

# Evaluating Population Exposure to Indoor Volatile Organic Compounds

Thomas Warburton

PhD

University of York

Chemistry

April 2025



# Abstract

Volatile organic compounds (VOCs) are a major source of air pollution with diverse indoor emission sources. Poor ventilation, solvent-containing products, and personal behaviours can elevate indoor VOC levels, though real-world data is limited. This thesis examines indoor VOC dynamics, focusing on emissions from household products and real-home exposure. Using a state-of-the-art gas chromatograph mass spectrometer, VOCs at sub-part per billion levels were identified and quantified alongside building characteristics such as age, and air change rates (ACR), as well as occupant activities such as cooking and cleaning times and frequency. In the first experiment, VOC emissions from liquid electrical (LE) fragrance diffusers were measured in 60 homes. Homes with the lowest ACR had the highest exposure to VOCs originating from LEs. A controlled booth experiment showed that monoterpene emissions from up to five LEs in a 10 m<sup>3</sup> booth were below their theoretical odour detection threshold. Moderating monoterpene content in fragrances could reduce formation of secondary air pollutants without affecting scent perception. It is possible that excessive off-label product use may be self-limiting as perceived fragrance intensity plateaued beyond two LEs operating simultaneously. A third study measured VOC concentrations in 124 homes in Bradford, UK over 12 months (2023–2024). Urban homes exhibited higher benzene, toluene, ethylbenzene and xylene (BTEX) concentrations due to outdoor pollution ingress. Acetaldehyde and carbon tetrachloride concentrations frequently exceeded lifetime cancer risk benchmarks. Scaling VOC concentrations to room volume and ACR into time-integrated emission rates revealed a seasonal trend, with rates generally peaking in summer and dipping in winter. A final chapter details a developed method to assess VOC emissions from aerosol products via gas chromatography, allowing for the analysis of potential product contamination, as well as identifying solutions to improve sampling rigour. This thesis advances understanding of indoor VOC sources, accumulation, and exposure in homes, providing contemporary real-home data to inform future research and improve indoor air quality models.



# Contents

<b>Abstract</b>	<b>iii</b>
<b>List of Figures</b>	<b>xi</b>
<b>List of Tables</b>	<b>xxi</b>
<b>List of Schemes</b>	<b>xxiii</b>
<b>List of Abbreviations</b>	<b>xxv</b>
<b>Acknowledgements</b>	<b>xxix</b>
<b>Declaration</b>	<b>xxxii</b>
<b>1 Introduction</b>	<b>1</b>
1.1 Scene setting . . . . .	1
1.1.1 VOCs from Hippocrates to Archer Martin . . . . .	1
1.1.2 Outdoor air pollution . . . . .	3
1.1.3 Outdoor VOC monitoring . . . . .	4
1.1.4 A brief history of indoor VOC research . . . . .	5
1.2 Indoor VOC emissions . . . . .	6
1.2.1 Review of indoor VOC emissions . . . . .	6
1.2.2 Source apportionment of indoor VOCs . . . . .	8
1.2.3 Sampling of indoor air . . . . .	8
1.2.4 Indoor-outdoor air relationships . . . . .	10
1.3 VOC removal pathways . . . . .	11
1.3.1 Oxidation reactions and associated chemistry . . . . .	12
1.3.1.1 Reaction with OH . . . . .	12
1.3.1.2 Reaction with O <sub>3</sub> . . . . .	13

---

1.3.1.3	Reaction with NO <sub>3</sub> . . . . .	14
1.3.1.4	Reaction with Cl . . . . .	16
1.3.1.5	Day-night cycles . . . . .	17
1.3.1.6	Oxidant and precursor reservoirs . . . . .	18
1.3.2	Surface interactions with VOCs . . . . .	19
1.3.3	Final remarks on VOC reaction and removal pathways . . . . .	21
1.4	Legislative impacts on indoor VOC exposure . . . . .	21
1.4.1	Ventilation requirements . . . . .	21
1.4.2	Air permeability . . . . .	22
1.4.3	Overheating . . . . .	22
1.4.4	Remarks on legislative impacts on IAQ . . . . .	22
1.5	Thesis structure . . . . .	23
1.6	References . . . . .	26
<b>2</b>	<b>Methodology</b>	<b>39</b>
2.1	General methodology . . . . .	39
2.1.1	Gas chromatography . . . . .	39
2.1.1.1	Carrier gases and columns . . . . .	40
2.1.1.2	Principles of separation . . . . .	40
2.1.1.3	Column efficiency . . . . .	41
2.1.1.4	Chromatographic resolution . . . . .	44
2.1.2	Thermal desorption . . . . .	45
2.1.2.1	VOC trapping . . . . .	45
2.1.2.2	Sample drying . . . . .	46
2.1.2.3	Peltier cooler . . . . .	47
2.1.2.4	Free-piston Stirling cooler . . . . .	48
2.1.3	Mass spectrometry . . . . .	49
2.1.3.1	Ionisation . . . . .	50
2.1.3.2	Quadrupole mass filter . . . . .	51
2.1.4	Flame ionisation detection . . . . .	53
2.1.4.1	Effective carbon number . . . . .	55
2.1.5	Whole air sampling . . . . .	57
2.1.5.1	Time-integrated canister sampling . . . . .	57
2.1.6	Sampling and instrument setup . . . . .	60
2.1.6.1	Canister preparation . . . . .	60
2.1.6.2	Sample collection . . . . .	61

---

2.1.6.3	Sample selection . . . . .	62
2.1.6.4	Sample drying . . . . .	62
2.1.6.5	Sample preconcentration . . . . .	62
2.1.6.6	Sample focusing and transfer . . . . .	62
2.1.6.7	Trap purging . . . . .	63
2.1.6.8	GC . . . . .	63
2.1.6.9	QMS . . . . .	65
2.1.6.10	Sample campaign sequencing . . . . .	67
2.1.6.11	Data workup . . . . .	69
2.2	Instrumentation and calibration . . . . .	69
2.2.1	Sampling canister stability . . . . .	70
2.2.2	Sample desorption . . . . .	74
2.2.3	Volume breakthrough . . . . .	80
2.2.4	FID carbon-wise response . . . . .	80
2.2.5	System contamination . . . . .	85
2.3	References . . . . .	90
<b>3</b>	<b>The impact of plug-in fragrance diffusers on indoor VOC concentrations</b>	<b>95</b>
3.1	Declaration, contributions and conflicts . . . . .	95
3.2	Abstract . . . . .	96
3.3	Introduction . . . . .	97
3.3.1	Objectives . . . . .	100
3.4	Methodology . . . . .	100
3.4.1	Experimental methodology . . . . .	100
3.4.2	Statistical approach . . . . .	106
3.4.3	Participant panel and survey . . . . .	108
3.5	Results . . . . .	108
3.5.1	Individual VOCs and TVOC . . . . .	108
3.5.2	Influence of CO <sub>2</sub> /ventilation on VOC exposure . . . . .	118
3.5.3	Participant effects and product use data . . . . .	120
3.5.4	Bottom-up estimates of increments in concentration . . . . .	122
3.5.5	Diffuser increment estimates . . . . .	124
3.5.6	Generation of secondary oxidation products from diffuser use . . . . .	127
3.6	Conclusions . . . . .	127
3.7	References . . . . .	130
<b>4</b>	<b>An assessment of VOC emissions and human strength perception of liquid</b>	

---

<b>electric fragrance diffusers</b>	<b>135</b>
4.1 Declaration, contributions and conflicts . . . . .	135
4.2 Abstract . . . . .	136
4.3 Introduction . . . . .	137
4.3.1 Objectives . . . . .	139
4.4 Methodology . . . . .	140
4.4.1 Canister preparation . . . . .	140
4.4.2 Sample collection and preparation for analysis . . . . .	141
4.4.3 Sample analysis . . . . .	143
4.4.4 Data visualisation and statistical analysis . . . . .	144
4.4.5 Olfactory methodology . . . . .	145
4.4.6 VOC metrics and modelling . . . . .	146
4.5 Results and discussion . . . . .	148
4.5.1 TVOC and fragrance species concentrations . . . . .	148
4.5.2 Comparison of LE emission rates . . . . .	151
4.5.3 Perceived intensity of LEs . . . . .	152
4.5.4 Modelling $\alpha$ -pinene increments . . . . .	155
4.5.5 Comparison with real-world analogues . . . . .	159
4.6 Conclusions . . . . .	161
4.6.1 Future work . . . . .	162
4.6.2 Limitations and considerations . . . . .	163
4.7 References . . . . .	164
<b>5 Yearlong study of indoor VOC variability: Insights into spatial, temporal, and contextual dynamics of indoor VOC exposure</b>	<b>173</b>
5.1 Declaration, contributions and conflicts . . . . .	173
5.2 Abstract . . . . .	174
5.3 Introduction . . . . .	174
5.4 Experimental and methodology . . . . .	176
5.4.1 Study area . . . . .	176
5.4.2 Participant selection and questionnaires . . . . .	177
5.4.3 Sample preparation, collection and preparation for analysis . . . . .	178
5.4.4 Sample analysis . . . . .	178
5.4.5 Calculation of ACR . . . . .	180
5.4.6 VOC metrics and manipulation . . . . .	182
5.4.6.1 Modified <i>Z-score</i> calculation . . . . .	182

---

5.4.6.2	Time-averaged emission rate calculation . . . . .	183
5.4.6.3	Sensitivity analysis . . . . .	184
5.4.7	IRIS benchmark calculations . . . . .	185
5.4.7.1	Lifetime cancer risk calculation . . . . .	185
5.4.7.2	Hazard quotient calculation . . . . .	186
5.4.8	Data visualisation and statistical analysis . . . . .	187
5.5	Results and discussion . . . . .	188
5.5.1	Indoor VOC concentrations . . . . .	188
5.5.1.1	Indoor concentrations of select VOCs . . . . .	188
5.5.1.2	Effect of geography on indoor VOC concentrations . . . . .	190
5.5.1.3	Lifetime cancer risk estimates . . . . .	190
5.5.1.4	Hazard quotients . . . . .	193
5.5.2	Air change rates . . . . .	196
5.5.3	Seasonality in VOC emissions . . . . .	197
5.6	Conclusions . . . . .	203
5.6.1	Limitations and strengths . . . . .	204
5.6.1.1	Limitations . . . . .	204
5.6.1.2	Strengths . . . . .	205
5.6.2	Future work . . . . .	206
5.7	References . . . . .	207
<b>6</b>	<b>Speciation and contaminant analysis of personal and home care aerosol products</b>	<b>219</b>
6.1	Background . . . . .	220
6.1.1	Contextualising previous work . . . . .	221
6.2	Methodology . . . . .	222
6.2.1	Aerosol dispensing and sampling . . . . .	223
6.2.1.1	Emission chamber . . . . .	223
6.2.1.2	Sample line . . . . .	224
6.2.1.3	Metal bellows pump . . . . .	224
6.2.2	Benzene analysis . . . . .	231
6.2.2.1	Sample drying . . . . .	233
6.2.2.2	GC heartcutting . . . . .	233
6.3	Conclusions . . . . .	237
6.4	References . . . . .	238
<b>7</b>	<b>Conclusions</b>	<b>241</b>

---

7.1	Synthesis of Key Findings . . . . .	241
7.2	Methodological Contributions . . . . .	242
7.3	Implications for Indoor Air Quality and Policy . . . . .	243
7.4	Limitations . . . . .	243
7.5	Future Research Directions . . . . .	244
7.6	Final Remarks . . . . .	244

# List of Figures

1.1	Structures of various monoterpenes, monoterpenoids and sesquiterpenes (Part 1). . . . .	2
1.2	Structures of various monoterpenes, monoterpenoids and sesquiterpenes (Part 2). . . . .	3
1.3	Photograph of Nelson’s Column in London during the Great Smog of 1952. Photograph taken by N T Stobbs and reproduced under the CC BY-SA 2.0 license. . . . .	4
1.4	Monthly median summed concentrations of 1,3-butadiene, benzene, toluene, ethylbenzene and xylene at rural and urban outdoor monitoring sites between January 2000 and July 2024, with $\log_{10}$ y-axis transformation. Curve smoothing was achieved using LOESS. Values were obtained from uk-air.defra.gov.uk using recorded data from the Automated Hydrocarbon Network. . . . .	5
1.5	Annual emission data of NMVOCs as a total, as well as the contributions of indoor NMVOCs originating from product use with $\log_{10}$ y-axis transformation. Data were obtained from the NAEI UK emissions data selector for NMVOCs across all sources. . . . .	12
1.6	The different emission and removal pathways for atmospheric VOCs through interactions with furnishings and building materials. . . . .	20
2.1	Diagram showing the internal structural differences between packed and capillary columns. In the capillary column, the stationary phase is a thin covering around the internal walls of the tube, in this diagram coloured brown. . . . .	41
2.2	Typical van Deemter curves for nitrogen, helium and hydrogen. . . . .	43
2.3	Separation of two imaginary peaks with a resolution of 0.5. The sum of the two elutions (chromatographic peak) is shown in black. Here there is significant co-elution of the two analytes, which would result in poor quantification. . . . .	44
2.4	Separation of two imaginary peaks with a resolution of 1.5. The sum of the two elutions (chromatographic peak) is shown in black. . . . .	44

---

2.5	A cross-sectional diagram illustrating sample drying using a Nafion hollow tube membrane. The Nafion membrane acts as a hollow tube, around which is the outer conduit, usually stainless steel, through which the purge gas flows.	48
2.6	A simplified diagram showing the workings of a free-piston Stirling cooler . . .	49
2.7	A 2D rendering of the production of analyte ions within the ion source. The analyte gas flow is orthogonal to the plane of the image, <i>i.e.</i> , entering from the front. . . . .	51
2.8	Electron impact mass spectrum of ethanol. Fragmentation structures as simple Lewis structures are annotated for select peaks. The peak labelled $M^+$ is the molecular ion, $C_2H_5OH^+$ . The mass spectrum was obtained from the National Institute of Standards and Technology (NIST) Chemistry WebBook, available at <a href="https://doi.org/10.18434/T4D303">https://doi.org/10.18434/T4D303</a> . <sup>[14]</sup> . . . . .	52
2.9	A simple diagram of the movement of two ions through a quadrupole mass selector. Ions with unstable trajectories, such as those that are too light or too heavy, are not detected. . . . .	53
2.10	A diagram showing the workings of a flame ionisation detector used following GC separation. . . . .	55
2.11	A diagram showing the final sampling assembly, with a flow-restrictive inlet and stabilising diaphragm, with sampling canister underneath. Labelled sections are as follows: 1. Inert in-line filter, 2. Goose neck to restrict entry of liquids, 3. Critical orifice flow restrictor, 4. Canister vacuum pressure gauge, 5. Internal diaphragm for flow rate stability, 6. Canister valve, 7. Canister. . .	58
2.12	Flow rate of flow-restrictive inlet affixed to the top of the evacuated sampling canisters. This figure is reproduced from Heeley-Hill <i>et al.</i> (2023) <sup>[27]</sup> using the same theme and colour scheme as in this thesis. . . . .	61
2.13	PLOT chromatogram for an ambient sample of residential indoor air. . . . .	64
2.14	WAX chromatogram for an ambient sample of residential indoor air. . . . .	64
2.15	WAX chromatogram for ambient air showing a large elution of unresolved $C_2$ to $C_6$ hydrocarbons. . . . .	66
2.16	PLOT chromatogram for ambient air without typically resolved species. . . .	66
2.17	WAX chromatogram for ambient air zoomed to show the other elutions from the ambient air sample. The unresolved hydrocarbon elution begins at $\approx 4.5$ min and finishes at $\approx 5$ min. . . . .	66
2.18	TIC for WAX-eluting species. The jump in baseline noise at $\approx 8.3$ min is due to the switching of the Deans switch towards both the QMS and the second FID. . . . .	66

---

2.19	PLOT chromatogram scaled between 18 mins and 21 mins to show the elutions of <i>i</i> -butane, <i>n</i> -butane and acetylene. . . . .	67
2.20	Scatter plots showing the changes in calibration mix concentration, with regression statistics and regression line equation calculated using Pearson's R. . . . .	72
2.21	The degradation plots as in figure 2.20 without the regression statistics and with selective scaling for each individual plot to better show the trend in species degradation. . . . .	73
2.22	Real-time water vapour mixing ratio in a whole air canister sample. The canister was first pressurised to 1 bar (gauge) with blank gas, connected to the analyser and the canister valve opened. . . . .	74
2.23	Layered chromatograms for PLOT elutions following preconcentration trap temperature variation. . . . .	76
2.24	Layered chromatograms for WAX elutions following preconcentration trap temperature variation. . . . .	77
2.25	Layered chromatograms for PLOT elutions following focus trap temperature variation. . . . .	78
2.26	Layered chromatograms for WAX elutions following focus trap temperature variation. . . . .	79
2.27	Facet wrapped plots of the linearity of peak area for calibrated gases with increasing sample volumes, from 5 mL to 1000 mL, using a 4 ppb multi-component standard. Regression statistics calculated using Spearman's Rho. Regression statistics for all species except ethene: $R = 1$ , $p = <0.001$ . Ethene regression statistics: $R = 0.89$ , $p = <0.001$ . . . . .	81
2.28	Segmented linear analysis of ethene peak areas against sample volume (mL). A vertical line is placed at the calculated breakthrough volume, $\approx 376$ mL. . . . .	82
2.29	PLOT chromatogram for no flow blank method. . . . .	86
2.30	WAX chromatogram for no flow blank method. . . . .	86
2.31	WAX chromatogram for no flow blank method following the replacement of the VF-WAX column. . . . .	87
2.32	TIC for WAX elutions of the no flow blank method. . . . .	87
2.33	The mass spectrum produced from the suspected benzene elution at $\approx 17$ min following background correction. . . . .	88
3.1	Flow schematic showing GCFIDQMS instrument setup. . . . .	102

---

3.2	Porous layer open tubular (PLOT) column elutions of a canister air sample with signal strength/response units on y-axis and retention time (RT)/acquisition time on x-axis. The first three signals from the left show a split ethane signal starting at roughly RT 9 min and ending at roughly RT 10.2 min, ethene signal just before RT 11 min, and a split propane signal starting at roughly RT 12 min and finishing at roughly RT 13 min. . . . .	106
3.3	The same canister sample run in figure 3.2 run a second time, showing better signal responses and resolution. Only data obtained from figure 3.3 was used in data workup. . . . .	107
3.4	Boxplot showing the spread of TVOC values from 60 homes, differentiated by whether the diffuser was off or on. Outliers above $10000 \mu\text{g m}^{-3}$ are removed from graphic to give equal presentation but are included in percentile calculations. . . . .	110
3.5	boxplot showing the spread of $\alpha$ -pinene values, differentiated by whether the diffuser was off or on, along with the calculated $\alpha$ -pinene increment. Outliers above $40 \mu\text{g m}^{-3}$ are removed from graphic to give equal presentation but are included in percentile calculations. . . . .	110
3.6	Boxplots showing different species concentration values, aggregated across all houses and separated by diffuser status, with y-axis $\log_{10}$ transformation. . .	113
3.7	Correlation matrix showing inter-VOC correlations when the diffuser was off. A forward slanting green line indicates a positive correlation, a full circle indicates no correlation, and a backward slanting red line indicates a negative correlation. A more intense colour and a narrower line indicates a stronger correlation. . . . .	114
3.8	Correlation matrix showing inter-VOC correlations when the diffuser was on. A forward slanting green line indicates a positive correlation, a full circle indicates no correlation, and a backward slanting red line indicates a negative correlation. A more intense colour and a narrower line indicates a stronger correlation. . . . .	115
3.9	The percentage chance a VOC showing any increase in concentration when the diffuser was turned on. A fully random outcome (half the homes higher, half lower) would occur at 50%. Only those coloured green deviate from random chance by a statistically significant amount. * denotes a species which was included in the fragrance formulation. . . . .	117

---

3.10	The relationship between CO <sub>2</sub> and TVOC. All measured values are included in the graphic and were included in the linear regression calculation. Diffuser off regression statistics: $R = 0.74$ , $p = 0.0093$ . Diffuser on regression statistics: $R = 0.58$ , $p = 0.014$ . . . . .	118
3.11	Boxplots showing the change in fragrance TVOC concentration when the diffuser was turned on for the houses with the poorest ventilation, the quartile with the highest baseline TVOC value. Outliers above 50 $\mu\text{g m}^{-3}$ were removed from the graphic to aid presentation, but were included in the calculation of quartiles and median concentration values. . . . .	118
3.12	A repeat of figure 3.10, however with the outlier at CO <sub>2</sub> fraction 2019 ppm and TVOC concentration 3084 $\mu\text{g m}^{-3}$ in the 'diffuser on' subset removed, with linear regression statistics re-run. Diffuser off regression statistics: $R = 0.74$ , $p = 0.0093$ . Diffuser on regression statistics: $R = 0.86$ , $p = 0.000024$ . . . . .	119
3.13	The relationship between the sum of fragrance VOCs and the distance between the sampling canister and the fragrance diffuser. Regression statistics were calculated using Pearson's R. Diffuser off regression statistics: $R = -0.012$ , $p = 0.89$ . Diffuser on regression statistics: $R = 0.057$ , $p = 0.055$ . . . . .	120
3.14	The sum of all measured VOCs ('TVOC') against total product use frequency from all houses. Pearson's $R = -0.015$ , $p = 0.81$ . Regression statistics calculated using a linear model. . . . .	121
3.15	The frequency of product use in each home over each three-day sampling period, differentiated by diffuser status. . . . .	121
3.16	Covariance matrix between selected VOC species and products for all homes when the diffuser was off. . . . .	122
3.17	Covariance matrix between selected VOC species and products for all homes when the diffuser was turned on. . . . .	122
3.18	A raster plot overlaid with contour lines showing the $\alpha$ -pinene increment expected for different room volumes and ventilation rates. A continuous colour scale was applied to $\alpha$ -pinene increment values, and the scale was transformed on a $\log_2$ scale to aid visualisation. . . . .	126
3.19	Calculated total SPCP values differentiated by diffuser status. Outliers below -4 and above +4 were removed from the graphic to aid presentation, but were included in the calculation of quartiles and median values. . . . .	128
3.20	Calculated SPCP from fragrance species, where data was available. Outliers above 1 were removed from the graphic to aid presentation, but were included in the calculation of quartiles and median values. . . . .	128

---

4.1	Top-down view of the large booth layout. Numbered elements are as follows: 1 - LE plug location, 2 - Air in flow vent, 3 - Canister sampling location, 4 - Air out flow vent, 5 - Access door. The height of the booth was 2.49 m, giving a final volume of 33.24 m <sup>3</sup> . . . . .	142
4.2	Top-down view of the toilet booth layout. Numbered elements are as follows: 1 - LE plug location, 2 - Air in flow vent, 3 - Canister sampling location, 4 - Air out flow vent, 5 - Access door. Ovals at the top of the schematic represent two toilets fitted on a plinth. The height of the booth was 2.6 m, giving a final volume of 9.48 m <sup>3</sup> . . . . .	142
4.3	Boxplots of the spread of fragrance TVOC concentrations in the large booth (left panel) and toilet booth (right panel). From bottom to top, each boxplot shows 5th percentile, 25th percentile, 50th percentile/median, 75th percentile, 95th percentile. Any outliers are given as single dots above or below the 5th/95th whisker. . . . .	149
4.4	Scatter plot showing median concentration results for fragrance species at each LE level (0 to 5) for the large booth. Regression statistics for each species: $\alpha$ -pinene $R = 1$ , $p = 0.0028$ ; $\gamma$ -terpinene $R = 0.83$ , $p = 0.058$ ; $p$ -cymene $R = 0.94$ , $p = 0.017$ ; eucalyptol $R = -0.6$ , $p = 0.24$ ; benzaldehyde $R = 0.66$ , $p = 0.18$ . . . . .	150
4.5	Scatter plot showing median concentration results for fragrance species at each LE level (0 to 5) for the toilet booth. Regression statistics for each species: $\alpha$ -pinene $R = 1$ , $p = 0.0028$ ; $\gamma$ -terpinene $R = 0.94$ , $p = 0.017$ ; $p$ -cymene $R = 0.89$ , $p = 0.033$ ; benzaldehyde $R = 1$ , $p = 0.0028$ . . . . .	150
4.6	Re-plot large booth benzaldehyde linearity, using the 0 LE concentration from the toilet booth to attempt to de-skew the regression caused by the outlying 0 LE large booth benzaldehyde concentration. The resulting linearity was of significance. Regression statistics( $R = 1$ , $p = 0.0028$ )the were calculated using Spearman's Rho. . . . .	151
4.7	A matrix which shows the mean change in perceived fragrance intensity at each combination of LE level from a scale of 0 to 100, 0 being the lowest/no change in perceived intensity and 100 being the highest. . . . .	153
4.8	Matrix showing $p$ -value results for each LE level pair following ANOVA and Benjamini-Hochberg <i>post-hoc</i> analysis for fragrance perception. . . . .	154
4.9	Matrix which shows $p$ -value results for each LE level pair following Kruskal-Wallis and Dunn <i>post-hoc</i> analysis for fragrance TVOC concentrations. . . . .	154

---

4.10	Raster plot showing expected increment concentration of $\alpha$ -pinene in $\mu\text{g m}^{-3}$ , against ventilation rates in units of $\text{h}^{-1}$ , and room volumes in units of $\text{m}^3$ . Concentrations were calculated using mean LE emission rates from this study. Increment concentrations graduate on a low-to-high colour scale from blue to red. . . . .	157
4.11	Comparison of concentrations collected in this study against the concentrations found in Warburton <i>et al.</i> (2023), <sup>[26]</sup> using the same LE device and liquid formulation. All concentrations are shown in $\mu\text{g m}^{-3}$ . Concentrations from Warburton <i>et al.</i> (2023) <sup>[26]</sup> are displayed on the plots as ‘Real homes’. From bottom to top, each boxplot shows 5th percentile, 25th percentile, 50th percentile/median, 75th percentile, 95th percentile. Any outliers are given as single dots above or below the 5th/95th whisker. . . . .	160
5.1	Measured indoor concentrations of a select group of VOCs measured in the INGENIOUS homes. Boxplots show values in the order of (from bottom-to-top): lower outliers, 5th percentile, 25th percentile, median value, 75th percentile, 95th percentile, and upper outliers. The y-axis has been logarithmically transformed to aid presentation. . . . .	189
5.2	Indoor concentrations of aromatic VOCs, treated through modified <i>Z-score</i> analysis, and separated by rural or urban status. Boxplots show values in the order of (from bottom-to-top): lower outliers, 5th percentile, 25th percentile, median value, 75th percentile, 95th percentile, and upper outliers. The y-axis has been logarithmically transformed to aid presentation. TMB = trimethylbenzene, BTEX = benzene, toluene, ethylbenzene and xylene. * denotes a change of significance ( $p\text{-value} \leq 0.05$ ). . . . .	191
5.3	Boxplots indoor-outdoor ratios of aromatic VOCs, separated by rural or urban status. Indoor-outdoor ratios were split into Boxplots show values in the order of (from bottom-to-top): lower outliers, 5th percentile, 25th percentile, median value, 75th percentile, 95th percentile, and upper outliers. TMB = trimethylbenzene. Here, individual xylene isomers have been grouped for consistency with the main text. . . . .	192

---

5.4	Calculated lifetime cancer risks (LCRs) for six VOCs. A horizontal dotted line is placed at the 0.000001 mark, representing the 1 in 1,000,000 chance threshold of developing cancer through a lifetime exposure to the exposure factor-adjusted concentration of the displayed VOC. Boxplots show values in the order of (from bottom-to-top): lower outliers, 5th percentile, 25th percentile, median value, 75th percentile, 95th percentile, and upper outliers. The y-axis has been logarithmically transformed to aid presentation. . . . .	193
5.5	Calculated hazard quotients (HQs) for the VOCs measured in this study with available reference concentration data from the integrated risk information system (IRIS). A horizontal dotted line is placed at $HQ = 1$ , above which a home occupant could develop symptoms based on a lifetime exposure to the exposure factor-adjusted concentration for the displayed VOC. Boxplots show values in the order of (from bottom-to-top): lower outliers, 5th percentile, 25th percentile, median value, 75th percentile, 95th percentile, and upper outliers. The y-axis has been logarithmically transformed to aid presentation. . . . .	195
5.6	The inferred air change rates ( $hr^{-1}$ ) by season. Boxplots show values in the order of (from bottom-to-top): lower outliers, 5th percentile, 25th percentile, median value, 75th percentile, 95th percentile, and upper outliers. The green diamonds indicate seasonal mean ACR. Error bars are calculated as 95% confidence intervals for the mean value using 1000 bootstrap resamples of the data. . . . .	196
5.7	Meteorological data gathered from UK Met Office for Bradford over 2023 and 2024, taken from a weather station at 53°48'46.8"N 1°46'19.2" W. Values were taken for each month. Data was collected for maximum and minimum mean temperature (°C), ground frost days per month, total rainfall (mm) and total sunshine hours per month. . . . .	197
5.8	Meteorological data gathered from UK Met Office for Bradford over 2023 and 2024, taken from a weather station at 53°48'46.8"N 1°46'19.2" W. Values were taken for each month. Data was collected for maximum and minimum mean temperature (°C), ground frost days per month, total rainfall (mm) and total sunshine hours per month. Values were taken for each month, with each month then being grouped into four seasons: winter (December, January, February), spring (March, April, May), summer (June, July, August), and autumn (September, October, November), and mean values for each meteorological measurement taken for each season. . . . .	198
5.9	Indoor TVOC concentrations by season. . . . .	199

---

5.10	Total indoor VOC emission rates by season. . . . .	199
5.11	Calculated individual VOC emission rates over the seasons. Outliers above 10 mg hr <sup>-1</sup> were removed from ethane and sum BTEX plots, and outliers above 1 mg hr <sup>-1</sup> were removed from 1,3-butadiene and sum TMB plots to aid presentation, but did not affect the calculation of quartiles for boxplots. Boxplots show values in the order of (from bottom-to-top): lower outliers, 5th percentile, 25th percentile, median value, 75th percentile, 95th percentile, and upper outliers. The y-axis has been logarithmically transformed to aid presentation. TMB = trimethylbenzene, BTEX = benzene, toluene, ethylbenzene and xylene. . . .	200
5.12	(a) Total fragrance product use, (b) total aerosol product use and (c) the sum of fragrance and aerosol product use. Statistics were gathered daily and then added together over the 72-hour sampling period. Boxplots show values in the order of (from bottom-to-top): lower outliers, 5th percentile, 25th percentile, median value, 75th percentile, 95th percentile, and upper outliers. . . . .	201
5.13	Seasonality in the summed normalised total VOC emissions. . . . .	202
5.14	Seasonality in the summed normalised monoterpene emissions. . . . .	202
5.15	Matrices of <i>p</i> -values following <i>post-hoc</i> Dunn tests for seasonality in (a) summed normalised VOC emission rates and (b) summed normalised monoterpene emission rates. A white coloured matrix cell indicates the <i>p</i> -value for the pairwise comparison was not of significance. Significant values ( <i>p</i> -value ≤ 0.05) graduate from red ( <i>p</i> -value = 0.05) to blue ( <i>p</i> -value → 0). . . . .	203
6.1	Pie chart showing the contribution of individual propellant types to the total 2012 propellant budget. HAP = hydrocarbon aerosol propellant; DME = dimethyl ether. Reproduced from Yeoman and Lewis (2021). <sup>[1]</sup> . . . . .	220
6.2	Diagram of the chamber used in the aerosol speciation study (not to scale). Reproduced from Yeoman <i>et al.</i> (Unpublished). . . . .	223
6.3	Schematic diagram of the AP sample line used for benzene analysis. During the main sampling campaign, the main line mass-flow controller, Nafion MD-070-96 and associated parts were removed, with all other components remaining. Symbols used within the diagram are as prescribed by the Piping and Instrument Diagrams (P&ID) standards. . . . .	225
6.4	PLOT chromatogram for 500 mL sample of blank gas drawn through the sampling manifold used to process the canister and pump blank samples. . .	226
6.5	WAX chromatogram for 500 mL sample of blank gas drawn through the sampling manifold used to process the canister and pump blank samples. . . .	226

---

6.6	Plot showing PLOT channel intensities following canister blank intensities being subtracted from the pump blank. . . . .	227
6.7	Plot showing WAX channel intensities following canister blank intensities being subtracted from the pump blank. . . . .	227
6.8	Plot showing the difference between canister and pump blank samples, zoomed in to the acetone peak, here showing splitting of the peak due to differences between acetone retention time between the canister and pump blank sample runs. . . . .	228
6.9	Original pump blank sample showing the acetone peak, with significant peak tailing, indicating there was band broadening due to high quantities of acetone in the volume sampled. . . . .	228
6.10	WAX elution for suspected D4 following liquid injection of 1 $\mu\text{L}$ into 3 L of blank gas into a Tedlar bag. The peak shows significant non-Gaussian characteristics, indicating an overloading of the column. While not ideal, it was evidence this was the elution of D4. . . . .	229
6.11	Mass spectrum for the peak shown in figure 6.10. . . . .	229
6.12	WAX elution for suspected D4 - originating from the same plot as figure 6.7, just scaled to retention times of 15.5 min and 16.5 min. . . . .	230
6.13	Mass spectrum for the peak shown in figure 6.12. Significant peaks at 32, 40 and 45 $m/z$ units originate from the background, identified as oxygen, argon, and small amounts of $\text{CO}_2$ , likely to originate from air due to a small leak. . . . .	230
6.14	QMS data from both total ion count (TIC) in green, and the 78 $m/z$ scan showing the benzene detection during the wide ethanol detection. The ethanol detection showed significant band broadening in the column due to the quantity of ethanol within the sample. . . . .	232
6.15	PLOT chromatogram for a 20 mL sample of the 30 component gas standard, with the absence of a benzene peak identified. . . . .	235
6.16	WAX chromatogram for a 20 mL sample of the 30 component gas standard, with the benzene peak identified. . . . .	235
6.17	PLOT chromatogram for a 20 mL sample of the 30 component gas standard using the heartcutting method, with the benzene peak identified. . . . .	236
6.18	WAX chromatogram for a 20 mL sample of the 30 component gas standard using the heartcutting method, with the absence of the benzene peak identified. There was a small reduction in baseline noise during the Deans switch actuation, owing to a slight reduction in pressure as the WAX eluent flow passed through the PLOT column. . . . .	236

# List of Tables

1.3	Residential concentrations in $\mu\text{g m}^{-3}$ of select VOCs in various studies. Where studies sampled in different indoor locations, only residential samples were used to display in table 1.3. BTEX concentrations displayed are the sum of individual benzene, toluene, ethylbenzene and xylene concentrations. Missing values are displayed as <i>ND</i> . . . . .	7
1.4	A summary of the different emissions from a variety of indoor activities and products . . . . .	8
2.1	The ECN contributions for different functional groups and elements used throughout these works. . . . .	56
2.2	The VOCs contained within the multi-component calibration standard mix. .	69
2.3	Sampling regimen for degradation testing of calibrated samples in sampling canisters. . . . .	71
2.4	A summary of carbon-wise responses from three sample runs using 200 mL samples of the multi-component calibration mix, including the column the VOC eluted from and the ECN used in the data workup. St. Dev. is the population standard deviation, while Rel. St. Dev is the relative standard deviation, calculated by dividing the standard deviation by the average of the carbon responses, and displayed as a percentage. . . . .	83
3.1	List of species quantified in this study and the quantification method used. .	103
3.2	Median, 5th and 95th percentile and standard deviation values for all quantified VOCs, differentiated by diffuser status. All median and percentile values are expressed in $\mu\text{g m}^{-3}$ . . . . .	111
3.3	Median, 5th and 95th percentile and standard deviation values for fragrance VOC emission rates, expressed in $\mu\text{g hr}^{-1}$ . . . . .	124
3.4	Median, 5th and 95th percentile and standard deviation values for fragrance VOC increment concentration, expressed in $\mu\text{g m}^{-3}$ . . . . .	124

---

4.1	Instrument limits of detection (LOD) and quantification (LOQ) for the six fragrance species $\alpha$ -pinene, $\beta$ -pinene, $\gamma$ -terpinene, <i>p</i> -cymene, eucalyptol, and benzaldehyde. . . . .	144
4.2	Comparison of LE emission rates and booth properties between this study and several other studies available in literature. . . . .	152
4.3	Comparison of median sampled concentrations from this study against UK indoor exposure thresholds available from Public Health England. <sup>[71]</sup> All concentrations are shown in $\mu\text{g m}^{-3}$ . . . . .	158
5.1	A table of the 30 VOCs contained within the 30-component NPL30 calibration standard used in this study. . . . .	180
5.2	Limits of detection (LOD) and quantification (LOQ) for VOCs resolved by the GC analysis. LODs were calculated by a signal-to-noise (SNR) ratio of 3:1, and LOQ using an SNR of 10:1. . . . .	181
5.3	Measured VOCs used for LCR analysis using inhalation unit risk data available from IRIS. . . . .	186
5.4	Measured VOCs used for HQ analysis using reference concentration data available from IRIS. . . . .	187

# List of Schemes

1.1	Formation of Criegee intermediate through ozonolysis of a generic alkene. . .	15
1.2	Resonance structures of the Criegee intermediate between zwitterions and a biradical. . . . .	15
1.3	Formation of a peroxyxynitrite intermediate following nitrate radical addition over a double-bond. . . . .	16
2.1	A flow schematic of sample preconcentration and focusing for canister samples through in-line cold traps. . . . .	47
2.2	A flow schematic for the sample sequencing used throughout the works in this thesis. . . . .	68
4.1	Flowcharts showing air sampling and olfactive assessment method flows. The flowchart begins at the top and works methodically through the steps downwards through to the bottom. Unless specifically stated, the time taken between the steps tended to vary based on logistics. . . . .	140



# List of Abbreviations

**LN<sub>2</sub>** Liquid Nitrogen.

***m/z*** Mass-to-Charge.

**AC** Alternating Current.

**ACR** Air Change Rate.

**ANOVA** Analysis Of Variation.

**AP** Aerosolised Product.

**ATSDR** Agency for Toxic Substances and Disease Registry.

**AURN** Automatic Urban and Rural Network.

**BiB** Born in Bradford.

**BTEX** Benzene, Toluene, Ethylbenzene and Xylene.

**CAZ** Clean Air Zone.

**CDU** Crude oil Distillation Unit.

**CEDA** Centre for Environmental Data and Analysis.

**CI** Criegee Intermediate.

**COP** Coefficient Of Performance.

**DC** Direct Current.

**ECN** Effective/Equivalent Carbon Number.

**EI** Electron Impact.

**EPA** Environmental Protection Agency.

**FID** Flame Ionisation Detection/Detector.

---

**FPSC** Free-Piston Stirling Cooler.

**GC** Gas Chromatography.

**HAP** Hydrocarbon Aerosol Propellant.

**HETP** Height-Equivalent of a Theoretical Plate.

**HQ** Hazard Quotient.

**IAQ** Indoor Air Quality.

**ID** Internal Diameter.

**INGENIOUS** Understanding the Sources, Transformations and Fates of Indoor Air Pollutants.

**IRIS** Integrated Risk Information System.

**IUPAC** International Union of Pure and Applied Chemistry.

**LC** Liquid Chromatography.

**LCR** Lifetime Cancer Risk.

**LE** Liquid Electrical.

**LEZ** Low Emission Zone.

**LLC** Limited Liability Company.

**LOD** Limit Of Detection.

**LOESS** Locally Estimated Scatterplot Smoothing.

**LOQ** Limit Of Quantification/Quantitation.

**MCM** Master Chemical Mechanism.

**MO<sub>x</sub>** Metal Oxide.

**MS** Mass Spectrometry.

**NAEI** National Atmospheric Emissions Inventory.

**NDIR** Nondispersion Infrared.

**NERC** Natural Environment Research Council.

**NMHC** Non-Methane Hydrocarbon.

---

**NMVOC** Non-Methane Volatile Organic Compound.

**NO<sub>x</sub>** Nitrogen oxides (NO + NO<sub>2</sub>).

**NPL** National Physical Laboratory.

**ODL** Odour Detection Limit.

**ODT** Odour Detection Threshold.

**ONS** Office for National Statistics.

**OVOC** Oxygenated Volatile Organic Compound.

**P&ID** Piping and Instrument Diagrams.

**PAN** Peroxy Acetyl Nitrate.

**PCP** Personal Care Product.

**PFA** Perfluorinated Alkane.

**PHE** Public Health England.

**PID** Photoionisation Detection/Detector.

**PLOT** Porous-Layer Open Tubular.

**PM** Particulate Matter.

**PPB** Parts Per Billion.

**PPE** Personal Protective Equipment.

**PPM** Parts Per Million.

**PPT** Parts Per Trillion.

**PTR** Proton Transfer Reaction.

**QMS** Quadrupole Mass Spectrometer.

**QQ** Quantile-Quantile.

**RF** Radio Frequency.

**SBS** Sick Building Syndrome.

**SIFT** Selected-Ion Flow-Tube.

**SOA** Secondary Organic Aerosol.

---

**SPCP** Secondary Product Creation Potential.

**SVOC** Semi-Volatile Organic Compound.

**TD** Thermal Desorption.

**TDU** Thermal Desorption Unit.

**TIC** Total Ion Count.

**TMB** Trimethylbenzene.

**TOF** Time Of Flight.

**TVOC** Total Volatile Organic Compound.

**UK** United Kingdom.

**ULEZ** Ultra-Low Emission Zone.

**US** United States (Of America).

**VOC** Volatile Organic Compound.

**VP** Vapour Pressure.

**WAS** Whole Air Samples.

**WHO** World Health Organisation.

# Acknowledgements

I would first like to thank my supervisor, Ally Lewis. Your support and guidance has been second-to-none. From all of the replies to my emails with plots and paper sections I bombarded you with, to being a constant source of encouragement for me through all the work a PhD brings, I appreciate you always setting time aside to read through all the waffling text I sent you (hopefully I'm a bit better now!). Thank you for taking a chance on me. I also would like to extend the same appreciation to my Independent Panel Member Terry Dillon - I always looked forward to our TAP meetings (yes it's sad, I know...).

A huge thanks also goes out to all of my colleagues at the Wolfson Atmospheric Chemistry Laboratories for all your constant positivity and support. In particular, Jim Hopkins, Steve Andrews and Martyn Ward - I feel very privileged to have been your student in all manner of technical things, you always had the solution every time the GC was having a mare! There aren't any other people on this planet I could have 30-minute conversations about Swage fittings with (yes it's sad, I know... there's a theme here). A big thanks also to everyone in Nicola Carslaw's Indoor Air Quality research group. You all provided a space where I could run through ideas and discuss my findings, and you helped make the work in this thesis stronger. And you let me whinge when things didn't quite work!

Thanks also to my friends, in particular Callum, Charlotte, Harry and Ross, for being my unwavering islands of (relative) normality, and providing welcome distractions away from periods of in depth work.

I would like to reserve my biggest thanks to my family - in particular, my brother (thank you also for being my R and stats troubleshooter), my sister-in-law, my cousin, my aunty and uncle, and above all my mum and my late father and grandparents. Without your companionship, love and kindness, none of this would have been possible. Shoutout also my nephews and niece!



# Declaration

I declare that this thesis is a presentation of original work and I am the sole author. This work has not previously been presented for an award at this, or any other, University. All sources are acknowledged as references.

This thesis is based on three original peer-reviewed publications for which I was first author, presented in chapters 3, 4 and 5. Author contributions are given at the start of chapters 3, 4, 5 and 6.

Warburton T, Grange S, Hopkins JR, Andrews SJ, Lewis AC, Owen N, Jordan C, Adamson G, Xia B. The impact of plug-in fragrance diffusers on residential indoor VOC concentrations. *Environ. Sci.: Processes & Impacts*, (2023), **25**, 805-817. <https://doi.org/10.1039/d2em00444e>

Warburton T, Lewis AC, Hopkins JR, Andrews SJ, Yeoman AM, Owen N, Jordan C, Adamson G, Xia B. An assessment of VOC emissions and human strength perception of liquid electric fragrance diffusers. *Environ. Sci.: Advances*, (2025), **5**, 739-752. <https://doi.org/10.1039/d4va00388h>

Warburton T, Hamilton JF, Carslaw N, McEachan RRC, Yang TC, Hopkins JR, Andrews SJ, Lewis AC. Yearlong study of indoor VOC variability: Insights into spatial, temporal, and contextual dynamics of indoor VOC exposure. *Environ. Sci.: Processes & Impacts*, (2025), **27**, 1025-1040. <https://doi.org/10.1039/D4EM00756E>

Chapter 6 discusses a methodology for work in another study for which I am second author, which at the time of writing is under consideration for publication in Scientific Reports, in the Household Air Pollution special issue.

Yeoman AM, Warburton T, Sidhu NK, Andrews SJ, Shaw M, Hopkins JR, Lewis AC. Updated speciation of VOCs emitted from European-market aerosol dispenser consumer products. Unpublished.



# Chapter 1

## Introduction

### 1.1 Scene setting

#### 1.1.1 VOCs from Hippocrates to Archer Martin

Volatile Organic Compounds (VOCs) are pervasive in 21<sup>st</sup> century life and their sources are myriad and complex, with personal exposure varying greatly according to individual activities, habits, and behaviours. In a most basic form, a VOC can be defined as an organic compound which has a low boiling point/high vapour pressure under standard atmospheric conditions (1 atm/101.325 kPa of pressure). However, there is no set definition on what constitutes a VOC, and definitions tend to vary depending on the context in which VOCs are defined.<sup>[1]</sup>

The concept of volatile compounds has been known about since the time of Hippocrates, who used the smell of patients' breath as an indicator of disease.<sup>[2]</sup> This antiquarian method was further developed more recently in the late-1800s when acetone concentrations were discovered to be elevated in the breath of diabetic patients.<sup>[3]</sup> Gas chromatography (GC) as it is known now was invented in 1952 by Anthony T. James and Archer J. P. Martin.<sup>[4]</sup> Quantifiable research into atmospheric VOCs became much more prevalent from the 1960s onwards following the advent of capillary column GC, allowing hitherto unprecedented resolution of complex gas-phase mixtures. Additional techniques such as thermal desorption (TD) allowed for further increased resolution of gas samples.

There are many sub-categories of VOCs commonly found in indoor environments: terpenes, hydrocarbons, and carbonyl-containing species to name a few. Terpene is an umbrella term for a group of chemicals whose formulae are multiples of isoprene ( $C_5H_8$ ). The two most com-

---

monly found indoor terpene classes are monoterpenes ( $C_{10}H_{16}$ ) and sesquiterpenes ( $C_{15}H_{24}$ ). There are additional similar classes called terpenoids, which possess a chemical formula not too dissimilar from that of a terpene class, but may deviate slightly by including other elements. Monoterpenes and sesquiterpenes are among the most reactive VOCs found in indoor environments and have high potential to create secondary products.<sup>[5,6]</sup> Some example structures of select monoterpenes, monoterpenoids and sesquiterpenes are shown in figures 1.1 and 1.2.

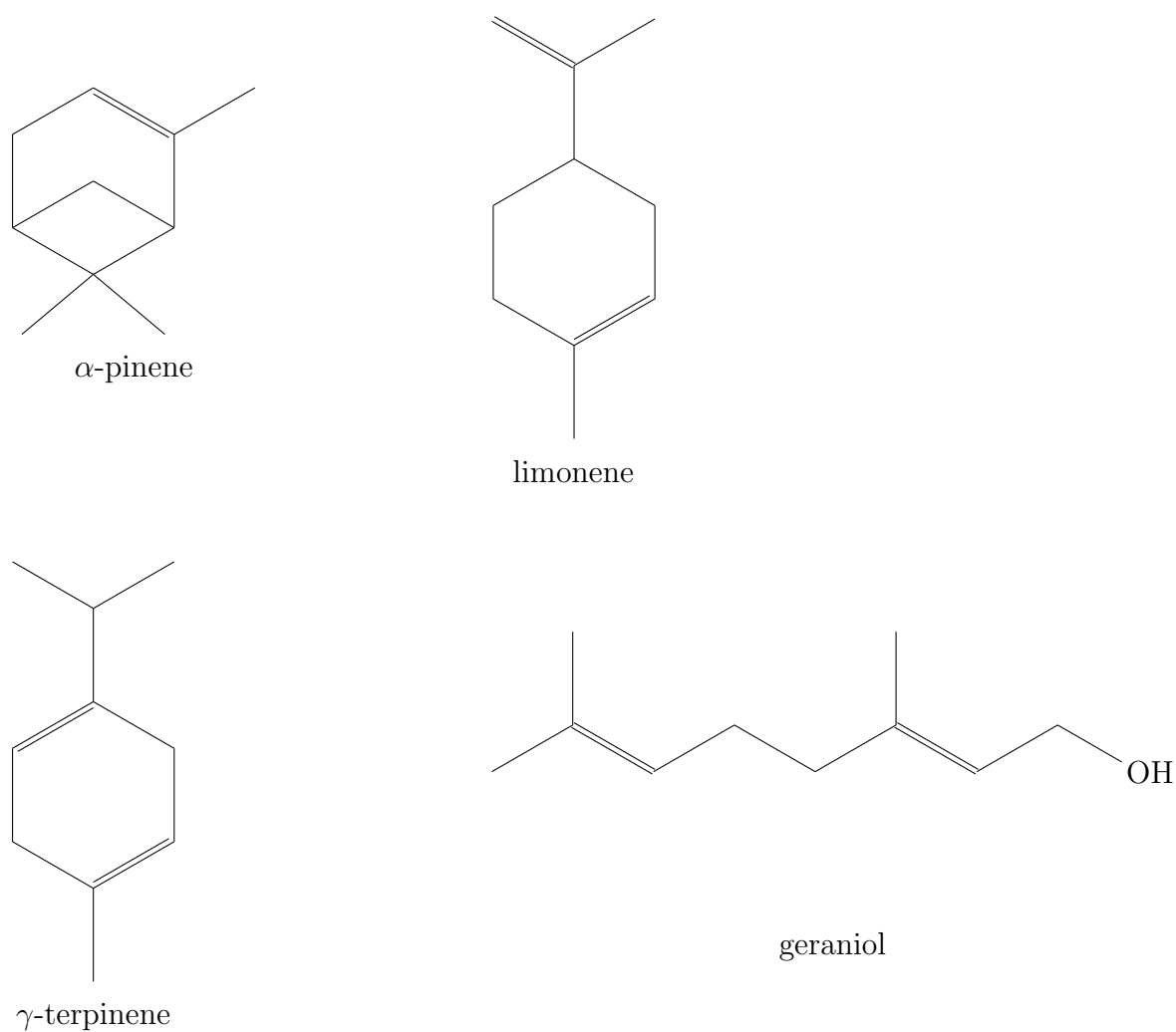


Figure 1.1: Structures of various monoterpenes, monoterpenoids and sesquiterpenes (Part 1).

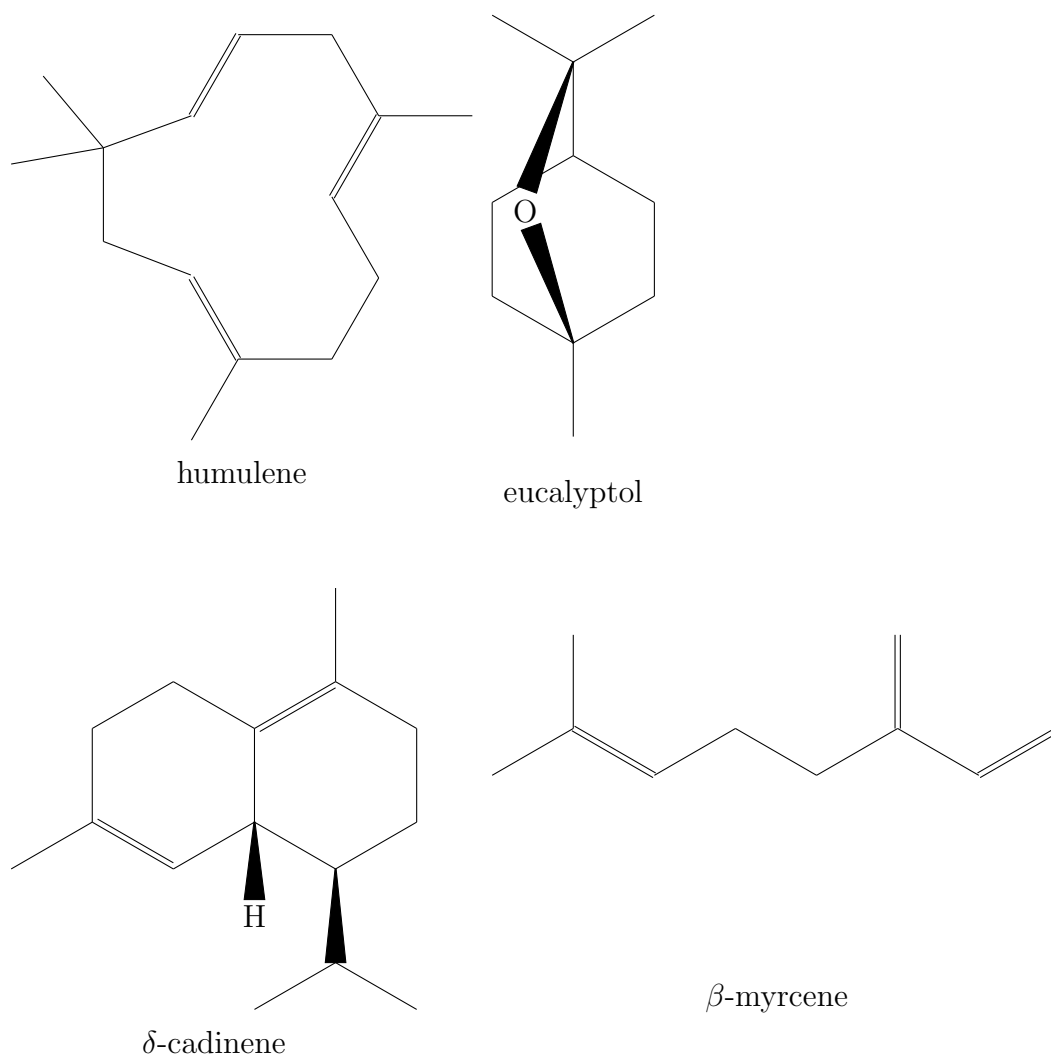


Figure 1.2: Structures of various monoterpenes, monoterpeneoids and sesquiterpenes (Part 2).

### 1.1.2 Outdoor air pollution

Air pollution is not a new concept, but was thrust into public attitudes and knowledge following deadly pollution events. Events such as the 1948 Donora smog, in which 20 people died and over 6000 people experienced respiratory difficulties caused by poisonous emissions from a steel works being trapped at ground-level by a temperature inversion, or the December 1952 London smog (often called the Great Smog of London), in which pollutants from coal-fired electricity generation stations were trapped by a windless anticyclone event where over an estimated 4000 people died. Figure 1.3 shows a photograph of Nelson's Column during



Figure 1.3: Photograph of Nelson's Column in London during the Great Smog of 1952. Photograph taken by N T Stobbs and reproduced under the CC BY-SA 2.0 license.

the Great Smog of London showing the poor visibility caused by airborne particulates and gases causing the smog. Before the Great Smog, London was already known for smogs and dense fogs from air pollution, colloquially called 'pea soupers' due to the yellow appearance of the fog (caused by sulphur dioxide), and while there are Acts of Parliament dating back to 1853 to tackle smoke emissions from industrial chimneys, pre-1956 air pollution legislation in the United Kingdom mainly treated air pollution as a nuisance rather than a cause for health concern. However, the United Kingdom Clean Air Act of 1956 is generally seen as a landmark act which aimed to lower pollution from both domestic and industrial emissions and treated air pollution as a cause of health issues.<sup>[7,8]</sup> Continuous outdoor monitoring of pollutants such as ozone ( $O_3$ ), sulphur dioxide ( $SO_2$ ), carbon monoxide (CO), both nitrogen monoxide (NO) and nitrogen dioxide ( $NO_2$ ), hereafter referred to together as NO<sub>x</sub>, and particulate matter (PM) has occurred in the UK since 1987 following the establishment of the Automatic Urban Monitoring Network, a predecessor of the current Automatic Urban and Rural Network (AURN).

### 1.1.3 Outdoor VOC monitoring

Outdoor hydrocarbon concentrations in the UK have been monitored continuously since 1992, following the establishment of the Automatic Hydrocarbon Network, with one rural monitoring site located south of Edinburgh, Scotland and the remaining three sites located in the south of England. There are also numerous non-automatic sites monitoring outdoor

---

hydrocarbon concentrations around the UK. Median monthly summed concentrations of 1,3-butadiene, benzene, toluene, ethylbenzene and xylene (all of which are hydrocarbons found largely from vehicle exhaust emissions<sup>[9]</sup>) at both the rural monitoring site and the urban site based at Marylebone Road, London are shown in figure 1.4. At the urban site, there has been a continued fall in hydrocarbon concentrations since 2000, while hydrocarbon concentrations at the rural site show a steady, fairly consistent concentration. Concentration differences between the urban and rural monitoring site currently are generally within an order of magnitude of each other, and mostly have been since hydrocarbon monitoring began at the rural site in 2008.

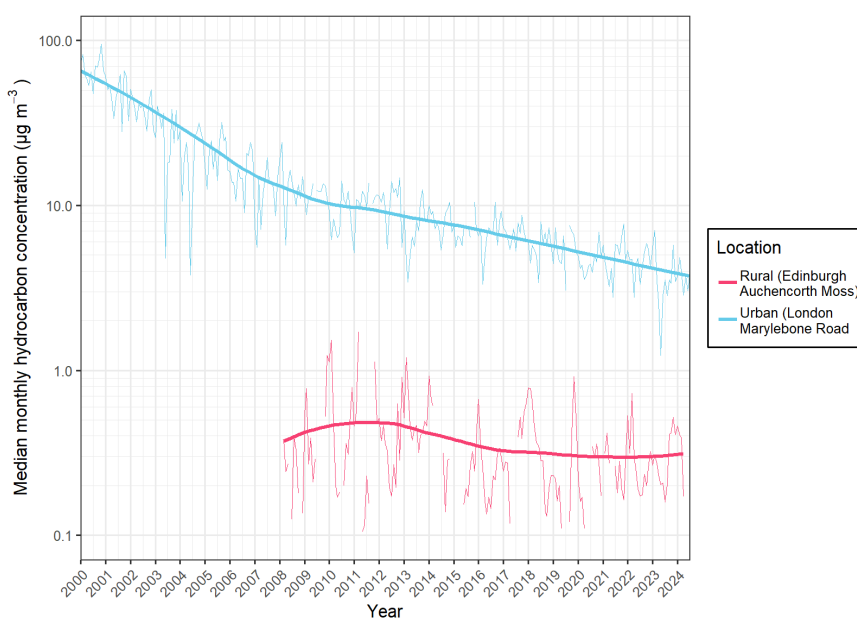


Figure 1.4: Monthly median summed concentrations of 1,3-butadiene, benzene, toluene, ethylbenzene and xylene at rural and urban outdoor monitoring sites between January 2000 and July 2024, with log<sub>10</sub> y-axis transformation. Curve smoothing was achieved using LOESS. Values were obtained from uk-air.defra.gov.uk using recorded data from the Automated Hydrocarbon Network.

### 1.1.4 A brief history of indoor VOC research

While outdoor air pollution has been researched and regulated against for over seven decades, along with over 30 years of outdoor hydrocarbon VOC monitoring in the UK, deep research into indoor air pollution is still relatively in its infancy. While indoor air research dating back to the 1970s exists, this research mostly looked at indoor-outdoor relationships with pollution, and was mostly in the context of observing 'outdoor pollutants' (those more commonly associated with combustion engines and industry such as SO<sub>2</sub>, CO and NO<sub>x</sub>) and their

---

ingress to indoor environments, rather than looking at indoor sources of air pollution.<sup>[10-12]</sup>

Indoor air quality research turned in the 1980s towards health concerns arising from building occupancy, which was coined 'sick building syndrome' (SBS). SBS is a condition where the occupants of a building are found to develop both acute and chronic health conditions and disease originating from the occupancy of a building where the occupants work or live. A series of World Health Organisation (WHO) meetings in the late-1970s and early-1980s discussed the impact of several pollutants, including SO<sub>2</sub>, CO and NO<sub>x</sub> but also discussing indoor formaldehyde emissions, concentrations and exposure in the context of SBS.<sup>[13-15]</sup> Focus on SBS also highlighted the emission of VOCs indoors, opening the door for future indoor VOC research.<sup>[16,17]</sup>

## 1.2 Indoor VOC emissions

### 1.2.1 Review of indoor VOC emissions

VOCs are known to be emitted from a multitude of sources, both anthropogenic and biogenic. Anthropogenic sources of indoor VOC emissions include the use of personal care products (PCPs), general homecare products, cooking and cleaning.<sup>[18-20]</sup> Biogenic sources of VOC emissions include human breath, body odour and skin oils.<sup>[21-23]</sup> Hundreds upon thousands of individual VOCs have been detected indoors, however total VOC (TVOC) concentrations are fairly consistently dominated by a few species, namely ethanol, methanol, butane and propane.<sup>[24-26]</sup>

People spend most of their indoor time in residential and occupational settings. Other indoor environments, such as those related to transport and recreation including shops, also contribute to total time spent indoors on a more episodic basis. Residential VOC concentrations are largely dependent on individual activities and behaviours within the space, whereas occupational VOC concentrations are largely dependent on the bulk activities taking place in the space. For instance, the mass contributions to TVOC concentrations of species commonly found in emissions from paint such as benzene, toluene, xylene isomers and ethylbenzene (commonly referred to collectively as 'BTEX') would be higher in settings such as builder's merchants and paint production factories than in an office block.<sup>[27]</sup> Guidance on indoor VOC concentrations exists in the UK, but is however limited to 11 VOCs.<sup>[28]</sup> Indoor VOC exposure is multi-faceted and limiting factors, such as wearing personal protective equipment (PPE) and increasing ventilation rates and air exchange, should be factored when considering indoor VOC exposure.

A concentration comparison of some commonly found residential VOCs from different studies can be seen in table 1.3. Residential VOC concentrations vary quite widely across different studies. For BTEX concentrations in these studies, toluene was always the largest individual component. Owing to the prevailing use of sorbent tubes for VOC sampling, studies will often focus their VOC reporting to more specific classes of VOCs, hence the often-missing data in table 1.3. While the use of whole air sampling canisters would allow for a broader potential for analysis, there are logistical implications with the use of canisters, and this is discussed in more detail in section 1.2.3.

Table 1.3: Residential concentrations in  $\mu\text{g m}^{-3}$  of select VOCs in various studies. Where studies sampled in different indoor locations, only residential samples were used to display in table 1.3. BTEX concentrations displayed are the sum of individual benzene, toluene, ethylbenzene and xylene concentrations. Missing values are displayed as *ND*.

VOC	Study concentration ( $\mu\text{g m}^{-3}$ )				
	Guo <i>et al.</i> (2003) <sup>[29]</sup>	Lai <i>et al.</i> (2004) <sup>[30]</sup>	Wang <i>et al.</i> (2017) <sup>[31]</sup>	Heeley-Hill <i>et al.</i> (2021) <sup>[25]</sup>	Halios <i>et al.</i> (2022) <sup>[32]</sup>
methanol	<i>ND</i>	<i>ND</i>	<i>ND</i>	0.30	<i>ND</i>
ethanol	<i>ND</i>	<i>ND</i>	<i>ND</i>	40.10	92.00
propane	<i>ND</i>	<i>ND</i>	<i>ND</i>	44.20	<i>ND</i>
<i>i</i> -butane	<i>ND</i>	<i>ND</i>	<i>ND</i>	40.40	4.00
<i>n</i> -butane	<i>ND</i>	<i>ND</i>	<i>ND</i>	107.00	12.00
BTEX	83.00	39.20	97.23	5.50	25.87
$\alpha$ -pinene	<i>ND</i>	16.50	15.02	8.00	12.10
<i>D</i> -limonene	<i>ND</i>	19.00	109.40	3.80	13.65

Indoor VOC exposure can be mitigated against by increasing air exchange between outdoor and indoor air. Increasing intra-building ventilation rates may also aid in VOC exposure mitigation, however this isn't as effective as increasing indoor-outdoor air exchange rates. Outdoor air in almost all circumstances has lower concentrations of VOCs than indoor air, and as such increasing the exchange between outdoors and indoors provides a mechanism by which indoor VOC exposure can be lowered. There are however times where this may not be possible or feasible in residential settings, such as during smog events, or during colder months where occupant comfort would be impacted. Compounding this with a growing trend in increased air tightness requirements in new dwellings, a reliance on mechanical ventilation means is emerging in newer, more energy efficient houses.<sup>[33,34]</sup> This is despite growing data which suggests a hybrid between natural ventilation (such as outdoor air ingress through the building, opening of windows and doors, and trickle vents) and mechanical ventilation to work most efficiently at lowering indoor VOC exposure.<sup>[35-37]</sup> For owners of homes with lower effi-

Table 1.4: A summary of the different emissions from a variety of indoor activities and products

Indoor activity	terpenes	alcohols	carbonyls	aliphatic hydrocarbons	aromatic hydrocarbons
Cooking	X	X	X	-	X
Cleaning	X	X	X	-	-
Aerosol products	X	X	X	X	X
Bathing products	X	X	X	-	-
Gas fires/stoves	-	-	-	X	X
Paints	X	X	X	X	X

ciency ratings who may wish to increase overall energy efficiency, such as through increasing air tightness and updating windows and doors to models with lower outdoor air infiltration capacity, a potential for inequality exists in the retro-fitting of mechanical ventilation means to maintain comfortable living standards.<sup>[38]</sup>

### 1.2.2 Source apportionment of indoor VOCs

Source apportionment refers to the identification of likely sources of VOCs in samples, mainly through analysis of VOC emission patterns. Specific VOCs are known to be released through specific activities, however assigning the presence of a specific VOC to a specific activity or product should be cautioned against. As mentioned earlier, butane and propane are present in indoor air, typically at relatively high concentrations.<sup>[24,25]</sup> Their presence in indoor air mostly arises from their use as propellants in aerosol products but may also arise from use of bottled gas appliances, and such emissions account for a large portion of total annual VOC emissions.<sup>[39]</sup> Monoterpenes typically emit indoors from cooking, especially when using seasoning and spices, but also arise from house plants, wooden furniture and the use of fragranced products.<sup>[40,41]</sup> Lower ( $C_1$  to  $C_4$ ) alcohols also evolve indoors through cooking, but additionally through the use of products such as deodorants, body sprays and hairsprays, as well as through recreational alcohol drinking for ethanol specifically.<sup>[42,43]</sup> A summary of the different emissions from a variety of indoor activities and using products indoors is shown in table 1.4.

### 1.2.3 Sampling of indoor air

Air sampling methods can be broadly split in two categories: passive and active. Active sampling is when an external source is required to move air from the atmosphere into the sampling container/line. This is seen in analytical methods such as selected-ion flow-tube

---

mass spectrometry (SIFT-MS) and proton-transfer reaction mass spectrometry (PTR-MS), which are known as 'on-line analysis', as well as in sorbent tube sampling where the sample air is pumped through the sorbent-packed tube. Passive sampling is when air being allowed to diffuse through/into the sampler, such as in vacuum-canister sampling or the use of settle plates, with settle plates typically used in the context of sampling airborne microorganisms. Each sampling methodology has advantages and disadvantages,<sup>[44–47]</sup> and care should be given when deciding the most appropriate sampling methodology in the context of the study itself. Sorbents such as Tenax or Carbopack can form ozone artifacts at ambient ozone concentrations, and there is evidence which shows sample degradation through ozonolysis for ozone-susceptible species such as terpenes.<sup>[48,49]</sup> The use of whole air sampling canisters also presents logistical issues, such as housing equipment to evacuate and store canisters, as well as potential issues with housing the canisters during sampling. Whole air sampling canisters do, however, present a simple solution to time-integrated sampling through the addition of a flow-restrictive inlet atop the canister valve. With this in mind, no one method can be satisfactorily declared superior, and as such decisions around sampling methods should be made with the target VOCs and logistical capabilities of the study in mind.

VOC sampling through sorbent-packed tubes has been used for nearly 40 years, and remains a standard sampling technique to this day.<sup>[50–52]</sup> In brief, this typically sees a relatively wide-bore ( $\leq 1/4''$ ) tube packed with a single or mixture of sorbents, such as Tenax or Carbopack. Air is pumped through the sorbent tube at a known flow rate over a recorded time span, but air can also be allowed to passively diffuse through the tube, the latter being more appropriate for wider-bore tubes. The analytes are then thermally desorbed by flash heating the tube, with the analytes desorbing into a stream of carrier gas. At this point the desorbed analytes can either be passed directly into the GC, or transferred to a narrow focusing trap. The purpose of a focus trap is to re-concentrate the analytes into narrow bands, and then transfer into the GC, resulting in sharper chromatographic peaks and increased resolution. This sampling method relies on the selectivity of the sorbent used to sample VOCs. Wide-bore tubes can also give poor chromatographic resolution without band focusing, which is discussed later in section 2.1.2. If a general VOC analysis of air is required, whole air samples in canisters can be taken to overcome selectivity of sorbent-tube sampling.<sup>[53–55]</sup>

Whole air samples can be taken by using vacuum-intake canisters. Canisters can either be uncoated/unpassivated or passivated. A lack of a passivated coating can present issues for VOC analysis through potential iron exposure in stainless-steel canisters, which provides reactive sites for VOC adsorption and breakdown.<sup>[56,57]</sup> Passivated canisters are coated in a formulation which masks the stainless-steel, to increase sample temporal stability. Canisters

---

with coatings are often given proprietary names, such as SUMMA<sup>®</sup> and Silonite<sup>™</sup> (Entech Instruments, CA USA), which are a nickel-chromium oxide coating and a silicone-based ceramic coating respectively, and SilcoCan<sup>®</sup> (Restek, PA, USA), which is another silicone-based ceramic coating. SUMMA<sup>®</sup>-coated canisters have generally been superseded by silicone-based coatings, due to the SUMMA<sup>®</sup> coating degradation exposing active iron sites, leading to relatively quick ( $\approx 1$  week) sample degradation.<sup>[58,59]</sup> Whole air samples stored in silicone-based internally-coated canisters have been shown to remain stable for a broad panel of VOCs up to 30 days.<sup>[60]</sup>

While not necessarily a sampler, low-cost sensors have become prevalent in recent years. In low-cost applications, these sensors typically contain a metal oxide (MOx) sensor chip which, through measuring changes in resistance on the MOx surface as oxidising gases make contact with the MOx surface, gives a projected total VOC (TVOC) mixing ratio (typically in parts per billion/ppb) within the sampled air. The output of a MOx sensor can also be a VOC index, loosely an indoor air quality (IAQ) index, often measured in ethanol equivalence. The sole use of these sensors to attempt to make quantified conclusions or extrapolations on IAQ could prove problematic, as they typically have high detection limits when compared to techniques such as GC, and do not provide the speciation often required for sufficient conclusions to be drawn on VOC exposure.<sup>[61]</sup> However, such sensors do have a place in qualitative research. Treating the readings as a vectorised time-series, that is observing the direction of the readings over time, will provide researchers, and indeed homeowners, with information regarding the impact of activities and individual behaviours in the home on IAQ.<sup>[62,63]</sup> The metric TVOC is itself used to reflect the total VOC concentrations identified within a specific study, however definitions of TVOC aren't static. An over-reliance on this metric could make cross-study comparisons difficult.

Sampler location in the home will also greatly impact the VOC make-up of the sampled air. For instance, air samples originating from a bedroom are unlikely to be greatly skewed by cooking emissions. As such to gain a complete overview of indoor VOC exposure, multiple samples from separate rooms within a house could be taken over the same sampling window to better understand indoor VOC exposure variability. However, this could have logistical implications involved, especially for larger-scale studies and campaigns.

#### **1.2.4 Indoor-outdoor air relationships**

The most efficient way a homeowner can limit their exposure to indoor air pollution and increase their IAQ is by increasing air exchange with less polluted air, typically outdoor air. Outdoor air exchange however only removes the issue from indoor environments and

---

moves the issue outdoors. Studies of indoor-outdoor air relationships tend to be focused toward the ingress of more typical outdoor pollutants, for instance NO<sub>x</sub> and particulates from vehicle emissions, rather than the egress of indoor emissions. From the studies which highlight indoor emissions as a source of outdoor air pollution, emissions originating from personal care product use tends to dominate overall egressed emissions.<sup>[64,65]</sup> Indoor VOC concentrations tend to be orders of magnitude higher than outdoors, and so egress of higher concentrations of VOCs in the presence of higher concentrations of atmospheric oxidising agents identified in section 1.3 would lead to a higher potential for oxidation products and SOAs to build in outdoor air.

The National Atmospheric Emissions Inventory (NAEI) gives annual emission data for various atmospheric pollutants over a number of different sectors in the UK. All non-methane VOCs (NMVOCs) are grouped together, and can be broadly split into indoor emissions and outdoor emissions based on the source and the activity. Figure 1.5 shows the trends in emissions of NMVOCs across all sectors, as well as the trend originating solely from indoor product use, which itself was dominated by aerosol use. Despite an overall fall in total NMVOC emissions across all sources, there has been a continued increase in NMVOC emissions originating from indoor product use over time. When records began in 1970, indoor product emissions contributed roughly 3.7% to total NMVOC emissions, rising to 19.5% in 2021. There was a high of 21.6% in 2020, however this is likely due to restrictions brought in requiring UK residents to stay at home meaning more time was spent indoors than normal, resulting in higher indoor emissions. The National Emission Ceilings Regulations were enacted into UK law in 2018, and sets targets for emissions of NMVOCs and other air pollutants, and has currently hit all targets set out in the 2020-2029 ceiling targets. The UK has also ratified the 1999 Gothenberg Protocol, also known as the Multi-effect Protocol, which aims to abate acidification, eutrophication and ground-level ozone formation.

### 1.3 VOC removal pathways

There are three main oxidative pathways for tropospheric removal of VOCs: reactions with ozone (O<sub>3</sub>), reactions with hydroxyl radicals (OH), and reactions with nitrate radicals (NO<sub>3</sub>). Reactions with Cl radicals are an additional source of VOC removal, with a likely higher significance in coastal areas or following indoor activities such as using bleach. It is also possible for VOCs to adsorb onto surfaces and sink into surfaces, which can either facilitate other removal pathways or gradual re-emission into the indoor atmosphere. Perhaps most significantly, exchange with cleaner air, typically outdoor air, provides the most efficient VOC exposure mitigation pathway, and was discussed in section 1.2.4.

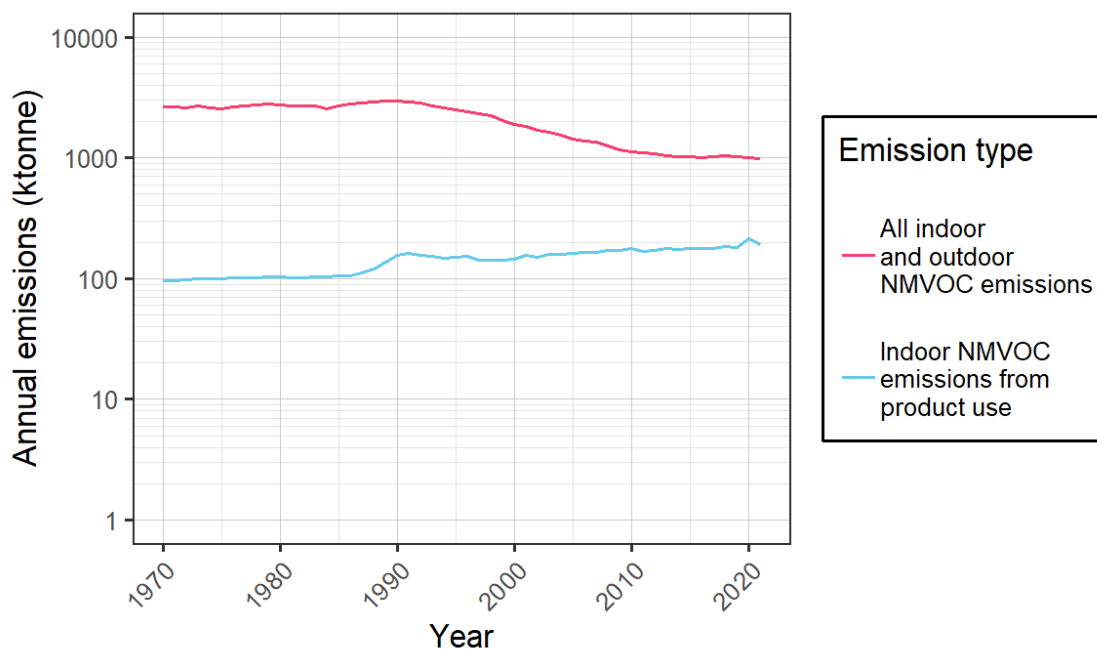


Figure 1.5: Annual emission data of NMVOCs as a total, as well as the contributions of indoor NMVOCs originating from product use with  $\log_{10}$  y-axis transformation. Data were obtained from the NAEI UK emissions data selector for NMVOCs across all sources.

### 1.3.1 Oxidation reactions and associated chemistry

#### 1.3.1.1 Reaction with OH

Taking a generic alkyl group-containing VOC as R, a hydroxyl radical-initiated VOC oxidative breakdown pathway can be summarised in reactions (R 1.1) to (R 1.6).<sup>[66,67]</sup> Here, the production of OH is initiated by photolysis of ozone to produce atomically excited oxygen,  $O(^1D)$ , which then reacts with atmospheric water vapour to produce two hydroxyl radicals.



---

The organic peroxy radical product in (R 1.4),  $\text{RO}_2$ , will undergo further reactions in air containing nitric oxide (NO) shown in (R 1.5), itself formed atmospherically from photolysis of nitrogen dioxide ( $\text{NO}_2$ ) and through various reactions originating from the Zeldovich mechanism.<sup>[68–70]</sup>



The alkoxy radical RO will then react with atmospheric oxygen to form the oxidised original VOC, RO, followed by the reformation of the hydroxyl radical from the reaction of  $\text{HO}_2$  with NO.



$\text{NO}_2$  produced in (R 1.5) and (R 1.7) is in its own right an atmospheric pollutant, here produced as a secondary emission but also originating as a primary emission from vehicle exhausts.<sup>[71]</sup>  $\text{NO}_2$  plays an important role in the production of tropospheric ozone, shown in (R 1.8) and (R 1.9). Aside from production through atmospheric oxidative reactions, ozone is present in the troposphere, the lowest atmospheric layer, in small concentrations due to stratospheric ozone infiltration, as well as the use of ozone as an air and surface disinfectant.<sup>[72,73]</sup>



Shown in (R 1.7), hydroxyl radicals are reproduced through atmospheric oxidation pathways, further aiding in the removal of VOCs in the atmosphere. Hydroxyl radicals are the most reactive of the three main tropospheric oxidisers, and react with most known trace gases.<sup>[74]</sup>

An additional source of hydroxyl radicals in indoor environments is the aerosol-surface photolysis of nitrous acid (HONO) into nitric oxide radicals and hydroxyl radicals, shown in (R 1.10).<sup>[75]</sup>

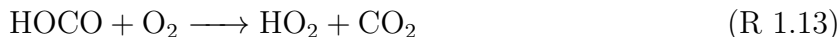


### 1.3.1.2 Reaction with $\text{O}_3$

Tropospheric ozone can be formed through the reaction of molecular oxygen with monoatomic oxygen radicals, as in (R 1.9), as well as through reactions between carbon monoxide and hydroxyl radicals to make the energised hydrocarboxyl radical (R 1.11), which once stabilised

---

following collisions with M (R 1.12) will react with molecular oxygen (R 1.13):



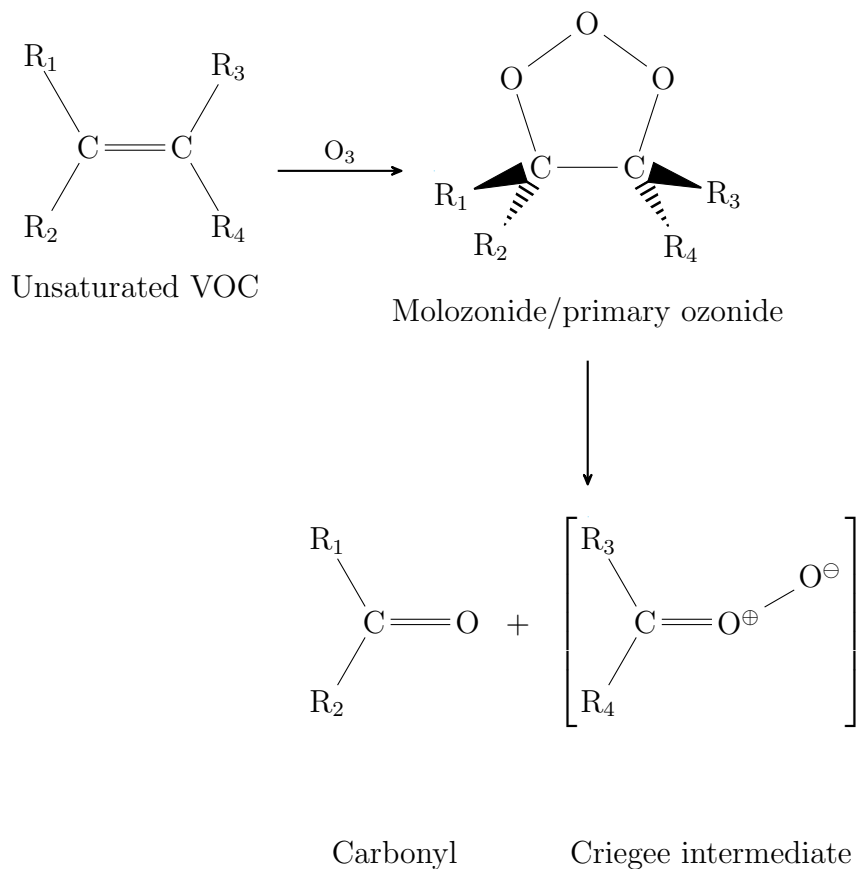
The resulting  $\text{HO}_2$  from (R 1.13) will then react through the steps shown in (R 1.7), (R 1.8) and (R 1.9) to form tropospheric ozone. However, ozone can also be transported from the stratosphere through stratosphere-troposphere exchange. This can occur through means such as strong upwinds, as well as through tropopause folds, a mechanism by which the tropopause (the boundary between the troposphere and the stratosphere) lowers in altitude due to events such as jet stream undulations and tropical cyclones. Stratospheric ozone also enters the troposphere through Brewer-Dobson circulation, which is the circulation of air through the tropopause into the stratosphere at the equator, and then downward through the tropopause back into the troposphere at the polar regions.

VOCs containing double bonds will react with ozone itself according to scheme 1.1. This ozonolysis reaction sees the formation of a carbonyl product, as well as the formation of a product called a Criegee intermediate. The Criegee intermediate (CI), a carbonyl oxide, exists in resonance structures as either zwitterions or a biradical species, as shown in scheme 1.2. It is these resonance structures which give rise to a multitude of potential products following double-bond ozonolysis. CIs can react with the product carbonyl in scheme 1.1 to form ozonides, they can unimolecularly decompose to form hydroxyl radicals, or can bimolecularly react to form hydroperoxides, known aerosol precursors, among many other degradation pathways.<sup>[76]</sup> The presence of aerosol precursors in the degradation pathways of CIs is of importance due to the known health effects of exposure to secondary organic aerosols (SOAs), in both chronic and acute cases.<sup>[77–79]</sup>

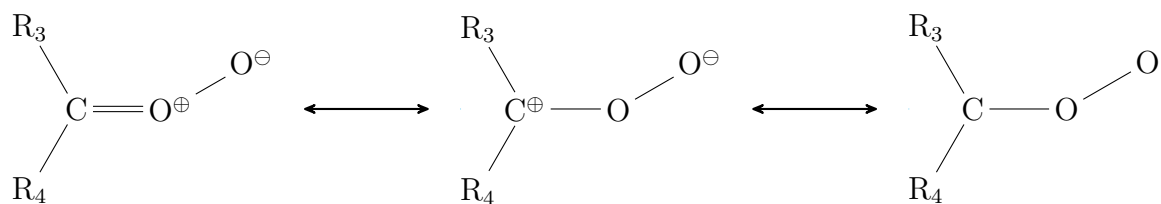
### 1.3.1.3 Reaction with $\text{NO}_3$

$\text{NO}_3$ , nitrate radicals, are another major source of atmospheric VOC-oxidant reactions. Nitrate radicals are formed through the reaction between  $\text{NO}_2$  and  $\text{O}_3$ :



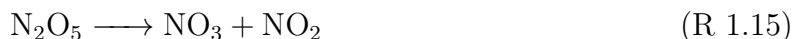


Scheme 1.1: Formation of Criegee intermediate through ozonolysis of a generic alkene.

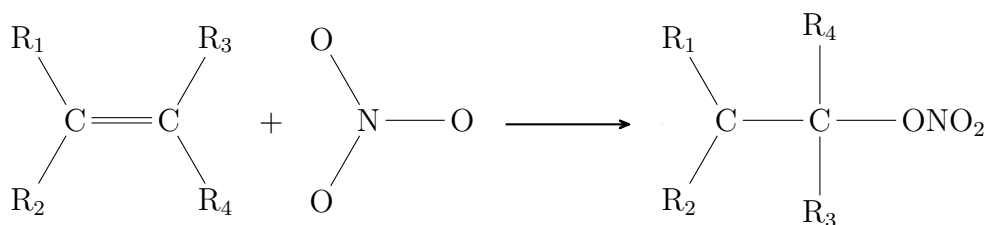


Scheme 1.2: Resonance structures of the Criegee intermediate between zwitterions and a biradical.

Nitrate radicals can also be formed through the decomposition of dinitrogen pentoxide,  $N_2O_5$ :



$NO_3$  reacts with VOCs, typically through  $NO_3$  addition across double-bonds in unsaturated VOCs but also through hydrogen abstraction (reacting favourably with surface-bound alcohols).<sup>[80,81]</sup> A scheme for the addition of  $NO_3$  on a generic unsaturated VOC (as in scheme 1.1) is given in scheme 1.3. The reactive peroxyxynitrite intermediate is then heavily implied in the later creation of secondary pollutants, including aerosols and larger particulates, aldehydes such as formaldehyde and other carbonyl species.<sup>[82-84]</sup>



Unsaturated VOC      Nitrate radical      Peroxyxynitrite intermediate

Scheme 1.3: Formation of a peroxyxynitrite intermediate following nitrate radical addition over a double-bond.

#### 1.3.1.4 Reaction with Cl

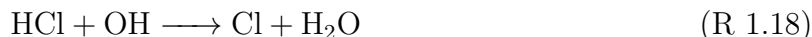
VOC removal through reactions with Cl radicals are not as significant as reactions with OH,  $O_3$  or  $NO_3$ , however they represent a source of VOC removal with the potential for a higher significance in coastal areas, as well as in indoor environments with higher concentrations of chlorinated-species.

Cl radicals can be formed through several different reactions, some of which are shown in reactions (R 1.16) and (R 1.17):



---

Cl radicals can additionally be formed through the reaction of HCl and OH, shown in reaction (R 1.18):



HCl itself can be formed prevalently in coastal areas through the reaction of suspended NaCl, itself a majority constituent of sea salt aerosols, and HNO<sub>3</sub>:



VOC - Cl reactions happen mainly through hydrogen abstraction (reaction (R 1.20)), but also through the addition of the chlorine radical over a double bond (reaction (R 1.21)).



### 1.3.1.5 Day-night cycles

Different atmospheric reactions dominate at different parts of the day. During the day time (*i.e.*, when there is sunlight), atmospheric VOC removal is dominated by reactions with hydroxyl radicals, while at night atmospheric VOC removal is dominated through reaction with nitrate radicals. Considering the four sources of VOC oxidation in the atmosphere discussed previously (OH, O<sub>3</sub>, NO<sub>3</sub> and Cl), hydroxyl radicals are formed through the quenching of excited oxygen, itself formed through the photodissociation of ozone, as in (R 1.1) and (R 1.2). During the daytime, nitrate radicals formed through reaction (R 1.14) quickly decompose through photolysis as in reaction (R 1.22) and (R 1.23):



NO<sub>3</sub> can also react with NO:



However, during night time hours where photodissociation cannot occur and reaction with NO happens less due to a lower night time concentration of NO<sub>x</sub>, nitrate radical concentrations

---

increase. In a general sense, VOC removal is dominated during the day through hydroxyl radical chemistry, and at night by nitrate radical chemistry. VOC reactions with ozone also occur throughout the day-night cycle.

### 1.3.1.6 Oxidant and precursor reservoirs

While the main oxidant formation pathways have been shown earlier, there are additional sources of the four main atmospheric oxidants listed. These are known as reservoirs, and they are typically a stable form of the constituent oxidants or oxidant precursors. One such reservoir is nitrous acid, HONO. HONO can either be formed as in the reverse reaction between NO and OH (shown as the dissociation of HONO in (R 1.10)), or through the reaction between NO<sub>2</sub> and wet surfaces, especially at night time:<sup>[85]</sup>



During the day, HONO quickly photolyses as in (R 1.10), however over night without sunlight to dissociate it, HONO can build in concentration. When sunlight becomes present again, accrued HONO will dissociate according to (R 1.10), becoming an important source of hydroxyl radicals during the first part of the morning cycle.

Another oxidant reservoir is peroxyacetyl nitrate (PAN). PAN is a greenhouse gas and a major component of smog, and so is a major pollutant in its own right. PAN also acts as a reservoir for ozone, as well as daytime nitrate radicals. There are no known primary emissions of PAN into the atmosphere, and so is a pure secondary pollutant. Following formation of the organic peroxy radical (RO<sub>2</sub>) such as in (R 1.4), another potential product of (R 1.5) is PAN:



PAN itself is thermally unstable, with a roughly 2 hr typical lifetime at 25 °C but up to a 1 month lifetime at 10 °C.<sup>[86]</sup> The decomposition route of PAN produces NO<sub>2</sub> as in (R 1.27):



The produced RO from (R 1.27) can then further produce more NO<sub>2</sub> and hydroxyl radicals through reactions (R 1.6) and (R 1.7). NO<sub>2</sub> can then further form ozone through reactions (R 1.8) and (R 1.9). PAN acts as a long-term reservoir which transports NO<sub>2</sub> and O<sub>3</sub>, and in smaller proportions OH, from cooler regions and therefore is an important source of

---

tropospheric ozone formation.

Another important reservoir is dinitrogen pentoxide,  $\text{N}_2\text{O}_5$ . During night hours, nitrate radicals can react with  $\text{NO}_2$  to form  $\text{N}_2\text{O}_5$ :



$\text{N}_2\text{O}_5$  is unstable photochemically, but in the absence of sunlight will build in concentration, much like HONO. During the first few hours of sunshine, accrued  $\text{N}_2\text{O}_5$  will then photodissociate in the reverse of reaction (R 1.28):

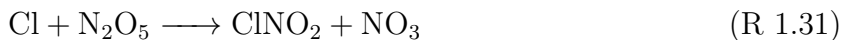


Any  $\text{NO}_3$  formed through the photodissociation of  $\text{N}_2\text{O}_5$  will then itself photodissociate according to reactions (R 1.22) and (R 1.23). Here,  $\text{N}_2\text{O}_5$  is a day-time source of  $\text{NO}_x$ . Another important consideration of  $\text{N}_2\text{O}_5$  is the formation of nitric acid through aerosol-surface quenching:



The nitric acid formed through this reaction therefore can become a component of acid rain, meaning  $\text{N}_2\text{O}_5$  is additionally a precursor to acid rain.<sup>[87,88]</sup>

Concentrations of  $\text{ClNO}_2$  increase in the absence of sunlight through the reaction shown in (R 1.31). In the first part of the morning cycle,  $\text{ClNO}_2$  quickly photolyses according to reaction (R 1.17), resulting in a sudden increase in Cl radical concentration in the early morning.



This reaction is likely to be of higher significance in coastal regions, where a higher concentration of atmospheric  $\text{Cl}^-$  ions occur due to a higher prevalence of sea salt aerosols within the troposphere.<sup>[89]</sup> This may in turn result in a higher concentration of nitrate radicals in the same coastal areas due to their formation in reaction (R 1.31).

### 1.3.2 Surface interactions with VOCs

VOCs also leave the atmosphere through sinking mechanisms, known as the 'sink effect'. Different materials in indoor environments can act as sinks for VOCs, with the construction and formulation of the building materials having implications towards the relative sink

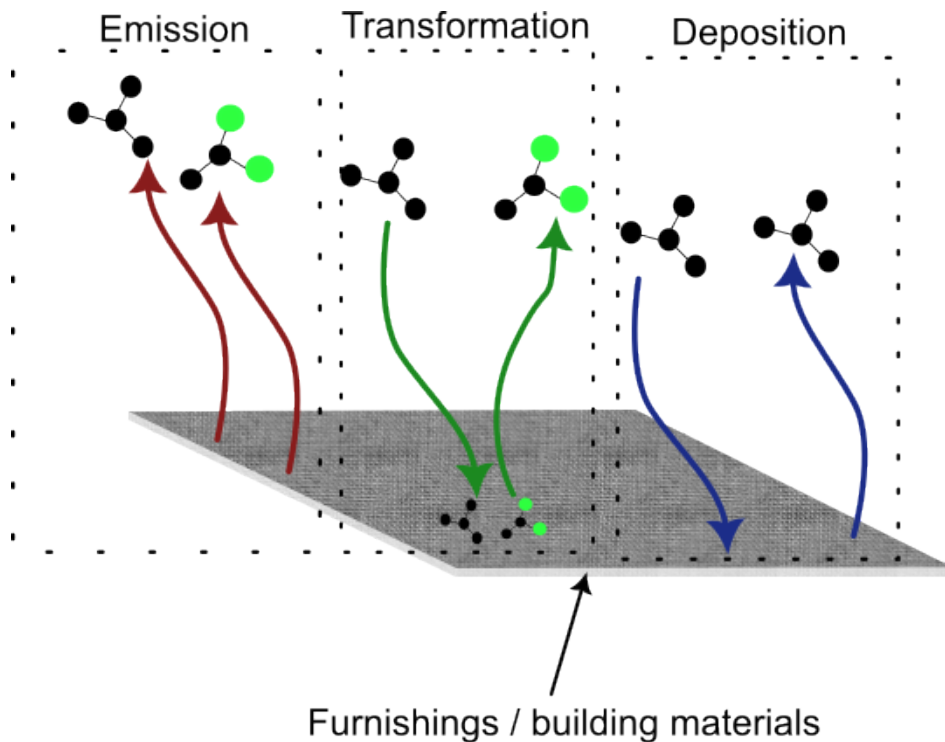


Figure 1.6: The different emission and removal pathways for atmospheric VOCs through interactions with furnishings and building materials.

potential for different VOCs. It is inherently difficult to measure deposition of VOCs onto and into surfaces in real, residential homes, however there are several models which exist through studies under laboratory conditions which have been applied to field tests, with generally good agreement between model predictions and measured values.<sup>[90,91]</sup> A diagram of the different VOC removal and emission pathways through furnishing and building materials is shown in figure 1.6.

Sinking and transformation, as in figure 1.6 can occur through either adsorption or absorption. Surface adsorption through the sinking method is usually explained through the Langmuir adsorption model, which assumes that adsorption occurs in a single layer, is uniform across the material surface, adsorption of the adsorbate is inert (not transformational), and adsorption is reversible. A transformational adsorption model can be either decompositional through similar kinetics to Michaelis-Menten kinetics, or bimolecular through either the Langmuir-Hinshelwood mechanism (through the reaction of two adsorbed molecules on neighbouring sites) or through the Eley-Rideal mechanism (through the reaction of one adsorbed molecule and another molecule still airborne). Surface absorption occurs when the molecule first adsorbs onto the material surface, and then penetrates the bulk material. Again, there are several mechanisms for this, such as Fickian diffusion, partitioning through

---

Henry's law and capillary action (in materials such as wood and concrete where capillary pores exist). While not the aim of the works within this thesis, it is clear that VOC removal, transformation and sinking pathways through material interactions are very complex.

### 1.3.3 Final remarks on VOC reaction and removal pathways

Great attention is normally given to outdoor VOC oxidation pathways, the impact of night and day on reaction rates, and further reactions of products with other pollutants. However these reactions do occur indoors,<sup>[92-94]</sup> and while concentrations of O<sub>3</sub>, OH, NO<sub>3</sub> and Cl may typically be lower indoors than outdoors, low air exchanges and increased occupancy must be borne in mind. Humans can spend up to 90% of their time indoors,<sup>[95]</sup> and there are members of society with no choice but to stay indoors. Additional attention should be paid to outdoor air pollution inequalities, generally found to be worse in areas of higher deprivation.<sup>[96]</sup> Air exchange between indoors and outdoors can only aid in mitigating potential harmful VOC and VOC-oxidation product exposure for as long as the outdoor air is cleaner than indoors.

## 1.4 Legislative impacts on indoor VOC exposure

With an increasing population, the need for new homes is clear.<sup>[97]</sup> Various pieces of legislation exist to regulate the building of new homes to meet certain standards, and in the context of indoor air these are given in The Building Regulations 2010 (as amended), and detailed in approved documents F (ventilation), L (energy efficiency, however only air permeability will be considered), and O (overheating). Requirements of each section will be listed first, with implications being discussed in section 1.4.4.

### 1.4.1 Ventilation requirements

Ventilation means must be present in kitchens, bathrooms and utility rooms in new UK homes. Ventilation must be between inside the room and outdoors, but may be either natural (through air bricks, vents or windows) or mechanical, such as through exhaust hoods or extractor fans. In new UK homes, supply air may only be provided by background ventilators, such as trickle vents, or through a continuous supply fan. Ventilation rates for the entire property is calculated by the number of bedrooms, starting at 19 L s<sup>-1</sup> for a 1-bedroom property increasing in increments of 6 L s<sup>-1</sup> for each additional bedroom. Each room must have purge ventilation exhausting to the outdoors, either manual such as a window or a door or through mechanical ventilation means.

---

The above values from the 2021 amendments for whole-dwelling ventilation rates are increased from 2010, which gave a ventilation rate of  $13 \text{ L s}^{-1}$  for a 1-bedroom property, increasing for each additional bedroom in increments of  $4 \text{ L s}^{-1}$ . In all versions of Approved Document F, a minimum ventilation rate of  $0.3 \text{ L s}^{-1} \text{ m}^{-2}$  of floor area is given. An increase in ventilation requirements has resulted in an increase in the prevalence of trickle vents and mechanical ventilation in newer houses to satisfy ventilation requirements.

### 1.4.2 Air permeability

Air permeability refers to the measure of the movement of air through a building, both outdoor air bleeding indoors and indoor air leaking outdoors, and is measured as a volume moving per unit of time per area of a building envelope. Air permeability requirements for new buildings in England and Wales were first introduced in 2002. Air permeability is usually measured using a pressure differential of 50 Pa, usually facilitated through the use of a 'blower door', which is an airtight fan unit fastened in the front door of a property. Air permeability requirements for new dwellings in England and Wales were  $2.78 \text{ L s}^{-1} \text{ m}^{-2}$  in 2010, and these were lowered to  $2.22 \text{ L s}^{-1} \text{ m}^{-2}$  in 2021, with a notional air permeability of  $1.39 \text{ L s}^{-1} \text{ m}^{-2}$  across all UK nations. Air permeability for new homes must not exceed  $2.78 \text{ L s}^{-1} \text{ m}^{-2}$  in Northern Ireland, and  $1.94 \text{ L s}^{-1} \text{ m}^{-2}$  in Scotland.

### 1.4.3 Overheating

Building overheating occurs when a building becomes too hot, with internal temperatures becoming excessively elevated. This can occur either through excessive heat retention or through solar heating. There are requirements on the extent to which a property facade or roof can be glazed with glass. Glazing has a known effect on building overheating, with large areas of glazing contributing to overheating not just in warmer months but also due to solar gain of infrared radiation, meaning overheating could occur during colder months.<sup>[98–100]</sup>

As well as causing lowered productivity and potential health effects,<sup>[101,102]</sup> overheating can also cause an increased rate of building material off-gassing (or outgassing), where sunk/captive VOCs are emitted from the material.<sup>[103,104]</sup> Overheating in the absence of adequate ventilation can therefore act as another mechanism by which VOC exposure can be increased.

### 1.4.4 Remarks on legislative impacts on IAQ

While overheating may not on the surface appear to cause an increase in indoor VOC exposure, the increase in temperature inside overheated homes/rooms causes VOCs which have

---

sunk into furnishings and surfaces to re-emit into the atmosphere.<sup>[105,106]</sup> Building materials are known to emit VOCs. Commonly emitted VOCs from building materials in new homes of note are the known carcinogen formaldehyde and the suspected carcinogen acetaldehyde.<sup>[107–109]</sup> Thus a combination of overheating and poor control of ventilation could result in unintentionally higher levels of exposure to indoor VOCs.

Combining the potential long-term (>1 year) emission of VOCs from new building materials along with decreased air permeability and increasing reliance on mechanical ventilation in new builds, new buildings may pose a risk of overexposure to potentially harmful VOCs. It has been shown that effective use of mechanical ventilation is only possible when the homeowner has a good understanding of the appropriate use of their mechanical ventilation system.<sup>[110,111]</sup> Making guidance easily available to homeowners on the proper use of both mechanical and manual ventilation such as trickle vents could aid in limiting over-exposure to VOCs in homes.

## 1.5 Thesis structure

This thesis will examine indoor VOC exposure, both in ambient settings and through VOC perturbation through known product use. This thesis provides insight into IAQ in homes across England and the multitude of factors which affect it, while also highlighting the more subtle VOC perturbing effects of product use which is otherwise masked through wide variability in real home VOC concentrations. Modelling of emission rates is then mapped across a range of plausible scenarios to offer insight into the possible room concentrations of VOCs associated with product use. Finally, analysis through the inference of air change rates (ACRs) and conversion of VOC concentrations to time-averaged emission rates reveals otherwise-hidden patterns in spatial and temporal VOC emissions.

Chapter 2 gives an overview of the instrumental and statistical methodology used throughout chapters 3, 4 and 5. Operating principles of the instrument are explored, along with methods for data processing and analysis. The work presented within chapter 2 was complementary to the publications in chapters 3, 4 and 5, however was not included within the publications for the sake of brevity.

Chapters 3, 4 and 5 of this thesis originated as published peer-reviewed articles, details of which are found in the thesis declaration. While these chapters remain faithful to the original articles as published, minor changes have been made to the themes of figures, referencing styles, headings and captions for consistency and clarity with the layout of this thesis, and additionally contain supplementary information and figures not present in the published

---

main article. Each chapter contains its own bibliography, renumbered at the beginning of each chapter.

Chapter 3 presents a study assessing the impact of plug-in fragrance diffusers on indoor VOC concentrations. In this study, 60 homes were sampled over a course of four-to-five consecutive weekend sampling periods. In the first week, a baseline sample was taken. Immediately prior to week two sampling commencement, a plug-in fragrance diffuser of known formulation was installed in the room being sampled, and left to run over weeks two and three of sampling. Immediately following the completion of the week three sample, the diffuser was removed. Week four (and week five for 30 of the houses) samples were a post-plug-in sample, to observe any decaying effects of the diffuser. This work aimed to quantify the effect of plug-in fragrance diffusers in real homes, as well as quantify variations of emissions across the cohort.

Chapter 4 is somewhat a continuation of the study in Chapter 3, inasmuch as it uses the same fragrance diffuser and the same fragrance formulation. In this study, the diffuser was simply placed into test booths (chambers), followed by the same VOC sampling and quantification methodology as in chapter 3. Booths used were either 30 m<sup>3</sup>, a volume roughly equivalent to an average UK living room, or 10 m<sup>3</sup>, a volume roughly equivalent to a small bathroom or ensuite toilet. In addition, human olfactory testing was completed in the 10 m<sup>3</sup> booths to assess human strength perception of the diffused fragrance. The purpose of this work was to assess both the stacking dynamics of simultaneous multiple diffuser use, and whether human perception of fragrance strength could play a part in self-limitation of VOC exposure.

Chapter 5 presents work completed as part of a wider project, INGENIOUS (Understanding the sources, transformations and fates of indoor air pollutants). In this work, over 120 homes in Bradford, UK had whole air samples collected between March 2023 and April 2024. Whole air samples were analysed through both GC-MS for VOC quantification, and greenhouse gas analysis for carbon dioxide, methane and water vapour quantification. Analysis was completed on both raw concentration data, as well as inferred emission rates through ACR calculation. Additional analyses on geographical disparities between rural and urban indoor air quality was also completed. This work was completed as part of a larger project assessing the emission and reactions of indoor air pollutants, and included additional particulate matter (PM) sampling, sampling through the use of low-cost sensors, as well as laboratory-based experiments on the emissions of cooking and use of cleaning products.

Chapter 6 presents a detailed overview of a developed method for sampling aerosol consumer products, including the construction of an emission chamber sampling line and the development of an analytical method using GC-MS to analyse VOC emissions from these

---

products.

Finally, Chapter 7 summarises the work presented in this thesis and draws overall conclusions based on the findings from each chapter. It also discusses the limitations of the studies conducted, explores potential future research directions, and considers the broader impacts on policy, future studies, and method development.

---

## 1.6 References

- [1] Marzio Invernizzi et al. “Lights and shadows of the voc emission quantification”. In: *Chemical Engineering Transactions* 85 (2021), pp. 109–114. DOI: [10.3303/CET2185019](https://doi.org/10.3303/CET2185019).
- [2] Flora Gouzerh et al. “Odors and cancer: Current status and future directions”. In: *Biochimica et Biophysica Acta (BBA) - Reviews on Cancer* 1877.1 (2022), p. 188644. DOI: [10.1016/J.BBCAN.2021.188644](https://doi.org/10.1016/J.BBCAN.2021.188644).
- [3] Roger S Hubbard. “Determination of acetone in expired air”. In: *J. Biol. Chem* 43 (1920), pp. 57–65.
- [4] Keith D Bartle and Peter Myers. “History of gas chromatography”. In: *TrAC Trends in Analytical Chemistry* 21.9 (2002), pp. 547–557. DOI: [https://doi.org/10.1016/S0165-9936\(02\)00806-3](https://doi.org/10.1016/S0165-9936(02)00806-3). URL: <https://www.sciencedirect.com/science/article/pii/S0165993602008063>.
- [5] N Carslaw and D Shaw. “Secondary product creation potential (SPCP): A metric for assessing the potential impact of indoor air pollution on human health”. In: *Environmental Science: Processes and Impacts* 21.8 (2019), pp. 1313–1322. DOI: [10.1039/c9em00140a](https://doi.org/10.1039/c9em00140a).
- [6] Peder Wolkoff. “Indoor air chemistry: Terpene reaction products and airway effects”. In: *International Journal of Hygiene and Environmental Health* 225 (2020), p. 113439. DOI: [10.1016/J.IJHEH.2019.113439](https://doi.org/10.1016/J.IJHEH.2019.113439).
- [7] J H Wyatt. “The Clean Air Act, 1956—Twelve Months’ Experience”. In: *Journal (Royal Society of Health)* 78.2 (1958), pp. 131–141.
- [8] J W S Longhurst et al. “Progress with air quality management in the 60 years since the UK clean air act, 1956. Lessons, failures, challenges and opportunities”. In: *International journal of sustainable development and planning* 11.4 (2016), pp. 491–499.
- [9] Wang Hong-li et al. “Volatile organic compounds (VOCs) source profiles of on-road vehicle emissions in China”. In: *Science of The Total Environment* 607-608 (2017), pp. 253–261. DOI: <https://doi.org/10.1016/j.scitotenv.2017.07.001>. URL: <https://www.sciencedirect.com/science/article/pii/S0048969717317047>.
- [10] William L Clink John E. Yocom and William A Cote. “Air Quality Relationships”. In: *Journal of the Air Pollution Control Association* 21.5 (1971), pp. 251–259. DOI: [10.1080/00022470.1971.10469525](https://doi.org/10.1080/00022470.1971.10469525). URL: <https://doi.org/10.1080/00022470.1971.10469525>.
- [11] Fredrick H Shair and Kenneth L Heitner. “Theoretical model for relating indoor pollutant concentrations to those outside”. In: *Environmental Science & Technology* 8.5 (May 1974), pp. 444–451. ISSN: 0013-936X. DOI: [10.1021/es60090a006](https://doi.org/10.1021/es60090a006). URL: <https://doi.org/10.1021/es60090a006>.

- 
- [12] William A Cote Willard A. Wade Iii and John E Yocom. “A Study of Indoor Air Quality”. In: *Journal of the Air Pollution Control Association* 25.9 (1975), pp. 933–939. DOI: [10.1080/00022470.1975.10468114](https://doi.org/10.1080/00022470.1975.10468114). URL: <https://doi.org/10.1080/00022470.1975.10468114>.
- [13] World Health Organization. *Indoor Air Pollutants: exposure and health effects*. Tech. rep. Copenhagen: World Health Organisation, June 1982. URL: <https://www.aivc.org/resource/indoor-air-pollutants-exposure-and-health-effects>.
- [14] V V Akimenko et al. “Report of a WHO subgroup on the “sick building” syndrome”. In: *Indoor Air* 6.D13 (1986), pp. 87–97.
- [15] World Health Organization Regional Office for Europe. *Indoor Air Quality Research: Report on a WHO Meeting, Stockholm, 27-31 August 1984*. World Health Organization, Regional Office for Europe, 1986. ISBN: 9789289012690. URL: <https://books.google.co.uk/books?id=je06AAAAIAAJ>.
- [16] Dan Norbäck, Ingegerd Michel, and John Widström. “Indoor air quality and personal factors related to the sick building syndrome”. In: *Scandinavian Journal of Work, Environment & Health* 16.2 (1990), pp. 121–128. URL: <http://www.jstor.org/stable/40965772>.
- [17] D Norbäck, M Torgén, and C Edling. “Volatile organic compounds, respirable dust, and personal factors related to prevalence and incidence of sick building syndrome in primary schools”. In: *British Journal of Industrial Medicine* 47.11 (1990), p. 733. DOI: [10.1136/oem.47.11.733](https://doi.org/10.1136/oem.47.11.733). URL: <http://oem.bmj.com/content/47/11/733.abstract>.
- [18] Shuiyuan Cheng et al. “Characterization of volatile organic compounds from different cooking emissions”. In: *Atmospheric Environment* 145 (2016), pp. 299–307. DOI: [10.1016/J.ATMOENV.2016.09.037](https://doi.org/10.1016/J.ATMOENV.2016.09.037).
- [19] A W Nørgaard et al. “Ozone-initiated VOC and particle emissions from a cleaning agent and an air freshener: Risk assessment of acute airway effects”. In: *Environment International* 68 (2014), pp. 209–218. DOI: [10.1016/J.ENVINT.2014.03.029](https://doi.org/10.1016/J.ENVINT.2014.03.029).
- [20] Amber M Yeoman et al. “Simplified speciation and atmospheric volatile organic compound emission rates from non-aerosol personal care products”. In: *Indoor Air* 30.3 (2020), pp. 459–472. DOI: <https://doi.org/10.1111/ina.12652>. URL: <https://onlinelibrary.wiley.com/doi/abs/10.1111/ina.12652>.
- [21] Dustin J Penn et al. “Individual and gender fingerprints in human body odour”. In: *Journal of The Royal Society Interface* 4.13 (2007), pp. 331–340. DOI: [10.1098/rsif.2006.0182](https://doi.org/10.1098/rsif.2006.0182). URL: <https://royalsocietypublishing.org/doi/abs/10.1098/rsif.2006.0182>.

- 
- [22] Jill D Fenske and Suzanne E Paulson. “Human Breath Emissions of VOCs”. In: *Journal of the Air & Waste Management Association* 49.5 (1999), pp. 594–598. DOI: [10.1080/10473289.1999.10463831](https://doi.org/10.1080/10473289.1999.10463831). URL: <https://doi.org/10.1080/10473289.1999.10463831>.
- [23] Ziwei Zou, Junzhou He, and Xudong Yang. “An experimental method for measuring VOC emissions from individual human whole-body skin under controlled conditions”. In: *Building and Environment* 181 (2020), p. 107137. DOI: <https://doi.org/10.1016/j.buildenv.2020.107137>. URL: <https://www.sciencedirect.com/science/article/pii/S0360132320305114>.
- [24] Thomas Warburton et al. “The impact of plug-in fragrance diffusers on residential indoor VOC concentrations”. In: *Environ. Sci.: Processes Impacts* 25.4 (2023), pp. 805–817. DOI: [10.1039/D2EM00444E](https://dx.doi.org/10.1039/D2EM00444E). URL: <http://dx.doi.org/10.1039/D2EM00444E>.
- [25] A C Heeley-Hill et al. “Frequency of use of household products containing VOCs and indoor atmospheric concentrations in homes”. In: *Environmental Science: Processes and Impacts* 23.5 (2021), pp. 699–713. DOI: [10.1039/d0em00504e](https://doi.org/10.1039/d0em00504e).
- [26] Nigel B Goodman et al. “Indoor volatile organic compounds at an Australian university”. In: *Building and Environment* 135 (2018), pp. 344–351. DOI: <https://doi.org/10.1016/j.buildenv.2018.02.035>. URL: <https://www.sciencedirect.com/science/article/pii/S0360132318301070>.
- [27] Safiye Ghobakhloo et al. “Exposure to volatile organic compounds in paint production plants: levels and potential human health risks”. In: *Toxics* 11.2 (2023), p. 111.
- [28] C Shrubsole et al. “IAQ guidelines for selected volatile organic compounds (VOCs) in the UK”. In: *Building and Environment* 165 (2019), p. 106382. DOI: <https://doi.org/10.1016/j.buildenv.2019.106382>. URL: <https://www.sciencedirect.com/science/article/pii/S036013231930592X>.
- [29] H Guo et al. “Source characterization of BTEX in indoor microenvironments in Hong Kong”. In: *Atmospheric Environment* 37.1 (2003), pp. 73–82. DOI: [https://doi.org/10.1016/S1352-2310\(02\)00724-0](https://doi.org/10.1016/S1352-2310(02)00724-0). URL: <https://www.sciencedirect.com/science/article/pii/S1352231002007240>.
- [30] H K Lai et al. “Personal exposures and microenvironment concentrations of PM<sub>2.5</sub>, VOC, NO<sub>2</sub> and CO in Oxford, UK”. In: *Atmospheric Environment* 38.37 (2004), pp. 6399–6410. DOI: <https://doi.org/10.1016/j.atmosenv.2004.07.013>. URL: <https://www.sciencedirect.com/science/article/pii/S1352231004006995>.
- [31] Chunting Michelle Wang et al. “Unexpectedly high concentrations of monoterpenes in a study of UK homes”. In: *Environmental Science: Processes & Impacts* 19.4 (2017),

- 
- pp. 528–537. DOI: [10.1039/c6em00569a](https://doi.org/10.1039/c6em00569a). URL: <https://dx.doi.org/10.1039/c6em00569a>.
- [32] Christos H Halios et al. “Chemicals in European residences – Part I: A review of emissions, concentrations and health effects of volatile organic compounds (VOCs)”. In: *Science of The Total Environment* 839 (2022), p. 156201. DOI: <https://doi.org/10.1016/j.scitotenv.2022.156201>. URL: <https://www.sciencedirect.com/science/article/pii/S0048969722032983>.
- [33] J Roberson. “Effect of building airtightness and fan size on the performance of mechanical ventilation systems in new US houses: a critique of ASHRAE Standard 62.2-2003”. In: (2004).
- [34] H el ene Niculita-Hirzel. “Latest Trends in Pollutant Accumulations at Threatening Levels in Energy-Efficient Residential Buildings with and without Mechanical Ventilation: A Review”. In: *International Journal of Environmental Research and Public Health* 19.6 (2022). DOI: [10.3390/ijerph19063538](https://doi.org/10.3390/ijerph19063538). URL: <https://www.mdpi.com/1660-4601/19/6/3538>.
- [35] Tom Ben-David and Michael S Waring. “Impact of natural versus mechanical ventilation on simulated indoor air quality and energy consumption in offices in fourteen U.S. cities”. In: *Building and Environment* 104 (2016), pp. 320–336. DOI: <https://doi.org/10.1016/j.buildenv.2016.05.007>. URL: <https://www.sciencedirect.com/science/article/pii/S0360132316301597>.
- [36] James F Montgomery, Stefan Storey, and Karen Bartlett. “Comparison of the indoor air quality in an office operating with natural or mechanical ventilation using short-term intensive pollutant monitoring”. In: *Indoor and Built Environment* 24.6 (2015), pp. 777–787. DOI: [10.1177/1420326X14530999](https://doi.org/10.1177/1420326X14530999). URL: <https://doi.org/10.1177/1420326X14530999>.
- [37] Jessica Berneiser et al. “Feeling the breeze? Ventilation practices and occupant requirements for mechanical ventilation in residential buildings”. In: *Energy and Buildings* 302 (2024), p. 113702. DOI: <https://doi.org/10.1016/j.enbuild.2023.113702>. URL: <https://www.sciencedirect.com/science/article/pii/S0378778823009325>.
- [38] Roderick J Lawrence. “Inequalities in urban areas: innovative approaches to complex issues”. In: *Scandinavian Journal of Public Health* 30.59 (2002), pp. 34–40. DOI: [10.1177/14034948020300030601](https://doi.org/10.1177/14034948020300030601). URL: <https://doi.org/10.1177/14034948020300030601>.
- [39] Amber M Yeoman and Alastair C Lewis. “Global emissions of VOCs from compressed aerosol products”. In: *Elementa: Science of the Anthropocene* 9.1 (2021), p. 177. DOI: [10.1525/elementa.2020.20.00177](https://doi.org/10.1525/elementa.2020.20.00177). URL: <https://doi.org/10.1525/elementa.2020.20.00177>.

- 
- [40] Felix Klein et al. “Quantification of the impact of cooking processes on indoor concentrations of volatile organic species and primary and secondary organic aerosols”. In: *Indoor Air* 29.6 (2019), pp. 926–942. DOI: <https://doi.org/10.1111/ina.12597>. URL: <https://onlinelibrary.wiley.com/doi/abs/10.1111/ina.12597>.
- [41] Christelle Marlet and Georges Lognay. “Monoterpenes: sources and implications in the indoor air quality”. In: *Biotechnology, Agronomy and Society and Environment* 15.4 (2011), pp. 611–622.
- [42] Otmar Geiss, Carmen Del Cacho, and Josefa Barrero-Moreno. “Catalytic Air Freshening Diffusers Based on Isopropyl Alcohol - A Major Source of Acetone Indoors”. In: *Aerosol and Air Quality Research* 14.1 (2014), pp. 177–184. DOI: [10.4209/aaqr.2013.02.0051](https://doi.org/10.4209/aaqr.2013.02.0051). URL: <http://dx.doi.org/10.4209/aaqr.2013.02.0051>.
- [43] Andreas T Güntner, Ines C Weber, and Sotiris E Pratsinis. “Catalytic Filter for Continuous and Selective Ethanol Removal Prior to Gas Sensing”. In: *ACS Sensors* 5.4 (2020), pp. 1058–1067. DOI: [10.1021/acssensors.9b02572](https://doi.org/10.1021/acssensors.9b02572). URL: <https://doi.org/10.1021/acssensors.9b02572>.
- [44] D K W Wang and C C Austin. “Determination of complex mixtures of volatile organic compounds in ambient air: canister methodology”. In: *Analytical and Bioanalytical Chemistry* 386.4 (2006), pp. 1099–1120. DOI: [10.1007/s00216-006-0466-6](https://doi.org/10.1007/s00216-006-0466-6). URL: <https://doi.org/10.1007/s00216-006-0466-6>.
- [45] Gwi Suk Heo et al. “Comparison of analytical methods for ozone precursors using adsorption tube and canister”. In: *Microchemical Journal* 70.3 (2001), pp. 275–283. DOI: [https://doi.org/10.1016/S0026-265X\(01\)00125-4](https://doi.org/10.1016/S0026-265X(01)00125-4). URL: <https://www.sciencedirect.com/science/article/pii/S0026265X01001254>.
- [46] Alan Rossner and Jean-Pierre Farant. “A Novel Personal Air Sampling Device for Collecting Volatile Organic Compounds: A Comparison to Charcoal Tubes and Diffusive Badges”. In: *Journal of Occupational and Environmental Hygiene* 1.2 (2004), pp. 69–81. DOI: [10.1080/15459620490275542](https://doi.org/10.1080/15459620490275542). URL: <https://doi.org/10.1080/15459620490275542>.
- [47] B Tolnai et al. “Advantages and disadvantages of different sampling techniques for sampling volatile organic hydrocarbons in air”. In: *Hungarian Journal of Industry and Chemistry* 28.1 (2000), pp. 44–47. DOI: [10.1515/hjic-2000-09](https://doi.org/10.1515/hjic-2000-09). URL: <https://hjic.mk.uni-pannon.hu/index.php/hjic/article/view/1097>.
- [48] Chunrong Jia Jae Hwan Lee Stuart A. Batterman and Sergei Chernyak. “Ozone Artifacts and Carbonyl Measurements Using Tenax GR, Tenax TA, Carbopack B, and Carbopack X Adsorbents”. In: *Journal of the Air & Waste Management Association*

- 
- tion 56.11 (2006), pp. 1503–1517. DOI: [10.1080/10473289.2006.10464560](https://doi.org/10.1080/10473289.2006.10464560). URL: <https://doi.org/10.1080/10473289.2006.10464560>.
- [49] Aggelos Calogirou et al. “Decomposition of Terpenes by Ozone during Sampling on Tenax”. In: *Analytical Chemistry* 68.9 (1996), pp. 1499–1506. DOI: [10.1021/ac950803i](https://doi.org/10.1021/ac950803i). URL: <https://doi.org/10.1021/ac950803i>.
- [50] M Even, E Juritsch, and M Richter. “Measurement of very volatile organic compounds (VVOCs) in indoor air by sorbent-based active sampling: Identifying the gaps towards standardisation”. In: *TrAC - Trends in Analytical Chemistry* 140 (2021). DOI: [10.1016/j.trac.2021.116265](https://doi.org/10.1016/j.trac.2021.116265).
- [51] P B Shepson, T E Kleindienst, and H B McElhoe. “A cryogenic trap/porous polymer sampling technique for the quantitative determination of ambient volatile organic compound concentrations”. In: *Atmospheric Environment (1967)* 21.3 (1987), pp. 579–587. DOI: [https://doi.org/10.1016/0004-6981\(87\)90040-0](https://doi.org/10.1016/0004-6981(87)90040-0). URL: <https://www.sciencedirect.com/science/article/pii/0004698187900400>.
- [52] N Van Den Hoed and M T H Halmans. “Sampling and Thermal Desorption Efficiency of Tube-Type Diffusive Samplers: Selection and Performance of Adsorbents”. In: *American Industrial Hygiene Association Journal* 48.4 (1987), pp. 364–373. DOI: [10.1080/15298668791384887](https://doi.org/10.1080/15298668791384887). URL: <https://doi.org/10.1080/15298668791384887>.
- [53] Kurt Haerens, Pieter Segers, and Toon Van Elst. “Sampling and stability of mercaptans: Comparison between bags, canisters and sorbent tubes”. In: *Chemical Engineering* 54 (2016), pp. 31–36.
- [54] A Castellnou, N Gonzalez-Flesca, and J O Grimalt. “On-site Comparison of Canister and Solid-Sorbent Trap Collection of Highly Volatile Hydrocarbons in Ambient Atmospheres”. In: *Environmental Monitoring and Assessment* 52.1 (1998), pp. 97–106. DOI: [10.1023/A:1005835023593](https://doi.org/10.1023/A:1005835023593). URL: <https://doi.org/10.1023/A:1005835023593>.
- [55] Balázs Tolnai et al. “Combination of canister and solid adsorbent sampling techniques for determination of volatile organic hydrocarbons”. In: *Microchemical Journal* 67.1-3 (2000), pp. 163–169.
- [56] Charles R Bryan and David Enos. *Results of stainless steel canister corrosion studies and environmental sample investigations*. Tech. rep. 2014.
- [57] Bruce Pate et al. “Temporal stability of polar organic compounds in stainless steel canisters”. In: *Journal of the Air & Waste Management Association* 42.4 (1992), pp. 460–462.
- [58] Della Wai-mei Sin et al. “Development of an analytical technique and stability evaluation of 143 C3–C12 volatile organic compounds in Summa® canisters by gas chromatography–mass spectrometry”. In: *Analyst* 126.3 (2001), pp. 310–321.

- 
- [59] Karen D Oliver, Joachim D Pleil, and William A McClenny. “Sample integrity of trace level volatile organic compounds in ambient air stored in SUMMA® polished canisters”. In: *Atmospheric Environment (1967)* 20.7 (1986), pp. 1403–1411. DOI: [https://doi.org/10.1016/0004-6981\(86\)90011-9](https://doi.org/10.1016/0004-6981(86)90011-9). URL: <https://www.sciencedirect.com/science/article/pii/0004698186900119>.
- [60] Catherine A Calvert Christopher C. Coffey Ryan F. LeBouf and James E Slaven. “Validation of an Evacuated Canister Method for Measuring Part-Per-Billion Levels of Chemical Warfare Agent Simulants”. In: *Journal of the Air & Waste Management Association* 61.8 (2011), pp. 826–833. DOI: [10.3155/1047-3289.61.8.826](https://doi.org/10.3155/1047-3289.61.8.826). URL: <https://doi.org/10.3155/1047-3289.61.8.826>.
- [61] Laurent Spinelle et al. “Review of Portable and Low-Cost Sensors for the Ambient Air Monitoring of Benzene and Other Volatile Organic Compounds”. In: *Sensors* 17.7 (2017). DOI: [10.3390/s17071520](https://doi.org/10.3390/s17071520). URL: <https://www.mdpi.com/1424-8220/17/7/1520>.
- [62] Alastair C Lewis et al. “Evaluating the performance of low cost chemical sensors for air pollution research”. In: *Faraday discussions* 189 (2016), pp. 85–103.
- [63] Juliana P Sá et al. “Application of the low-cost sensing technology for indoor air quality monitoring: A review”. In: *Environmental Technology & Innovation* 28 (2022), p. 102551. DOI: <https://doi.org/10.1016/j.eti.2022.102551>. URL: <https://www.sciencedirect.com/science/article/pii/S2352186422001432>.
- [64] Brian C McDonald et al. “Volatile chemical products emerging as largest petrochemical source of urban organic emissions”. In: *Science* 359.6377 (Feb. 2018), pp. 760–764. DOI: [10.1126/science.aaq0524](https://doi.org/10.1126/science.aaq0524). URL: <https://doi.org/10.1126/science.aaq0524>.
- [65] Nicholas J Nassikas et al. “Indoor Air Sources of Outdoor Air Pollution: Health Consequences, Policy, and Recommendations: An Official American Thoracic Society Workshop Report”. In: *Annals of the American Thoracic Society* 21.3 (2024), pp. 365–376. DOI: [10.1513/AnnalsATS.202312-1067ST](https://doi.org/10.1513/AnnalsATS.202312-1067ST). URL: <https://doi.org/10.1513/AnnalsATS.202312-1067ST>.
- [66] Mark Jacob Goldman, William H Green, and Jesse H Kroll. “Chemistry of Simple Organic Peroxy Radicals under Atmospheric through Combustion Conditions: Role of Temperature, Pressure, and NO<sub>x</sub> Level”. In: *J. Phys. Chem. A* 125 (2021), pp. 10303–10314. DOI: [10.1021/acs.jpca.1c07203](https://doi.org/10.1021/acs.jpca.1c07203). URL: <https://doi.org/10.1021/acs.jpca.1c07203>.

- 
- [67] Dwayne E Heard and Michael J Pilling. “Measurement of OH and HO<sub>2</sub> in the Troposphere”. In: *Chemical Reviews* 103.12 (2003), pp. 5163–5198. DOI: [10.1021/cr020522s](https://doi.org/10.1021/cr020522s). URL: <https://doi.org/10.1021/cr020522s>.
- [68] Roger Atkinson. “Atmospheric chemistry of VOCs and NO<sub>x</sub>”. In: *Atmospheric Environment* 34.12-14 (2000), pp. 2063–2101. DOI: [10.1016/S1352-2310\(99\)00460-4](https://doi.org/10.1016/S1352-2310(99)00460-4).
- [69] Ya B Zeldvich. “The oxidation of nitrogen in combustion and explosions”. In: *J. Acta Physicochimica* 21 (1946), p. 577.
- [70] Emre Özgül and Hasan Bedir. “Fast NO emission prediction methodology via one-dimensional engine performance tools in heavy-duty engines”. In: *Advances in Mechanical Engineering* 11 (2019), pp. 168781401984595–168781401984595. DOI: [10.1177/1687814019845954](https://doi.org/10.1177/1687814019845954).
- [71] Michael Rößler et al. “Mechanisms of the NO<sub>2</sub> Formation in Diesel Engines”. In: *MTZ worldwide* 78.7 (2017), pp. 70–75. DOI: [10.1007/s38313-017-0057-2](https://doi.org/10.1007/s38313-017-0057-2). URL: <https://doi.org/10.1007/s38313-017-0057-2>.
- [72] Elena Grignani et al. “Safe and Effective Use of Ozone as Air and Surface Disinfectant in the Conjunction of Covid-19”. In: *Gases* 1.1 (2021), pp. 19–32. ISSN: 2673-5628. DOI: [10.3390/gases1010002](https://doi.org/10.3390/gases1010002). URL: <https://www.mdpi.com/2673-5628/1/1/2>.
- [73] Juno Hsu and Michael J Prather. “Stratospheric variability and tropospheric ozone”. In: *Journal of Geophysical Research: Atmospheres* 114.D6 (2009). DOI: <https://doi.org/10.1029/2008JD010942>. URL: <https://agupubs.onlinelibrary.wiley.com/doi/abs/10.1029/2008JD010942>.
- [74] R G Prinn et al. “Evidence for variability of atmospheric hydroxyl radicals over the past quarter century”. In: (2005). DOI: [10.1029/2004GL022228](https://doi.org/10.1029/2004GL022228). URL: <https://agupubs.onlinelibrary.wiley.com/doi/10.1029/2004GL022228>.
- [75] Francesca Spataro and Antonietta Ianniello. “Sources of atmospheric nitrous acid: State of the science, current research needs, and future prospects”. In: *Journal of the Air & Waste Management Association* 64.11 (2014), pp. 1232–1250. DOI: [10.1080/10962247.2014.952846](https://doi.org/10.1080/10962247.2014.952846). URL: <https://doi.org/10.1080/10962247.2014.952846>.
- [76] Rebecca L Caravan, Michael F Vansco, and Marsha I Lester. “Open questions on the reactivity of Criegee intermediates”. In: *Communications Chemistry* 4.1 (2021), p. 44. DOI: [10.1038/s42004-021-00483-5](https://doi.org/10.1038/s42004-021-00483-5). URL: <https://doi.org/10.1038/s42004-021-00483-5>.
- [77] Faria Khan et al. “Toxicological Responses of  $\alpha$ -Pinene-Derived Secondary Organic Aerosol and Its Molecular Tracers in Human Lung Cell Lines”. In: *Chemical Research in Toxicology* 34.3 (2021), pp. 817–832. DOI: [10.1021/acs.chemrestox.0c00409](https://doi.org/10.1021/acs.chemrestox.0c00409). URL: <https://doi.org/10.1021/acs.chemrestox.0c00409>.

- 
- [78] Michal Pardo et al. “Exposure to naphthalene and  $\beta$ -pinene-derived secondary organic aerosol induced divergent changes in transcript levels of BEAS-2B cells”. In: *Environment International* 166 (2022), p. 107366. DOI: <https://doi.org/10.1016/j.envint.2022.107366>. URL: <https://www.sciencedirect.com/science/article/pii/S0160412022002938>.
- [79] Tanguy Déméautis et al. “Weight loss and abnormal lung inflammation in mice chronically exposed to secondary organic aerosols”. In: *Environ. Sci.: Processes Impacts* 25.3 (2023), pp. 382–388. DOI: [10.1039/D2EM00423B](https://doi.org/10.1039/D2EM00423B). URL: <http://dx.doi.org/10.1039/D2EM00423B>.
- [80] M Pilar Pérez-Casany et al. “Ab Initio Study on the Mechanism of Tropospheric Reactions of the Nitrate Radical with Alkenes: Ethene”. In: *The Journal of Organic Chemistry* 63.20 (1998), pp. 6978–6983. DOI: [10.1021/jo980779j](https://doi.org/10.1021/jo980779j). URL: <https://doi.org/10.1021/jo980779j>.
- [81] Yafen Zhang and John R Morris. “Hydrogen Abstraction Probability in Reactions of Gas-Phase NO<sub>3</sub> with an OH-Functionalized Organic Surface”. In: *The Journal of Physical Chemistry C* 119.26 (2015), pp. 14742–14747. DOI: [10.1021/acs.jpcc.5b00562](https://doi.org/10.1021/acs.jpcc.5b00562). URL: <https://doi.org/10.1021/acs.jpcc.5b00562>.
- [82] J Hjorth et al. “Products and mechanisms of the gas-phase reactions between nitrate radical and a series of alkenes”. In: *Journal of Physical Chemistry* 94.19 (1990), pp. 7494–7500.
- [83] Ian Barnes et al. “Kinetics and products of the reactions of nitrate radical with monoalkenes, dialkenes, and monoterpenes”. In: *Journal of Physical Chemistry* 94.6 (1990), pp. 2413–2419.
- [84] M Dam et al. “Observations of gas-phase products from the nitrate-radical-initiated oxidation of four monoterpenes”. In: *Atmospheric Chemistry and Physics* 22.13 (2022), pp. 9017–9031. DOI: [10.5194/acp-22-9017-2022](https://doi.org/10.5194/acp-22-9017-2022). URL: <https://acp.copernicus.org/articles/22/9017/2022/>.
- [85] Jiaqi Wang et al. “Observation of nitrous acid (HONO) in Beijing, China: Seasonal variation, nocturnal formation and daytime budget”. In: *Science of The Total Environment* 587-588 (2017), pp. 350–359. DOI: <https://doi.org/10.1016/j.scitotenv.2017.02.159>. URL: <https://www.sciencedirect.com/science/article/pii/S0048969717304084>.
- [86] Yuhong Liu et al. “Formation of peroxyacetyl nitrate (PAN) and its impact on ozone production in the coastal atmosphere of Qingdao, North China”. In: *Science of The Total Environment* 778 (2021), p. 146265. DOI: <https://doi.org/10.1016/j.scitotenv.2021.146265>.

- 
- scitotenv.2021.146265. URL: <https://www.sciencedirect.com/science/article/pii/S0048969721013334>.
- [87] Roger Atkinson, Arthur M Winer, and James N Pitts. “Estimation of night-time N<sub>2</sub>O<sub>5</sub> concentrations from ambient NO<sub>2</sub> and NO<sub>3</sub> radical concentrations and the role of N<sub>2</sub>O<sub>5</sub> in night-time chemistry”. In: *Atmospheric Environment (1967)* 20.2 (1986), pp. 331–339. DOI: [https://doi.org/10.1016/0004-6981\(86\)90035-1](https://doi.org/10.1016/0004-6981(86)90035-1). URL: <https://www.sciencedirect.com/science/article/pii/0004698186900351>.
- [88] D M Huff et al. “Deposition of dinitrogen pentoxide, N<sub>2</sub>O<sub>5</sub>, to the snowpack at high latitudes”. In: *Atmospheric Chemistry and Physics* 11.10 (2011), pp. 4929–4938.
- [89] A M M Manders et al. “Sea salt concentrations across the European continent”. In: *Atmospheric Environment* 44.20 (2010), pp. 2434–2442. ISSN: 1352-2310. DOI: <https://doi.org/10.1016/j.atmosenv.2010.03.028>. URL: <https://www.sciencedirect.com/science/article/pii/S1352231010002396>.
- [90] Doyun Won et al. “Validation of the surface sink model for sorptive interactions between VOCs and indoor materials”. In: *Atmospheric Environment* 35.26 (2001), pp. 4479–4488. DOI: [https://doi.org/10.1016/S1352-2310\(01\)00223-0](https://doi.org/10.1016/S1352-2310(01)00223-0). URL: <https://www.sciencedirect.com/science/article/pii/S1352231001002230>.
- [91] Xiaoyu Liu et al. “VOC Sink Behaviour on Building Materials – Model Evaluation”. In: *Indoor and Built Environment* 20.6 (2011), pp. 661–676. DOI: [10.1177/1420326X11409461](https://doi.org/10.1177/1420326X11409461). URL: <https://doi.org/10.1177/1420326X11409461>.
- [92] Junfeng Zhang and Paul J Lioy. “Ozone in Residential Air: Concentrations, I/O Ratios, Indoor Chemistry, and Exposures”. In: *Indoor Air* 4.2 (1994), pp. 95–105. DOI: <https://doi.org/10.1111/j.1600-0668.1994.t01-2-00004.x>. URL: <https://onlinelibrary.wiley.com/doi/abs/10.1111/j.1600-0668.1994.t01-2-00004.x>.
- [93] Golam Sarwar et al. “Hydroxyl radicals in indoor environments”. In: *Atmospheric Environment* 36.24 (2002), pp. 3973–3988. DOI: [https://doi.org/10.1016/S1352-2310\(02\)00278-9](https://doi.org/10.1016/S1352-2310(02)00278-9). URL: <https://www.sciencedirect.com/science/article/pii/S1352231002002789>.
- [94] Wenjuan Wei, Corinne Mandin, and Olivier Ramalho. “Reactivity of Semivolatile Organic Compounds with Hydroxyl Radicals, Nitrate Radicals, and Ozone in Indoor Air”. In: *International Journal of Chemical Kinetics* 49.7 (2017), pp. 506–521. DOI: <https://doi.org/10.1002/kin.21093>. URL: <https://onlinelibrary.wiley.com/doi/abs/10.1002/kin.21093>.

- 
- [95] Neil E Klepeis et al. “The National Human Activity Pattern Survey (NHAPS): a resource for assessing exposure to environmental pollutants”. In: *Journal of exposure science & environmental epidemiology* 11.3 (2001), pp. 231–252.
- [96] Nathan R Gray, Alastair C Lewis, and Sarah J Moller. “Deprivation based inequality in NOx emissions in England”. In: *Environmental Science: Advances* 2.9 (2023), pp. 1261–1272.
- [97] Alan Holmans. “New estimates of housing demand and need in England, 2011 to 2031”. In: *Town & Country Planning Tomorrow Series Paper* 16.4 (2013).
- [98] Miloslav Bagoňa et al. “Analysis of impact of selected glass units for energy consumption and the risk of overheating in the school building using simulation”. In: *12th Conference of International Building Performance Simulation Association*. Nov. 2011.
- [99] P Cooper and R R Kulkarni. “Overheating and thermal stratification in multi-storey glazed spaces”. In: *Annual Conference of the Australian and New Zealand Solar Energy Society*. Sydney, Dec. 1994, pp. 333–338.
- [100] Hasim Altan et al. “Daylight, solar gains and overheating studies in a glazed office building”. In: *Int. J. Energy Environ* 2 (2008), pp. 129–138.
- [101] Claire Tam et al. “Mitigation Strategies for Overheating and High Carbon Dioxide Concentration within Institutional Buildings: A Case Study in Toronto, Canada”. In: *Buildings* 10.7 (2020). DOI: [10.3390/buildings10070124](https://doi.org/10.3390/buildings10070124). URL: <https://www.mdpi.com/2075-5309/10/7/124>.
- [102] Chima Cyril Hampo, Leah H Schinasi, and Simi Hoque. “Surviving indoor heat stress in United States: A comprehensive review exploring the impact of overheating on the thermal comfort, health, and social economic factors of occupants”. In: *Heliyon* 10.3 (2024). DOI: [10.1016/j.heliyon.2024.e25801](https://doi.org/10.1016/j.heliyon.2024.e25801). URL: <https://doi.org/10.1016/j.heliyon.2024.e25801>.
- [103] Samuel Stamp et al. “Seasonal variations and the influence of ventilation rates on IAQ: A case study of five low-energy London apartments”. In: *Indoor and Built Environment* 31.3 (2021), pp. 607–623. DOI: [10.1177/1420326X211017175](https://doi.org/10.1177/1420326X211017175). URL: <https://doi.org/10.1177/1420326X211017175>.
- [104] Roger Clive Birchmore et al. “Thermal performance and indoor air quality in new, medium density houses – Auckland, New Zealand”. In: *International Journal of Building Pathology and Adaptation* 41.1 (2023), pp. 279–300. DOI: [10.1108/IJBPA-08-2021-0110](https://doi.org/10.1108/IJBPA-08-2021-0110). URL: <https://doi.org/10.1108/IJBPA-08-2021-0110>.

- 
- [105] R Otson. “Effects of ventilation, temperature, sources, and sinks on VOC levels in a residence”. In: *Indoor Air Quality, Ventilation and Energy Conservation in Buildings*. 2. Montreal, May 1995, pp. 85–92.
- [106] Chen Zhou et al. “Combined effects of temperature and humidity on indoor VOCs pollution: Intercity comparison”. In: *Building and Environment* 121 (2017), pp. 26–34. DOI: <https://doi.org/10.1016/j.buildenv.2017.04.013>. URL: <https://www.sciencedirect.com/science/article/pii/S0360132317301737>.
- [107] J S Park and K Ikeda. “Variations of formaldehyde and VOC levels during 3 years in new and older homes”. In: *Indoor Air* 16.2 (2006).
- [108] Norimichi Suzuki et al. “Indoor Air Quality Analysis of Newly Built Houses”. In: *International Journal of Environmental Research and Public Health* 16.21 (2019). DOI: [10.3390/ijerph16214142](https://doi.org/10.3390/ijerph16214142). URL: <https://www.mdpi.com/1660-4601/16/21/4142>.
- [109] N Suzuki et al. “Changes in the concentration of volatile organic compounds and aldehydes in newly constructed houses over time”. In: *International Journal of Environmental Science and Technology* 17.1 (2020), pp. 333–342. DOI: [10.1007/s13762-019-02503-3](https://doi.org/10.1007/s13762-019-02503-3). URL: <https://doi.org/10.1007/s13762-019-02503-3>.
- [110] Jarek Kurnitski et al. “Use of mechanical ventilation in Finnish houses”. In: *European Blower Door Symposium*. Vol. 2. Kassel, Mar. 2007, pp. 152–161.
- [111] J Sonne, C Withers, and R Vieira. “Are residential whole-house mechanical ventilation systems reliable enough to mandate tight homes”. In: *ASHRAE and AIVC IAQ 2016* (2016).



# Chapter 2

## Methodology

This methodology will be split into two sections. The first section will look at a general overview of the analytical methods used in the studies within this thesis, while the second section will discuss the specific instrumentation and data methodologies used for the following chapters in this thesis. Within this second section, calibration will be discussed, along with data processing and workup methodologies.

### 2.1 General methodology

#### 2.1.1 Gas chromatography

Chromatography is a technique in which mixtures, often complex, are separated into their constituent parts. There are several different types of chromatography, but all maintain the fundamental principle of separation. A common high school demonstration is the separation of dyes in ink from a felt-tip pen through a coffee filter using water; an accessible form of paper chromatography, which has now been superseded by thin layer chromatography. All chromatography techniques have three components: the mixture to be separated, a mobile phase, and a stationary phase. The stationary phase is the separation medium, the element of the technique which facilitates the separation of the mixture. The mobile phase is the component which moves the mixture over the stationary phase.

In gas chromatography (GC), the mobile phase is known as a carrier gas and the stationary phase is known as a column. The selection of carrier gases and columns is made relative to the mixture being analysed. Additional techniques may be required for deeper analysis of potential trace constituents, such as preconcentration and focusing of trace constituents and

---

mass spectrometry (MS), all of which are discussed later.

### 2.1.1.1 Carrier gases and columns

In GC, the role of the carrier gas is to sweep the mixture and resulting separated analytes through the instrument(s). In the case of a front-end thermal desorbing unit (TDU) and back-end mass spectrometers (MS), then the carrier gas also acts to sweep the mixture and resulting separated analytes through these components, too. The selection of an appropriate carrier gas relies on the required resolution of the resulting chromatogram, as well as the separation efficiency of the column, length and inner diameter (ID) of the column, and the carrier gas linear velocity. Typically, nitrogen, helium, or hydrogen are used for GC, and these are discussed further later in this sub-section.

The stationary phase is a component of the column being used to separate the mixture. The first GC columns were between 1 m and 5 m in length and up to 5 mm ID.<sup>[1]</sup> These GC columns were packed with particles which were themselves coated in the stationary phase. The short lengths, wide bores and packing methods restricted the chromatographic resolution, and only more 'simple' separation was initially possible.<sup>[2,3]</sup> Capillary columns, where the stationary phase coats the inner walls of the column, allow for much narrower column bores, integral for maintaining pressure across the column. While packed columns do have a place in air sample analysis, such as applications requiring large sample volumes or with less complex mixtures, capillary columns provide high efficiency separation of complex mixtures. A simple diagram showing the differences between packed and capillary columns can be seen in figure 2.1.

### 2.1.1.2 Principles of separation

Separation of mixtures through GC works on the principle that different analytes within the mixture will interact varyingly with the stationary phase. A specific analyte, A, partitions between the carrier gas ( $A_M$ ) and the column ( $A_S$ ) as an equilibrium as it traverses through the column as shown in reaction (R 2.1), the speed of which is dictated by the equilibrium constant K (partition coefficient).



The partition coefficient for each analyte, therefore the directional favourability of reaction (R 2.1), depends on the strength of the analyte's partitioning onto the stationary phase. This can be measured by the capacity factor (also called the retention factor),  $K'$ . The capacity factor describes the relative ability of a column to retain an analyte ( $t_R$ ), relative to the void

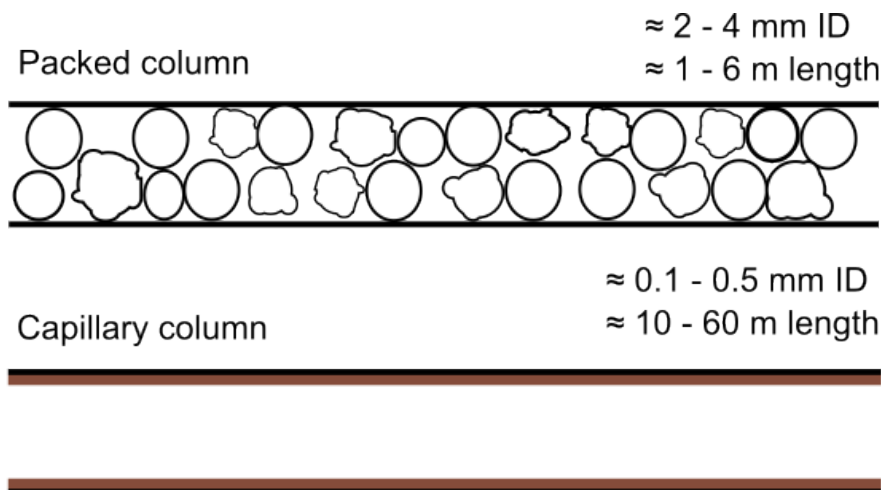


Figure 2.1: Diagram showing the internal structural differences between packed and capillary columns. In the capillary column, the stationary phase is a thin covering around the internal walls of the tube, in this diagram coloured brown.

time ( $t_M$ ), which itself is the time taken for an unretained analyte to traverse the column.  $K'$  can be calculated using equation 2.1.

$$K' = \frac{(t_R - t_M)}{t_M} \quad (2.1)$$

Capacity factor can additionally be calculated from the partition coefficient if the volumes of mobile and stationary phase are known ( $V_m$  and  $V_s$  respectively), according to equation 2.2.

$$K' = K \frac{V_s}{V_m} \quad (2.2)$$

Capacity factor and partition coefficient are proportional to each other. Good separation of a mixture is not dictated by having high or low capacity factors or partition coefficients, however. For example, a high capacity factor means there would be a longer retention time of an analyte in the column, which could be impractical for analysis. Therefore, column efficiencies need to be described in a column-specific manner.

### 2.1.1.3 Column efficiency

Efficiency in GC is measured by theoretical plates. The term originates from column distillation, where a physical plate, or tray, would provide a contact point where a liquid-gas equilibrium could be established; essentially, a plate was a contact point for a gas to condense. With more plates came greater distillation efficiency, and so it is for GC with theoretical plates.

---

The number of theoretical plates of a column refers to the column's separation efficiency, and can be calculated by equation 2.3.

$$N = 16 \left( \frac{t_R}{W} \right)^2 \quad (2.3)$$

Here,  $N$  refers to the number of theoretical plates (dimensionless),  $t_R$  is the analyte column retention time (min), and  $W$  is the peak base width (min). This assumes the analyte peak has a gaussian distribution.

The height equivalent of a theoretical plate (HETP) is a measure of the length of the column required for one theoretical plate's worth of mobile-to-stationary phase partitioning. This can be calculated simply by dividing the length of the column by the number of theoretical plates, as in 2.4:

$$HETP = \frac{L}{N} \quad (2.4)$$

where  $L$  is the column length (m), while HETP is usually expressed in mm. A low HETP indicates less of the column is required to house one theoretical plate, resulting in greater separation efficiency, assuming an even distribution of stationary phase within the column. HETP is also affected by the carrier gas. Figure 2.2 shows the change of carrier gas HETP with linear velocity, defined as how fast the carrier gas flows through the column, for nitrogen, helium and hydrogen.

Figure 2.2 can be derived through the use of either equation 2.5 or 2.6, known as the van Deemter equation and Golay equation, respectively. Here, HETP is defined as a function of band broadening, the dispersion of an analyte through the column.

$$HETP = A + \frac{B}{u} + u(C_m + C_s) \quad (2.5)$$

$$HETP = \frac{B}{u} + u(C_m + C_s) \quad (2.6)$$

Here,  $u$  is defined as the linear velocity of the carrier gas through the column,  $A$  is defined as the eddy diffusion term,  $B$  is the longitudinal diffusion term, and  $C_m$  and  $C_s$  is the mass transfer term for the mobile phase and stationary phase, respectively. In capillary columns, there is no eddy diffusion as there is only a single pathway for the analyte to traverse through the column, setting the  $A$  term to 0 and giving equation 2.6.

Shown in figure 2.2, nitrogen offers a low HETP for a short range of linear velocities, while helium and hydrogen offer a low HETP over a broader range of linear velocities. Purely by observing figure 2.2, one would assume hydrogen to be the superior carrier gas, however the

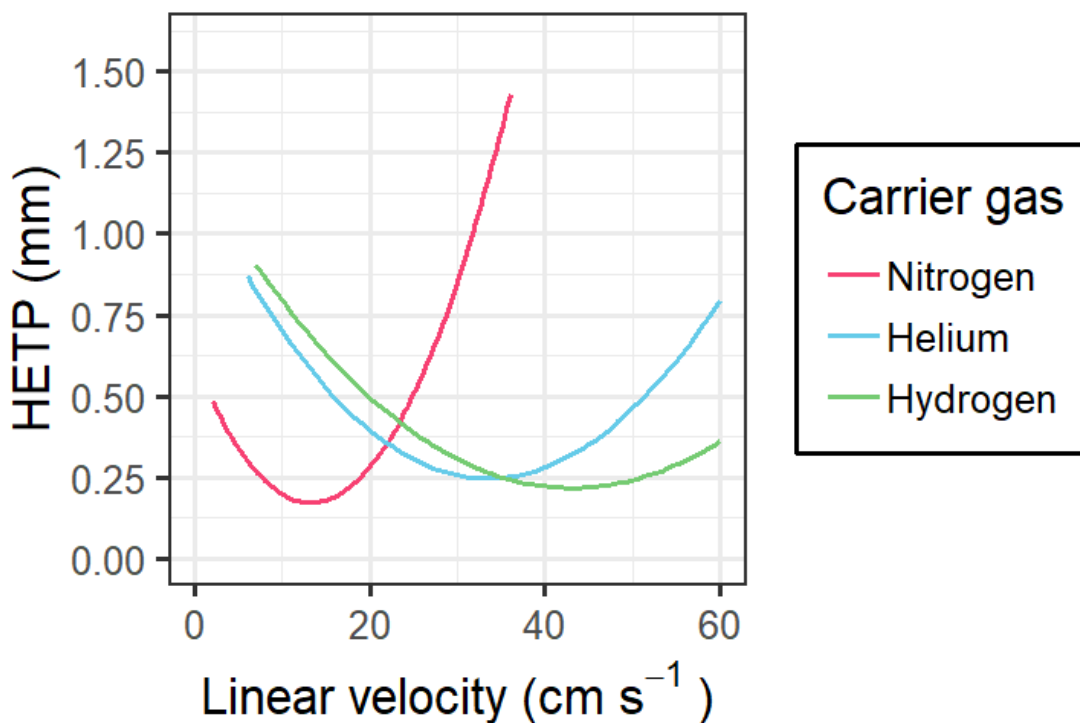


Figure 2.2: Typical van Deemter curves for nitrogen, helium and hydrogen.

choice of carrier gas is more nuanced than this, especially when using GC coupled with a mass spectrometer (MS, or GCMS in tandem). For most common applications, the selection of a carrier gas is usually a decision between hydrogen and helium, as nitrogen typically offers to narrow a range of linear velocities for high efficiency column separation and narrow elution bands.

An MS can ionise analytes through different methods following GC, such as electron impact ionisation (EI) or chemical ionisation (CI). Hydrogen has the potential to ionise within the MS itself which could result in increased noise. Moreover, the use of hydrogen as a carrier gas can result in analyte degradation through hydrogenation and de-chlorination within the MS.<sup>[4]</sup> Hydrogen carrier gas use can also result in metallurgic interactions between hydrogen and the ionisation source in the MS for non-hydrogen inert source surfaces, potentially shortening the life of the source and giving signal artifacts in the MS spectrum.<sup>[5]</sup> Hydrogen has a lower viscosity than helium or nitrogen, so the MS vacuum pump must operate harder to achieve the vacuum required for the MS to operate. Finally, hydrogen also has safety implications through flammability. While laboratory mitigations can be made to keep risk of explosion low, accumulation of hydrogen within the MS presents a risk of explosion and so must be treated with care.

---

While helium does not present the issues above, helium is in short supply and is expensive. Hydrogen can be generated somewhat easily within a laboratory itself using an electrolytic hydrogen generator, whereas helium must be supplied in cylinders.

#### 2.1.1.4 Chromatographic resolution

Resolution is measured as the separation of two analytes relative to each other. If two analytes experience significant band broadening within the column, the resulting elutions of the two analytes may overlap and give low resolution. The resolution of two peaks A and B ( $R_{A,B}$ ) can be described by relating the retention times of the two peaks with the individual peak base widths ( $W_A$  and  $W_B$ ), according to equation 2.7.

$$R_{A,B} = \frac{t_{R,A} - t_{R,B}}{0.5(W_A + W_B)} = \frac{2\Delta t_R}{(W_A + W_B)} \quad (2.7)$$

Resolution itself is dimensionless. A resolution of 0.5 is indicative of poor separation between the two analytes, resulting in co-elution of the analytes, shown in figure 2.3. A resolution of 1.5 is the lowest desirable resolution between two peaks for peak separation and accurate quantification, shown in figure 2.4, representing a 0.1% overlap between elutions.

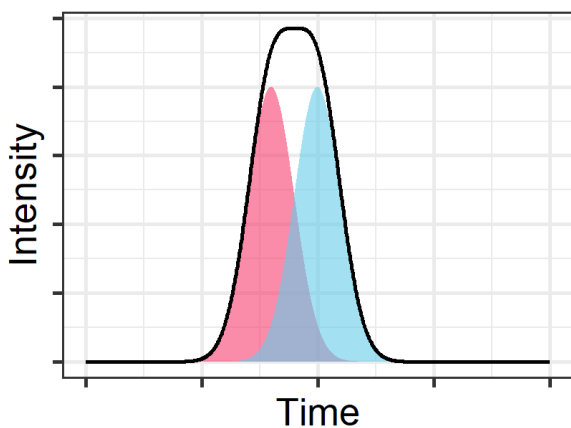


Figure 2.3: Separation of two imaginary peaks with a resolution of 0.5. The sum of the two elutions (chromatographic peak) is shown in black. Here there is significant co-elution of the two analytes, which would result in poor quantification.

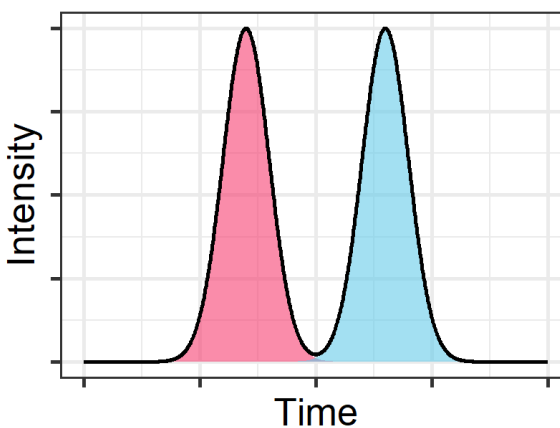


Figure 2.4: Separation of two imaginary peaks with a resolution of 1.5. The sum of the two elutions (chromatographic peak) is shown in black.

---

## 2.1.2 Thermal desorption

Air is a complex matrix, of which VOCs are a minor constituent typically at parts per billion (ppb) mixing ratios. Low concentrations typically require large sample volumes for successful analysis. Large sample volumes present issues with maintaining efficiency and resolution. For VOC analysis, undesired bulk constituents of air, such as oxygen and nitrogen, effectively act as diluents; the cause of requiring large volumes for whole air sample analysis. These diluents can be reduced through preconcentration. Preconcentration allows for analysis of species with low concentrations in the original air sample with the use of much lower volumes of carrier gas which, when done successfully, maintains resolution and efficiency integrity. Preconcentration is achieved through thermal desorption (TD).

Historically, TD was achieved through the heating of a sample to release components into the gas phase, which would then be swept into the GC with a carrier gas. This in itself is pyrolysis-GC, a technique still commonly used for analysis of nonvolatile species. With scientific improvements came more sophisticated TD capabilities with the use of cryogenically-cooled trapping media for preconcentration.<sup>[6,7]</sup> Trapping at low temperatures results in increased absorption of volatile species in the preconcentration trap. The cooled trap is then flash heated to desorb the trapped species into the flow of carrier gas. While this method is extremely efficient, the use of liquid nitrogen (LN<sub>2</sub>) means that certain issues can arise such as blockage of the trapping tube (narrow-bore tubing such as glass or stainless steel), and the requirement for a supply of LN<sub>2</sub> which has considerable risks associated with its use. Achieving low temperatures through non-cryogenic means can be done through the use of Peltier or Stirling coolers, and is discussed later.

### 2.1.2.1 VOC trapping

For preconcentration, VOCs in air are typically trapped using a sorbent-packed tube. VOC trapping can be achieved through the sampling mechanism itself (as in sorbent tube sampling), or in-line (also called 'on-line') through a front-end thermal desorber. Both methods utilise the same principle of VOC trapping, while allowing for diluent gases to pass over unaffected by the sorbent. Common sorbent materials include charcoal-based materials such as Carbo-pack™(Sigma-Aldrich, Merck KGaA, Germany) and Carbograph™(LARA S.r.l, Italy), or polymer-based materials such as Tenax™-packed tubes (trademark owned by Buchem B.V., Netherlands) or divinylbenzene-based co-polymers. Common features of sorbent materials are that they are often hydrophobic, trap compounds primarily through intermolecular interactions, and their trapping efficiency depends on sorbent pore size and surface area. Smaller pore sizes typically retain smaller molecules more effectively. Mesh size refers to the particle

---

size of the sorbent material, affecting flow resistance rather than analyte selectivity. When different mesh sizes are used, they are given as a range, such as 60-80. In this example, a 60-80 mesh sorbent means the sorbent particles have passed through a 60-mesh screen and would not pass through an 80-mesh screen. A wider range of mesh sizes means a larger variety of molecule sizes can be trapped, and vice versa.

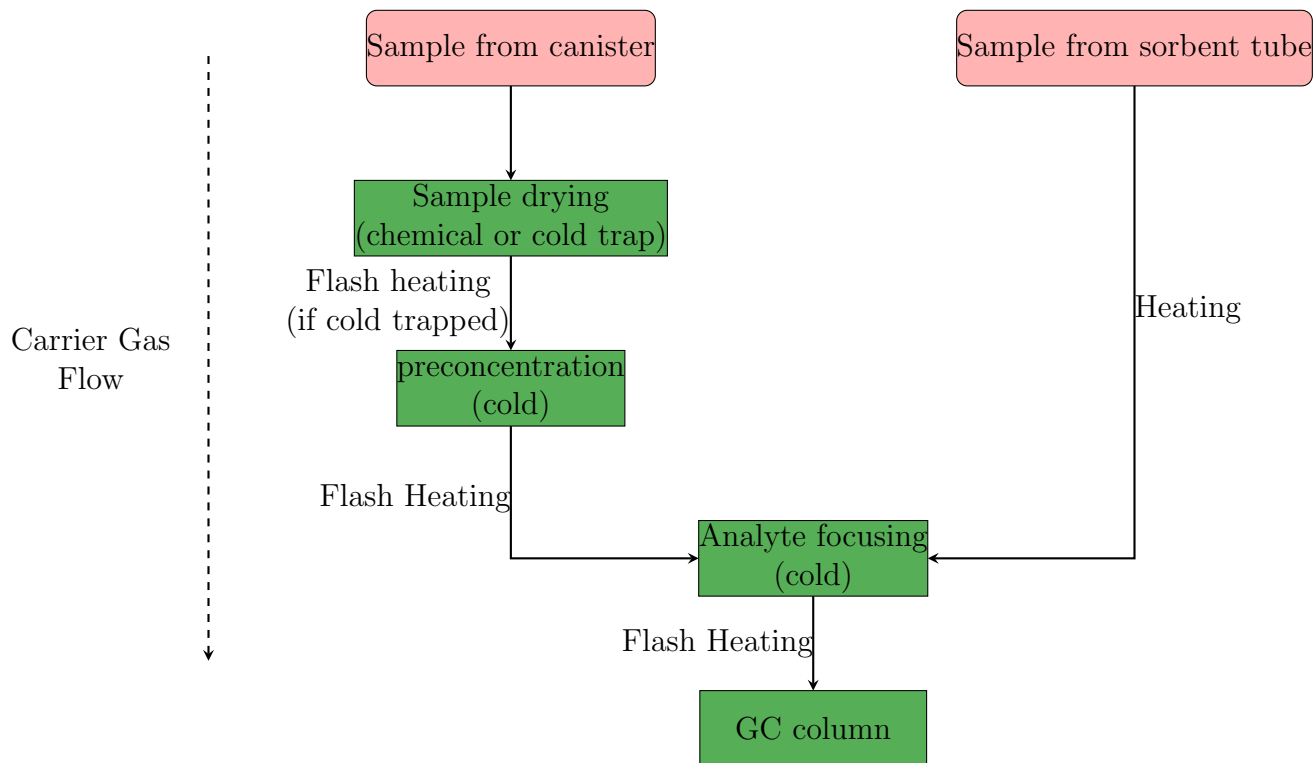
However, preconcentration for air samples collected through vacuum-intake canisters, collection methods for which are detailed in section 1.2.3, must be done in-line before GC injection. In-line preconcentration is achieved in a narrow-bore (typically  $1/16''$ ) tube, typically stainless-steel and lined with fused-silica, packed with a small quantity of sorbent cooled to a low temperature. The canister sample (pressurised with a blank gas) is then swept through the tube with carrier gas, at which point VOCs will adsorb onto the sorbent, while unretained gases are purged. After a period of time, the tube is then flash heated to desorb the trapped VOCs into the stream of carrier gas, at which point the concentrated analytes can then either be injected into the GC column, or focused. If the trap is cooled lower than  $-80\text{ }^{\circ}\text{C}$ , consideration must be given to the retention of  $\text{CO}_2$  in the preconcentrator, with an initial warming stage to  $\geq -80^{\circ}\text{C}$  to allow  $\text{CO}_2$  to purge, before fully heating the trap to desorb VOC analytes.

Sample focusing is much the same procedure as preconcentration. A tube with a narrower bore than the preconcentration tube is cooled, and the concentrated analytes are swept through the tube by the carrier gas. Again, after a period of time the tube is then flash heated, and the desorbed analytes are passed into the GC column. The narrower bore of the focusing tube serves multiple purposes. Primarily it focuses the analytes into narrow bands, crucial for maintaining high chromatographic resolution. Additionally, it limits back pressure build-up into the GC column, which often have internal diameters of less than  $1/162''$ . A simple flow scheme for sample preconcentrating and focusing is given in scheme 2.1.

### 2.1.2.2 Sample drying

Retention of water vapour in air samples presents issues for VOC analysis, such as blockage of the trapping tube with ice and absorption of water vapour into the trapping sorbent, as well as possible damage to the GC columns and MS ion source.<sup>[8]</sup> The presence of water vapour can also disturb the elution of analytes from the GC column, such as through peak splitting, co-eluting and diminished resolution.<sup>[9]</sup> So before a sample can be effectively preconcentrated for VOC analysis, it must first be dried.

Sample drying can be done chemically through the use of Nafion (Chemours, DA, USA), a trademarked name for a sulphonated tetrafluoroethylene co-polymer. In this application,



Scheme 2.1: A flow schematic of sample preconcentration and focusing for canister samples through in-line cold traps.

Nafion acts as a membrane between the humid sample gas and a dry purge gas, shown in figure 2.5. Water binds to the sulphonated terminal groups in the Nafion chains, which can then diffuse through the membrane into the stream of dry purge gas.

Issues can arise with the use of Nafion dryers for VOC analysis, as Nafion also removes oxygenated and sulphonated species, resulting in either absent expected elutions or artificially lower elutions. A positive implication of this effect is discussed in section 6.2.2. Sample drying can be achieved through the flash freezing of water vapour in a narrow-bore glass tube (a 'water trap'). Sample drying must occur quickly through deposition of water vapour, as if the water vapour was allowed to condense first then VOC loss could occur through dissolution into the liquid water and subsequent freezing of the water-VOC solution. Cooling of a water trap (and preconcentration traps) through non-cryogenic results in a more compact system with increased portability.

### 2.1.2.3 Peltier cooler

A Peltier cooler utilises the thermoelectric effect (also called the Seebeck-Peltier effect) to allow for low-temperature refrigeration without the use of cryogenics. The Peltier effect refers

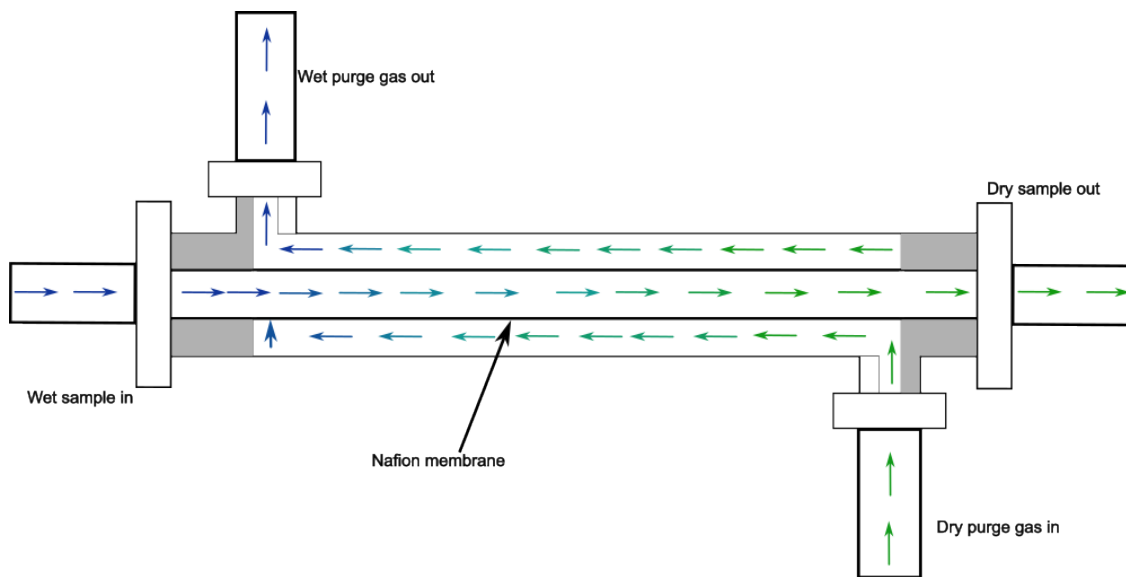


Figure 2.5: A cross-sectional diagram illustrating sample drying using a Nafion hollow tube membrane. The Nafion membrane acts as a hollow tube, around which is the outer conduit, usually stainless steel, through which the purge gas flows.

to the generation of a temperature differential through the application of an electric current across a junction of two dissimilar conductive materials or semiconductors, resulting in heat absorption at one junction (cold side) and heat release at the other (hot side). These plates are commonly stacked in series so one Peltier plate removes the heat generated by the cold side of another, resulting in a lower achievable temperature. While Peltier plates are non-moving, requiring little maintenance, and can in theory be stacked limitlessly, in practice they are inefficient and require additional components such as heat sinks to increase cooling efficiency. Coefficients of performance (COP) can be used to describe the efficiency of a heat pump/refrigeration system, and is defined according to equation 2.8.

$$COP = \frac{|Q|}{W} \quad (2.8)$$

$|Q|$  is the heat produced or removed by the system (expressed as an absolute value), and  $W$  is the net work put into the system. Peltier plates typically have a low COP for cooling ( $\ll 1$ ),<sup>[10,11]</sup> indicating relatively low operating efficiencies. The use of free-piston Stirling coolers (FPSC) can provide lower temperatures, integral for analysis of semi-volatile species.

#### 2.1.2.4 Free-piston Stirling cooler

An FPSC uses the Stirling cycle to produce cooling, and a simplified diagram is shown in figure 2.6. In this cycle, there is cyclic compression and expansion of a working gas (typically

helium) within a sealed chamber. The system consists of two main pistons: a displacer and a power piston (labelled in figure 2.6 simply as 'piston'), both moving freely without mechanical linkages. The displacer moves the gas between the cold and hot ends of the cylinder, ensuring effective heat exchange. During the cycle, the power piston compresses the gas, raising its temperature, and the heat is expelled at the hot end through a heat exchanger. Then the gas expands, reducing its temperature, and it absorbs heat at the cold end through another heat exchanger, thereby producing cooling. This cycle is repeated, transferring heat from the cold head to the hot head, thus providing refrigeration. FPSCs typically also have low COPs ( $< 1$ ).<sup>[12,13]</sup> However, FPSCs can achieve much lower temperatures than Peltier plates with comparable (if not slightly higher) COPs, allowing for a greater VOC trapping potential with a comparable efficiency to that of a Peltier cooler.

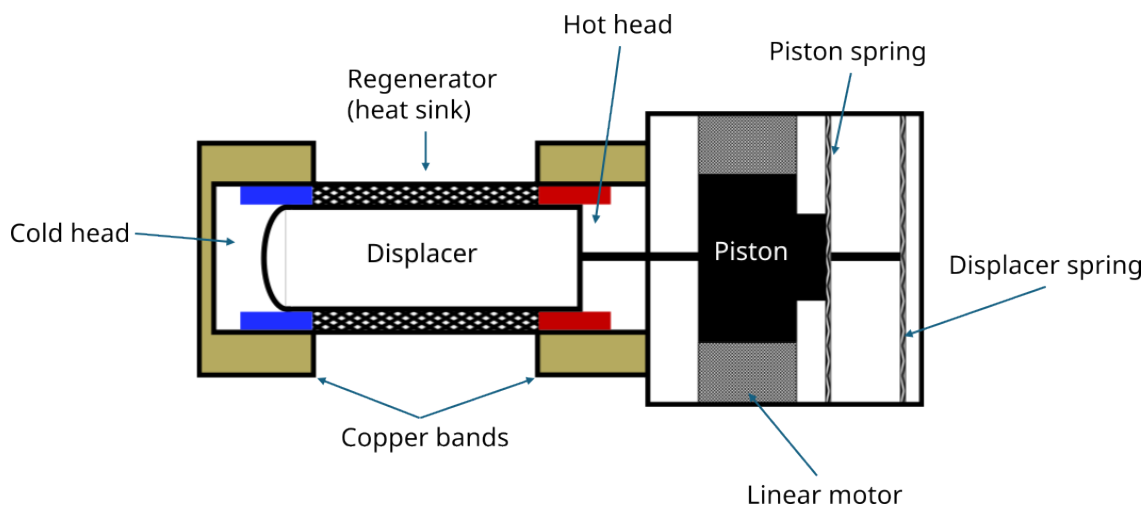


Figure 2.6: A simplified diagram showing the workings of a free-piston Stirling cooler .

### 2.1.3 Mass spectrometry

Mass spectrometry (MS) serves to identify a chemical species based on its mass-to-charge ratio ( $m/z$ ). Broadly, MS can be broken into five main sections: vapourisation, ionisation, acceleration, ion separation, and detection. MS instruments operate within vacuums, firstly to ensure the ion separation (drift/deflection) region is clear of gases which could increase collisions and affect drift/deflection results, but also to remove contaminant gases. A small level of mixture separation can occur within an MS, due to the different separation methods employed. In a time-of-flight (TOF) MS, ionised molecules are accelerated into a field-free drift tube, where separation occurs based on the mass of the ionised molecule. In a sector MS, a deflection zone (with either an applied magnetic or electric field) causes ionised molecules to travel along a curved path. In this zone, a lighter molecule travels along a more curved path

---

and a heavier molecule less curved path. However, MS is not itself a separation technique and the ions produced through ionisation are not separated effectively to produce clear, separate mass spectra. An MS does not apply well to complex mixtures, and is therefore often best used in tandem with a separation technique to ensure a high resolution is maintained, through effectively separating a mixture into its constituent parts prior to introduction to the MS.

Vapourisation in the context of GC-MS tandem doesn't apply as the eluent of the GC column is already vapourised, and can be transferred through heated tubing straight into the MS. However, in the context of liquid techniques such as liquid chromatography-MS (LC-MS) this presents an issue. In LC-MS a solvent is used to dissolve the analyte mixture. Relative to the volume of mixture, there would be several orders of magnitude more solvent present, and if this was immediately vapourised into the MS, the quantity of vapour created would cause an increase in noise and potentially damage the ion source (discussed later). The increase in noise would occur due to the level of solvent vapour being evacuated through the vacuum, causing a drop in the vacuum pressure, collisions between solvent vapour and analytes and potentially allowing for the infiltration of air into the MS. LC-MS systems typically begin transfer of analytes from the LC column to the MS with a solvent delay, meaning the MS transfer would only begin once the solvent had finished eluting from the column, leaving just the analytes to be detected by MS.

### 2.1.3.1 Ionisation

The way in which a species gains a charge (ionisation) varies according to the context of the application and deployment of an MS system. Electron impact (EI) is a common technique in which a stream of high energy electrons are fired at the vapourised analyte. Electrons are produced through thermionic emission by flowing a current through a filament, typically made of tungsten or rhenium. This causes the filament to heat up, and once the electrons gain enough thermal energy to overcome the work function of the metal, electrons are emitted. By applying a voltage across the filament and an anode, this will concentrate the electrons into a focused beam. The beam will then collide with the analyte gas flow (which enters orthogonally to the plane of the ion source), ionising the analytes according to equation (R 2.2).



A simplified, 2D figure of ion production with the EI source is given in figure 2.7. The positively charged analyte ions are then pushed out of the ion source by the repeller plate. The ion flow is then focused by a series of electrostatic Einzel lenses, three hollow electrodes through which a potential difference is applied, inducing an electric field. This electric field

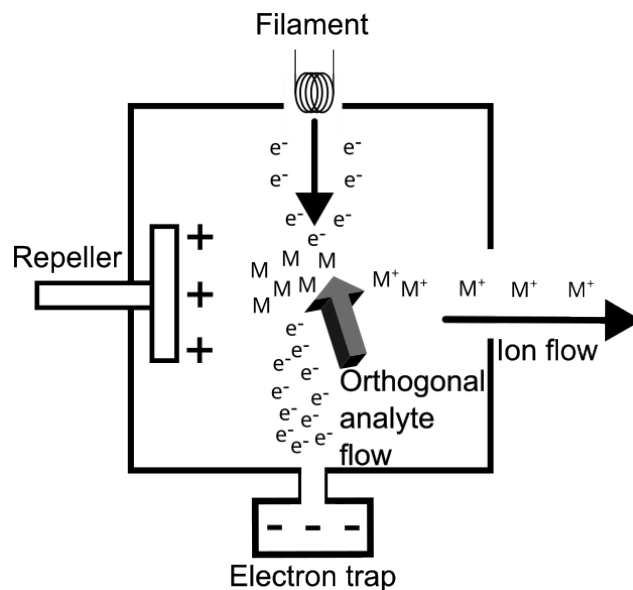


Figure 2.7: A 2D rendering of the production of analyte ions within the ion source. The analyte gas flow is orthogonal to the plane of the image, *i.e.*, entering from the front.

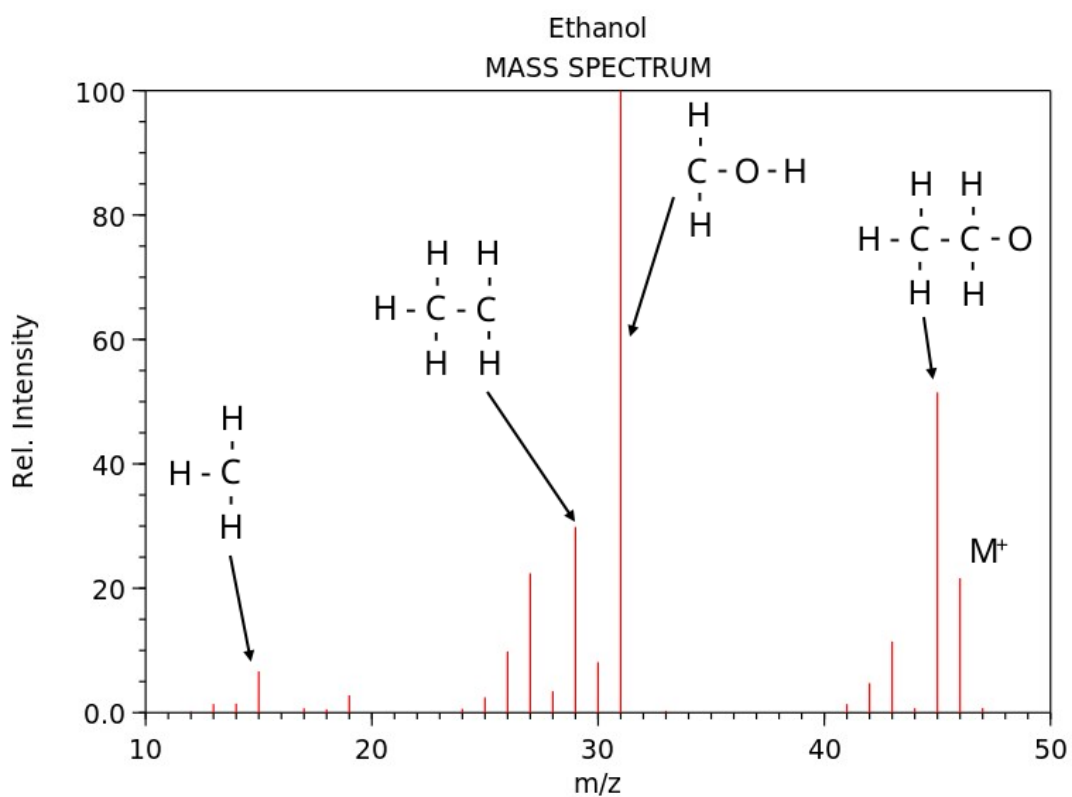
then causes the ions to diverge and converge according to the voltages applied, focusing the ion flow into a beam. For the MS used throughout these works, the ion beam will then flow through to the quadrupole mass filter, which is discussed in section 2.1.3.2.

This process will cause both ionisation and fragmentation of the analyte in question, breaking the molecule into several charged parts. Fragmentation can be both helpful and unhelpful. For the analysis of ions through accurate masses (as opposed to nominal masses), preservation of the parent molecule would be required, and as such soft techniques such as electrospray or chemical ionisation would be required. However, fragmentation also allows for an in depth picture of a molecule's structure to be drawn, as shown in figure 2.8. By using a constant electron energy, typically 70 eV, fragmentation will be regular among all users of EI, allowing for a large library to be constructed of EI mass spectra.

### 2.1.3.2 Quadrupole mass filter

A quadrupole mass filter is designed to separate ions based on their  $m/z$  ratio. It consists of four parallel metal rods, typically around 10 cm in length, arranged in a square configuration. If the rods are cylindrical rather than hyperbolic, placing them so that the distance between diagonally opposite rods is  $1/1.148$  times the rod diameter provides a good approximation of the ideal hyperbolic field. Opposing pairs of rods are electrically connected.

A combination of radio frequency (RF) voltage and direct current (DC) voltage is applied such that one pair of rods receives a potential of  $+U + V \cos(\omega t)$ , while the opposing pair



NIST Chemistry WebBook (<https://webbook.nist.gov/chemistry>)

Figure 2.8: Electron impact mass spectrum of ethanol. Fragmentation structures as simple Lewis structures are annotated for select peaks. The peak labelled  $M^+$  is the molecular ion,  $C_2H_5OH^+$ . The mass spectrum was obtained from the National Institute of Standards and Technology (NIST) Chemistry WebBook, available at <https://doi.org/10.18434/T4D303>.<sup>[14]</sup>

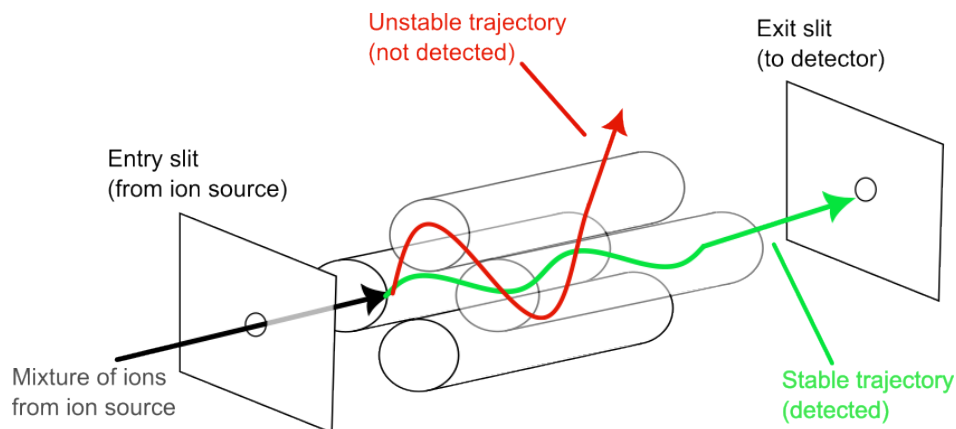


Figure 2.9: A simple diagram of the movement of two ions through a quadrupole mass selector. Ions with unstable trajectories, such as those that are too light or too heavy, are not detected.

receives  $-U - V \cos(\omega t)$ . Here,  $U$  is the DC voltage,  $V$  is the amplitude of the RF voltage, and  $\omega$  is the angular frequency. This oscillating electric field creates a dynamic potential that allows only ions of a specific mass-to-charge ratio to pass through the quadrupole at a given time.

As ions travel along the axis of the quadrupole, the electric field selectively stabilizes the trajectories of ions with a specific  $m/z$  ratio, allowing them to pass through the filter, while others are deflected and lost. A simplified diagram of this process is shown in figure 2.9. By adjusting the RF and DC voltages, the quadrupole can target different  $m/z$  ratios, effectively acting as a tunable mass filter. Ions with too high an  $m/z$  ratio do not respond quickly with the oscillating field, and eventually collide with the quadrupole rods. Ions with a low  $m/z$  ratio respond too quickly to the field, and either collide with the rods or are ejected from the field entirely. Once ions collide with the rods, they lose their charge and as such are no longer influenced by the quadrupole. Over time this can cause a buildup of deposited fragments and so should be cleaned to maintain performance. The low  $m/z$  ions which escape the quadrupole will be removed through the vacuum applied throughout the MS/QMS. The RF transformer and DC power supply are essential for generating and controlling the required voltages, ensuring precise ion selection and mass resolution in the QMS.

#### 2.1.4 Flame ionisation detection

The Flame Ionization Detector (FID) is a device that detects organic compounds by measuring organic ions produced during combustion. The FID operates through a series of precise steps, involving the generation, collection, and quantification of ions. It can act as a stan-

---

alone analytical technique as in the monitoring of landfill and fugitive gases,<sup>[15,16]</sup> however it is commonly used as a detector following GC separation. The FID requires at least two separate gases, and in some cases three, as well as the column eluent. Hydrogen is required for the flame, and oxygen (or purified air free of contaminants) is used to ensure the flame burns completely. For some FIDs a makeup gas is required. The purpose of the makeup gas is to optimise the flow rate of the column eluent to the FID. Some modern FIDs are derivatives of older FID units which were built to work with packed columns, from which a higher carrier gas flow rate would be needed. However as capillary columns require a low flow rate of carrier (relative to packed columns), a makeup gas is required to account for the lower flow rate for capillary columns. Some FIDs are designed to work exclusively for capillary columns, for which makeup gas ports may not be included.

The separated analytes and carrier gas elutions from the GC column are mixed with hydrogen gas and air before entering the FID's combustion chamber. Here, the mixture is ignited, producing a flame. Organic analytes undergo pyrolysis in this flame, breaking down into smaller fragments, predominantly carbon-containing ions (and electrons). The flame acts as the ionization source.

Inside the FID, there are two electrodes, commonly referred to as the collector and the nozzle head. The positive electrode is the nozzle head where the flame is produced, while the negative electrode acts as a collector due to the attraction between the ions and the negatively charged electrode. When the ions hit the collector, a current is produced. This current is extremely small, often in the picoampere (pA) range, and is directly proportional to the number of carbon atoms within the analyte eluted from the GC. The signal is then plotted as a function of time, which is the final chromatogram. The eluent peak area is proportional to the 'amount' of analyte detected, either through a change in sample volume or sample concentration. A diagram showing the workings of a flame ionisation detector is shown in figure 2.10.

The FID is highly sensitive to carbon-containing compounds, making it a powerful tool for detecting hydrocarbons and other organic molecules. The linearity of FID responses over a range of volumes and concentrations is discussed further in section 2.2.

The concentration of a species is directly proportional to the area under the peak produced by that species' detection in the FID. The mixing ratio of a species separated from a mixture can be calculated by dividing the area of the analyte peak by the response factor (RF) of the

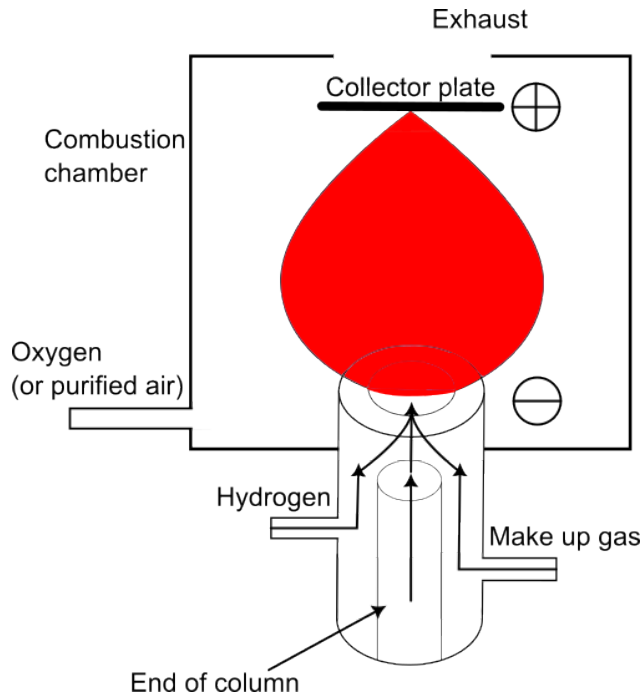


Figure 2.10: A diagram showing the workings of a flame ionisation detector used following GC separation.

same species from a calibrated gas, according to equation 2.9.

$$\text{fraction}_{\text{analyte}} = \frac{\text{area}_{\text{analyte}}}{RF_{\text{cal}}} = \frac{\text{area}_{\text{analyte}}}{\left(\frac{\text{area}_{\text{cal}}}{\text{ratio}_{\text{cal}}}\right)} \quad (2.9)$$

#### 2.1.4.1 Effective carbon number

As the response produced by the FID is proportional to the number of carbon atoms within the analyte, a stable carbon-wise response allows for quantification of species which are not directly calibrated against. The application of a method where the response of a calibrated species is used to calculate the concentration of an uncalibrated species using a carbon ratio between the two species is known as using effective (or equivalent) carbon number (ECN). These steps are shown in equations 2.10 and 2.11.

$$RF_{\text{uncalibrated}} = \frac{RF_{\text{cal}}}{\left(\frac{ECN_{\text{cal}}}{ECN_{\text{uncalibrated}}}\right)} \quad (2.10)$$

$$\text{ppb}_{\text{uncalibrated}} = \frac{\text{area}_{\text{uncalibrated}}}{RF_{\text{uncalibrated}}} \quad (2.11)$$

$ECN_{\text{uncalibrated}}$  is the effective carbon number of the uncalibrated species.  $ECN_{\text{cal}}$  and  $RF_{\text{cal}}$  must be for the same species, with  $RF_{\text{cal}}$  originating from a calibration run immediately before or after the sample requiring quantifying to protect against instrument response drift. Using an ECN and RF of a directly calibrated species essentially turns this species into a proxy for the quantification of uncalibrated species. Stability in the carbon number-to-response ratio is paramount in the successful execution of this method for the quantification of uncalibrated species.

Oxygenated species produce a lower FID signal. The presence of oxygen within the molecule will cause a more complete burn, producing more  $\text{CO}_2$ ,  $\text{CO}$  and  $\text{H}_2\text{O}$  which aren't detected by the FID, rather than organic ions. If a species is directly calibrated using the RF of the calibration sample, this lower response should not impact analysis. As a general rule of thumb, a rough ECN can be calculated by adding up the number of carbon atoms within the analyte, and subtracting 0.5 per oxygen atom. Following this rule, ethanol would have an ECN of 1.5, and propan-1-ol would have an ECN of 2.5. However, the location of the oxygen atom(s) within the molecule, as well as other adjoining atoms, will impact the ECN for the molecule. The ECN rules used in the works contained within this thesis, informed from several different studies,<sup>[17-21]</sup> are shown in table 2.1. Instrument analysis on carbon-to-response ratios is given in section 2.2.4.

Table 2.1: The ECN contributions for different functional groups and elements used throughout these works.

Functional group	ECN contribution
Paraffinic carbon	1.0
Olefinic carbon	0.95
Aromatic carbon	1.0
Aldehyde	-1.0
Ketone	-1.0
Primary alcohol	-0.6
Secondary alcohol	-0.75
Tertiary alcohol	-0.25
Ether	-1.0
Ester	-1.5
Nitrogen (amines)	Treated as oxygen
Nitrogen (nitrile)	-0.5
Cl (adjoining paraffinic C)	-0.12
Cl (adjoining olefinic C)	0.05

---

## 2.1.5 Whole air sampling

As discussed in section 1.2.3, air samples can be collected through a variety of methods, but consideration needs to be placed on not just the chemical analysis to be completed, but also issues such as sample storage, sampler preparation, and sampler logistics. Sorbent tubes are commonplace and can be highly effective for detecting trace VOCs.<sup>[22-24]</sup> This would typically see one or several tubes packed with a sorbent deployed into a setting, and have the sample air pumped through the tube at a fixed rate over a span of time. Sorbent tubes are small and take up little space over the sampling duration. Sorbent tube transportation and storage requires the tubes being kept at low-to-sub-zero (°C) temperatures in order to preserve sample integrity. The sorbent used within the tubes are typically hydrophobic, but higher relative humidity in air being sampled can lead to a reduced VOC recovery.<sup>[25,26]</sup> Additionally, as is discussed in section 2.2.3, sorbent tubes are subject to 'breakthrough', where the volume of a sample flowing through the sorbent tube becomes a limiting factor in the proportion of VOC retained by the sorbent. Finally, sorbents can exhibit a degree of retention selectivity, and as such analysis from sorbent tube samples tend to be focused on select VOCs. However, they are relatively cheap and simple to use.

A solution to sampling selectivity is to take whole air samples (WAS) using evacuated canisters. A sampling canister is typically of stainless-steel construction, and is internally coated in a proprietary passivation layer to inhibit sample-canister interactions. Throughout this thesis, a combination of canister brands were used (Restek, PA, USA and Entech, CA, USA), however all were 6 L stainless-steel canisters internally treated with a silica-based ceramic passivation coating. Flow restrictors (Entech, CA, USA) were fitted atop the canisters in the studies in chapters 3, 4 and 5 to reduce the canister sample flow rate and thus time integrate the sample. A fully evacuated canister, discussed in section 2.1.6.1, would take  $\approx 30$  seconds to take a full sample, resulting in an average flow rate of  $\approx 12 \text{ L min}^{-1}$ . Such samples are often referred to as 'grab' samples, as they can result in a whole air sample over a much shorter time window, giving potential for deeper analysis into VOC exposure through momentary activities. However, using such samples to infer longer-period VOC exposure would present difficulties. Using in-line flow restrictors to give a time-integrated sample therefore limits potential skewing of these activities on the sample being taken. An example diagram of a canister with flow restrictor inlet is shown in figure 2.11

### 2.1.5.1 Time-integrated canister sampling

The flow-restrictive inlets used throughout this thesis utilised a critical orifice to achieve the flow restriction. This simply consists of a plate with a hole drilled through the middle. While

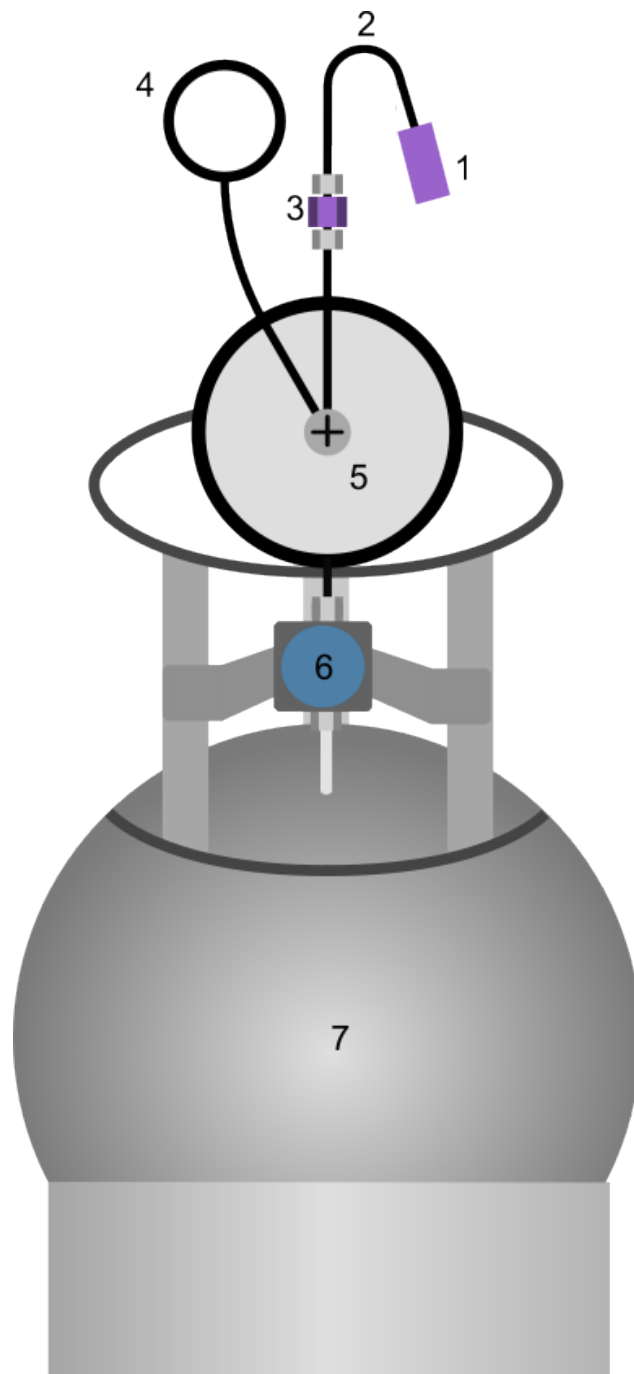


Figure 2.11: A diagram showing the final sampling assembly, with a flow-restrictive inlet and stabilising diaphragm, with sampling canister underneath. Labelled sections are as follows: 1. Inert in-line filter, 2. Goose neck to restrict entry of liquids, 3. Critical orifice flow restrictor, 4. Canister vacuum pressure gauge, 5. Internal diaphragm for flow rate stability, 6. Canister valve, 7. Canister.

---

simple in construction, the critical orifice is a sophisticated piece of engineering which can be designed to give a range of potential flow rates. The small diameter hole (the critical orifice) creates a choked (or sonic) flow when the condition in equation 2.12 is met. Choked flow is a condition where the flow rate of a fluid reaches a limit due to the gas velocity at the exit plane being equal to the speed of sound, and is said to be at sonic conditions.

$$\frac{P_2}{P_1} \leq \left( \frac{2}{\gamma + 1} \right)^{\frac{\gamma}{\gamma - 1}} \quad (2.12)$$

In equation 2.12,  $P_1$  and  $P_2$  are the upstream (inlet side) and downstream (canister/vacuum side) absolute pressures respectively, and  $\gamma$  is the ratio of specific heats (also called the adiabatic index or Laplace's coefficient) of the gas in question. For air,  $\gamma = 1.4$ . Substituting this into equation 2.12 gives a condition of choked flow being achieved when the downstream pressure is less than or equal to 0.528 times (52.8%) the upstream pressure. In the case of atmospheric upstream conditions and a downstream vacuum, both the air velocity and the mass flow rate become choked when a sonic velocity is reached through the orifice. Once choked flow is achieved, the choked mass flow rate can be determined using equation 2.13.

$$\dot{m} = C_d A \sqrt{\gamma \rho_1 P_1 \left( \frac{2}{\gamma + 1} \right)^{\frac{\gamma + 1}{\gamma - 1}}} \quad (2.13)$$

$\dot{m}$  is the mass flow rate,  $C_d$  is the discharge coefficient of the orifice,  $A$  is the cross-sectional area of the orifice,  $\rho_1$  and  $P_1$  are the density and pressure of the upstream gas respectively. However, as  $\rho$  can be calculated according to equation 2.14, where  $R$  is the ideal gas constant and  $T_1$  is the temperature of the gas:

$$\rho = \frac{P_1}{RT_1} \quad (2.14)$$

this can then can in turn be substituted into equation 2.13 to form equation 2.15.

$$\dot{m} = C_d A P_1 \sqrt{\frac{\gamma}{RT_1} \left( \frac{2}{\gamma + 1} \right)^{\frac{\gamma + 1}{\gamma - 1}}} \quad (2.15)$$

Assuming a constant density ( $\rho$ ) final conversion from mass flow rate to volumetric flow rate ( $Q$ ) can be determined by equation 2.16:

$$Q = \frac{\dot{m}}{\rho} \quad (2.16)$$

---

or can be directly substituted into equation 2.15 using equation 2.16 to give equation 2.17:

$$Q = \frac{C_d A P_1}{\sqrt{RT_1}} \sqrt{\gamma \left( \frac{2}{\gamma + 1} \right)^{\frac{\gamma+1}{\gamma-1}}} \quad (2.17)$$

For the 6 L canisters used throughout this thesis, assuming the air being sampled is dry and acts as an ideal gas, achieving a full sample over 72 hours (assuming a constant flow rate) would require a volumetric flow rate of 1.39 mL min<sup>-1</sup>. An orifice internal diameter can be derived using equation 2.18 and assuming  $P_1 = 101325$  Pa,  $T_1 = 293$  K,  $R = 287$  J kg · K<sup>-1</sup>,  $\gamma = 1.4$ , and that  $C_d$  is between 0.6 and 1, which results in orifice internal diameters from between 0.0008 mm and 0.0006 mm.

$$A = \frac{Q \sqrt{RT_1}}{C_d P_1 \sqrt{\gamma \left( \frac{2}{\gamma+1} \right)^{\frac{\gamma+1}{\gamma-1}}}} = \frac{Q}{C_d P_1} \sqrt{\frac{RT_1}{\gamma \left( \frac{2}{\gamma+1} \right)^{\frac{\gamma+1}{\gamma-1}}}} \quad (2.18)$$

Thus what seemingly appears to be a disc with a hole in the middle becomes a highly technical and expertly calibrated piece of engineering.

## 2.1.6 Sampling and instrument setup

One sampling and instrumental setup was used throughout the studies and calibration work within this thesis. In short, this comprised a custom-built thermal desorbing unit (TDU), which then directly injected into a two-column gas chromatograph (GC), eluents from both columns detected through flame ionisation detection (FID), with one column having further detection through a quadropole mass spectrometer (QMS). Together, they make the TD-GC-FID-QMS instrument. A simplified flow-chart is given in chapter 3 figure 3.1, however a more detailed discussion of the instrument setup is presented here.

### 2.1.6.1 Canister preparation

To begin with, 6 L stainless-steel canisters internally treated with a proprietary silica-based ceramic passivation layer (Restek, PA, USA and Entech, CA, USA) were evacuated to a pressure  $\leq 0.1$  Pa. The evacuation process was completed *via* a two-step process. Canisters were first evacuated using an Edwards XDS10 dry scroll pump (Edwards Ltd, Sussex, UK) from ambient pressure to  $\approx 1$  Pa. Canisters were then attached to an Edwards nXDS10i dry scroll pump (Edwards Ltd, Sussex, UK) affixed with an Alcatel 5011 molecular drag pump (Alcatel Vacuum Products is now known as Adixen Vacuum Products, part of Pfeiffer Vacuum, Wetzlar, Germany). The molecular drag pump acted as a turbomolecular pump,

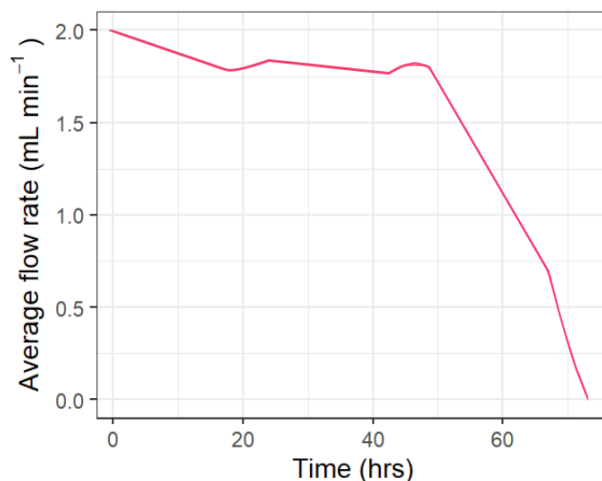


Figure 2.12: Flow rate of flow-restrictive inlet affixed to the top of the evacuated sampling canisters. This figure is reproduced from Heeley-Hill *et al.* (2023)<sup>[27]</sup> using the same theme and colour scheme as in this thesis.

which helped achieve the final vacuum of  $\leq 0.1$  Pa.

### 2.1.6.2 Sample collection

Sample canisters were affixed with a flow-restrictive inlet which time-integrated the 6 L canister samples over a 72 hour period. The inlet flow rate, while relatively stable throughout the first 48 hours of sampling, experienced a reduced flow rate throughout the final 24 hours of sampling, coinciding with the canister vacuum approaching ambient pressure, as shown in figure 2.12 (reproduced from Heeley-Hill *et al.* (2023)<sup>[27]</sup>). As such, samples had an inherent bias towards the first 48 hours of sampling.

After 48 hours of sampling using time-integrated, flow-restrictive inlets, approximately 90% of the total canister volume has been collected. During the final 24 hours, the flow rate decreases broadly linearly from  $1.75 \text{ mL min}^{-1}$  to  $0 \text{ mL min}^{-1}$ , contributing only around 10% of the total sample volume despite accounting for one-third of the sampling duration. Consequently, high-emission events occurring between 48 and 72 hours may be underrepresented in the final sample.

Notably, by approximately 52 hours, 95% of the total sample volume has been collected, suggesting that the vast majority of the representative air mass is captured within the first two days. In future campaigns, sampling durations could be reduced to 48 hours without significant loss of representativeness, offering a more time-efficient approach while maintaining an effectively uniform flow-weighted sample.

---

### 2.1.6.3 Sample selection

Whole air samples from stainless steel canisters (discussed later in section 2.1.5) were drawn through a 16-port manifold. Originally, this was through a Valco microelectric actuator multi-position valve (VICI Valco Instruments Co. Inc., TX, USA), and this was eventually replaced by a manifold composed of 16-port solenoid-actuated bellows valves (Swagelok Company, OH, USA) using a high-pressure air line to open and close the valves, connected in parallel to a main delivery line which then connected into a port on the TD unit. Samples were drawn at 15 mL min<sup>-1</sup>, through the water trap and then into the preconcentration trap.

### 2.1.6.4 Sample drying

The TD unit was composed of three traps to dry, preconcentrate and focus analytes prior to GC injection. The first trap was a 30 cm long 1/16" stainless steel fused-silica tube held at a temperature of -40 °C. This first trap acted as a drier ('water trap'). As discussed in section 2.1.2.2, water vapour must physically transform through deposition of the vapour immediately into ice and not transition through the liquid phase to limit VOC loss through dissolution into liquid water. -40 °C was chosen as the water trapping temperature to avoid preconcentrating the VOCs analysed through this methodology in the water trap, but still be at a cold enough temperature to deposit water vapour into ice.

### 2.1.6.5 Sample preconcentration

Through the water trap, the sample stream continued into the preconcentration trap. This comprised a 30 cm length of 1/16" stainless steel fused-silica tube, as with the water trap, and was packed with Carboxen<sup>TM</sup>40-60 mesh and Carboxen<sup>TM</sup>60-80 mesh adsorbents (Merck KGaA, Darmstadt, Germany) and fritted with glass wool. Both the preconcentration and focus traps were set to a temperature of -180 °C, not with the expectation of achieving this temperature but to set the trap holding temperature at the lowest temperature the system could achieve, invariably between -125 °C and -110 °C. Once sample collection had finished, the preconcentration trap was heated to -80 °C for 4 minutes in the flow of carrier to purge any CO<sub>2</sub> from the trap. After 4 minutes, the carrier flow was reversed and the preconcentration trap was heated to 190 °C to desorb analytes into the focus trap.

### 2.1.6.6 Sample focusing and transfer

The focus trap comprised a 20 cm section of 1/32" stainless steel fused-silica tube, again packed with Carboxen<sup>TM</sup>40-60 mesh and Carboxen<sup>TM</sup>60-80 mesh adsorbents (Merck KGaA, Darmstadt, Germany). As with the preconcentration trap, the focus trap was held at the

---

lowest achievable temperature for analyte trapping. The analytes were held in the focus trap until the GC was ready to begin a new method. This was at least 2 minutes. Once the GC was ready, the focus trap was flash heated to 200 °C to transfer analytes into the GC oven for 2 minutes.

#### **2.1.6.7 Trap purging**

Following analyte transfer, the preconcentration and focus traps were backflushed with carrier and heated to 230 °C to purge any remaining organic material. The water trap was heated to 100 °C to remove any residual water, and all desorbed gases from trap purging would then be vented to the atmosphere. The traps and carrier flow were then reset to their holding conditions, and would be left in this state for a delay to ensure traps were back to their holding conditions before new method commencement.

#### **2.1.6.8 GC**

In these works, an Agilent 7890A GC was used for separation. The GC oven was held at 35 °C for 7 minutes following method commencement, and then heated to 200 °C at a 5 °C min<sup>-1</sup> ramp rate over 33 minutes, achieving the final oven temperature of 200 °C at 40 minutes, after which the oven temperature would be held at 200 °C for a further 5 minutes. The GC method ran for 45 minutes each sample.

Analytes were desorbed from the flash-heated focus trap through a 60 m long, 150 μm ID VF-WAXms column (referred to afterwards as both VF-WAX or just WAX) with a film thickness of 0.50 μm (Agilent Technologies, CA, USA) at a flow rate of 1.6 mL min<sup>-1</sup> with a carrier gas pressure of 35 psi. VF-WAX columns are intended for the analysis of trace species which are typically used in foods, as well as fragrances and flavourings. VF-WAX columns use a polyethylene glycol (PEG) stationary phase. The VF-WAX column would not resolve lower hydrocarbons C<sub>2</sub> to C<sub>6</sub>. These unresolved hydrocarbons would elute from the VF-WAX column in a broad band from the start of the method to roughly 7.5 minutes. To resolve these species, a Deans switch (Agilent Technologies, CA, USA) would divert the unresolved hydrocarbon eluent into a 50 m, 320 μm ID, 5 μm film thickness Na<sub>2</sub>SO<sub>4</sub>-deactivated Al<sub>2</sub>O<sub>3</sub> porous-layer open tubular (PLOT) column. Elutions from the PLOT column would directly flow through to a flame ionisation detector (FID). After 8.3 minutes, once the unresolved analytes had passed onto the PLOT column, the Deans switch would divert VF-WAX eluent flow through a 2m, 150 μm ID length of fused silica, which would then further split to either another FID through a 0.91 m, 150 μm ID length of fused silica, or to the quadrupole mass spectrometer (QMS) through a 2.1 m, 150 μm ID length of fused silica.

Chromatograms from FID responses for a typical indoor air sample are given in figures 2.13 and 2.14. Only select species are labelled on the plots for brevity. In practice, over 120 different VOC species were detected at various stages of analysis. However, as indoor air is highly changeable, it was rare that all detectable species were found within samples, and as such total/summed VOC concentrations typically represented a smaller subset of the total number of detectable species.

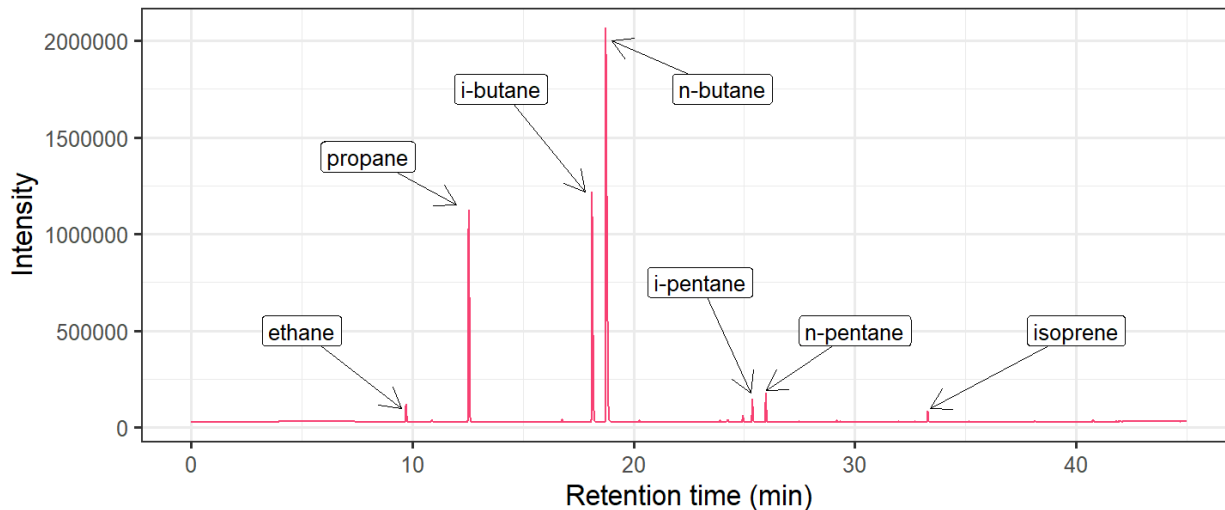


Figure 2.13: PLOT chromatogram for an ambient sample of residential indoor air.

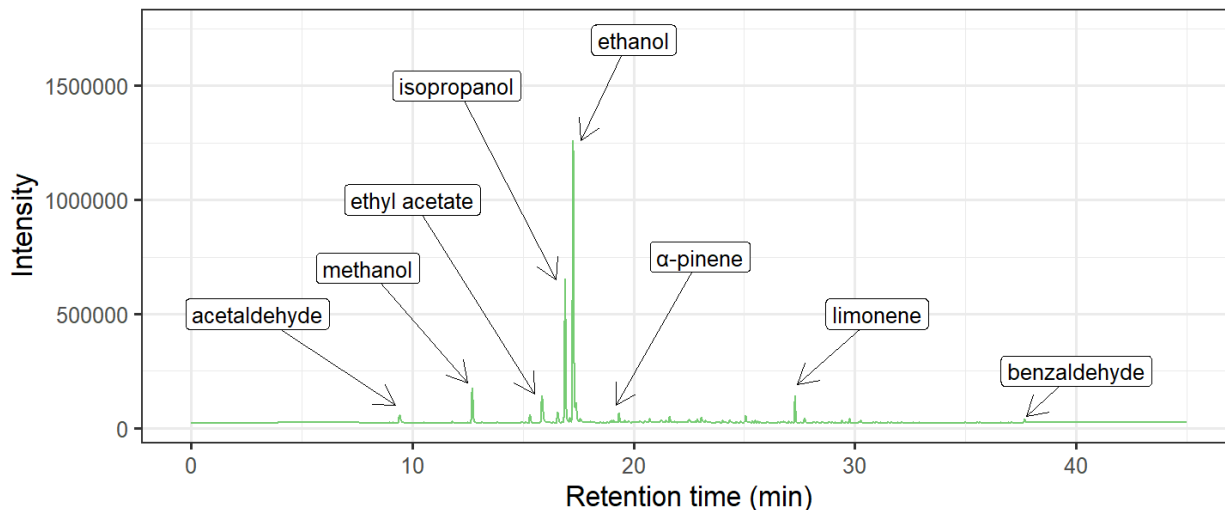


Figure 2.14: WAX chromatogram for an ambient sample of residential indoor air.

Chromatograms showing the unresolved analytes as a VF-WAX elution, which would otherwise pass onto the PLOT column can be seen in figure 2.15. This chromatogram was produced following the analysis of ambient air. This shows a very intense, relatively broad

---

elution lasting roughly 30 seconds. A correspondingly empty PLOT chromatogram, save two trace analytes associated with the mistimed Deans switch actuation which caused the unresolved analytes to pass immediately through to the VF-WAX FID, is shown in figure 2.16. A zoomed version of figure 2.15 showing the other resolved analytes from the VF-WAX column is shown in figure 2.17. The total ion count (TIC) for the same WAX elutions are shown in figure 2.18. Here, the unresolved species were not detected through MS as there was a 7 minute solvent delay applied to the MS method, which is expounded upon later.

The PLOT column elutions were generally in order of boiling point, however the WAX elutions were in order of polarity. There were deviations from the boiling point order from PLOT elutions, such as acetylene (boiling point  $-84\text{ }^{\circ}\text{C}$ ) which eluted after *n*-butane (boiling point  $-1\text{ }^{\circ}\text{C}$ ), as in figure 2.19. This was generally seen in unsaturated molecules when compared with their saturated analogues.

In principle, a non-polar column will elute by boiling point. However the PLOT column stationary phase was coated in a deactivating salt,  $\text{Na}_2\text{SO}_4$ . The alumina stationary phase is highly polar and contains many active sites, meaning that without deactivation, more polar analytes such as alkenes and alkynes would be very strongly retained on the stationary phase surface, causing band broadening and poor resolution, and in some cases total retention. Covering the alumina in a deactivation layer reduces the stationary phase surface polarity and number of active sites as well as increasing the column stability over time, giving a more reproducible and predictable elution pattern. KCl can also be used as a deactivation salt for alumina columns, but deactivation by  $\text{Na}_2\text{SO}_4$  provides a more polar surface than KCl, resulting in higher retention of more polar molecules. Due to the higher polarity of acetylene, the elution of acetylene sees significant peak tailing, shown in figure 2.19. This would also be seen with propyne (methyl acetylene).

#### 2.1.6.9 QMS

Elutions from the VF-WAX column following the Deans switch actuation at 8.3 mins were sent to both an FID and the QMS, with the flow pathway split using lengths of fused-silica to balance pressures. The QMS method began at 7 mins following an in-built solvent delay in the software used to control the GC and QMS and acquire data. The software used for GC-MS control can be applied to LC-MS control as well, and so a solvent delay is applied as default to avoid overwhelming the MS detector with solvents used during LC analysis. An example total ion count (TIC) for wax-eluting species is given in figure 2.18. This was a TIC for the same sample run as in figures 2.15, 2.16 and 2.17. The ion source was run at a temperature of  $230\text{ }^{\circ}\text{C}$  (maximum of  $250\text{ }^{\circ}\text{C}$ ), while the QMS was run at  $150\text{ }^{\circ}\text{C}$  (maximum

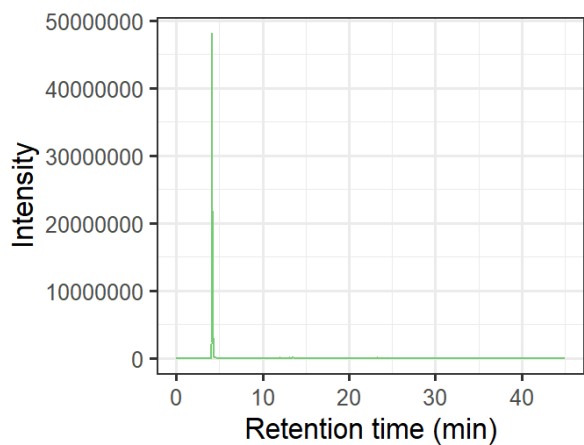


Figure 2.15: WAX chromatogram for ambient air showing a large elution of unresolved  $C_2$  to  $C_6$  hydrocarbons.

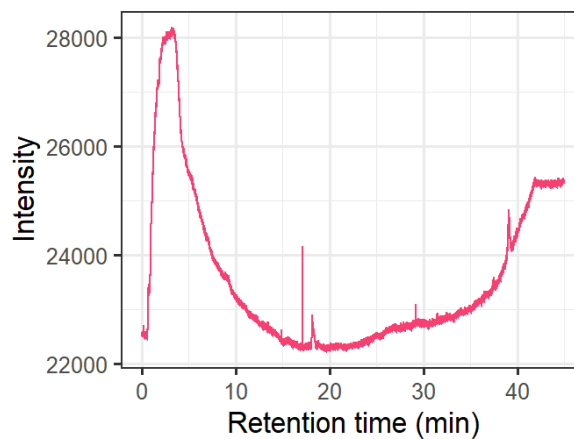


Figure 2.16: PLOT chromatogram for ambient air without typically resolved species.

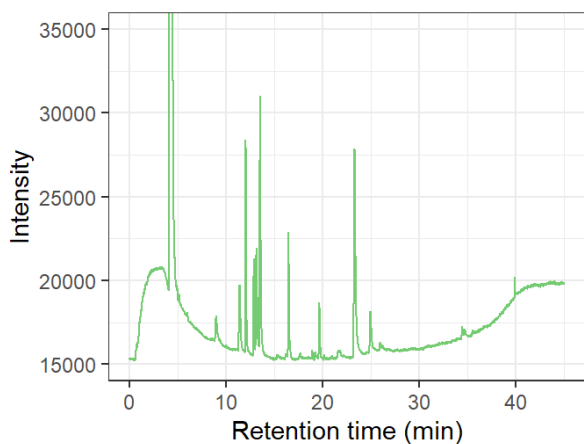


Figure 2.17: WAX chromatogram for ambient air zoomed to show the other elutions from the ambient air sample. The unresolved hydrocarbon elution begins at  $\approx 4.5$  min and finishes at  $\approx 5$  min.

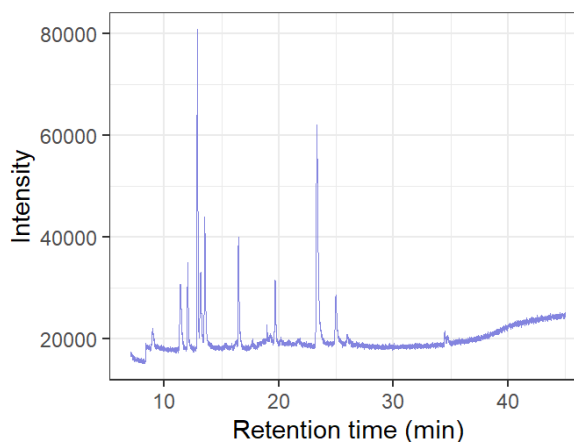


Figure 2.18: TIC for WAX-eluting species. The jump in baseline noise at  $\approx 8.3$  min is due to the switching of the Deans switch towards both the QMS and the second FID.

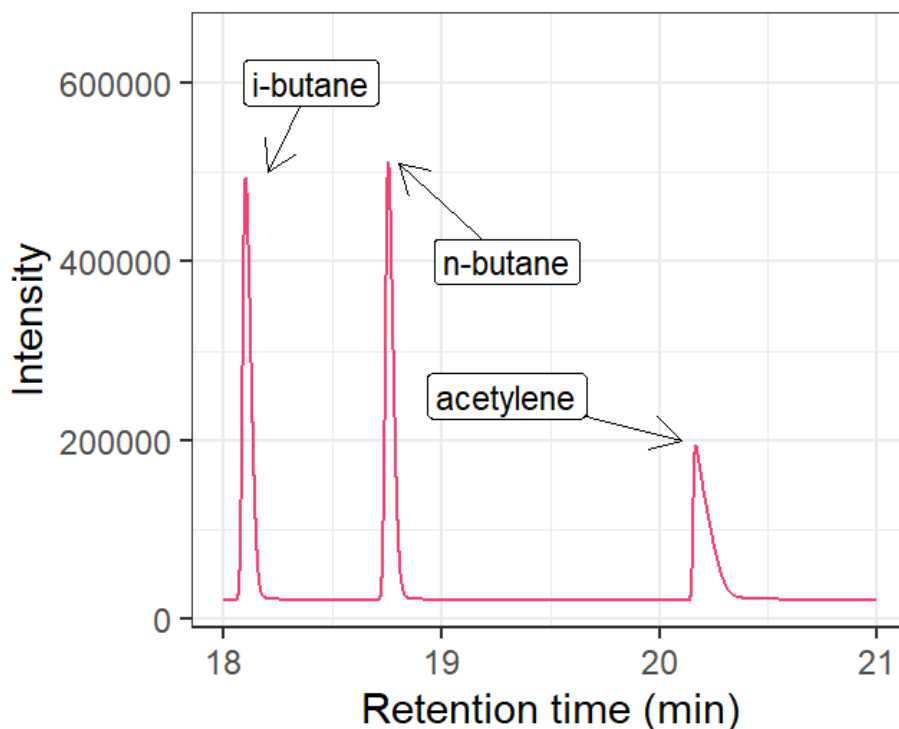


Figure 2.19: PLOT chromatogram scaled between 18 mins and 21 mins to show the elutions of *i*-butane, *n*-butane and acetylene.

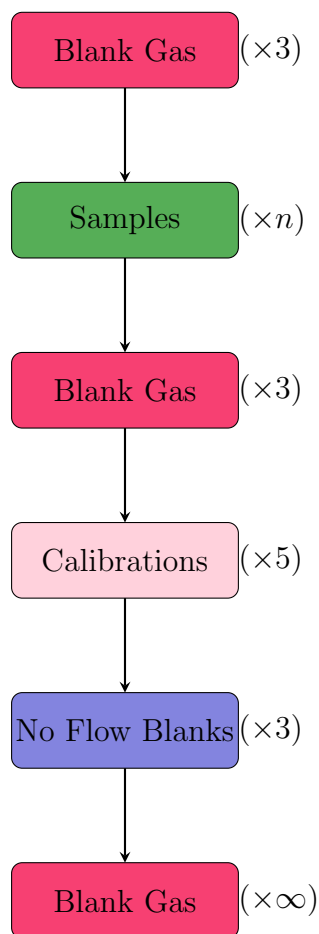
of 200 °C). The electron energy was 70 eV, and the quadrupole was set to scan between an  $m/z$  range of 30 and 150 units.

Chromatograms could be extracted for single  $m/z$  units, allowing for the deconvolution of overlapping peaks by separating elutions into constituent mass contributions. As the VF-WAX column is selective towards low-to-mid polarity species such as lower ( $C_2$  to  $C_6$  aldehydes and ketones,  $C_7$  to  $C_{12}$  hydrocarbons, monoterpenes,  $C_1$  to  $C_5$  alcohols), there were many elutions over the GC running method, some of which occurred simultaneously, thus are said to have co-eluted.

#### 2.1.6.10 Sample campaign sequencing

A standard sequencing procedure through a sampling campaign helps ensure valid cross-campaign comparisons. Throughout the works contained within this thesis, a common sampling sequence was used, as shown in scheme 2.2.

Blank gas was used to ensure that all TD traps were purged between sequence steps. In ambient indoor sampling campaigns, these blank gas sequence steps were included to ensure that comparisons could be made accurately with other campaigns that used this instrument,



Scheme 2.2: A flow schematic for the sample sequencing used throughout the works in this thesis.

some of which may have had much higher VOC concentrations and required the trap cleanup, which these blank gas steps achieved. In other campaigns which used this instrument and it was known prior to use that samples were likely to have high VOC concentrations ( $\gg$  ppm fractions), blank gas was run between the samples to ensure complete trap cleanup between samples. Details on the 'no flow blank' method are discussed in section 2.2.5. 500 mL of sample was drawn for each run, except in the no flow blank methods where no volume was drawn. For the analysis completed in chapter 6, only 25 mL of sample was drawn to avoid saturating the FIDs and QMS. Low sample volumes can cause larger errors in systems due to potentially unswept internal volumes, however the TDU used here had very low internal volumes, and each method included a purge step to sweep internal volumes with 150 mL of sample prior to introduction to the water and preconcentration traps. GC errors are discussed in section ??

Table 2.2: The VOCs contained within the multi-component calibration standard mix.

Species			
1,2,3-trimethylbenzene	1,2,4-trimethylbenzene	1,3,5-trimethylbenzene	1,3-butadiene
but-1-ene	acetylene	benzene	<i>cis</i> -but-2-ene
<i>cis</i> -pent-2-ene	ethane	ethene	ethylbenzene
<i>n</i> -hexane	<i>i</i> -butane	<i>i</i> -octane	<i>i</i> -pentane
isoprene	<i>m</i> -xylene	<i>n</i> -butane	<i>n</i> -heptane
<i>n</i> -pentane	<i>o</i> -xylene	propene	propane
<i>p</i> -xylene	toluene	<i>trans</i> -but-2-ene	<i>trans</i> -pent-2-ene

### 2.1.6.11 Data workup

The area directly underneath the peak of a chromatogram is proportional to the mixing ratio of the eluted species. Peak integration therefore is a crucial, albeit often overlooked, area of data workup. Manual integration of peaks can often result in reproducibility issues, and can be subject to several sources of error. For the works within this thesis, GCWerks (GC Soft Inc., CA, USA) was used to process chromatograms and TICs generated by Agilent Chemstation software.

## 2.2 Instrumentation and calibration

For the following experiments, the multi-component calibration mix detailed in table 2.2 was used. There were cases, as with LOD and LOQ calculations in later sections, in which the use of a precalibrated mix was necessitated. For other tests, the calibrated mix was still used because of the longevity testing of the instrument, which was completed separately from these works. Assessing instrument response over time requires the use of the same standard over a longer period of time. Each VOC within the calibration mix, made by the National Physical Laboratory (Teddington, UK), was mixed to a ratio of 4 ppb.

Here, the prefix *i*- was used to refer to isomers of the preceding species. The preferred IUPAC (International Union of Pure and Applied Chemistry) name for the isomerised species in this mix were: *i*-butane as 2-methylpropane, *i*-pentane as 2-methylbutane, and *i*-octane as 2,2,4-trimethylpentane. The prefix *n*- was used to specify that the preceding species was the unbranched, or 'straight-chain', form (*n*- being shorthand for 'normal'). Trimethylbenzene was shortened to 'TMB' in the figures for the following calibration to aid in the presentation of the graphics within the page margins and limits.

---

These following tests formed part of a larger, separate long-term calibration analysis for the instrument which was completed throughout this thesis. As such, a readily-available supply of a calibrated sample was required to ensure these tests could be completed several times over a span of several years and could be directly comparable with each other. The use of a calibrated mix with species other than hydrocarbons, such as oxygenated VOCs (OVOCs), would offer a deeper insight into the different behaviours of a variety of VOCs throughout these tests. However in the context of a multi-year instrument analysis within a busy laboratory, there was no guaranteed regular supply of a calibrated standard which contained this ideal blend of VOCs.

Important to consider would be the stability of the inclusion of OVOCs within a blend. All gas samples and standards have a shelf life, and for calibration cylinders this is typically a conservative estimation. Including OVOC species which would be ideal to analyse in the following tests, such as ethanol or methanol, would begin to present an issue with sample stability over time.<sup>[28,29]</sup> While inclusion of OVOCs would present a calibration somewhat more akin to indoor air, a short shelf life of the standard is a considerable financial restraint for a multi-year analysis. Additionally, consistent access to calibration standards for other commonly quantified species, such as monoterpenes, was limited. This was due in part to the shared use of a single monoterpene standard within a busy laboratory environment, meaning availability could not be guaranteed when required. With this all borne in mind, the standard calibration mix shown in table 2.2 was used for all the following calibration tests.

### **2.2.1 Sampling canister stability**

The sampling canisters used throughout the works in this thesis could be used to store samples for a theoretically infinite length of time. In longer, more complex sampling campaigns, it is a possibility that canisters would have to be stored for several days, indeed weeks, before the sample could be processed on the instrument, due either to logistical implications of transport or fitting the samples into a busy laboratory schedule. As such, the stability of samples in the sampling canister needed to be assessed.

For this test, six canisters were each filled from fully evacuated to 1 bar (gauge) with the multi-component calibration standard. Following the canister filling, initial samples were drawn immediately, and then the samples were left for up to 119 days to assess the stability of the samples throughout an elongated period of storage. Table 2.3 shows the sampling regimen over the testing period. There was a heavier bias towards the initial storage period (up to 22 days after filling) as this was more likely to be within the storage period of collected field samples. However, the testing period was extended beyond the typical  $\leq 1$  month period

seen in most stability tests<sup>[30,31]</sup> up to  $\approx 4$  months after filling. 100 mL of canister sample was drawn for each run for this assessment, to use minimal volumes of canister gas and aid in extending the test duration. Brass caps were added to each canister between uses and tightened to limit potential leaks.

Table 2.3: Sampling regimen for degradation testing of calibrated samples in sampling canisters.

	First sample	Second sample	Third sample	Fourth sample	Fifth sample
Day	1	12	22	109	119

Median canister mixing ratios were used for the degradation plot shown in figure 2.20. The fifth sample from one canister had to be discarded due to the canister valve having failed, leading to the canister leaking the sample and reaching ambient pressure, which resulted in the GC being unable to draw a volume of sample equal to the others. At the time of this sample being taken, blank gas was not readily available to re-pressurise the canister and allow for it to be run and quantified, and so for the fifth sample,  $n = 5$ , however for the remaining samples  $n = 6$ . A scaled version of figure 2.20 is shown in figure 2.21 to better highlight the degradation trend.

All species showed general stability throughout the tests, however as expected there was a decrease in species mixing ratio over time. While there was a large time gap between the third and fourth tests, the degradation appeared to be mostly linear throughout the sampling period, with regression slopes ranging from  $-0.002x$  to  $-0.005x$ , representing a sample degradation of between 0.002 and 0.005 ppb day<sup>-1</sup>. Aromatic and unsaturated species tended to experience higher rates of degradation than saturated species. Some species, specifically C<sub>2</sub> to C<sub>5</sub> hydrocarbons except acetylene and 1,3-butadiene, exhibited a somewhat more logarithmic-like decay, however within the sampling period the degradation did not significantly accelerate. Sample stability would also be dependent on other variables such as relative humidity and storage temperature, and it would be expected that species with higher reactivities such as OVOCs and monoterpenes would experience higher rates of degradation. As such, samples were not stored for longer than 21 days throughout the works in this thesis.

Species such as *p*-xylene and 1,2,3-trimethylbenzene exhibited an exponential-like degradation. The initially rapid degradation, however, was likely due to a reduced concentration of these species in the gas phase. This reduction was attributed to their preferential partitioning onto the internal walls of the canisters. In ambient indoor air, where relative humidity typically ranges between 30% and 70%, water vapor preferentially adsorbs onto the canister

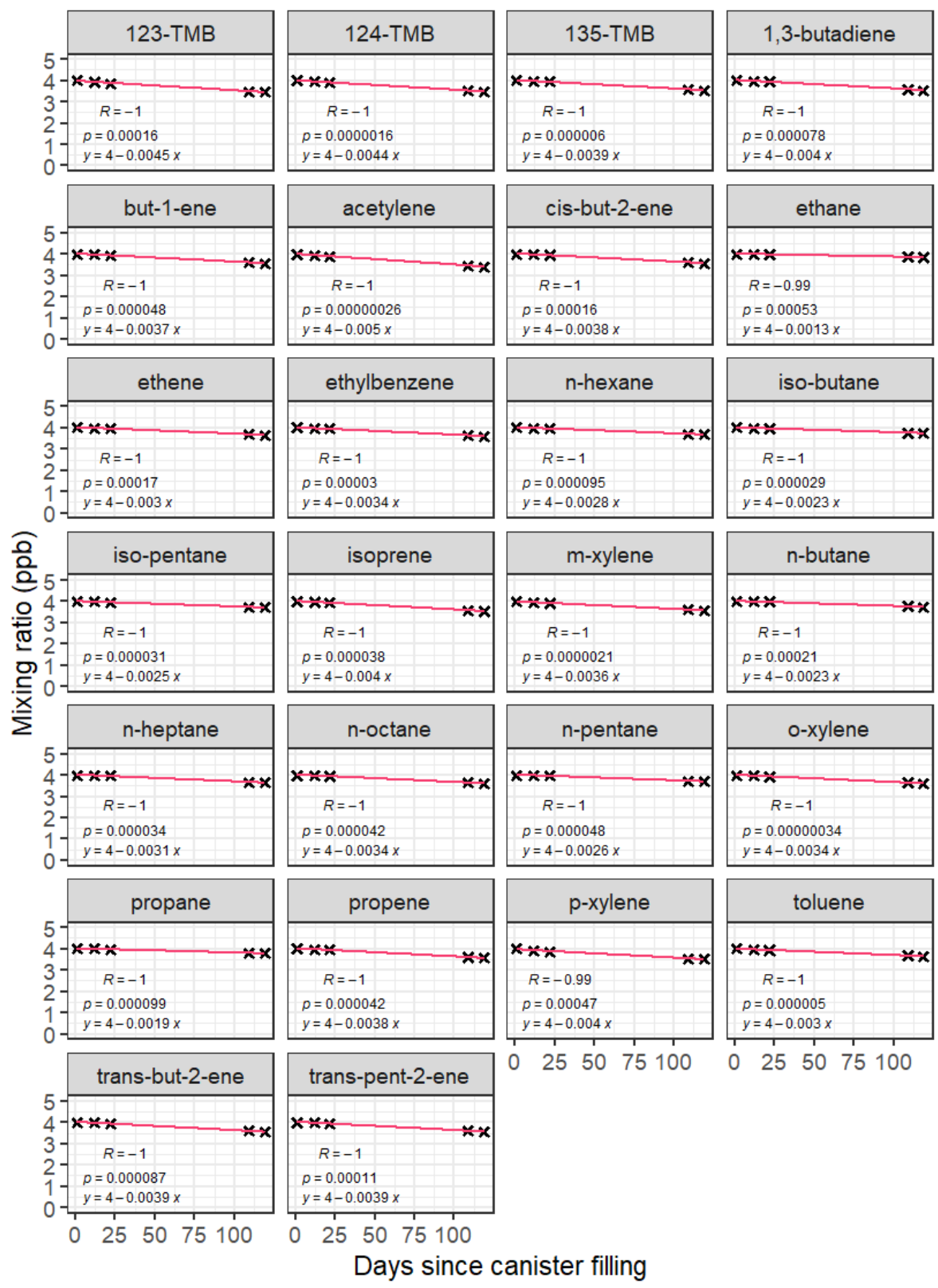


Figure 2.20: Scatter plots showing the changes in calibration mix concentration, with regression statistics and regression line equation calculated using Pearson's R.

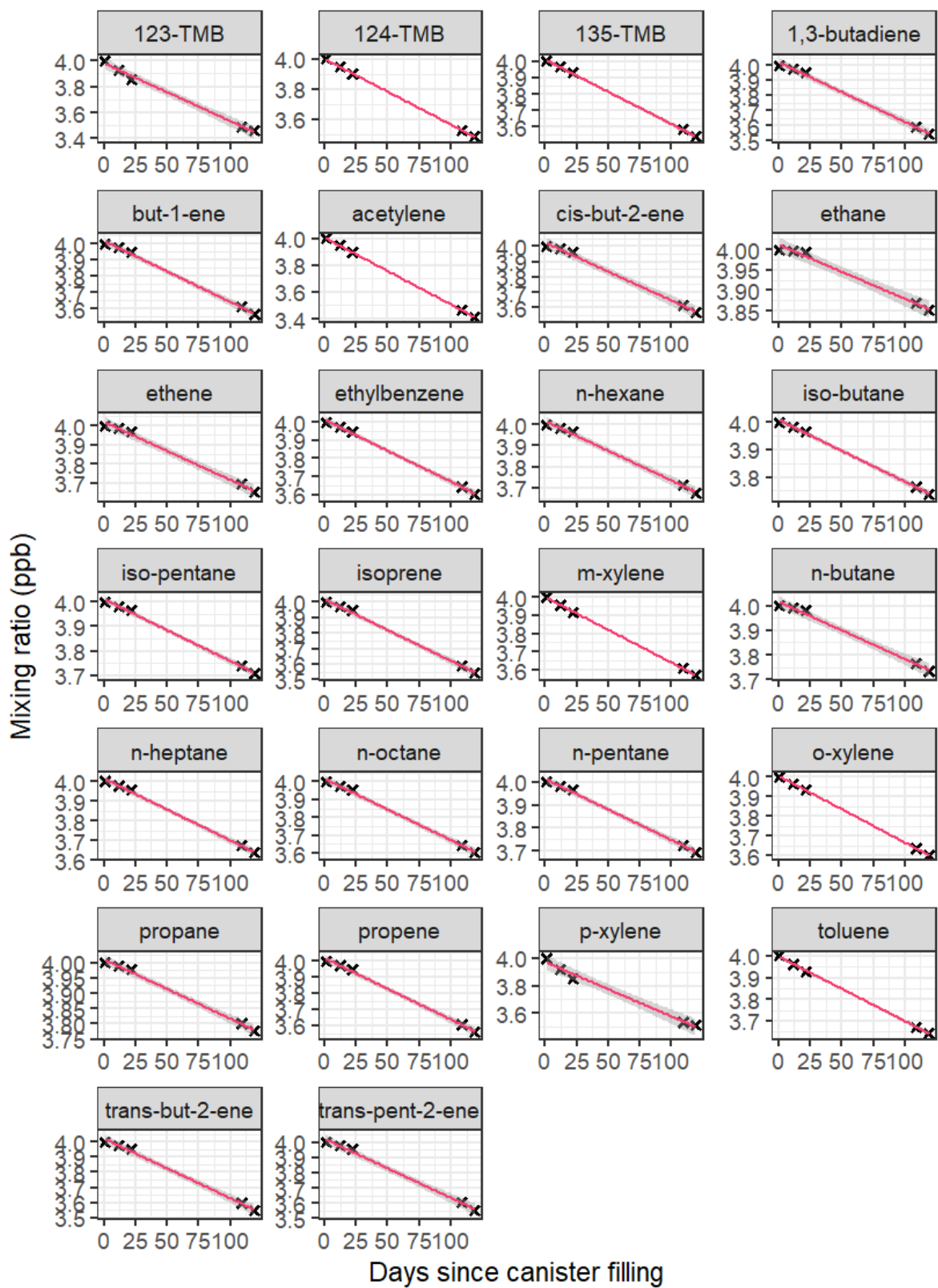


Figure 2.21: The degradation plots as in figure 2.20 without the regression statistics and with selective scaling for each individual plot to better show the trend in species degradation.

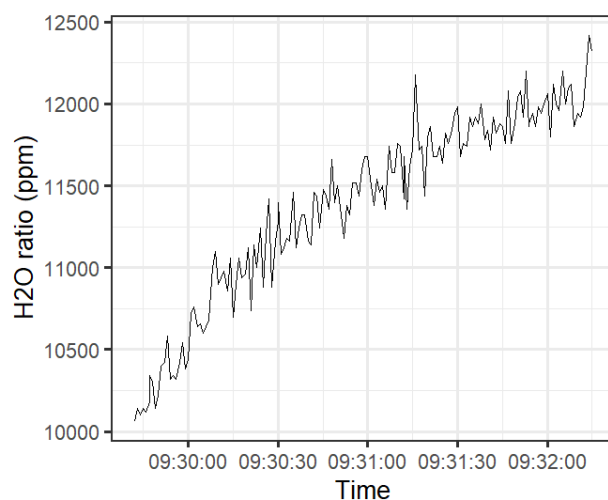


Figure 2.22: Real-time water vapour mixing ratio in a whole air canister sample. The canister was first pressurised to 1 bar (gauge) with blank gas, connected to the analyser and the canister valve opened.

walls over polar VOCs. As a result, in humid samples, these species would likely remain in the gas phase, preventing the partitioning behavior observed in figure 2.21. The partitioning of water vapor between the gas phase and canister walls is illustrated in figure 2.22. In this experiment, a whole air sample was collected in a 6 L evacuated canister, which was then pressurized to 1 bar (gauge) with blank gas. The canister outlet was subsequently connected to a greenhouse gas laser absorption analyser (Ultraportable Greenhouse Gas Analyser, Los Gatos Research Inc., CA, USA), and the canister valve was opened. Over time, the fraction of water vapor in the gas phase appeared to increase. As the canister pressure decreased, water previously adsorbed onto the walls re-entered the gas phase. While this confirms that canisters are best suited for humidified sampling, it also highlights that whole air sampling canisters are unsuitable for accurately reporting water vapor mixing ratios. In the degradation tests, the calibration standard was dispensed into evacuated canisters without prior humidification. Consequently, the more polar species likely underwent slight partitioning onto the canister walls.

## 2.2.2 Sample desorption

The selection of desorption temperatures for the preconcentration and focus traps will impact the analyte recovery. It is therefore crucial to assess ideal desorption temperatures to ensure a balance is struck between successful trap desorption without either sample degradation or retention. For the following tests, a range of temperatures were used to assess analyte desorption efficiencies.

---

The multi-component calibration mix was run over a sequence of decreasing desorption temperatures. PLOT and WAX column elutions are shown in figures 2.23 and 2.24 for the preconcentration trap, and 2.25 and 2.26 for the focus trap. In the following plots, the 'Control' temperature was the standard method temperatures referenced in sections 2.1.6.5 and 2.1.6.6 for the preconcentration trap and focus trap desorption, respectively. Chromatograms for all desorption temperatures are shown in totality on the left of each of the following four plots, with specific VOCs picked to show a closer analysis of each desorption temperature on the right of each plot. For PLOT column desorptions, acetylene and isoprene were chosen for the 'zoomed' plots: acetylene as it represents the most volatile of the VOCs analysed on the PLOT column and has often been seen to be among the first species to respond to calibration experiments, and isoprene due to it being a larger species with a much later elution. For WAX column elutions, trimethylbenzenes and benzene were picked: trimethylbenzenes, as they are more viscous than most VOCs analysed throughout these works and thus were more prone to smearing and band broadening through poor preconcentration and focus desorption, and benzene, due to its importance in IAQ and health impact assessments.

Irrespective of the temperatures used, even down to half the regular desorption temperatures, there was total analyte recovery throughout. Baseline noise was variable, however this was thought to have originated externally to the instrument, and there was no reason to believe this was due to the experiments being run. Noticeable on the PLOT column, there was a subtle but general shift in retention time for both acetylene and isoprene, seen here mostly as a change in the time elution maxima were detected. This is a display of band broadening, There additionally were artifacts found between 0 and 5 mins on the preconcentration desorption control chromatograms. These artifacts appeared at the same retention times on both PLOT and WAX columns, so were not due to a specific column elution. The cause was found to be a fluctuation in the FID hydrogen supply pressure, resulting in a baseline magnitude rise and decay.

Throughout the works within chapters 3, 4 and 5, the standard desorption temperatures given in sections 2.1.6.5 and 2.1.6.6 were still used, as while the results of desorption temperature variation showed total recovery at relatively low temperatures (when compared with the standard method), this was using a calibration mix and was not necessarily reflective of a regular ambient indoor sample. These experiments did however indicate that sample recovery should be expected to be very high (if not complete) for ambient indoor samples for a range of desorption temperatures.

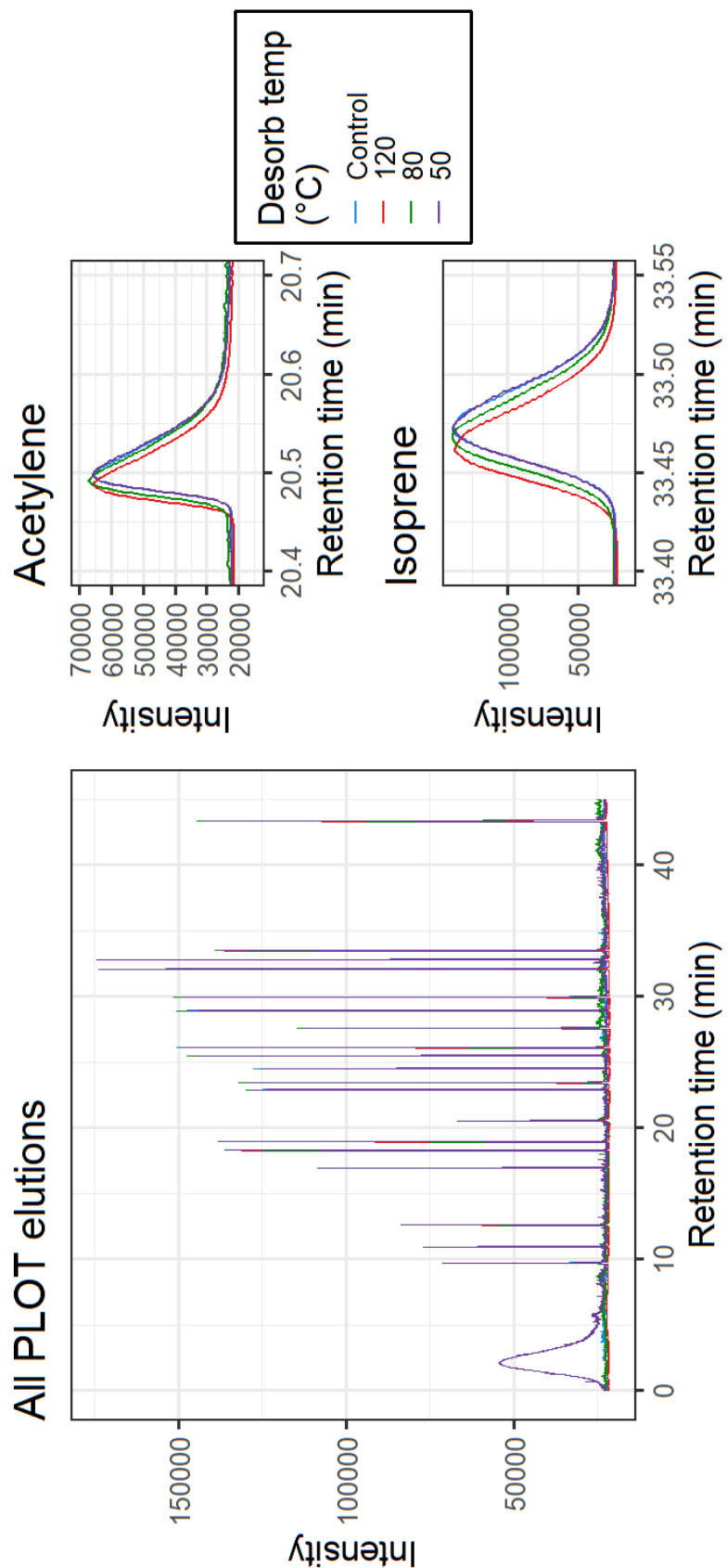


Figure 2.23: Layered chromatograms for PLOT elutions following preconcentration trap temperature variation.

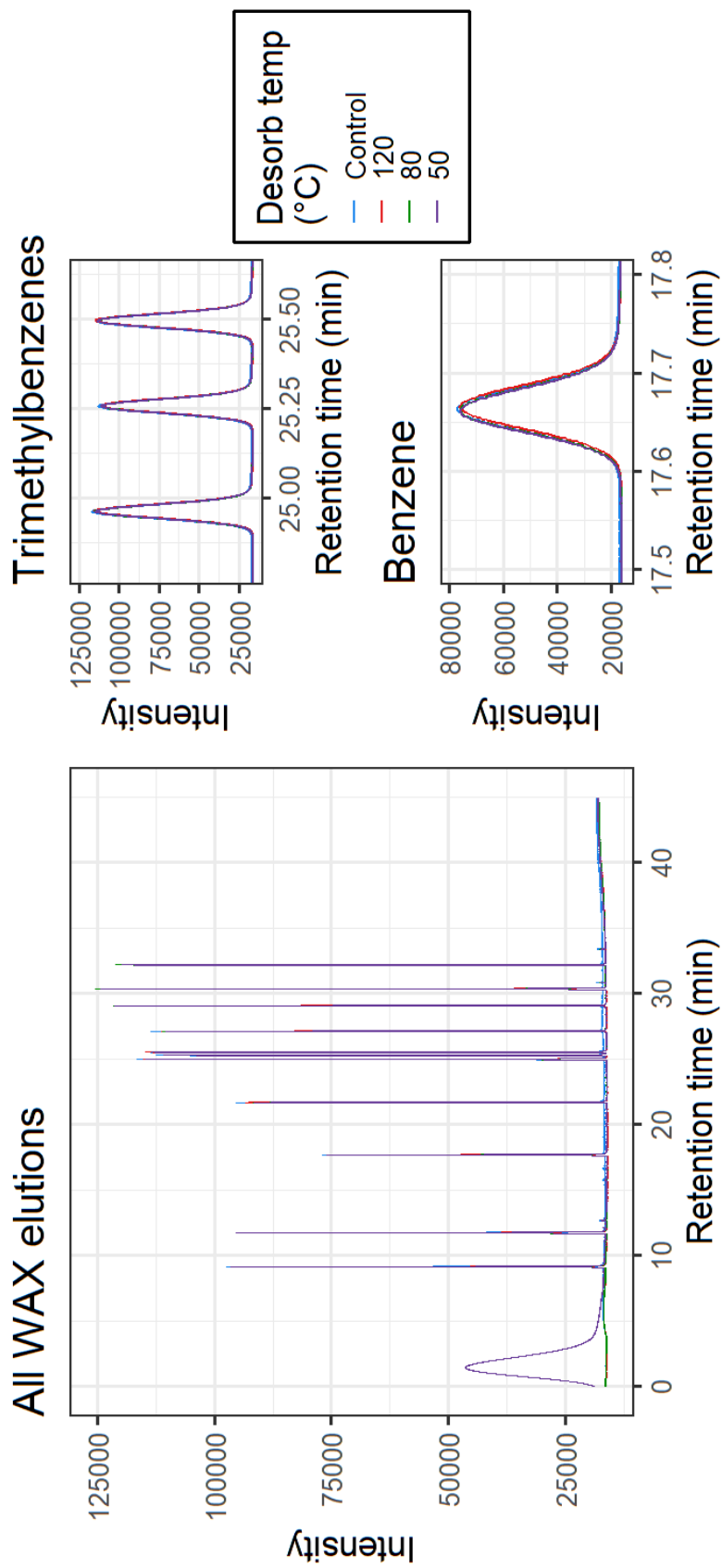


Figure 2.24: Layered chromatograms for WAX elutions following preconcentration trap temperature variation.

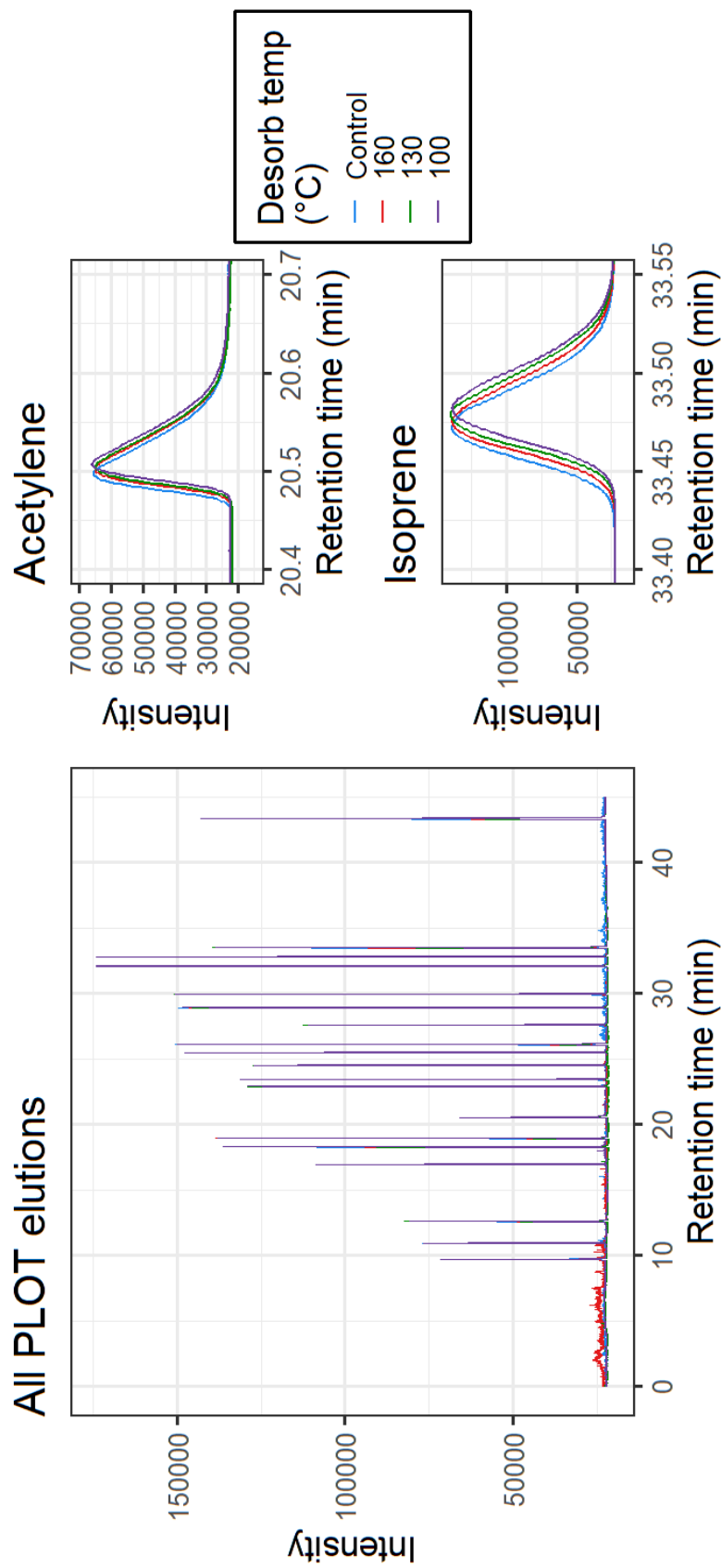


Figure 2.25: Layered chromatograms for PLOT elutions following focus trap temperature variation.

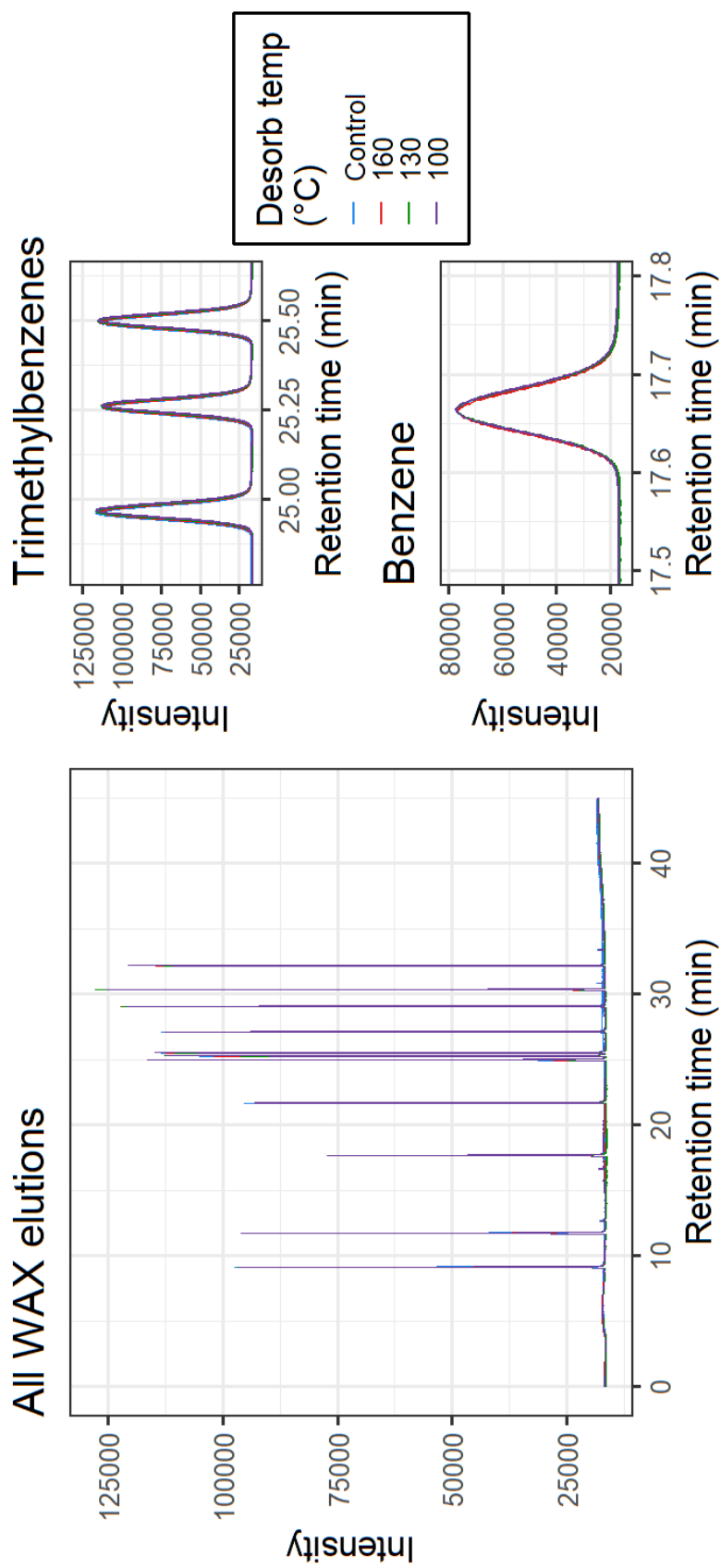


Figure 2.26: Layered chromatograms for WAX elutions following focus trap temperature variation.

---

### 2.2.3 Volume breakthrough

Dependent on the concentration of analytes within the sampled gas, samples of widely differing volumes will need to be drawn. A packed thermal desorber trap behaves like a small GC column, with analytes trapping at different rates, and migrating through the trap in the direction of the carrier gas flow. The breakthrough volume refers to the point at which so much sampled gas (or carrier gas) has passed through the trap, the analytes have traversed the length of the trap and have 'broken through', ultimately being swept by the carrier gas to purge. A low breakthrough volume indicates larger sample volumes will trap inefficiently resulting in inaccurate quantification for species which break through. This is important to consider is particularly concerning for VOCs at low ambient concentrations, where larger volumes may be required to produce a large enough signal to quantify. Large breakthrough volumes with linearity over a range of sample volumes are ideal, giving the user flexibility in the volumes of samples being analysed, resulting in the potential for analysis of samples with very low concentrations.

Figure 2.27 shows volume breakthrough testing for VOCs with a range of volatilities over a range of sampled volumes.

All species except ethene showed total linearity over volumes from 5 mL to 1000 mL. Ethene showed a somewhat logarithmic relationship between peak area and volume, indicating breakthrough. By applying a linear model to the data for ethene, the residuals of the model can be found. Segmented linear models were then applied to break the curved data for ethene into multiple separate linearities, shown in figure 2.28. A break in linearity was found to occur at  $V_{\text{break}} \approx 376$  mL. Concentrations returned from any analysis at sample volumes higher than  $\approx 376$  mL therefore indicate a lower measured concentration of ethene than was actually present in the sample. For this instrument, a compromise sampling volume of 500 mL was chosen to ensure sufficient signal strength for trace analytes such as monoterpenes, compounds of greater atmospheric relevance than ethene, despite the known breakthrough effects observed for ethene.

### 2.2.4 FID carbon-wise response

The response of FIDs to the carbon content of VOCs should be linear; that is, each carbon atom, depending on its neighbouring atoms, should yield a similar FID response, regardless of the parent molecule. Consequently, dividing the peak area by the ECN of the molecule responsible for the peak should result in a comparable response, regardless of the parent molecule. However, this is influenced by column retention features, such as peak tailing, as

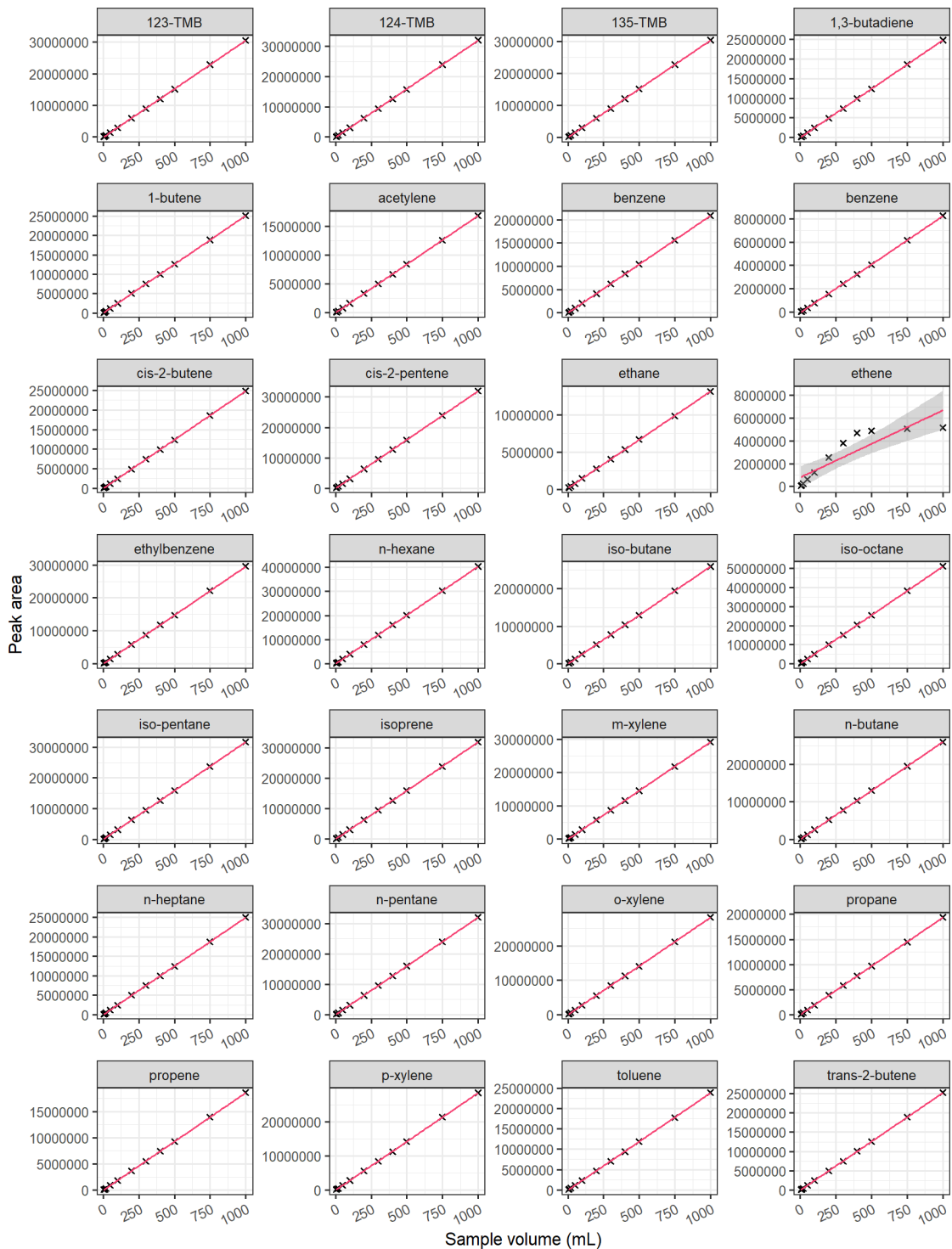


Figure 2.27: Facet wrapped plots of the linearity of peak area for calibrated gases with increasing sample volumes, from 5 mL to 1000 mL, using a 4 ppb multi-component standard. Regression statistics calculated using Spearman's Rho. Regression statistics for all species except ethene:  $R = 1$ ,  $p = <0.001$ . Ethene regression statistics:  $R = 0.89$ ,  $p = <0.001$ .

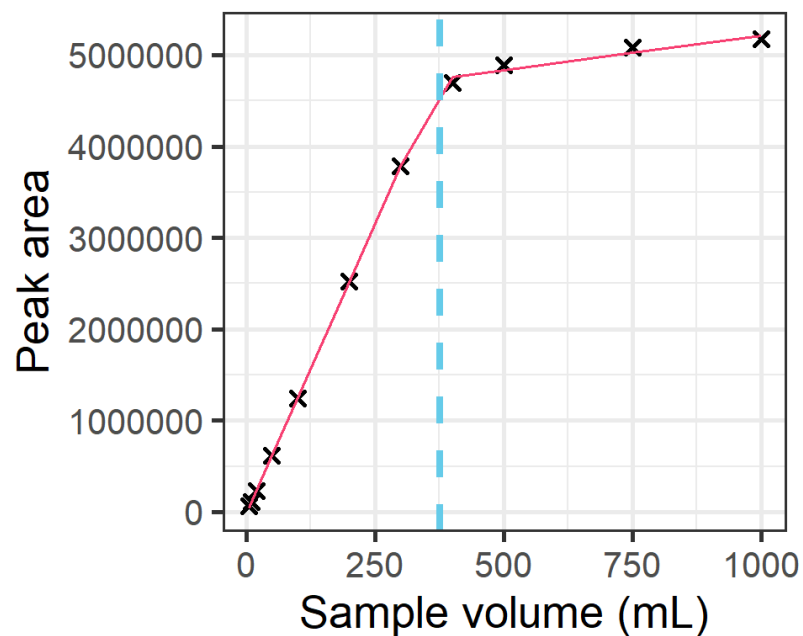


Figure 2.28: Segmented linear analysis of ethene peak areas against sample volume (mL). A vertical line is placed at the calculated breakthrough volume,  $\approx 376$  mL.

well as volume breakthrough at higher sample volumes.

To evaluate the responses of the FIDs, the multi-component calibration standard was analysed in triplicate using 200 mL samples. The carbon-wise response was then determined by dividing the FID peak area by the calculated ECN, as shown in Table 2.1. The various carbon-wise responses are presented in Table 2.4.

Table 2.4: A summary of carbon-wise responses from three sample runs using 200 mL samples of the multi-component calibration mix, including the column the VOC eluted from and the ECN used in the data workup. St. Dev. is the population standard deviation, while Rel. St. Dev. is the relative standard deviation, calculated by dividing the standard deviation by the average of the carbon responses, and displayed as a percentage.

Species	ECN	Sample run carbon response			St. Dev.	Rel. St. Dev. (%)	Eluting column
		1	2	3			
1,2,3-trimethylbenzene	9.0	1 764 455.556	1 660 706.222	1 670 462.556	46 778.193	2.75	VF-WAX
1,2,4-trimethylbenzene	9.0	1 699 437.778	1 742 098.778	1 746 852.556	21 319.580	1.23	VF-WAX
1,3,5-trimethylbenzene	9.0	1 627 264.111	1 658 901.889	1 664 912.667	16 514.277	1.00	VF-WAX
1,3-butadiene	3.8	3 226 417.632	3 225 643.158	3 222 394.474	1742.908	0.05	PLOT
but-1-ene	3.9	3 149 612.152	3 154 411.392	3 149 118.734	2387.197	0.08	PLOT
acetylene	1.9	4 330 627.895	4 366 067.368	4 359 418.421	15 380.577	0.35	PLOT
benzene	6.0	1 717 262.000	1 722 819.500	1 718 220.333	2425.708	0.14	VF-WAX
<i>cis</i> -but-2-ene	3.9	2 972 225.385	3 144 105.385	3 138 430.256	79 721.042	2.58	PLOT
<i>cis</i> -pent-2-ene	4.9	3 227 665.306	3 223 030.408	3 220 931.429	2813.323	0.09	PLOT
ethane	2.0	3 311 320.000	3 308 744.000	3 304 062.000	3004.357	0.09	PLOT
ethene	1.9	2 525 748.947	2 533 821.053	2 541 524.211	6440.811	0.25	PLOT
ethylbenzene	8.0	1 802 687.250	1 818 755.250	1 824 324.000	9173.274	0.51	VF-WAX
<i>n</i> -hexane	6.0	3 275 978.667	3 322 056.333	3 327 877.333	23 215.194	0.70	PLOT
<i>i</i> -butane	4.0	3 216 472.750	3 212 003.750	3 207 654.500	3600.146	0.11	PLOT
<i>i</i> -octane	8.0	3 153 415.500	3 150 913.750	3 151 886.750	1029.701	0.03	PLOT
<i>i</i> -pentane	5.0	3 106 640.000	3 141 385.000	3 139 305.600	15 911.493	0.51	PLOT
isoprene	4.8	2 825 832.708	3 277 890.208	3 277 623.333	213 039.074	6.81	PLOT
<i>m</i> -xylene	8.0	1 755 866.000	1 798 811.375	1 806 319.375	22 226.657	1.24	VF-WAX
<i>n</i> -butane	4.0	3 218 305.000	3 211 974.500	3 206 628.000	4772.754	0.15	PLOT

Continued on next page

Table 2.4: A summary of carbon-wise responses from three sample runs using 200 mL samples of the multi-component calibration mix, including the column the VOC eluted from and the ECN used in the data workup. St. Dev. is the population standard deviation, while Rel. St. Dev is the relative standard deviation, calculated by dividing the standard deviation by the average of the carbon responses, and displayed as a percentage. (continued)

Species	ECN	Sample run carbon response			St. Dev.	Rel. St. Dev. (%)	Eluting column
		1	2	3			
<i>n</i> -heptane	7.0	1 765 676.571	1 763 022.286	1 764 307.286	1083.790	0.06	VF-WAX
<i>n</i> -pentane	5.0	3 178 471.800	3 168 300.800	3 172 662.000	4166.308	0.13	PLOT
<i>o</i> -xylene	8.0	1 728 169.250	1 743 639.250	1 740 871.125	6735.652	0.39	VF-WAX
propane	3.0	3 213 656.333	3 208 790.667	3 209 134.000	2217.208	0.07	PLOT
propene	2.9	3 173 198.276	3 166 070.000	3 166 704.138	3221.254	0.10	PLOT
<i>p</i> -xylene	8.0	1 729 340.000	1 753 870.625	1 756 656.875	12 273.397	0.70	VF-WAX
toluene	7.0	1 674 028.714	1 676 926.000	1 671 565.571	2190.777	0.13	VF-WAX
<i>trans</i> -but-2-ene	3.9	3 190 486.667	3 189 322.564	3 187 347.692	1295.651	0.04	PLOT
<i>trans</i> -pent-2-ene	4.9	3 135 062.857	3 130 822.041	3 131 057.755	1945.962	0.06	PLOT

---

Excluding acetylene and ethene, the overall standard deviation of PLOT column elutions was 173716, representing a 5.5% relative standard deviation. The overall standard deviation of WAX column elutions was 51225, which represented a 3.0% relative standard deviation. WAX column elutions exhibited a lower carbon-wise response when compared to PLOT column elutions. However, in the context of this instrument where the WAX elution flow was split between the FID and the QMS, this would logically result in a lower FID signal for the WAX elutions.

While the carbon-wise response of both acetylene and ethene were internally consistent, they were not consistent with the other elutions on the PLOT column. It is known that the  $\text{Na}_2\text{SO}_4$  deactivation salt used on the PLOT column causes increased retention of both ethene and acetylene (as well as other species with higher number of unsaturated bonds, such as propyne and isoprene), which also causes peak tailing, as shown in figure 2.19 for acetylene. This causes issues when comparing these peaks with species with more symmetric elution profiles such as *n*-butane and propane. However, as the elutions of ethene and acetylene were consistent between runs and their carbon-wise response was internally consistent; this was simply a characteristic of the instrument.

While isoprene, 1,2,3-trimethylbenzene, and *cis*-but-2-ene exhibited comparatively higher standard deviations than the other species, this increased variance was confined to the first run of the sequence. No consistent or systematic cause for this anomaly was identified, and similar irregularities were occasionally observed throughout the studies described in this thesis. As such, the variation was attributed to sporadic, non-reproducible factors rather than any specific issue with the instrument. To ensure robust methodology, the calibration responses used for sample workup throughout this thesis were checked for variation, and results which varied greatly from the expected response were discarded.

### 2.2.5 System contamination

To assess any inherent contamination within the instrument, referred to here as 'system contamination', a method was developed to mimic a regular sampling run without drawing any sample through the TD ports. This method was coined the 'no flow blank'. In this method, the TD port selection valve was switched off, however the TD traps themselves were still cooled and heated at the regular temperatures and for regular times. Additionally, while the sample volume was set to 0 mL, the sampling time was set to the equivalent time a sample would be drawn over (for a 500 mL volume at a sampling rate of  $15 \text{ ml min}^{-1}$  this would take  $\approx 33.3$  mins). This resulted in an equal volume of carrier gas flowing through the traps as in a regular sampling run. The sampling time could easily be adjusted for the different vol-

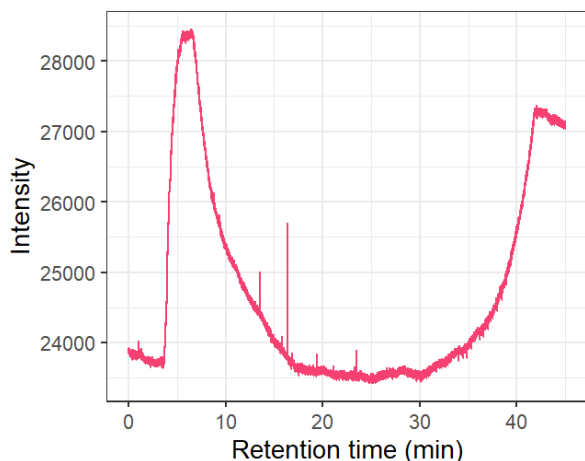


Figure 2.29: PLOT chromatogram for no flow blank method.

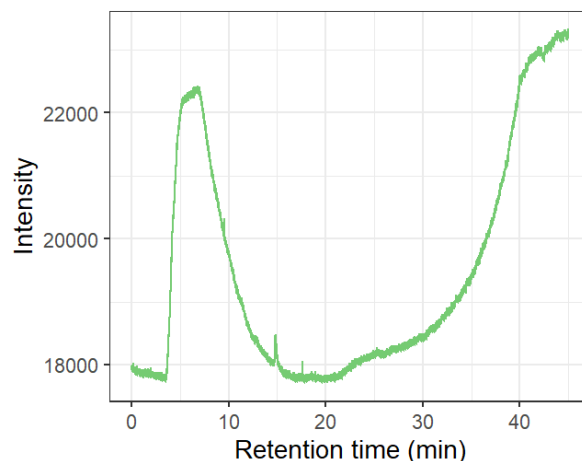


Figure 2.30: WAX chromatogram for no flow blank method.

umes taken by the instrument in other campaigns. This resulting chromatograms therefore allowed for analysis on any potential carrier gas or instrument contamination. Figures 2.29 and 2.30 show PLOT and WAX column elutions for a no flow blank method. There were several spikes in electrical signals in both methods, however these did not represent chromatographic elutions. The only elution was that of benzene, shown at  $\approx 15$  min in figure 2.30. Although not explicitly stated in the literature, this was colloquially an occurrence in similar instruments which utilise the trapping procedure laid out in this thesis, such as the GC-FID instruments at the Cape Verde Atmospheric Observatory and across the National Environment Research Council (NERC) Air Quality Network Supersites. In the studies contained within this thesis, the occurrence of benzene within the no flow blank method was included within the methodology, allowing for other researchers to investigate the origin of this feature.

Using process of elimination, as there was no sample being drawn, benzene could not have originated solely from the sampling manifold. Benzene contamination did not originate in the column, as benzene was still eluted after a VF-WAX replacement, shown in figure 2.31, albeit with a slightly shifted retention time. Overlaying with the TIC for the same run (figure 2.32 showed that the peak was still benzene, confirmed in the mass spectrum for the peak shown in figure 2.33. The presence of benzene in the TIC additionally ruled out that it originated from the FID hydrogen, makeup or air supply; a contamination from these sources would be detected as elevated baseline noise throughout the method as opposed to a singular elution. This finally left the possibility that the benzene originated from the carrier gas or

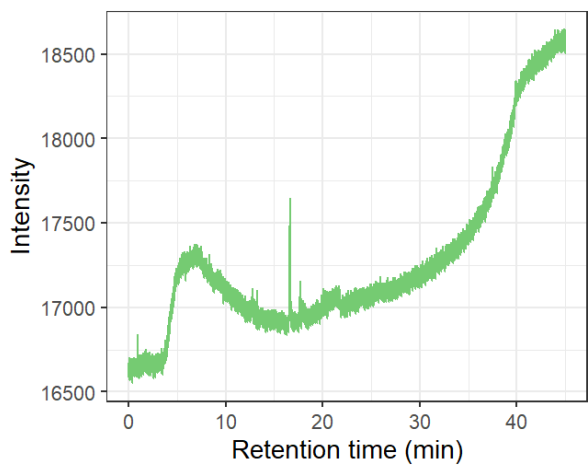


Figure 2.31: WAX chromatogram for no flow blank method following the replacement of the VF-WAX column.

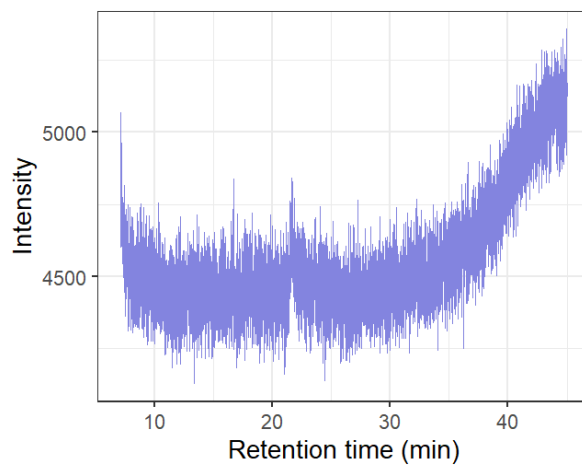


Figure 2.32: TIC for WAX elutions of the no flow blank method.

from somewhere within the TD.

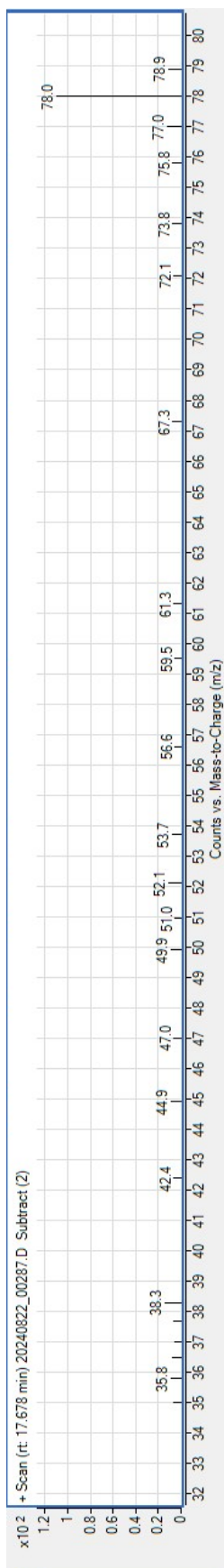


Figure 2.33: The mass spectrum produced from the suspected benzene elution at  $\approx 17$  min following background correction.

---

The carrier gas was usually purified by passing the carrier through a bed of platinum beads at  $\approx 300$  °C, through which any VOCs present would be fully oxidised to CO<sub>2</sub> and H<sub>2</sub>O. The presence of CO<sub>2</sub> from this purification process was attributed to the large rise and decay seen between  $\approx 4$  and  $\approx 15$  mins on chromatograms. Removal of this purification step (resultant WAX chromatogram shown in figure 2.31), but all other steps remaining the same between methods, resulted in the smaller rise and decay shown when comparing figure 2.30 and figure 2.31. However, the benzene elution still produced the same response. Given the reproducibility of the contamination and the likelihood this was an inherent contaminant through using this methodology (given the colloquial occurrence of this contamination throughout several similar instruments), the no flow blank method was used to correct whole air samples for system-related contamination. The inclusion of the no flow blank method in the sampling sequence, shown in scheme 2.2, resulted in whole air samples being effectively corrected for all known sources of contamination.

---

## 2.3 References

- [1] Keith D Bartle and Peter Myers. “History of gas chromatography”. In: *TrAC Trends in Analytical Chemistry* 21.9 (2002), pp. 547–557. DOI: [https://doi.org/10.1016/S0165-9936\(02\)00806-3](https://doi.org/10.1016/S0165-9936(02)00806-3). URL: <https://www.sciencedirect.com/science/article/pii/S0165993602008063>.
- [2] N H Ray. “Gas chromatography. I. The separation and estimation of volatile organic compounds by gas-liquid partition chromatography”. In: *Journal of Applied Chemistry* 4.1 (1954), pp. 21–25. DOI: <https://doi.org/10.1002/jctb.5010040106>. URL: <https://onlinelibrary.wiley.com/doi/abs/10.1002/jctb.5010040106>.
- [3] Edward M Fredericks and Francis R Brooks. “Gas chromatography analysis of gaseous hydrocarbons by gas-liquid partition chromatography”. In: *Analytical Chemistry* 28.3 (1956), pp. 297–303.
- [4] Spencer M Steinberg and David W Emerson. “On-line dechlorination–hydrogenation of chlorinated paraffin mixtures using GC and GC/MS”. In: *Environmental Monitoring and Assessment* 184.4 (2012), pp. 2119–2131. DOI: [10.1007/s10661-011-2104-9](https://doi.org/10.1007/s10661-011-2104-9). URL: <https://doi.org/10.1007/s10661-011-2104-9>.
- [5] Víctor Cutillas et al. “Beyond helium: hydrogen as a carrier gas in multiresidue pesticide analysis in fruits and vegetables by GC-MS/MS”. In: *Analytical Methods* 16.11 (2024), pp. 1564–1569.
- [6] William A McClenny et al. “Automated cryogenic preconcentration and gas chromatographic determination of volatile organic compounds in air”. In: *Analytical Chemistry* 56.14 (1984), pp. 2947–2951.
- [7] Yoko Yokouchi, Yoshinari Ambe, and Tsuneaki Maeda. “Automated analysis of C3-C13 hydrocarbons in the atmosphere by capillary gas chromatography with a cryogenic preconcentration”. In: *Analytical sciences* 2.6 (1986), pp. 571–575.
- [8] Maria Rosa Ras, Francesc Borrull, and Rosa Maria Marcé. “Sampling and preconcentration techniques for determination of volatile organic compounds in air samples”. In: *TrAC Trends in Analytical Chemistry* 28.3 (2009), pp. 347–361.
- [9] Nobuo Ochiai, Shigeki Daishima, and Daniel B Cardin. “Long-term measurement of volatile organic compounds in ambient air by canister-based one-week sampling method”. In: *J. Environ. Monit.* 5.6 (2003), pp. 997–1003. DOI: [10.1039/B307777M](https://doi.org/10.1039/B307777M). URL: <http://dx.doi.org/10.1039/B307777M>.
- [10] Gao Min and D M Rowe. “Improved model for calculating the coefficient of performance of a Peltier module”. In: *Energy Conversion and Management* 41.2 (2000), pp. 163–171. DOI: [https://doi.org/10.1016/S0196-8904\(99\)00102-8](https://doi.org/10.1016/S0196-8904(99)00102-8). URL: <https://www.sciencedirect.com/science/article/pii/S0196890499001028>.

- 
- [11] Faraz Afshari. “Experimental Study for Comparing Heating and Cooling Performance of Thermoelectric Peltier”. In: *Politeknik Dergisi* 23.3 (2020), pp. 889–894. DOI: [10.2339/politeknik.713600](https://doi.org/10.2339/politeknik.713600).
- [12] Chunfeng Song, Jingwen Lu, and Yutaka Kitamura. “Study on the COP of free piston Stirling cooler (FPSC) in the anti-sublimation CO<sub>2</sub> capture process”. In: *Renewable Energy* 74 (2015), pp. 948–954. DOI: <https://doi.org/10.1016/j.renene.2014.08.071>. URL: <https://www.sciencedirect.com/science/article/pii/S0960148114005412>.
- [13] Kyeong Ho Jang, Hong Seok Kim, and Seong Hyuk Lee. “Numerical analysis of free-piston stirling cooler systems for improving cooling performance”. In: *Case Studies in Thermal Engineering* 37 (2022), p. 102272. DOI: <https://doi.org/10.1016/j.csite.2022.102272>. URL: <https://www.sciencedirect.com/science/article/pii/S2214157X22005184>.
- [14] William E Wallace. *NIST Chemistry WebBook, NIST Standard Reference Database Number 69*. Gaithersburg: National Institute of Standards and Technology, 2024.
- [15] Susan Hennigan. “Method 21 monitors fugitive emissions”. In: *Environmental Protection* 4.9 (1993), pp. 22–23.
- [16] V Lebrun et al. “Landfill gas (LFG) fugitive emissions on landfill surface—Comparative test of on site analysis devices”. In: *International Waste Management and Landfill Symposium*. Sardinia, Apr. 2007.
- [17] C L Faiola et al. “Quantification of biogenic volatile organic compounds with a flame ionization detector using the effective carbon number concept”. In: *Atmospheric Measurement Techniques* 5.8 (2012), pp. 1911–1923. DOI: [10.5194/amt-5-1911-2012](https://doi.org/10.5194/amt-5-1911-2012). URL: <https://amt.copernicus.org/articles/5/1911/2012/>.
- [18] Andrew D Jorgensen, Kurt C Picel, and Vassilis C Stamoudis. “Prediction of gas chromatography flame ionization detector response factors from molecular structures”. In: *Analytical Chemistry* 62.7 (1990), pp. 683–689.
- [19] Benjamin Frank, Zai-Lai Xie, and Annette Trunschke. “Higher Alcohol Synthesis: Product Analysis Using the Concept of Effective Carbon Numbers”. In: *Chemie Ingenieur Technik* 85.8 (2013), pp. 1290–1293. DOI: <https://doi.org/10.1002/cite.201300006>. URL: <https://onlinelibrary.wiley.com/doi/abs/10.1002/cite.201300006>.
- [20] M Kállai and J Balla. “The effect of molecular structure upon the response of the flame ionization detector”. In: *Chromatographia* 56.5 (2002), pp. 357–360. DOI: [10.1007/BF02491945](https://doi.org/10.1007/BF02491945). URL: <https://doi.org/10.1007/BF02491945>.

- 
- [21] M Kállai, Z Veres, and J Balla. “Response of flame ionization detectors to different homologous series”. In: *Chromatographia* 54.7 (2001), pp. 511–517. DOI: [10.1007/BF02491209](https://doi.org/10.1007/BF02491209). URL: <https://doi.org/10.1007/BF02491209>.
- [22] Elizabeth Woolfenden. “Sorbent-based sampling methods for volatile and semi-volatile organic compounds in air: Part 1: Sorbent-based air monitoring options”. In: *Journal of Chromatography A* 1217.16 (2010), pp. 2674–2684. DOI: <https://doi.org/10.1016/j.chroma.2009.12.042>. URL: <https://www.sciencedirect.com/science/article/pii/S0021967309018470>.
- [23] Chiung-Yu Peng and Stuart Batterman. “Performance evaluation of a sorbent tube sampling method using short path thermal desorption for volatile organic compounds”. In: *J. Environ. Monit.* 2.4 (2000), pp. 313–324. DOI: [10.1039/B003385P](https://doi.org/10.1039/B003385P). URL: <http://dx.doi.org/10.1039/B003385P>.
- [24] Karen D Oliver William A. McClenny and E Hunter Daughtrey Jr. “Analysis of VOCs in Ambient Air Using Multisorbent Packings for VOC Accumulation and Sample Drying”. In: *Journal of the Air & Waste Management Association* 45.10 (1995), pp. 792–800. DOI: [10.1080/10473289.1995.10467409](https://doi.org/10.1080/10473289.1995.10467409). URL: <https://doi.org/10.1080/10473289.1995.10467409>.
- [25] Maxim Wilkinson et al. “Effects of high relative humidity and dry purging on VOCs obtained during breath sampling on common sorbent tubes”. In: *Journal of Breath Research* 14.4 (2020), p. 46006. DOI: [10.1088/1752-7163/ab7e17](https://doi.org/10.1088/1752-7163/ab7e17). URL: <https://dx.doi.org/10.1088/1752-7163/ab7e17>.
- [26] Alba Maceira et al. “New approach to resolve the humidity problem in VOC determination in outdoor air samples using solid adsorbent tubes followed by TD-GC-MS”. In: *Science of The Total Environment* 599-600 (2017), pp. 1718–1727. DOI: <https://doi.org/10.1016/j.scitotenv.2017.05.141>. URL: <https://www.sciencedirect.com/science/article/pii/S0048969717312445>.
- [27] A C Heeley-Hill et al. “Frequency of use of household products containing VOCs and indoor atmospheric concentrations in homes”. In: *Environmental Science: Processes and Impacts* 23.5 (2021), pp. 699–713. DOI: [10.1039/d0em00504e](https://doi.org/10.1039/d0em00504e).
- [28] Stephen Vaughan. “Gas Mixtures and Standards”. In: *Trace Analysis of Specialty and Electronic Gases* (2013), pp. 275–300.
- [29] Steve Scheuring and Daniel Bartel. “How To Buy Gas Calibration Mixes”. In: *LC-GC Europe* 18.10 (2005).
- [30] Thomas J Kelly and Michael W Holdren. “Applicability of canisters for sample storage in the determination of hazardous air pollutants”. In: *Atmospheric Environment* 29.19 (1995), pp. 2595–2608.

- 
- [31] Tanja J Schuck et al. “Stability of halocarbons in air samples stored in stainless-steel canisters”. In: *Atmospheric Measurement Techniques* 13.1 (2020), pp. 73–84.



# Chapter 3

## The impact of plug-in fragrance diffusers on indoor VOC concentrations

### 3.1 Declaration, contributions and conflicts

This chapter is based on the following publication:

Warburton T, Grange S, Hopkins JR, Andrews SJ, Lewis AC, Owen N, Jordan C, Adamson G, Xia B. The impact of plug-in fragrance diffusers on residential indoor VOC concentrations. *Environ. Sci.: Processes & Impacts*, (2023), **25**, 805-817. <sup>†</sup>

Note that figures 5, 8 and 9 from the original publication's electronic supplementary information (ESI) have been omitted from this thesis for brevity, and references to them in-text have been removed. These referenced the participant survey used to capture product use statistics, mean changes in VOC concentration separated by diffuser status (by treating each house as a separate series of samples), and total product use broken down into ventilation quantiles, respectively. All ESI figures remain freely available through the paper's DOI (see footnote).

In this work, ACL, TW, NO, CJ, BX and GA designed the original experiment. JRH and SJA developed the analytical instruments and methods and TW, JRH and SJA performed the laboratory analysis. TW undertook the data analysis and visualisations and SKG and

---

<sup>†</sup><https://doi.org/10.1039/D2EM00444E>

---

ACL guided the statistical and data methods. All authors contributed to the writing of the manuscript and the development of its conclusions.

NO, CJ, and GA are employees of Givaudan UK Ltd, Givaudan Fragrances Corp. and BX is an employee of Bath & Body Works, Inc. who are industrial suppliers of chemicals and finished household and personal care products. To support independence all analytical work and data analysis was undertaken by University of York and no restrictions placed on freedoms to publish. While the fragrance oil formulation was known to researchers at the University of York, the full composition is not disclosed in this work, aside from the identification of six detectable VOCs ( $\alpha$ -pinene,  $\beta$ -pinene,  $\gamma$ -terpinene, *p*-cymene, benzaldehyde, and eucalyptol) and the mass percentage contribution of  $\alpha$ -pinene to the total formulation. The fragrance oil is a modified, commercially available product, and due to commercial sensitivities and confidentiality agreements between researchers and industry partners, the complete formulation cannot be revealed.

## 3.2 Abstract

Plug-in fragrance diffusers are one of myriad volatile organic compound-containing consumer products that are commonly found in homes. The perturbing effects of using a commercial diffuser indoors were evaluated using a study group of 60 homes in Ashford, UK. Air samples were taken over 3 day periods with the diffuser switched on and in a parallel set of control homes where it was off. At least four measurements were taken in each home using vacuum-release into 6 L silica-coated canisters and with >40 VOCs quantified using gas chromatography with FID and MS (GC-FID-QMS). Occupants self-reported their use of other VOC-containing products. The variability between homes was very high with the 72 hour sum of all measured VOCs ranging between 30 and >5000  $\mu\text{g m}^{-3}$ , dominated by *n*/i-butane, propane, and ethanol. For those homes in the lowest quartile of air exchange rate (identified using  $\text{CO}_2$  and TVOC as proxies) the use of a diffuser led to a statistically significant increase (*p*-value < 0.02) in the summed concentration of detectable fragrance VOCs and some individual species, e.g.  $\alpha$ -pinene rising from a median of 9  $\mu\text{g m}^{-3}$  to 15  $\mu\text{g m}^{-3}$  (*p*-value < 0.02). The observed increments were broadly in line with model-calculated estimates based on fragrance weight loss, room sizes and air exchange rates.

---

### 3.3 Introduction

The use of room fragrance products is an acknowledged source of emission for a range of different volatile organic compounds (VOCs) indoors. Quantifying the emission rate characteristics and speciation of fragranced products is central to understanding how they may impact indoor air in real-world settings.<sup>[1]</sup> The wider health effects of VOCs indoors are well explored and documented; it is clear that long-term exposure to high concentrations of certain VOCs may carry with it an increased likelihood of experiencing negative health effects.<sup>[2]</sup> In 2019, Public Health England (PHE) released a set of recommended exposure limits for selected VOCs in indoor settings, based on literature data collated by Shrubsole *et al.*<sup>[3]</sup> Not all VOCs are included in these guidelines, unsurprising given that many thousands of different VOCs exist. For many VOCs there are still some basic uncertainties related to what are representative concentrations indoors, the variability between different indoor spaces, and the emission sources that control concentrations. VOCs such as monoterpenes (including  $\alpha$ -pinene and limonene) have particularly complex emissions. They are released from natural sources such as building materials, plants and food products and are also included as fragrance ingredients in many cleaning and personal care products. There is limited information on individual source strengths and a general lack of quantitative assessment of the contributions made to indoor VOCs from individual commercial products. This limits the development of regulatory and/or industry guidance and best practice that might be effective in managing VOC emissions and overall exposure.

Previous work evaluating the relationship between air fresheners, room fragrances and indoor air quality has been mixed, with only limited relationships found between air fresheners/room fragrance use and elevated VOC concentrations in real-world indoor residential settings.<sup>[4,5]</sup> This is in contrast to a larger number of laboratory studies which have evaluated emissions from air fresheners/room fragrances in (often smaller) test chambers, with marked increases in VOC concentrations after product use.<sup>[6,7]</sup> It has also been shown in test chambers that removal of room fragrance products, such as plug-in diffusers, results in a rapid decay in concentration of those VOCs derived from the fragrance formulation.<sup>[7]</sup> This is in contrast to real-world studies which have shown a lingering of VOCs indoors after products have been removed.<sup>[8,9]</sup> A possible reason for this discrepancy is the absence of representative surface materials such as building materials and room furnishings within test facilities – materials which may act as temporary reservoirs for VOCs. This surface sink effect can also be considered as a mechanism for VOC removal.<sup>[10]</sup>

The effects of exposure to high VOC concentrations are complex and varied, ranging from mild-to-moderate exacerbation of respiratory symptoms to cardiac rhythm interruption.<sup>[11–13]</sup>

---

While ambient concentrations typically found in residential settings are unlikely to contribute to widespread acute health effects, long-term exposure to VOCs in residential settings is less well evidenced in terms of impacts. Previous studies exploring links between the exacerbation of asthma symptoms and allergic reactions to VOC exposure have been inconsistent in their conclusions, and sometimes of poor design quality.<sup>[14]</sup> There are studies, however, which highlight the importance of monitoring indoor VOC concentrations to mitigate potential exacerbation of respiratory symptoms in vulnerable people.<sup>[15,16]</sup> Additionally, a recent study has shown a correlation between VOC metabolites, indicative of personal VOC exposure, and atopic dermatitis.<sup>[17]</sup>

Analytical approaches to sampling VOCs can vary in indoor air studies. Diffusive air sampling using sorbent-packed tubes remains a popular and low-cost option allowing for bulk testing. Sorbent tube sampling followed by thermal desorption (TD) and gas chromatographic (GC) methods remains the international standard for VOC identification in indoor and test chamber facilities, ISO 16000-6: 2021. However, there are limits to the VOCs that can be sampled, which are dependent on the sorbent materials used, as well as potential interferences and reduced species sensitivity from the co-adsorption of water and ozone.<sup>[18,19]</sup> Whole air sampling using silica-treated inert canisters is another possible technique and is used in this study. This uses a canister evacuated to vacuum, then exposed to either the test chamber, target room, or connected to a sampling gas line. With sorbent tubes air can enter through natural diffusion or be actively pumped. In vacuum-treated canisters air enters due to a differential in pressure, often through a fixed flow or critical orifice restrictor. Active sampling, either onto tubes, or using vacuum-treated inert canisters generally requires more expensive equipment however it offers a quantitative route to measuring the most volatile VOCs.<sup>[20]</sup>

The relationships between amount/frequency of chemical product use and total volatile organic compound (TVOC) concentrations found indoors are complex, with literature results varying between no relationships seen, to significant correlation between the two variables.<sup>[4,21,22]</sup> This is likely influenced by factors such as testing conditions, locations and sampling methods as well as being impacted by a lack of common methodology and speciation. Intuition would suggest that using VOC-containing products such as cleaning products or personal care products should increase VOC concentrations within the room the product was used in. Indeed, it has been found that VOCs typically found in cleaning products and VOCs emitted through cooking tend to dominate indoor air samples and include some fragrance VOCs.<sup>[23-25]</sup> Increases in frequency of cleaning and cooking activities in indoor settings might therefore be reflected in an increase in concentrations of specific marker VOCs.

---

Plug-in diffusers belong to the class of air fresheners, differing from most products in that fragrance output is kept constant over a period of time. These devices use mains electricity to deliver a constant low heat to aid in the diffusion of the fragrance oil through a wick. Some devices may have variable output settings, resulting in a varied emission rate. In this study the device used had a fixed output rate.

The effect of air change rate (ACR) on VOC concentrations is well established, with the relationship between the two inversely proportional; as ACR increases, indoor VOC concentrations decrease for constant indoor emission rates.<sup>[5,26]</sup> The relative influence of variable ventilation rates compared with varying usage of VOC-containing products is uncertain, in large part because individual activity- and product-based emission rates are not well defined and ACR is building- and occupant-specific. There has been some investigation of the relationships between temperatures, sink effects and ventilation rates on VOC concentrations, with results showing a dominance of ventilation over temperature and sink effects for short periods.<sup>[27]</sup> Using the methods employed in this study, the measurement of ACR in real settings requires key information for its calculation, such as internal and external carbon dioxide mole fractions/ppm, room occupancy, room volume, as well as CO<sub>2</sub> generation within the room.<sup>[28]</sup> This data can prove difficult to obtain for large scale residential indoor air studies, which often necessitates the use of proxy indicators for ACR.

CO<sub>2</sub> has long been used as an indicator for ventilation rates, both in terms of indoor pollutant exposure and risk to airborne-disease infection, which has been particularly prominent during the SARS-CoV-2 pandemic.<sup>[22,29,30]</sup> The work of Jia *et al.* (2021)<sup>[31]</sup> demonstrated a link between CO<sub>2</sub> and total VOC concentration in highly-occupied university lecture theatres, as well as a link between room occupancy levels and TVOC concentrations. This is potentially helpful as it means ACR, CO<sub>2</sub> mixing ratios and TVOC concentration may be inferred from one another, if only a subset of these data were available. We note however that the terminology and definition of TVOC is problematic in so much as it is operationally defined by the method of measurement and is rarely calibrated or directly comparable between studies. Whilst there is no universal definition of what TVOC means, it remains a widely quoted metric in indoor air studies, and despite the lack of comparability it has utility as a means for any study to express the totality of VOC behaviours. The methods used in this paper differ from Jia *et al.*, who used photoionisation detectors (PID) to evaluate TVOC concentrations, and nondispersive infrared (NDIR) sensors to measure CO<sub>2</sub> mixing ratios continuously. Here TVOC concentrations are calculated by summing all individually measured VOCs, and CO<sub>2</sub> determined through using laser absorption spectroscopy, both based on a 3 day sampling period. While the method in this paper does not show real-time

---

changes in atmospheric VOC composition related to changes in room occupancy, activities or product use, it does give a representative insight into summed VOC/CO<sub>2</sub> concentrations over time, and it illuminates whether the relationship shown by Jia *et al.* is seen in residential settings using an alternative methodology. A study by Murakami *et al.* (2019)<sup>[32]</sup> showed a weak positive correlation between TVOC and CO<sub>2</sub> concentrations in classrooms with air conditioning, however, the TVOC definition in the work of Murakami *et al.* differed again to that of Jia *et al.* These differences in measurement methods and operational definitions of TVOC does make comparison between studies difficult.

### 3.3.1 Objectives

The purpose of this study was to identify in real-world home settings the incremental impacts on ambient indoor VOC concentrations arising from using a single well-controlled VOC-emitting consumer product with known emission rate. The study was conducted across a group of 60 homes in Ashford, UK. Having established a baseline set of indoor VOC observations in all homes,<sup>[4]</sup> a commercially available plug-in diffuser was used releasing VOCs from a modified commercial fragrance formulation. The study split homes into those that would use the product (switched on), and those where it was switched off, the latter acting as a parallel control group. The use throughout of a control group was to account for any systematic and large-scale changes to ventilation rates arising from regional scale meteorological effects acting across the cohort as a whole, for example high windspeeds systematically increasing ACR or high/low temperatures leading to changes in window opening. The study explored the relationships between use of the plug-in diffuser, observed VOCs (both individual VOCs and summed VOC concentration), indoor CO<sub>2</sub> mole fraction (as a proxy for ACR) and wider self-reported chemical product use statistics from occupants in the homes.

## 3.4 Methodology

### 3.4.1 Experimental methodology

Homes were selected from a pre-existing non-trained fragrance industry panel cohort based in the Ashford area, UK. Each homeowner was given a commercially available mains-powered fragrance diffuser (referred to as ‘the diffuser’) with known liquid fragrance formulation. The fragrance was contained in a dipropylene glycol carrier liquid. Homes were split into two groups of 30 homes, each group studied over a four-to-five-week period. The first 30 homes were sampled between October and December 2021, and the second 30 homes between January and March 2022. Sampling was into 6 Litre stainless-steel canisters internally treated

---

with silica (Restek, PA, USA and Entech, CA, USA) attached to a flow restrictor to limit sample into the canister to 1 Litre every 8 hours ( $\approx 2 \text{ mL min}^{-1}$ ). Heeley-Hill *et al.* found these flow restrictors to sample linearly over a 48 hour period, with a reduced rate between 48 hours and 72 hours, achieving the full 6 L sample at ambient pressure after 72 hours.<sup>[4]</sup> Canisters were tagged with unique identifiers, evacuated to at least 0.1 Pa then sent for dispersal among the participants. Samples were taken over weekend periods, starting at 7 am on Friday and finishing at 7 am the following Monday. Filled samples were then returned for processing and analysis. Canisters were then evacuated once again, and the process repeated. Personal details relating to the participants and their homes were fully blinded to the University of York and anonymity of the participants maintained throughout the study.

At least four consecutive weekend samples were taken from each home:

1. an initial sample with the diffuser switched off (baseline sample),
2. a sample taken after the diffuser had been switched on at the start of the in-use period,
3. a further sample taken a week later from (2) where the diffuser remained switched on throughout and,
4. a final sample taken several days after the diffuser had been switched off (post-diffuser sample).

This gave as a minimum two ‘diffuser off’ samples and two ‘diffuser on’ samples for each home. 15 houses from each group provided a second post-diffuser sample two weeks after the diffuser was switched off.

On return to the lab the canisters were pressurised and thus diluted to 1 bar (gauge pressure) with highly purified air, free of VOCs. This diluent air was purified by passing compressed ambient air through a bed of platinum beads heated to 400 °C to fully oxidise any VOCs present. The same purified air was directly analysed by the instrument in order to quantify any impurities or interfering compounds contained therein (none were found). Samples were analysed using a custom thermal desorption unit (TDU) coupled to an Agilent 7890A gas chromatograph (GC) fitted with flame ionisation detectors (FID) and an Agilent 5977A quadrupole mass spectrometer (QMS) manufactured by Agilent Technologies, CA, USA (GC-FID-QMS). A flow chart for the system can be seen in figure 3.1.

Sample canisters and blank samples were connected to the TDU through a 16-port Valco microelectric actuator multi-position valve (VICI Valco Instruments Co. Inc., TX, USA). 500 mL was withdrawn from each sample and first passed through a water trap, comprising a 30 cm length of 1/16” silica-coated stainless-steel tube held at -40 °C, which removed

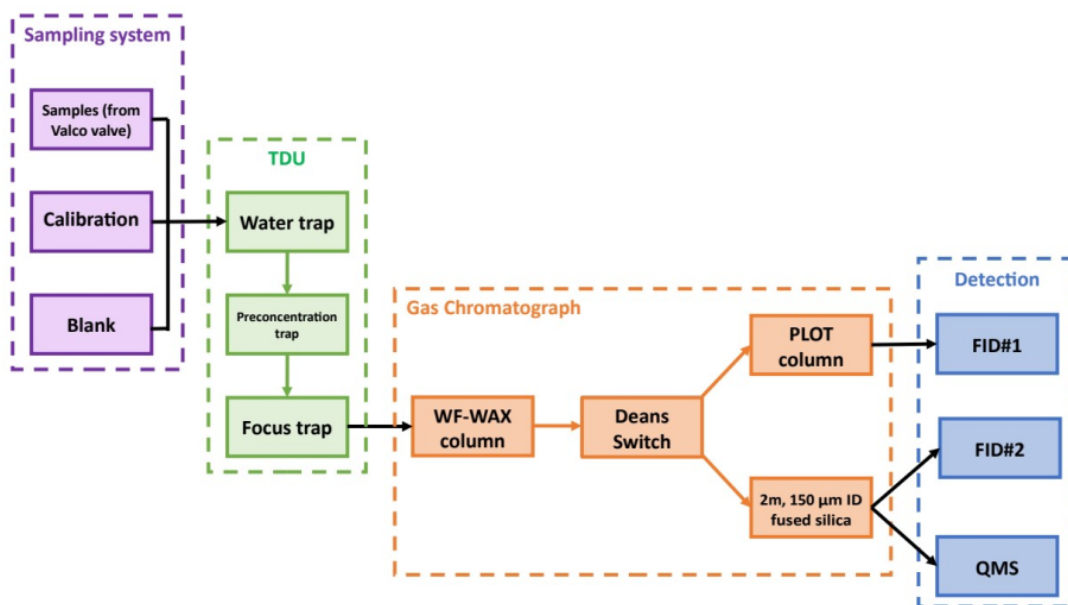


Figure 3.1: Flow schematic showing GCFIDQMS instrument setup.

moisture from the samples. The dried samples were then passed through a pre-concentration trap comprising a 30 cm length of  $\frac{1}{16}$ " silica-coated stainless-steel tube packed with both Carbpac<sup>TM</sup> X 40-60 mesh and Carbpac<sup>TM</sup> B 60-80 mesh adsorbents (Sigma-Aldrich, subsidiary of Merck KGaA, Darmstadt, Germany) fritted with glass wool and held at the lowest achievable temperature the unit could maintain, always less than  $-120$  °C. After sample collection, the pre-concentration trap was warmed to  $-80$  °C and purged with helium carrier gas (in the same direction of flow) for 4 minutes to remove  $\text{CO}_2$  from the trap which would otherwise interfere with the analytical method. The trap was then heated to  $190$  °C for 3 minutes in a flow of helium in the opposite direction of flow to desorb the volatile gases onto the focus trap. The focus trap comprised a 20 cm length of  $\frac{1}{32}$ " silica-coated stainless-steel tube packed with Carbpac<sup>TM</sup> X 40-60 mesh and Carbpac<sup>TM</sup> B 60-80 mesh adsorbents and held at the lowest achievable temperature the unit could maintain, always less than  $-120$  °C. Upon complete transfer of the analytes of interest, the focus trap was purged with helium and rapidly heated to  $200$  °C for 2 minutes during transfer to the GC oven for separation and analysis. During the GC analysis phase, the pre-concentration and focus traps were back-flushed with carrier gas and heated to  $230$  °C to remove any remaining organic material, in preparation for following samples, while the water trap was back-flushed and heated to  $100$  °C to remove any water.

Upon transfer into the GC oven, the analytes were initially passed onto a 60 m long,  $150$   $\mu\text{m}$  internal diameter (ID) VF-WAX column with a film thickness of  $0.50$   $\mu\text{m}$  (Agilent Tech-

nologies, CA, USA) at a flow rate of 1.6 mL min<sup>-1</sup> (carrier gas pressure of 35 psi). Initially, the unresolved analytes (C<sub>2</sub>-C<sub>6</sub> non-methane hydrocarbons/NMHCs) eluting from the WAX column were passed onto a Na<sub>2</sub>SO<sub>4</sub>-deactivated Al<sub>2</sub>O<sub>3</sub> porous-layer open tubular (PLOT) column (50 m × 320 μm ID, with a film thickness of 5 μm), via a Deans switch, for separation and detection by FID. After 8.3 minutes, the Deans switch was actuated to divert the analytes onto a length of fused silica (2 m × 150 μm ID) to balance column flows at the Deans switch and subsequently split between the second FID and the QMS for simultaneous detection via sections of 150 μm ID fused silica of length 0.91 m and 2.1 m, respectively. Quantification of VOCs was mostly completed using FID peak integration, however for some species QMS data was used when mass resolution was required to deconvolve overlapping peaks. MS quantification was limited to benzene, benzaldehyde, and all speciated monoterpenes and monoterpeneoids. A thirty-component mix of NMHCs in nitrogen (in the region of 4 ppb) provided by the National Physical Laboratory, Teddington, UK, cylinder number D933515 (hereafter referred to as ‘NPL 30’), was used for quantification of the components contained therein while equivalent carbon responses were used to quantify all other species. A table of which species were directly calibrated, and which used equivalent carbon numbers for quantification is shown in table 3.1. Direct calibration of monoterpene species was not employed in this study, owing to time constraints given the sequential timeline of the study and logistical implications.

Table 3.1: List of species quantified in this study and the quantification method used.

Species name	Quantification method
Ethane	Direct calibration using NPL 30
Ethene	Direct calibration using NPL 30
Propane	Direct calibration using NPL 30
Propene	Direct calibration using NPL 30
<i>i</i> -butane	Direct calibration using NPL 30
<i>n</i> -butane	Direct calibration using NPL 30
Acetylene	Direct calibration using NPL 30
But-1-ene	Direct calibration using NPL 30
<i>cis</i> -but-2-ene	Direct calibration using NPL 30
<i>i</i> -pentane	Direct calibration using NPL 30
<i>n</i> -pentane	Direct calibration using NPL 30
<i>cis</i> -pent-2-ene	Direct calibration using NPL 30
<i>n</i> -hexane	Direct calibration using NPL 30

*Continued on next page*

Table 3.1: List of species quantified in this study and the quantification method used (continued).

Species name	Quantification method
Isoprene	Direct calibration using NPL 30
<i>n</i> -heptane	Direct calibration using NPL 30
<i>n</i> -octane	Direct calibration using NPL 30
Ethylbenzene	Direct calibration using NPL 30
<i>m</i> -xylene	Direct calibration using NPL 30
<i>o</i> -xylene	Direct calibration using NPL 30
1,3,5-trimethylbenzene	Direct calibration using NPL 30
1,2,4-trimethylbenzene	Direct calibration using NPL 30
1,2,3-trimethylbenzene	Direct calibration using NPL 30
Benzene	Direct calibration using NPL 30
Toluene	Direct calibration using NPL 30
Styrene	Equivalent carbon number using toluene as reference
Acetone	Equivalent carbon number using toluene as reference
Acetaldehyde	Equivalent carbon number using toluene as reference
Hexanal	Equivalent carbon number using toluene as reference
Butan-2-one	Equivalent carbon number using toluene as reference
Methanol	Equivalent carbon number using toluene as reference
Benzaldehyde	Equivalent carbon number using toluene as reference
Ethanol	Equivalent carbon number using toluene as reference
Ethyl acetate	Equivalent carbon number using toluene as reference
Butyl acetate	Equivalent carbon number using toluene as reference
Propyl acetate	Equivalent carbon number using toluene as reference
Acetonitrile	Equivalent carbon number using toluene as reference
Dichloromethane	Equivalent carbon number using toluene as reference
$\alpha$ -pinene	Equivalent carbon number using toluene as reference
$\beta$ -pinene	Equivalent carbon number using toluene as reference
<i>D</i> -limonene	Equivalent carbon number using toluene as reference
Eucalyptol	Equivalent carbon number using toluene as reference
$\beta$ -terpinene	Equivalent carbon number using toluene as reference
$\gamma$ -terpinene	Equivalent carbon number using toluene as reference
$\delta$ -terpinene	Equivalent carbon number using toluene as reference

*Continued on next page*

Table 3.1: List of species quantified in this study and the quantification method used (continued).

Species name	Quantification method
3-carene	Equivalent carbon number using toluene as reference
$\beta$ -myrcene	Equivalent carbon number using toluene as reference
<i>p</i> -cymene	Equivalent carbon number using toluene as reference

Canisters were randomly selected for blank canister tests to ensure there was no carry-over between samples, and blank tests (using the highly purified air used to dilute canister samples) were interspersed in the sample sequence, along with NPL 30 calibrations. A typical sequence would see a group of 15 canisters run consecutively, followed by three blank runs, five NPL 30 calibration runs, and then further blank gas samples between sequences. All blank gas and NPL 30 tests also used 500 mL of gas. A selection of households from the second cohort of houses ( $n = 22$ ) were chosen after samples had been processed through GC-FID-QMS for analysis for carbon dioxide (CO<sub>2</sub>) mole fraction (measured in ppm). This was done by flowing the sample at 600 mL min<sup>-1</sup> into a laser absorption spectrometer (Ultraportable Greenhouse Gas Analyser, Los Gatos Research Inc., CA, USA), to 300 ppb detection limit at 1 Hz frequency.

Chromatograms were integrated using *GCWerks* software (GC Soft Inc., CA, USA) and using the NPL 30 standards, concentrations for each species were determined in  $\mu\text{g m}^{-3}$ . In total, 47 VOC species were quantified, of which six were known to be contained in the diffuser fragrance formulation. In this study, TVOC was defined as being the sum of all individual species found in a sample, although on many occasions only a subset of 47 VOC species were present in detectable quantities. As discussed in the introduction, it is important to note that TVOC as defined above is not a true representation of the absolute amount of reactive carbon content of the indoor air sampled, but is used here as a helpful metric that is reflective of the sum total concentration of the species quantified. Summing concentrations of all 47 species quantified might be better expressed as ‘sum VOC concentration’, however due to the pervasiveness of use of the term ‘TVOC’, it will continue to be referred to as such in this paper.

Occasionally chromatograms obtained from samples would present with disrupted elution of ethane, ethene and propane peaks, shown in figure 3.2. This effect was seen multiple times in each batch of 15 canisters, anecdotally associated with high CO<sub>2</sub> mole fractions. When this occurred, samples were re-run at lower canister pressures until a good chromatogram

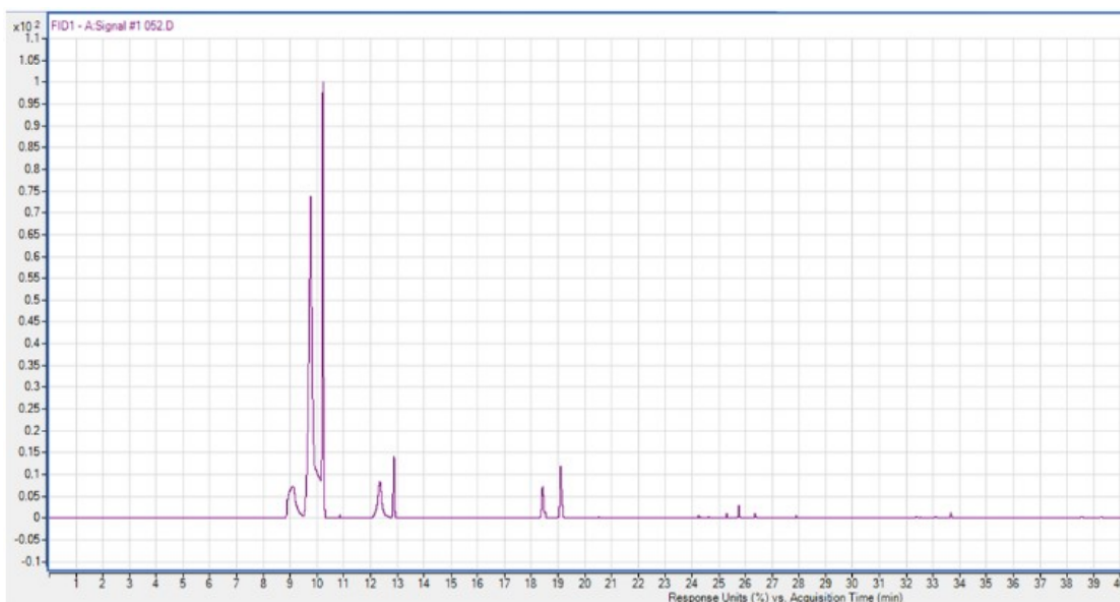


Figure 3.2: Porous layer open tubular (PLOT) column elutions of a canister air sample with signal strength/response units on y-axis and retention time (RT)/acquisition time on x-axis. The first three signals from the left show a split ethane signal starting at roughly RT 9 min and ending at roughly RT 10.2 min, ethene signal just before RT 11 min, and a split propane signal starting at roughly RT 12 min and finishing at roughly RT 13 min.

was produced. Figure 3.3 shows the same sample canister which produced the data in figure 3.2 but after being re-analysed. While this effect added time it was not detrimental to the overall data capture. A small number of samples ( $n = 3$ ) were discounted due to canisters not having taken a full sample (indicated by the canister not being at ambient pressure upon arrival at University of York). This was likely due to participants (all from the same home) not successfully opening the sampling valve. A small number of samples ( $n = 2$ ) were deemed spoiled as the canisters had been exposed to a leak from the diffuser during transport. After these samples were removed, this left a total of  $n = 259$  individual useable samples.

The fragrance formulation was known to the investigation team at University of York, however the formulation is commercially sensitive information and, beyond what is shown in this work, therefore cannot be disclosed in its entirety.

### 3.4.2 Statistical approach

All data processing and analysis was completed using the R programming language (v.4.1.3), through *RStudio* Software. Data manipulation was completed using packages contained within the *Tidyverse* collection of packages, mainly *ggplot2* and *dplyr*. Boxplots show values in the order of (from bottom-to-top): lower outliers, 5th percentile, 25th percentile, median

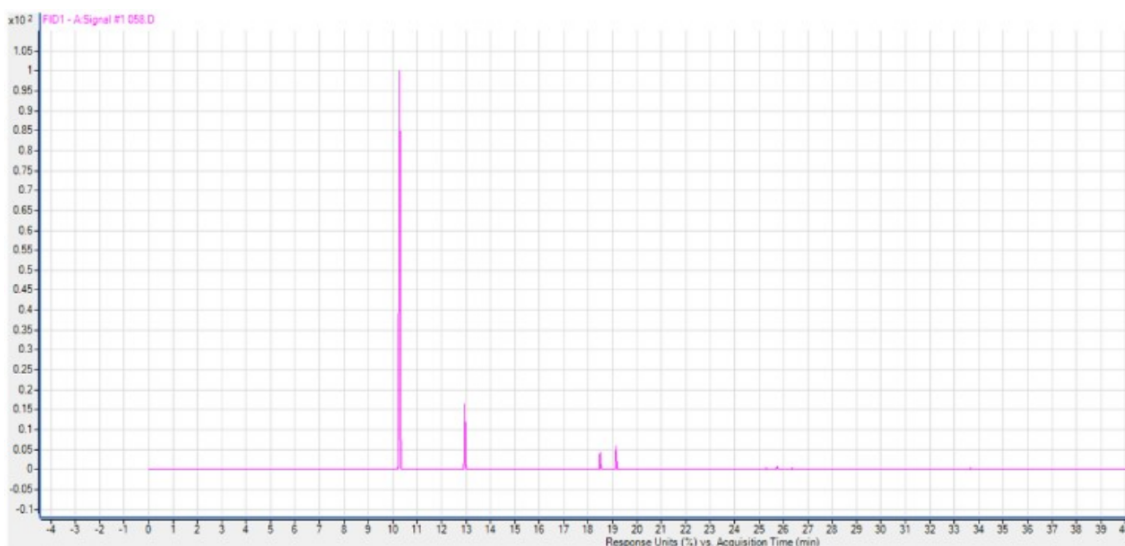


Figure 3.3: The same canister sample run in figure 3.2 run a second time, showing better signal responses and resolution. Only data obtained from figure 3.3 was used in data workup.

value, 75th percentile, 95th percentile, and upper outliers, along with mean values displayed as a red diamond on select boxplots. Statistical testing was completed using Wilcoxon signed-rank tests, using a confidence interval of  $\alpha = 0.95$ . Statistical significance using this approach was defined as a  $p$ -value yielded from a Wilcoxon signed-rank test lower than 0.05. Unless stated otherwise in the paper, it should be assumed this is our threshold for significance for all statistical testing done. Mean values were not used in data visualisation but were used in statistical testing. Tests were completed using the house the sample originated from as the identifier, so observations were aggregated into groups typically of 1 or 2, which would not yield a difference whether mean or median values were used in statistical testing. Sensitivity tests were completed using median values for statistical analyses however, which confirmed that both methods gave the same conclusions. Important to note is that while a change in species concentration may be of statistical significance, this does not necessarily mean the change in species concentration was large in absolute terms of  $\mu\text{g m}^{-3}$ . Correlation matrices were produced using the *corrplot* package using visual aids to help show correlations: a forward slanting blue line indicates a positive correlation, a full circle indicates no correlation, and a backward slanting red line indicates a negative correlation. A more intense colour and a narrower line indicates a stronger correlation (both for positive and negative correlations). Covariance analysis was completed through initially rescaling concentration and product use data from 0 to 1. Covariance values were then calculated and assigned, then rescaled from 0 to 100 using *BBMisc*. The matrix was then displayed graphically using the *tile* function in *ggplot2*. Diffuser increment plots were produced using the *raster* and *contour\_filled* functions in *ggplot2*, with additional contour lines and contour line labels added using the *contour2*

---

and *geom\_text\_contour* functions in the *metR* package.

TVOC concentrations were calculated as being the sum of all individually quantified VOC in each sample. These included C<sub>2</sub> to C<sub>8</sub> hydrocarbons, and a range of monoterpenes and oxygenated VOCs (oVOCs) such as esters and alcohols. An additional metric of ‘fragrance TVOC’ was defined as the sum of individual concentrations for  $\alpha$ -pinene,  $\beta$ -pinene,  $\gamma$ -terpinene, benzaldehyde, *p*-cymene and eucalyptol. Important to note however is that these six species do not reflect the total fragrance formulation, and there were many species within the fragrance which were not detectable in ambient air, owing to limits with the analytical method and often very low compound vapour pressures. For transparency, all data gathered, including survey answers, species concentrations and statistical test results, have been uploaded to the Centre for Environmental Data and Analysis (CEDA) repository.

### 3.4.3 Participant panel and survey

Each participant was provided with a tablet-based questionnaire which included questions on property and construction details, occupancy, participant activities and household VOC product use. Product use information was gathered on a cumulative basis over the 3 day sampling period. Product use statistics were limited to frequency of use of product types (*e.g.* paints, air fresheners, sealants *etc.*), and not brands or sub-types, or absolute quantities. Instructions on use of the sampler (how to open and close the sampling valve, and when) and where to place it were given in written form to the participants. The canisters were placed in the main living space within the house, in most cases the living room. Approximate distances between the diffuser and sampling canisters were reported by each participant. There was a 100% response rate to the survey.

## 3.5 Results

### 3.5.1 Individual VOCs and TVOC

Table 3.2 shows the median concentration, 5th percentile, 95th percentile and standard deviation for each of the 47 species, separated into diffuser off and diffuser on values for all 60 homes combined. Running Wilcoxon signed-rank tests were conducted on the aggregated data paired by the house the sample came from. Statistically significant increases (*p*-values for all following species were less than 0.05) in mean concentration were seen for 20 species, including  $\alpha$ -pinene, eucalyptol, ethanol, benzaldehyde and TVOC with the diffuser turned on. There were also statistically significant decreases (*p*-value for all following species were less

---

than 0.05) in aggregated mean concentrations, again paired by house, when the diffuser was turned on: acetone,  $\delta$ -terpinene,  $\gamma$ -terpinene and *o*-xylene. Figure 3.4 shows TVOC values graphically through boxplots, differentiated by diffuser off and diffuser on values.  $\alpha$ -pinene constituted  $\approx 5\%$  of the fragrance formulation and was the most volatile aroma compound by vapour pressure. The diffuser off and diffuser on values for  $\alpha$ -pinene can be seen in figure 3.5, alongside the emission-estimated diffuser  $\alpha$ -pinene increment. This increment is elaborated on later in the paper and compared to estimated values based on emissions rates, ACR and room sizes. To confirm that the diffuser was delivering a detectable fragrance, occupants were asked to note whether there was a perceivable odour. 55 homes had at least one occupant report a detectable fragrance attributable to use of the diffuser. For occupants that reported being unable to detect the fragrance, diffuser operation was alternatively confirmed by a negative mass-change (range of 5 g to 7 g of liquid fragrance lost), indicating that the lack of perceived fragrance may have arisen due to those individuals' odour detection response, or other factors such as a high ACR, or presence of other more dominant fragrance-emitting sources. All diffusers used in the study were confirmed to work before deployment. Statistical mean weight loss across all diffusers with available data, excluding those which leaked, was 6.84 g with a standard deviation of 1.93 g. Boxplots for other species as well as fragrance TVOC are shown in figure 3.6.

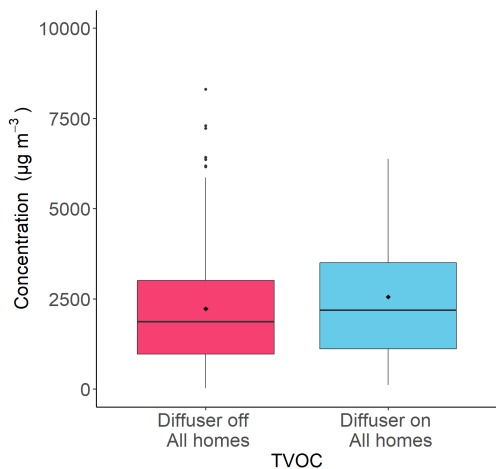


Figure 3.4: Boxplot showing the spread of TVOC values from 60 homes, differentiated by whether the diffuser was off or on. Outliers above  $10000 \mu\text{g m}^{-3}$  are removed from graphic to give equal presentation but are included in percentile calculations.

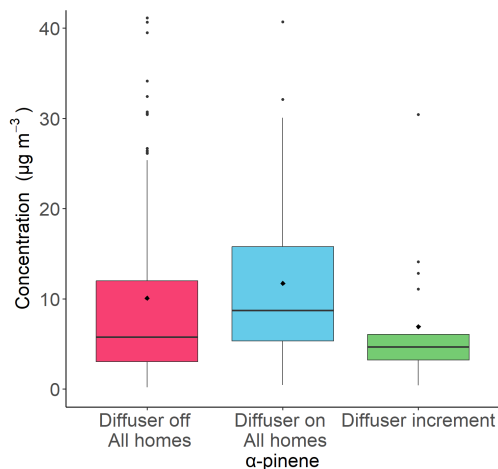


Figure 3.5: boxplot showing the spread of  $\alpha$ -pinene values, differentiated by whether the diffuser was off or on, along with the calculated  $\alpha$ -pinene increment. Outliers above  $40 \mu\text{g m}^{-3}$  are removed from graphic to give equal presentation but are included in percentile calculations.

Points and lines on boxplot from bottom up are as follows: low outliers as points (if present), 5th percentile, 25th percentile, median value as black line in middle of box, mean values as a black diamond, 75th percentile, 95th percentile, and high outliers (if present) as points.

Table 3.2: Median, 5th and 95th percentile and standard deviation values for all quantified VOCs, differentiated by diffuser status. All median and percentile values are expressed in  $\mu\text{g m}^{-3}$ .

Species	Median concentration		5th Percentile		95th Percentile		Standard deviation	
	Diffuser off	Diffuser on	Diffuser off	Diffuser on	Diffuser off	Diffuser on	Diffuser off	Diffuser on
ethane	6.9	8.5	1.9	3.4	160	140	100	94
ethene	1.2	1.3	0.34	0.45	4.1	4	4.8	6.5
propane	99	150	4.3	5.3	960	1300	330	400
propene	0.4	0.58	0.13	0.19	1.6	1.7	7.9	11
<i>i</i> -butane	120	210	2.1	4.2	1200	1300	380	390
<i>n</i> -butane	230	310	6.1	9.3	1300	1300	460	500
acetylene	0.35	0.47	0.17	0.24	1.3	1.7	0.81	1
but-1-ene	0.15	0.22	<0.1	<0.1	0.61	0.68	0.24	0.37
<i>cis</i> -but-2-ene	0.67	1.6	0.2	0.19	5.6	12	2.4	3.9
<i>i</i> -pentane	4.1	7.8	0.79	1.3	42	48	13	20
<i>n</i> -pentane	1.4	1.5	0.42	0.61	11	8	5.1	2.6
<i>cis</i> -pent-2-ene	<0.1	0.1	<0.1	<0.1	0.29	0.45	<0.1	0.18
<i>n</i> -hexane	0.23	0.29	0.12	0.15	1.2	0.92	0.83	0.28
isoprene	2.1	2.2	0.49	0.57	6.4	5.7	2	1.9
<i>n</i> -heptane	1.1	0.42	<0.1	0.12	6.4	3	2.3	1.1
<i>n</i> -octane	0.21	0.29	<0.1	0.11	1.6	4.7	1.3	1.9
Ethylbenzene	0.63	0.61	<0.1	0.12	3.4	4.8	6.7	1.9
<i>m</i> -xylene	0.62	0.73	0.17	0.21	2.7	4.5	4.5	2.1
<i>o</i> -xylene	1.5	0.68	0.18	0.1	23	4.4	8.1	19
1,3,5-trimethylbenzene	0.17	0.25	<0.1	<0.1	0.94	2.9	1	1.7
1,2,4-trimethylbenzene	0.76	1.1	0.28	0.2	3.1	3.8	1.6	1.9
1,2,3-trimethylbenzene	0.16	0.25	<0.1	<0.1	1.3	1.1	0.95	0.83
benzene	0.46	0.44	0.15	0.15	1.2	1.3	0.42	0.43
toluene	2.4	2.5	0.72	0.8	11	11	3.2	4.6
styrene	0.18	0.16	<0.1	<0.1	0.82	0.47	0.47	0.16

Continued on next page

Table 3.2: Median, 5th and 95th percentile and standard deviation values for all quantified VOCs, differentiated by diffuser status. All median and percentile values are expressed in  $\mu\text{g m}^{-3}$ . (continued)

Species	Median concentration		5th Percentile		95th Percentile		Standard deviation	
	Diffuser off	Diffuser on	Diffuser off	Diffuser on	Diffuser off	Diffuser on	Diffuser off	Diffuser on
acetone	36	36	13	14	150	130	81	150
acetaldehyde	11	11	3.7	3.8	28	24	52	7.3
hexanal	5.3	5	<0.1	<0.1	13	14	4.4	4.5
butan-2-one	4	4.5	0.85	0.86	21	31	8.5	11
methanol	48	49	16	11	160	170	49	58
benzaldehyde	0.17	0.18	<0.1	<0.1	0.36	0.38	<0.1	0.11
ethanol	730	1000	130	250	3100	2700	960	980
ethyl acetate	5.3	4.6	0.43	0.48	50	56	39	23
butyl acetate	1.4	1.5	0.21	0.15	20	18	20	15
propyl acetate	1.9	2.1	0.15	0.21	14	50	10	20
acetonitrile	7.5	6.1	1.6	0.32	16	37	10	18
dichloromethane	0.35	0.41	0.11	0.15	2.6	3.4	1.5	2.3
$\alpha$ -pinene	5.8	8.7	1.2	2.5	32	27	12	8.8
$\beta$ -pinene	1.5	1.8	0.4	0.46	8.2	5.3	4.8	1.9
<i>D</i> -limonene	8.9	10	1.4	1.6	38	40	14	18
eucalyptol	<0.1	<0.1	<0.1	<0.1	0.39	0.53	0.62	0.18
$\beta$ -terpinene	0.12	<0.1	<0.1	<0.1	0.64	0.64	0.46	0.23
$\gamma$ -terpinene	0.3	0.26	<0.1	<0.1	2.5	1.8	0.99	0.53
$\delta$ -terpinene	<0.1	<0.1	<0.1	<0.1	0.82	0.58	0.32	0.2
3-carene	0.63	0.61	0.13	0.13	3.3	2.7	1.2	1.4
$\beta$ -myrcene	0.18	0.19	<0.1	<0.1	0.72	0.7	0.25	0.46
<i>p</i> -cymene	0.78	0.68	0.23	0.24	2.9	2.5	1	0.84

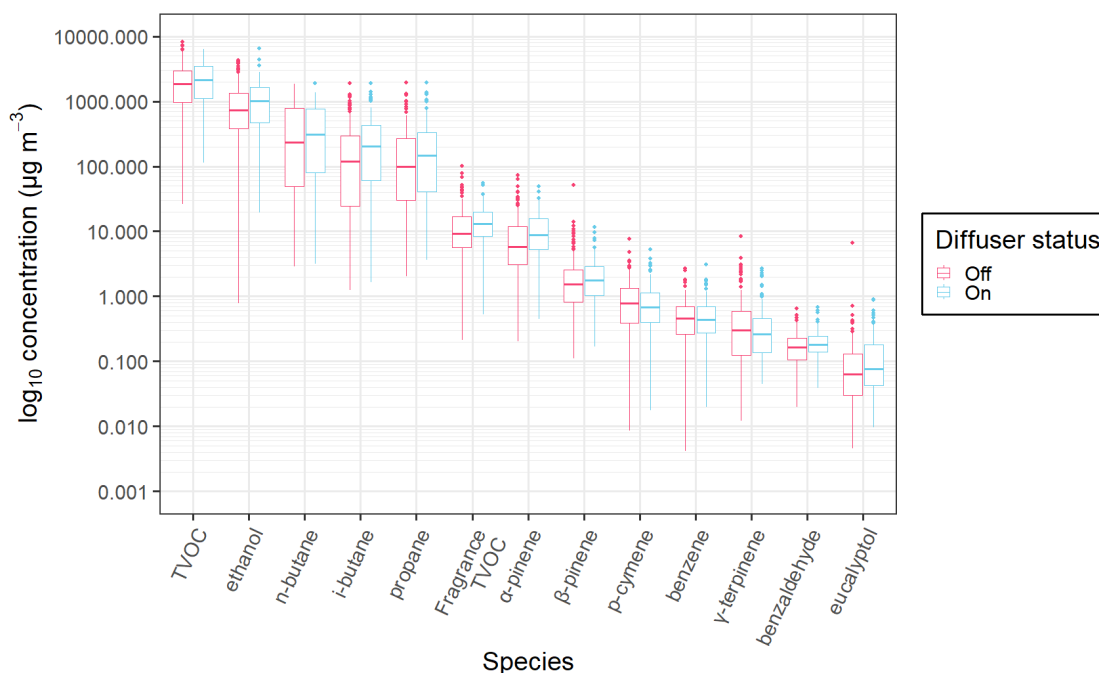


Figure 3.6: Boxplots showing different species concentration values, aggregated across all houses and separated by diffuser status, with  $y$ -axis  $\log_{10}$  transformation.

There are often common patterns for VOCs related to common emission sources, time of day/year, temperature, building materials and many other variables.<sup>[33–35]</sup> To study any correlation between quantified species, correlation matrices were constructed between all quantified species, shown in figures 3.7 and 3.8 for diffuser off and diffuser on correlations, respectively. Inter-fragrance VOC correlations were generally strengthened when the diffuser was turned on. Most fragrance VOCs exhibited a positive correlation with each other both with the diffuser off and when on. There were mostly positive correlations between other non-methane hydrocarbons (NMHCs)  $C_2$  to  $C_6$ , seen most strongly between  $C_2$  to  $C_4$  NMHCs. Species which show stronger correlations with each other mostly arise from similar sources, for example  $C_3$  and  $C_4$  hydrocarbons commonly derive from aerosols, monoterpenes from natural and fragranced products, and monoaromatic compounds from solvents and combustion of petroleum-derived fuels.<sup>[36–38]</sup>

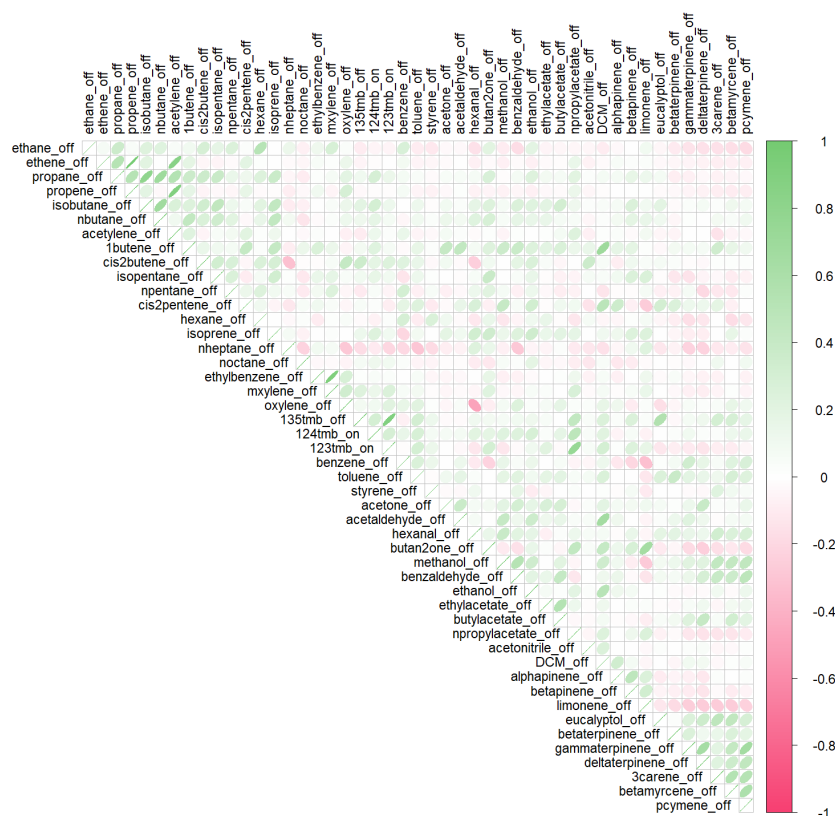


Figure 3.7: Correlation matrix showing inter-VOC correlations when the diffuser was off. A forward slanting green line indicates a positive correlation, a full circle indicates no correlation, and a backward slanting red line indicates a negative correlation. A more intense colour and a narrower line indicates a stronger correlation.



Figure 3.8: Correlation matrix showing inter-VOC correlations when the diffuser was on. A forward slanting green line indicates a positive correlation, a full circle indicates no correlation, and a backward slanting red line indicates a negative correlation. A more intense colour and a narrower line indicates a stronger correlation.

To assess the changes in individual species concentration when the diffuser was on versus off, Wilcoxon signed-rank tests were performed. These tests were initially conducted on aggregated values, differentiated by diffuser status, and statistics were paired by the house the sample was taken from. Taking observations on a home-by-home basis – that is treating each house as a stand-alone series of four/five samples – a further test can be made evaluating individually whether a simple increment or decrement in concentration was observed when the diffuser was turned on. Aggregating this simple binary outcome (VOC = higher or lower with the diffuser on) across all homes, it is possible to evaluate whether the occurrence of increments (or decrements) systematically varied by more than would be expected from random chance. This is shown for each VOC in figure 3.9, along with a marker to indicate

---

whether the deviation from chance is statistically significant. As discussed earlier, the tests completed to yield figure 3.9 used matched mean values, rather than median values. Most VOCs that showed an increment in concentration with the diffuser switched on by this simple binary metric were NMHCs C<sub>2</sub> to C<sub>6</sub>, and only eucalyptol from the fragrance species showed a statistically significant probability of being higher in a home with the diffuser on. Changes to all the other fragrance VOCs, other than  $\gamma$ -terpinene which showed a statistically significant decrease in probability of being higher in a home with the diffuser on, did not deviate by more than would be expected via random chance, however any changes seen in figure 3.9, whether of significance or otherwise, cannot be satisfactorily assessed to originate through diffuser use alone. Given the highly changeable nature of indoor air seen in this study, there may be background fluctuations which could influence the sampled concentration of a VOC. As such, changes of significance should not be presumed to arise through diffuser use alone.

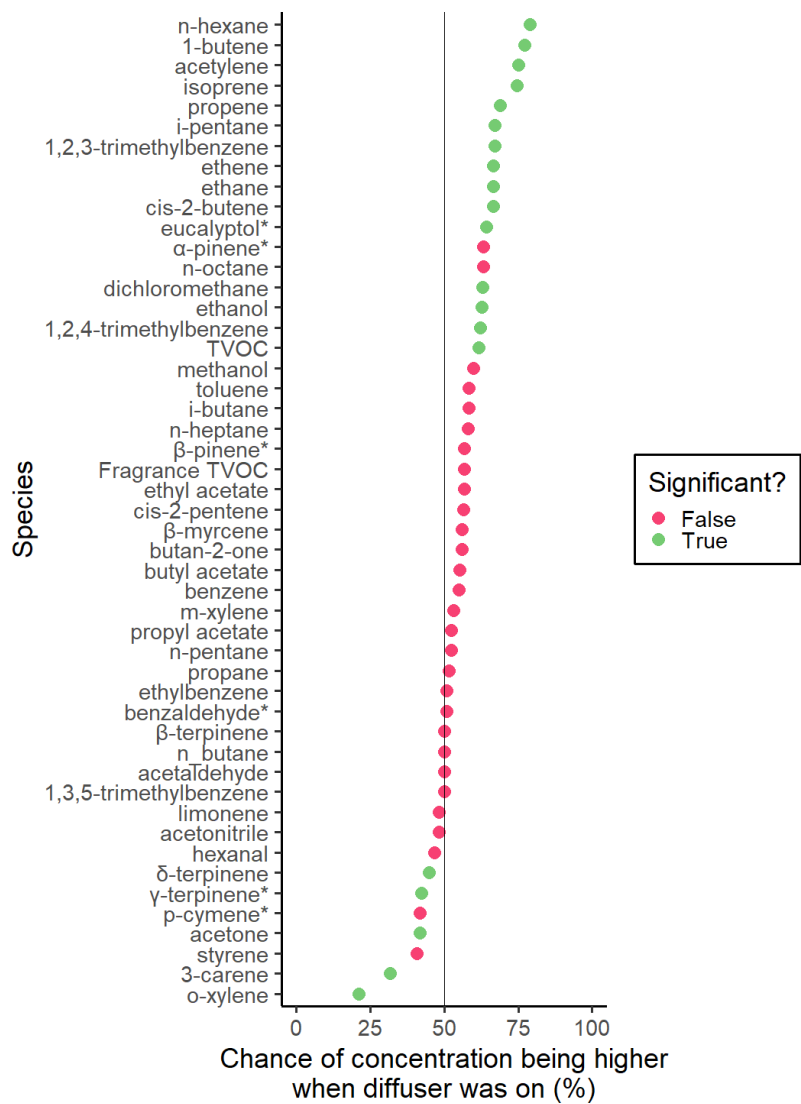


Figure 3.9: The percentage chance a VOC showing any increase in concentration when the diffuser was turned on. A fully random outcome (half the homes higher, half lower) would occur at 50%. Only those coloured green deviate from random chance by a statistically significant amount. \* denotes a species which was included in the fragrance formulation.

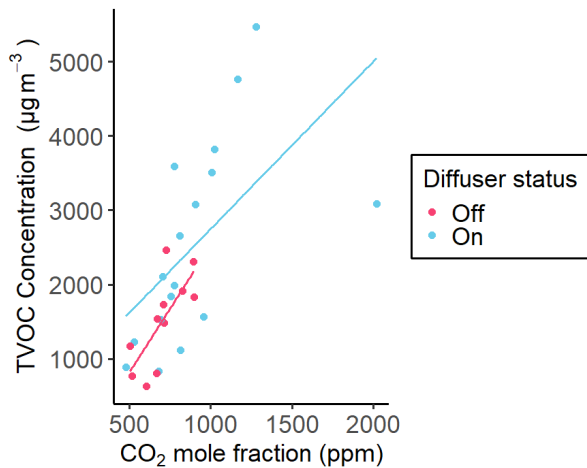


Figure 3.10: The relationship between CO<sub>2</sub> and TVOC. All measured values are included in the graphic and were included in the linear regression calculation. Diffuser off regression statistics:  $R = 0.74$ ,  $p = 0.0093$ . Diffuser on regression statistics:  $R = 0.58$ ,  $p = 0.014$ .

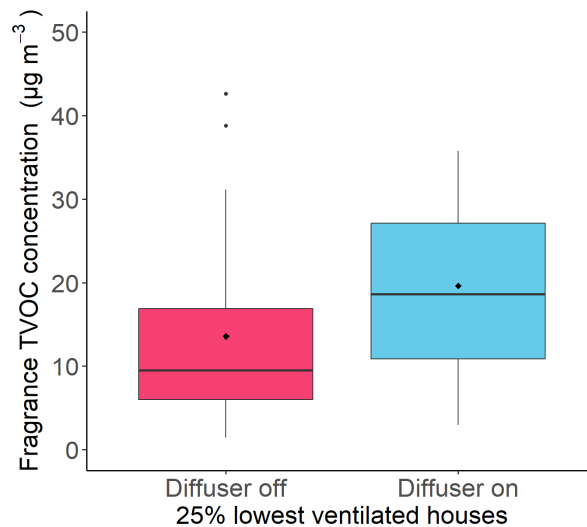


Figure 3.11: Boxplots showing the change in fragrance TVOC concentration when the diffuser was turned on for the houses with the poorest ventilation, the quartile with the highest baseline TVOC value. Outliers above  $50 \mu\text{g m}^{-3}$  were removed from the graphic to aid presentation, but were included in the calculation of quartiles and median concentration values.

### 3.5.2 Influence of CO<sub>2</sub>/ventilation on VOC exposure

72 hour time-integrated CO<sub>2</sub> mole fraction was quantified from a sub-set of houses ( $n = 28$ ) in the second cohort, ranging from 482 ppm to 2019 ppm. CO<sub>2</sub> mole fraction was compared against TVOC values from the same sample, shown in figure 3.10. Lines of regression were calculated using a linear model, with  $R$  and  $p$  values being calculated using Pearson's  $R$ . A positive correlation between CO<sub>2</sub> fraction and TVOC concentration is seen in both 'diffuser off' and 'diffuser on' samples. However, in the 'diffuser on' subset there was one outlier with a CO<sub>2</sub> fraction of 2019 ppm and a TVOC concentration of  $3084 \mu\text{g m}^{-3}$ , which deviates the regression line for 'diffuser on' samples away from 'diffuser off' samples. While the use of CO<sub>2</sub>-emitting products such as candles during this sampling window was not extraordinary, it should be noted that ambient outdoor temperatures in locality to the sampling cohort were lower than previous or following weeks. Indeed, most higher CO<sub>2</sub> fractions were recorded during this sampling period. This may have resulted in lower ventilation rates due to closing of windows and internal doors, or more-than-normal use of appliances such as gas fires.

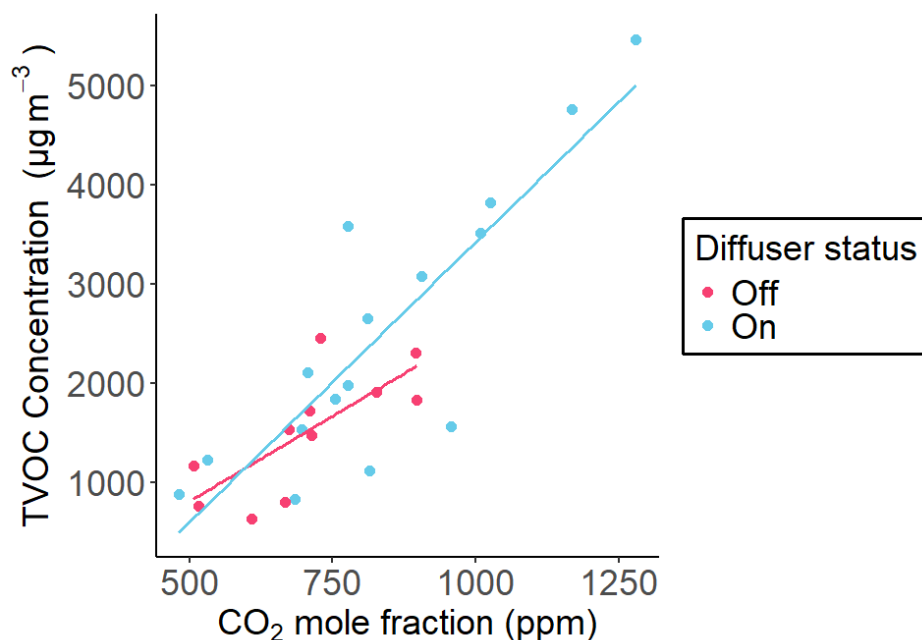


Figure 3.12: A repeat of figure 3.10, however with the outlier at CO<sub>2</sub> fraction 2019 ppm and TVOC concentration 3084 μg m<sup>-3</sup> in the 'diffuser on' subset removed, with linear regression statistics re-run. Diffuser off regression statistics:  $R = 0.74$ ,  $p = 0.0093$ . Diffuser on regression statistics:  $R = 0.86$ ,  $p = 0.000024$ .

Removal of this outlier still produces a plot which exhibits a positive relationship between CO<sub>2</sub> fraction and TVOC concentration, shown in figure 3.12. Removal of this outlier did not change the conclusions drawn from the relationship between TVOC and CO<sub>2</sub> in this dataset, and so to maintain transparency the outlier was left in the dataset.

Since CO<sub>2</sub> data was only available for a subset of samples, but TVOC concentrations were available for all samples, quartiles were constructed using baseline TVOC concentration as an indicator of ACR, based on the relationship seen in figure 3.10 and with CO<sub>2</sub> used as the ACR proxy. Only baseline data were used to infer ACR to remove any potential circular influence of the diffuser itself. To construct the quartiles, samples were ranked from highest to lowest baseline TVOC: Q1 (highest 25% baseline TVOC concentrations) to Q4 (lowest 25% baseline TVOC concentrations). The change in fragrance TVOC concentration when the diffuser was turned on for Q1, the 25% of homes with notionally the lowest ACR are shown in figure 3.11. For homes in the lowest ACR quantile, the sum of fragrance VOCs doubled for 'diffuser on' samples, a statistically significant increase ( $p$ -value < 0.02), and more pronounced than when evaluated for all homes. A statistically significant increase in  $\alpha$ -pinene concentration was also seen for homes in this quantile ( $p$ -value < 0.02). For the other quartiles however, the differences between diffuser on and off reduced as baseline TVOC

---

values lowered, in line with figure 3.5.

### 3.5.3 Participant effects and product use data

Each participant self-reported the distance between the diffuser and the sampling canister, specific to each sample taken. To observe how well the fragrance diffused into the airspace in the room, the sum of VOCs was plotted against the distance between the sampling canister and the diffuser, shown in figure 3.13. Distances between sampling canister and diffuser ranged from between 0.5 m to 6 m. No relationship was observed with proximity of sampler to diffuser, implying the diffuser emission was well mixed in the room.

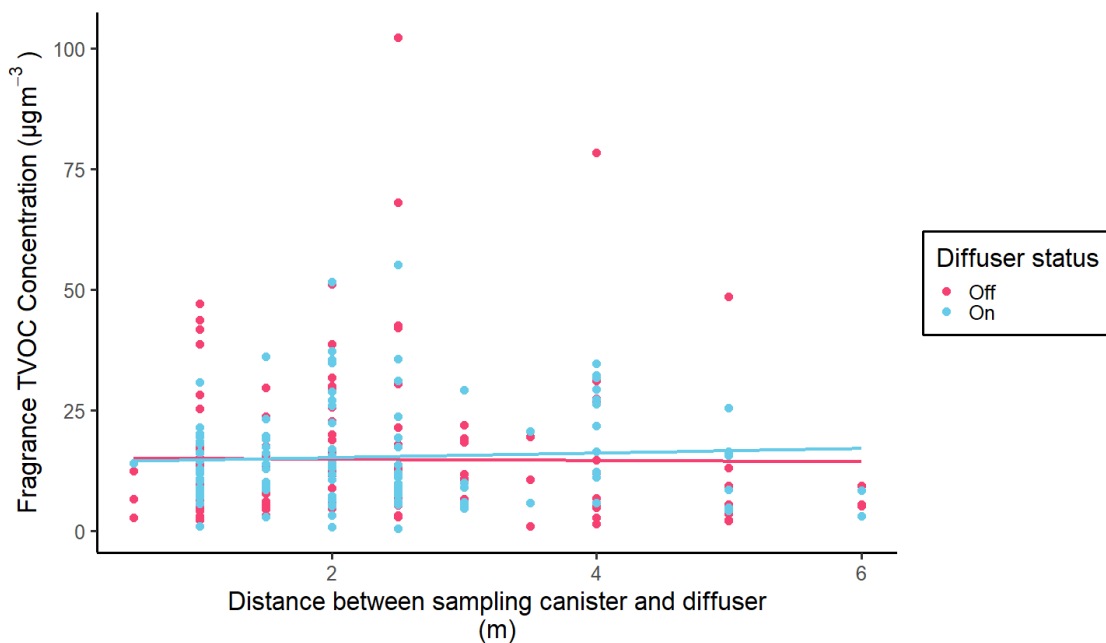


Figure 3.13: The relationship between the sum of fragrance VOCs and the distance between the sampling canister and the fragrance diffuser. Regression statistics were calculated using Pearson's R. Diffuser off regression statistics:  $R = -0.012$ ,  $p = 0.89$ . Diffuser on regression statistics:  $R = 0.057$ ,  $p = 0.055$

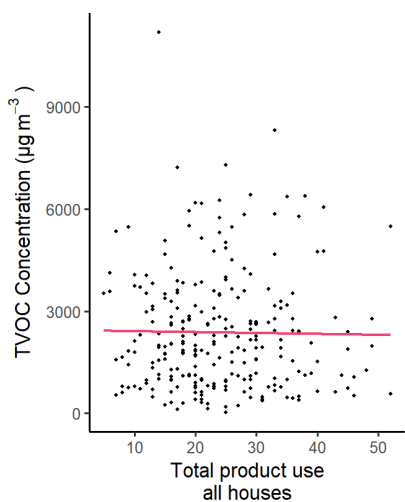


Figure 3.14: The sum of all measured VOCs (‘TVOC’) against total product use frequency from all houses. Pearson’s  $R = -0.015$ ,  $p = 0.81$ . Regression statistics calculated using a linear model.

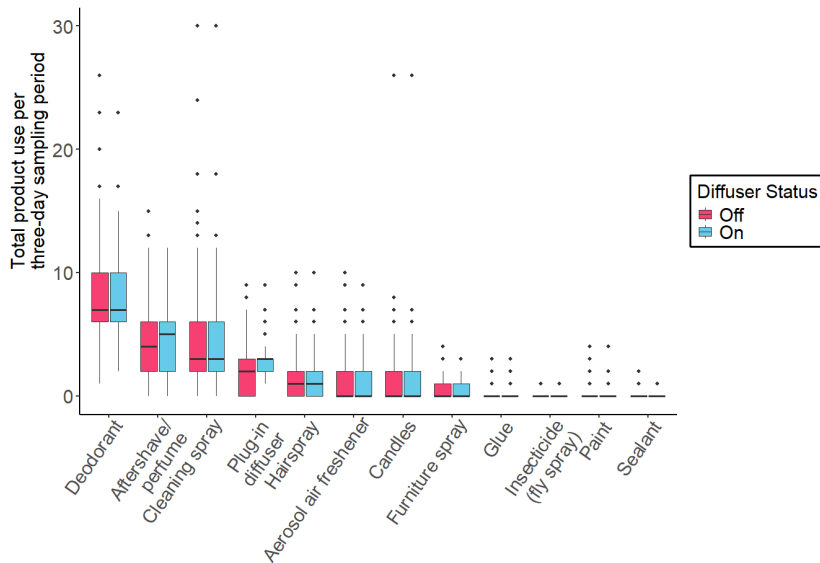


Figure 3.15: The frequency of product use in each home over each three-day sampling period, differentiated by diffuser status.

Cumulative product use statistics, limited to product type and number of uses within the 72 hour period, were self-reported by occupants. These values were then plotted against TVOC concentration shown in figure 3.14. Figure 3.15 shows individual product use data for the three-day sampling period, with deodorants being the most used VOC-containing product.

To test for any relationship between the frequency of use of particular VOC-containing products and variability observed in individual VOCs, covariance matrices were produced with the four most abundant contributors to TVOC (propane, n-butane, iso-butane and ethanol) along with three fragrance species,  $\alpha$ -pinene,  $\beta$ -pinene and eucalyptol.  $\alpha$ -Pinene contributed the most to the fragrance formulation;  $\beta$ -pinene is typically used in other fragranced products along with  $\alpha$ -pinene, and eucalyptol was included owing to its relatively low concentrations found in the baseline samples. Deodorant, cleaning sprays and aftershave were chosen as the products for comparison since they were the most frequently used. Plug-in diffuser was included as it was known that the use value for this product use increased by exactly 1 per day during the ‘diffuser on’ sampling period. The matrices produced are seen in figure 3.16

for the diffuser off matrix, and figure 3.17 for the diffuser on matrix. It is clear that few significant relationships exist between frequency of usage of individual products and variability in specific VOC concentrations indoors.

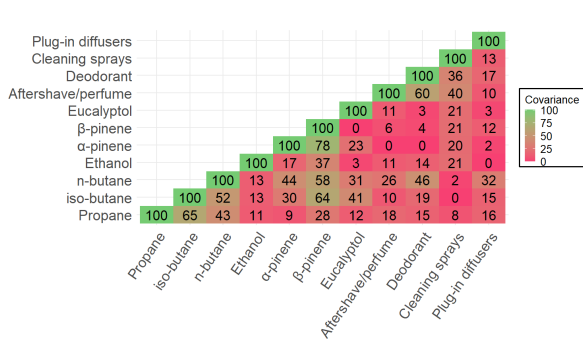


Figure 3.16: Covariance matrix between selected VOC species and products for all homes when the diffuser was off.

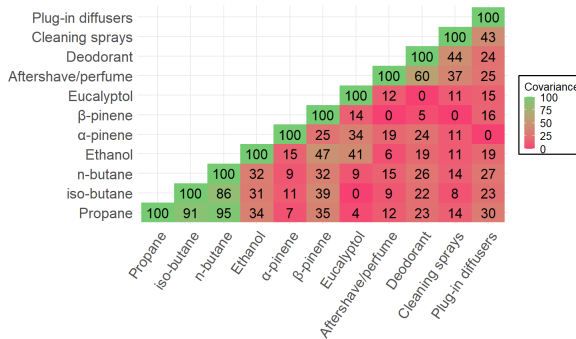


Figure 3.17: Covariance matrix between selected VOC species and products for all homes when the diffuser was turned on.

Product use statistics and species concentrations were rescaled on a 0 to 1 scale prior to covariance calculations being completed. Covariance values were then rescaled from 0 to 100.

### 3.5.4 Bottom-up estimates of increments in concentration

Diffusers were chosen for this study because their emission rates are well controlled and are not affected by user behaviour. By weighing each diffuser before and after use the mass of fragrance and VOC emitted can be quantified. If a constant rate of loss is assumed, then this can be converted into an emission rate in units of  $\mu\text{g h}^{-1}$ . An assumption is made that the profile of VOCs emitted from the diffuser does not substantially change over the 72 hour period (or indeed over the study period). Industry norms of technical performance for products of this type would aim to meet this expectation in order to deliver a consistent fragrance to consumers.

Using weight loss data for each diffuser along with the fragrance formulation, the emission rate for each fragrance VOC could be calculated. Additionally, for samples with known  $\text{CO}_2$  mole fractions, ACR was calculated as an expression of air changes per hour (ACH). To calculate this metric, some conservative assumptions were made: where the volume of the room the sample was obtained from was not reported by the homeowner, a room volume of  $30 \text{ m}^3$  was used derived from data available from the Royal Institution of British Architects (RIBA) that the room experienced air exchange only with (cleaner) outdoor air and not the

---

rest of the house; external CO<sub>2</sub> mole fractions were assumed to be 450 ppm for all samples; natural CO<sub>2</sub> generation was estimated to be 0.46 L per min per person, as per the work of Batterman (2017),<sup>[28]</sup> and the recorded number of occupants in the house were present in the room being sampled. ACR was calculated using a one-compartment box model. This was justified as figure 3.13 indicated that there appeared to be no ‘personal cloud’ of higher fragrance concentrations in the immediate proximity to the diffuser. ACR was calculated according to equation 3.1:

$$ACR = \frac{6 \times 10^4 n G_p}{V(C_{in} - C_{ex})} \quad (3.1)$$

where  $n$  is the number of room occupants,  $G_p$  is natural CO<sub>2</sub> generation per person (L min<sup>-1</sup>),  $V$  is room volume (m<sup>3</sup>),  $C_{in}$  is the internal CO<sub>2</sub> mole fraction within the room being sampled (ppm), and  $C_{ex}$  is the external CO<sub>2</sub> mole fraction (ppm). Once  $A_H$  was calculated, this then allowed for the calculation of the contribution the diffuser had to elevating a fragrance VOC concentration in a model room. This can be calculated using equation 3.2:

$$C = \left( \frac{q}{A_H V (1 - e^{-A_H t})} \right) 10^6 \quad (3.2)$$

where  $C$  is concentration of the species (μg m<sup>-3</sup>), and  $q$  is the emission rate of the species (g hr<sup>-1</sup>). All other variables remain the same as previously stated. However, as  $t$  approaches infinity, the calculation can be simplified, shown in equation 3.3:

$$C = \left( \frac{q}{A_H V} \right) 10^6 \quad (3.3)$$

Fragrance VOC emission rates are shown in table 3.3. Equation 3.3 was used in the calculation of fragrance VOC concentration increase within the modelled room. The bottom-up estimated increment in concentrations shown in table 3.4 fall broadly within the range of observed  $\alpha$ -pinene concentration increments, shown as the third boxplot in figure 3.5. It should be recognised that these increment values do not account for simultaneous removal through oxidative reaction pathways or any surface loss of fragrance species into VOC reservoirs or sinks.

Table 3.3: Median, 5th and 95th percentile and standard deviation values for fragrance VOC emission rates, expressed in  $\mu\text{g hr}^{-1}$ .

Species	Median	5th Percentile	95th Percentile	Standard deviation
$\alpha$ -pinene	1270	680	1830	360
$\beta$ -pinene	24.5	13.2	35.4	6.96
benzaldehyde	39.6	21.2	57.2	11.2
<i>p</i> -cymene	5.42	2.91	7.83	1.54
eucalyptol	71.6	38.4	103	20.3
$\gamma$ -terpinene	2.83	1.52	4.08	0.803

Table 3.4: Median, 5th and 95th percentile and standard deviation values for fragrance VOC increment concentration, expressed in  $\mu\text{g m}^{-3}$ .

Species	Median	5th Percentile	95th Percentile	Standard deviation
$\alpha$ -pinene	4.69	1.10	17.40	7.15
$\beta$ -pinene	0.0907	0.0213	0.336	0.138
benzaldehyde	0.265	0.0624	0.982	0.404
<i>p</i> -cymene	0.0201	0.00472	0.0743	0.0306
eucalyptol	0.146	0.0345	0.543	0.224
$\gamma$ -terpinene	0.0105	0.00246	0.0388	0.016

### 3.5.5 Diffuser increment estimates

Using a variety of room volumes and ventilation rates, as well as a constant diffuser output rate based on values from this study, a spread of diffuser increments in VOC concentrations can be calculated for all combinations of room volume and ACR. Plotting these values with room volume on the  $x$ -axis, ventilation rate on the  $y$ -axis, and with a colour gradient of species concentration as a  $z$ -axis variable, a contour plot can be produced for any species included in the diffuser formulation. The contour plot of increments in  $\alpha$ -pinene from a single diffuser are shown in figure 3.18. Ventilation rates and room volumes were capped at  $20 \text{ hr}^{-1}$  and  $50 \text{ m}^3$  respectively, with the vast majority of physically plausible combinations of ACR and room sizes experiencing a predicted increment of no more than  $100 \mu\text{g m}^{-3}$ . Whilst this model cannot replicate exactly homes tested in the real world, the bottom-up calculation is helpful in demonstrating that the modest increases in VOCs such as  $\alpha$ -pinene that were measured when a single diffuser was used are of the same order of magnitude

---

as would be predicted using a bottom-up methodology. For reference the  $\alpha$ -pinene 1 day exposure limit was recommended at  $4500 \mu\text{g m}^{-3}$  by PHE; this does not however necessarily constitute a long-term exposure recommendation. A single diffuser used in a typical domestic room volume of  $30 \text{ m}^3$  (RIBA average room and house sizes for south-east England) and a recommended minimum ACR of  $6 \text{ hr}^{-1}$  would be predicted to give rise to a room increment of around  $10 \mu\text{g m}^{-3}$  in  $\alpha$ -pinene, again broadly in line with the observations. We note that the loss of VOC from a room is assumed to be solely from ventilation and dilution and that oxidation or deposition are ignored, hence figure 3.18 is likely to represent an upper bound of increment. We additionally note that the recommended minimum ACR of  $6 \text{ hr}^{-1}$  is high compared to the commonly found residential ACRs of roughly between  $0.5 \text{ hr}^{-1}$  to  $2 \text{ hr}^{-1}$ . This recommended minimum likely incorporates occupational environments, which often require high ACRs, which may skew this recommended minimum value.

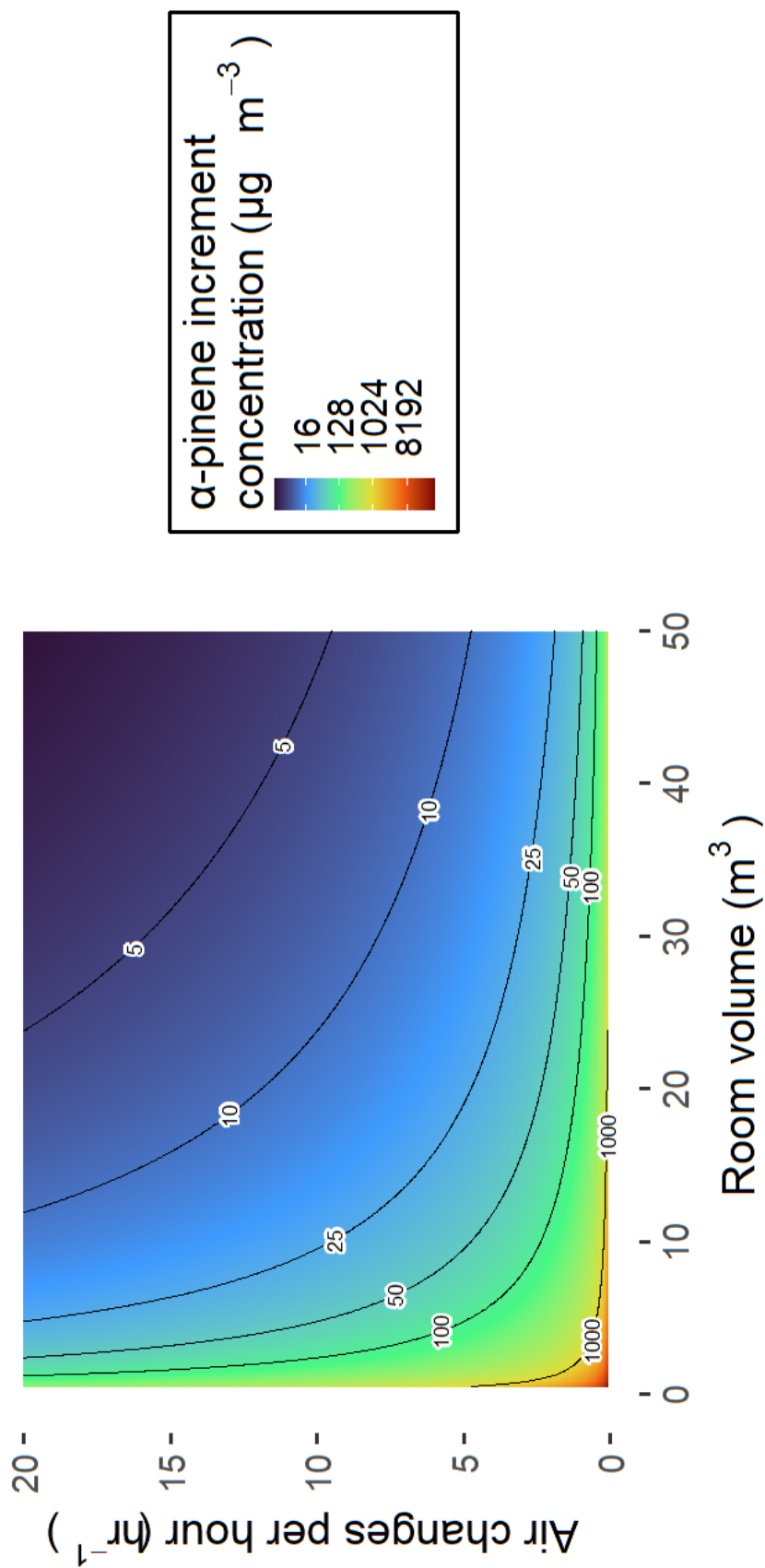


Figure 3.18: A raster plot overlaid with contour lines showing the  $\alpha$ -pinene increment expected for different room volumes and ventilation rates. A continuous colour scale was applied to  $\alpha$ -pinene increment values, and the scale was transformed on a  $\log_2$  scale to aid visualisation.

---

### 3.5.6 Generation of secondary oxidation products from diffuser use

Carslaw and Shaw (2019) described an operational metric to indicate the potential of a VOC to undergo further reactions within indoor airspaces and create secondary products, named the secondary product creation potential (SPCP).<sup>[39]</sup> The SPCP is defined as the sum of a range of secondary products created from degradation of a VOC, divided by the mixing ratio of the primary species added, in units of ppb of secondary products per ppb of VOC. It is of relevance for health since secondary products derived from VOC oxidation can play a role in the formation of secondary aerosols<sup>[40]</sup> and include other more directly harmful products such as formaldehyde.<sup>[41–43]</sup> It is useful to apply the metric here since indoor air in the homes studied were often dominated in mass terms by relatively unreactive species such as propane and butane that have low SPCP multipliers. Monoterpenes are known to have higher reactivities and SPCP, hence use of this metric ensures that the potential wider effects of increments in by-products are also evaluated. Similar to figures 3.4 and 3.5, calculated SPCP values were differentiated by the diffuser status for TVOC and for the sum of the fragrance VOCs where there is SPCP data ( $\alpha$ -pinene,  $\beta$ -pinene and benzaldehyde). This is shown in figures 3.19 and 3.20. There was no discernible change for SPCP - mole fraction product in figure 3.19, but a slightly larger increase in SPCP - mole fraction product for fragrance species in figure 3.20. Noteworthy, however, is the increase in relative contribution of fragrance species data to the overall SPCP values, when compared to their mass contributions, reflecting a higher potential for monoterpene species to lead secondary products compared to high mass contributors such as propane, i-butane, n-butane and ethanol.

## 3.6 Conclusions

The use of room fragrance products such as plug-in diffusers undoubtedly impacts on the airspace composition within the area the product is used. Clearly using any VOC-containing products in poorly ventilated spaces will result in a higher VOC concentration and higher exposure to the user than would occur in a well-ventilated space. In this study virtually all participants reported that they could detect the presence of fragrance when the diffusers were switched on indicating that in a purely functional sense the devices were working as intended by the manufacturer. However quantitatively determining by how much VOCs were incrementally raised by using the diffuser was not straightforward since the diffuser emitted VOCs into an already highly congested indoor atmosphere containing many VOCs at higher concentrations, including some species that were also in fragrance formulation.

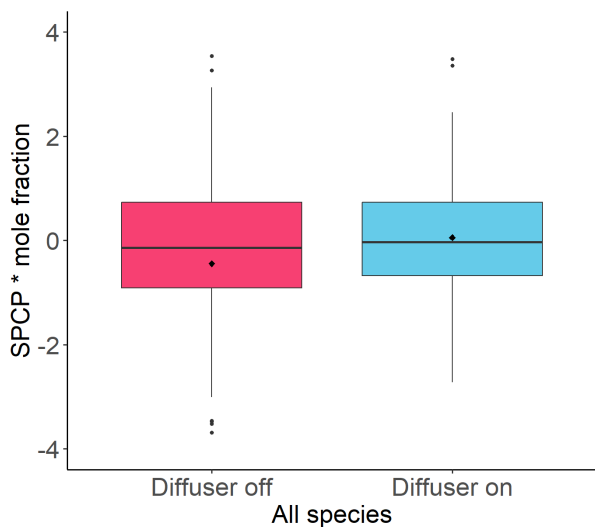


Figure 3.19: Calculated total SPCP values differentiated by diffuser status. Outliers below -4 and above +4 were removed from the graphic to aid presentation, but were included in the calculation of quartiles and median values.

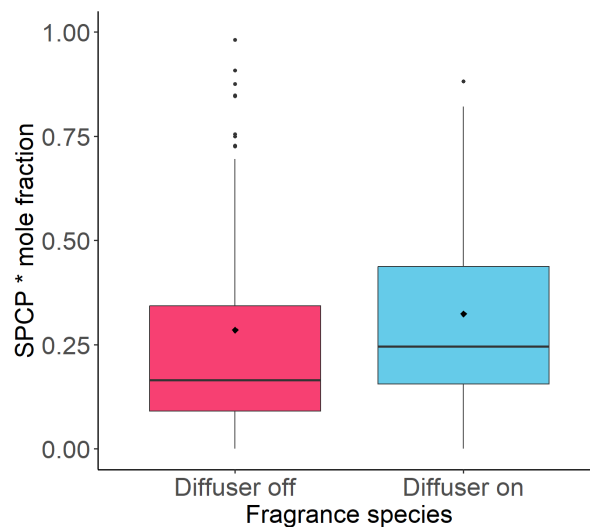


Figure 3.20: Calculated SPCP from fragrance species, where data was available. Outliers above 1 were removed from the graphic to aid presentation, but were included in the calculation of quartiles and median values.

The  $\text{SPCP} \times \text{mole fraction}$  product is given in units of ppb.

---

Future inclusion of appliance use data in surveys may prove insightful, as the frequency of use of appliances such as gas fires may help with interpreting the presence of high CO<sub>2</sub> fractions that may not be from respiration.

When the study homes were segmented by air exchange rate, inferred from concurrent CO<sub>2</sub> measurements acting as a proxy, then a small increment in diffuser-originating VOCs could be detected. For homes in the lowest ventilation quartile,  $\alpha$ -pinene concentrations increased on average from 9 to 14.5  $\mu\text{g m}^{-3}$ , with the median value increasing from 6  $\mu\text{g m}^{-3}$  to 14.1  $\mu\text{g m}^{-3}$ . This increment in  $\alpha$ -pinene was set against a background mean TVOC concentration in that quartile of >3500  $\mu\text{g m}^{-3}$ . By using the weight loss of fragrance from the diffuser, a bottom up estimate of increment increase in  $\alpha$ -pinene was calculated to be around 10  $\mu\text{g m}^{-3}$ , assuming an ACR of 6 hr<sup>-1</sup>, a typical room volume of 30 m<sup>3</sup> and no oxidative/depositional losses. In this regard the use of a fragrance diffuser for studies in real-world settings is helpful since the emission rate is well controlled, formulation is known, and amounts released are not subject to end-user variability. Using a more targeted metric related to secondary product creation potential did not lead to any substantial change in conclusions. Whilst fragrance-related VOCs made up a larger fractional contribution to the SPCP metric there was no statistically significant increase in calculated SPCP across all homes when diffusers were used. A bottom-up model for estimating the incremental increases in a VOC when a single diffuser is used indicated that increments of >450  $\mu\text{g m}^{-3}$  (a high safety margin of 1/10th the 24 hour exposure recommendation) are physically plausible but would require a combination of very small room volumes (below 5 m<sup>3</sup>) and very low air exchange rates. It is possible that additional user instruction might provide guidance against use in such unusual situations.

---

## 3.7 References

- [1] E Uhde and N Schulz. “Impact of room fragrance products on indoor air quality”. In: *Atmospheric Environment* 106 (2015), pp. 492–502. DOI: [10.1016/j.atmosenv.2014.11.020](https://doi.org/10.1016/j.atmosenv.2014.11.020).
- [2] D A Sarigiannis et al. “Exposure to major volatile organic compounds and carbonyls in European indoor environments and associated health risk”. In: *Environment International* 37.4 (2011), pp. 743–765. DOI: [10.1016/j.envint.2011.01.005](https://doi.org/10.1016/j.envint.2011.01.005).
- [3] C Shrubsole et al. “IAQ guidelines for selected volatile organic compounds (VOCs) in the UK”. In: *Building and Environment* 165 (2019), p. 106382. DOI: <https://doi.org/10.1016/j.buildenv.2019.106382>. URL: <https://www.sciencedirect.com/science/article/pii/S036013231930592X>.
- [4] A C Heeley-Hill et al. “Frequency of use of household products containing VOCs and indoor atmospheric concentrations in homes”. In: *Environmental Science: Processes and Impacts* 23.5 (2021), pp. 699–713. DOI: [10.1039/d0em00504e](https://doi.org/10.1039/d0em00504e).
- [5] C Jia, S Batterman, and C Godwin. “VOCs in industrial, urban and suburban neighborhoods- Part 2: Factors affecting indoor and outdoor concentrations”. In: *Atmospheric Environment* 42.9 (2008), pp. 2101–2116. DOI: [10.1016/j.atmosenv.2007.11.047](https://doi.org/10.1016/j.atmosenv.2007.11.047).
- [6] E Höllbacher et al. “Emissions of indoor air pollutants from six user scenarios in a model room”. In: *Atmospheric Environment* 150 (2017), pp. 389–394. DOI: [10.1016/j.atmosenv.2016.11.033](https://doi.org/10.1016/j.atmosenv.2016.11.033).
- [7] X Liu et al. “Full-scale chamber investigation and simulation of air freshener emissions in the presence of ozone”. In: *Environmental Science and Technology* 38.10 (2004), pp. 2802–2812. DOI: [10.1021/es030544b](https://doi.org/10.1021/es030544b).
- [8] N Goodman et al. “Evaluating air quality with and without air fresheners”. In: *Air Quality, Atmosphere and Health* 13.1 (2020), pp. 1–4. DOI: [10.1007/s11869-019-00759-9](https://doi.org/10.1007/s11869-019-00759-9).
- [9] N B Goodman et al. “Emissions from dryer vents during use of fragranced and fragrance-free laundry products”. In: *Air Quality, Atmosphere and Health* 12.3 (2019), pp. 289–295. DOI: [10.1007/s11869-018-0643-8](https://doi.org/10.1007/s11869-018-0643-8).
- [10] A Lamplugh, A Nguyen, and L D Montoya. “Optimization of VOC removal using novel, low-cost sorbent sinks and active flows”. In: *Building and Environment* 176 (2020). DOI: [10.1016/j.buildenv.2020.106784](https://doi.org/10.1016/j.buildenv.2020.106784).
- [11] S Senthilkumaran et al. “Ventricular fibrillation after exposure to air freshener-death just a breath away”. In: *Journal of Electrocardiology* 45.2 (2012), pp. 164–166. DOI: [10.1016/j.jelectrocard.2011.05.002](https://doi.org/10.1016/j.jelectrocard.2011.05.002).

- 
- [12] D Vethanayagam et al. “Fragrance materials in asthma: A pilot study using a surrogate aerosol product”. In: *Journal of Asthma* 50.9 (2013), pp. 975–982. DOI: [10.3109/02770903.2013.822079](https://doi.org/10.3109/02770903.2013.822079).
- [13] J E M Gibbs. “Essential oils, asthma, thunderstorms, and plant gases: A prospective study of respiratory response to ambient biogenic volatile organic compounds (BVOCs)”. In: *Journal of Asthma and Allergy* 12 (2019), pp. 169–182. DOI: [10.2147/JAA.S193211](https://doi.org/10.2147/JAA.S193211).
- [14] U B Nurmatov et al. “Volatile organic compounds and risk of asthma and allergy: A systematic review”. In: *European Respiratory Review* 24.135 (2015), pp. 92–101. DOI: [10.1183/09059180.00000714](https://doi.org/10.1183/09059180.00000714).
- [15] J H Lee et al. “Relationship between indoor air pollutant levels and residential environment in children with atopic dermatitis”. In: *Allergy, Asthma and Immunology Research* 6.6 (2014), pp. 517–524. DOI: [10.4168/aair.2014.6.6.517](https://doi.org/10.4168/aair.2014.6.6.517).
- [16] J Y Chin et al. “Levels and sources of volatile organic compounds in homes of children with asthma”. In: *Indoor Air* 24.4 (2014), pp. 403–415. DOI: [10.1111/ina.12086](https://doi.org/10.1111/ina.12086).
- [17] E K Ha et al. “Personal Exposure to Total VOC is Associated With Symptoms of Atopic Dermatitis in Schoolchildren”. In: *Journal of Korean Medical Science* 37.8 (2022). DOI: [10.3346/JKMS.2022.37.E63](https://doi.org/10.3346/JKMS.2022.37.E63).
- [18] E Woolfenden. “Monitoring vocs in air using sorbent tubes followed by thermal desorption-capillary gc analysis: Summary of data and practical guidelines”. In: *Journal of the Air and Waste Management Association* 47.1 (1997), pp. 20–36. DOI: [10.1080/10473289.1997.10464411](https://doi.org/10.1080/10473289.1997.10464411).
- [19] M Even, E Juritsch, and M Richter. “Measurement of very volatile organic compounds (VVOCs) in indoor air by sorbent-based active sampling: Identifying the gaps towards standardisation”. In: *TrAC - Trends in Analytical Chemistry* 140 (2021). DOI: [10.1016/j.trac.2021.116265](https://doi.org/10.1016/j.trac.2021.116265).
- [20] Gabriela Ventura et al. “Active vs passive sampling of VOCs in IAQ field studies in selected energy-efficient European office and residential buildings”. In: *Indoor Air*. Beijing, 2005.
- [21] K Pytel, R Marcinkowska, and B Zabiegała. “Investigation on air quality of specific indoor environments—spa salons located in Gdynia, Poland”. In: *Environmental Science and Pollution Research* 28.42 (2021), pp. 59214–59232. DOI: [10.1007/s11356-020-09860-4](https://doi.org/10.1007/s11356-020-09860-4).
- [22] S Mentese and D Tasdibi. “Assessment of residential exposure to volatile organic compounds (VOCs) and carbon dioxide (CO<sub>2</sub>)”. In: *Global Nest Journal* 19.4 (2017), pp. 726–732. DOI: [10.30955/gnj.002278](https://doi.org/10.30955/gnj.002278).

- 
- [23] Rufus D Edwards et al. “VOC concentrations measured in personal samples and residential indoor, outdoor and workplace microenvironments in EXPOLIS-Helsinki, Finland”. In: *Atmospheric Environment* 35.27 (2001), pp. 4531–4543. DOI: [https://doi.org/10.1016/S1352-2310\(01\)00230-8](https://doi.org/10.1016/S1352-2310(01)00230-8). URL: <https://www.sciencedirect.com/science/article/pii/S1352231001002308>.
- [24] C Arata et al. “Volatile organic compound emissions during HOMEChem”. In: *Indoor Air* 31.6 (2021), pp. 2099–2117. DOI: [10.1111/ina.12906](https://doi.org/10.1111/ina.12906).
- [25] M Cheng et al. “Factors controlling volatile organic compounds in dwellings in Melbourne, Australia”. In: *Indoor Air* 26.2 (2016), pp. 219–230. DOI: [10.1111/ina.12201](https://doi.org/10.1111/ina.12201).
- [26] Ľudmila Mečiarová et al. “Factors Effecting the Total Volatile Organic Compound (TVOC) Concentrations in Slovak Households”. In: *International Journal of Environmental Research and Public Health* 14.12 (2017). DOI: [10.3390/ijerph14121443](https://doi.org/10.3390/ijerph14121443). URL: <https://www.mdpi.com/1660-4601/14/12/1443>.
- [27] R Otson. “Effects of ventilation, temperature, sources, and sinks on VOC levels in a residence”. In: *Indoor Air Quality, Ventilation and Energy Conservation in Buildings*. 2. Montreal, May 1995, pp. 85–92.
- [28] S Batterman. “Review and extension of CO<sub>2</sub>-based methods to determine ventilation rates with application to school classrooms”. In: *International Journal of Environmental Research and Public Health* 14.2 (2017). DOI: [10.3390/ijerph14020145](https://doi.org/10.3390/ijerph14020145).
- [29] L Chatzidiakou, D Mumovic, and A Summerfield. “Is CO<sub>2</sub> a good proxy for indoor air quality in classrooms? Part 1: The interrelationships between thermal conditions, CO<sub>2</sub> levels, ventilation rates and selected indoor pollutants”. In: *Building Services Engineering Research and Technology* 36.2 (2015), pp. 129–161. DOI: [10.1177/0143624414566244](https://doi.org/10.1177/0143624414566244).
- [30] Z Peng and J L Jimenez. “Exhaled CO<sub>2</sub> as a COVID-19 infection risk proxy for different indoor environments and activities”. In: *Environmental Science and Technology Letters* 8.5 (2021), pp. 392–397. DOI: [10.1021/acs.estlett.1c00183](https://doi.org/10.1021/acs.estlett.1c00183).
- [31] Y Jia et al. “Investigation of indoor total volatile organic compound concentrations in densely occupied university buildings under natural ventilation: Temporal variation, correlation and source contribution”. In: *Indoor and Built Environment* 30.6 (2021), pp. 838–850. DOI: [10.1177/1420326X20914000](https://doi.org/10.1177/1420326X20914000).
- [32] K Murakami et al. “A field survey on indoor air pollution in school classrooms with different ventilation methods”. In: *E3S Web of Conferences*. Vol. 111. 2019. DOI: [10.1051/e3sconf/201911101020](https://doi.org/10.1051/e3sconf/201911101020).

- 
- [33] Y Zhang and Y Xu. “Characteristics and correlations of VOC emissions from building materials”. In: *International Journal of Heat and Mass Transfer* 46.25 (2003), pp. 4877–4883. DOI: [10.1016/S0017-9310\(03\)00352-1](https://doi.org/10.1016/S0017-9310(03)00352-1).
- [34] N Fu et al. “Indoor volatile organic compounds in densely occupied education buildings of four universities: Target list, concentration levels and correlation analysis”. In: *Building and Environment* 191 (2021). DOI: [10.1016/j.buildenv.2021.107599](https://doi.org/10.1016/j.buildenv.2021.107599).
- [35] C Lutes et al. “Observation of Conditions Preceding Peak Indoor Air Volatile Organic Compound Concentrations in Vapor Intrusion Studies”. In: *Groundwater Monitoring and Remediation* 41.2 (2021), pp. 99–111. DOI: [10.1111/gwmr.12452](https://doi.org/10.1111/gwmr.12452).
- [36] Felix Klein et al. “Quantification of the impact of cooking processes on indoor concentrations of volatile organic species and primary and secondary organic aerosols”. In: *Indoor Air* 29.6 (2019), pp. 926–942. DOI: <https://doi.org/10.1111/ina.12597>. URL: <https://onlinelibrary.wiley.com/doi/abs/10.1111/ina.12597>.
- [37] T Barboni and N Chiaramonti. “BTEX emissions during prescribed burning in function of combustion stage and distance from flame front”. In: *Combustion Science and Technology* 182.9 (2010), pp. 1193–1200. DOI: [10.1080/00102201003660199](https://doi.org/10.1080/00102201003660199).
- [38] Biljana D Škrbić, Vesna B Marinković, and Saša Spaić. “Assessing the impact of combustion and thermal decomposition properties of locally available biomass on the emissions of BTEX compounds by chemometric approach”. In: *Fuel* 282 (2020), p. 118824. DOI: <https://doi.org/10.1016/j.fuel.2020.118824>. URL: <https://www.sciencedirect.com/science/article/pii/S0016236120318202>.
- [39] N Carslaw and D Shaw. “Secondary product creation potential (SPCP): A metric for assessing the potential impact of indoor air pollution on human health”. In: *Environmental Science: Processes and Impacts* 21.8 (2019), pp. 1313–1322. DOI: [10.1039/c9em00140a](https://doi.org/10.1039/c9em00140a).
- [40] X Niu et al. “Surface characterization of secondary organic aerosols from ozonolysis of monoterpene and the effects of acute lung injury in mice”. In: *Aerosol and Air Quality Research* 20.7 (2020), pp. 1675–1685. DOI: [10.4209/aaqr.2019.12.0628](https://doi.org/10.4209/aaqr.2019.12.0628).
- [41] T Liu et al. “Significant Production of Secondary Organic Aerosol from Emissions of Heated Cooking Oils”. In: *Environmental Science and Technology Letters* 5.1 (2018), pp. 32–37. DOI: [10.1021/acs.estlett.7b00530](https://doi.org/10.1021/acs.estlett.7b00530).
- [42] M Takhar, Y Li, and A W. H. Chan. “Characterization of secondary organic aerosol from heated-cooking-oil emissions: Evolution in composition and volatility”. In: *Atmospheric Chemistry and Physics* 21.6 (2021), pp. 5137–5149. DOI: [10.5194/acp-21-5137-2021](https://doi.org/10.5194/acp-21-5137-2021).

- 
- [43] Z Zhang et al. “Formation and evolution of secondary organic aerosols derived from urban-lifestyle sources: Vehicle exhaust and cooking emissions”. In: *Atmospheric Chemistry and Physics* 21.19 (2021), pp. 15221–15237. DOI: [10.5194/acp-21-15221-2021](https://doi.org/10.5194/acp-21-15221-2021).

# Chapter 4

## An assessment of VOC emissions and human strength perception of liquid electric fragrance diffusers

### 4.1 Declaration, contributions and conflicts

This chapter is based on the following publication:

Warburton T, Lewis AC, Hopkins JR, Andrews SJ, Yeoman AM, Owen N, Jordan C, Adamson G, Xia B. An assessment of VOC emissions and human strength perception of liquid electric fragrance diffusers. *Environ. Sci.: Advances*, (2025), **5**, 739-752. <sup>†</sup>

All figures, both in the main text and in the supplementary information have been included in the following chapter, with in-text references to these figures edited accordingly. The flowchart given here in figure 4.1 has been recreated using *Tikz* to better suit presentation within this thesis, however otherwise remains unchanged. The original version of this work remains freely available through the paper's DOI (see footnote below).

The experiments were designed by TW, ACL, NO, CJ, GA and BX. TW, JRH, SJA and AMY supported the VOC analytical measurements used in this study, NO, CJ led the olfactory testing component. TW and ACL undertook the data analysis and subsequent interpretation. All authors contributed to the drafting and reviewing of the manuscript.

NO, CJ, and GA are employees of Givaudan UK Ltd, Givaudan Fragrances Corp. and

---

<sup>†</sup><https://doi.org/10.1039/D4VA00388H>

---

BX is an employee of Bath & Body Works, Inc. who are industrial suppliers of chemicals and finished household and personal care products. To support independence, all analytical work and data analysis was undertaken by University of York with no restrictions placed on freedoms to publish. While the fragrance oil formulation was known to researchers at the University of York, the full composition is not disclosed in this work, aside from the identification of six detectable VOCs ( $\alpha$ -pinene,  $\beta$ -pinene,  $\gamma$ -terpinene, *p*-cymene, benzaldehyde, and eucalyptol) and the mass percentage contribution of  $\alpha$ -pinene to the total formulation. Other than the schematic, not-to-scale diagrams shown in figures 4.1 and 4.2, no scale diagrams or photographs of the emission booths are provided. The fragrance oil is a modified, commercially available product, and the emission booths are housed within a commercially-sensitive fragrance product development and assessment facility. Due to commercial sensitivities and confidentiality agreements between researchers and industry partners, both the full formulation and detailed booth specifications remain undisclosed.

## 4.2 Abstract

Fragrance products are commonplace in everyday life and their air quality effects extensively studied. In this study the use of multiple plug-in diffusers (liquid electricals/LEs) was assessed by quantifying VOC concentrations in controlled test rooms ('toilet booth' and 'large booth') with up to 5 LEs of known formulation in concurrent use. Olfactive strength tests were completed under the same conditions in blind assessments. Air samples were analysed using thermal desorption- (TD) gas chromatography (GC) coupled to flame ionisation (FID) and mass spectrometry (MS) detectors. Significant positive linearities were found for several VOCs (e.g  $\alpha$ -pinene toilet booth and large booth  $R = 1$  and  $p = 0.0028$ , *p*-cymene toilet booth  $R = 0.94$  and  $p = 0.017$ , large booth  $R = 0.89$  and  $p = 0.033$ ), with  $\alpha$ -pinene presenting the highest measurable gas-phase concentration (mean  $25 \mu\text{g m}^{-3}$ , toilet booth with 5 LEs present). All measurable linearities for fragrance species in toilet booths were significant. However, olfactive intensity assessment showed a plateauing in fragrance perception after the addition of 2 LEs. Only very volatile fragrance ingredients such as  $\alpha$ -pinene and benzaldehyde could be detected in the gas phase, but at ambient concentrations that were always lower than literature values for their individual odour detection thresholds. The plateauing of the perception of fragrance strength may aid in limiting potential off-instruction use, thereby limiting end-user exposure to potentially high concentrations of emitted VOCs. The drivers of human fragrance perception here appeared to be lower vapour pressure constituents of fragrance formulations like sesquiterpenes. Moderation of the concentration of monoterpenes used in room fragrance formulations may be a practical solution in limiting possible air

---

quality impacts of product use, whilst still maintaining end-user fragrance perception.

## 4.3 Introduction

Fragrances have been used by humans since antiquity and are well-documented in many different cultures and regions through history, and the use of fragranced products is commonplace in 21st century life.<sup>[1-4]</sup> Common gas phase emissions from fragranced products include monoterpenes, alcohols and esters.<sup>[5,6]</sup> Monoterpenes are also emitted from many other sources indoors including from flowers, fruit, cooking and cleaning.<sup>[7-10]</sup> Since they are relatively reactive to oxidation indoors they are potential precursors to the production of secondary organic aerosols (SOAs).<sup>[9,11-13]</sup> Monoterpenes are typically included in fragrance formulations for their individual fragrance notes and are known to be important in the perception of fragrance.<sup>[14,15]</sup> Through electroencephalography, common emissions from fragrance products such as limonene and terpinolene can be linked to changes in brain function, including an increased perception of relaxation and pleasure in humans.<sup>[16-18]</sup>

Monoterpenes are only one of many classes of compound found in fragranced products,<sup>[19-21]</sup> however they are often some of the most volatile present and hence generate some of the highest gas-phase indoor concentrations when a product is used. They are more amenable to analysis by methods such as thermal desorption gas chromatography-mass spectrometry (TD-GC-MS) or on-line mass spectrometry such as proton transfer reaction (PTR) and selection ion flow tube (SIFT) MS than less volatile fragrance components such as terpene oxides and sesquiterpenes. Some monoterpenoids, such as geraniol and borneol, while commonly described as ‘volatile’, have vapour pressures comparative with sesquiterpenes and as such are often not easily quantified. There is an understandable attraction in air quality science for using gas-phase measurements of monoterpenes as a proxy for the presence of fragrance, despite many non-fragrance sources of these species also existing indoors. Those species which likely impact substantially on human perception of fragrance are often not detectable by most analytical methods in ambient air due to very low gas-phase concentrations and vapour pressures.

Fragrance diffusers belong to a group of home fragrance products that actively emit into an air space. This is commonly through passive diffusion, e.g. using wooden sticks/reeds to enhance evaporation, or using an electrically powered element (commonly called ‘plug ins’, referred to commercially as Liquid Electricals/LEs). LEs can be further differentiated into those that use a heated wick to actively diffuse fragrance into the airspace, or so-called ‘nebulisers’ which aerosolises fragrance oil. LEs are designed to deliver a constant rate of emission of volatile

---

organic compounds (VOCs) and semi-volatile organic compounds (SVOCs) associated with the scent.<sup>[22]</sup> The concentration in air of each VOC/SVOC emitted is dependent on the fragrance formulation and compound vapour pressure.<sup>[10,23]</sup> There has been some research into the differences in VOC emissions arising from passive and plug-in fragrance diffusers; the formulation of fragrance generally having more influence than the diffuser type.<sup>[22,24]</sup> Using a constant-emission fragrance device within an airspace leads to an initial increase in VOC concentration before reaching a steady state concentration that is determined by the balance of emission with loss processes including fresh air ventilation rate, surface deposition and in-room oxidation.<sup>[10,23]</sup>

Evaluation of the indoor air effects of LE devices has predominantly been conducted in small laboratory test chambers; these generate gas phase concentrations much higher than are seen in real-world home settings.<sup>[22,25–27]</sup> Test chambers allow for greater experimental control, such as chamber air change rate (ACR) and chemical composition of diluent air.<sup>[28]</sup> Evaluating effects of LEs on indoor air quality and in human perception of fragrance is complicated by pre-existing VOCs from other sources and widely different product use behaviours and varying air change rates.<sup>[26,29–31]</sup> Warburton *et al.* (2023)<sup>[26]</sup> showed that incremental indoor VOC increases from using a single LE in real homes were difficult to discern and that air ventilation and location in the home (and associated properties such as room size) were key factors.<sup>[32–34]</sup> Ventilation in homes is highly variable but is generally reducing in residential properties as they are made more energy efficient. Fragranced products including LEs must perform well from an environmental and human perception perspective in both old and new/retrofitted housing stock.

Any solvent-containing product (e.g. paints, glues, aerosols, adhesives) used in a manner that deviates substantially from its intended method of application has the potential for health harms.<sup>[35–39]</sup> This might occur, for example if users do not follow labelling instructions for frequency/duration of use, quantity/amount of product intended to be used, or ventilation requirements. Theoretically high concentrations of fragranced-derived VOCs could be generated indoors if numerous products (or multiples of the same product) were used off-instruction, such as in small rooms that had poor ventilation. Fragrance species are one constituent within a complex matrix of chemicals within product formulations however, and concentrations of each must be borne in mind while assessing safety of use.

VOCs associated with fragrance possess an odour detection threshold (ODL). This is defined as the minimum concentration required for a human to reliably perceive the presence of the VOC. Any human-based olfactive assessment has the potential for uncertainties given person-to-person variability, and as such ODLs can change between studies.<sup>[40–42]</sup> The ODL

---

of a compound depends greatly on its shape, size, vapour pressure, polarity and reactivity.<sup>[43,44]</sup> Certain malodours are detectable in low atmospheric mixing ratios, while some commonly used ingredients such as  $\alpha$ -pinene have ODLs orders of magnitude above these thresholds.<sup>[45,46]</sup> There has additionally been shown to be some moderate discrepancies in ODL between younger and older adults, with younger adults tending to have lower VOC-specific ODLs.<sup>[47]</sup> While ODLs may differ and vary person-to-person, they provide a useful benchmark for assessing the impact of VOC-releasing products on user perception. However, the use of ODLs in comparison to indoor VOC concentrations originating from product emissions remain relatively understudied.

### 4.3.1 Objectives

This study aims to uniquely combine the indoor air quality effects arising from using a well-controlled LE source in realistic but controlled rooms and the olfactive strength of that source. It remains a possibility that the non-standard, off-instruction and excessive use of any VOC-containing products may lead to unintentional harm in the home, with the most significant hazards arising where there is poor or no olfactory detection of the emitted VOCs. The indoor concentrations of odourless VOCs such propane or butane might reach many hundreds of parts per million before being perceived. In these worst cases, there is a risk of fatality with longer-term chronic exposure potentially leading to sub-acute effects.

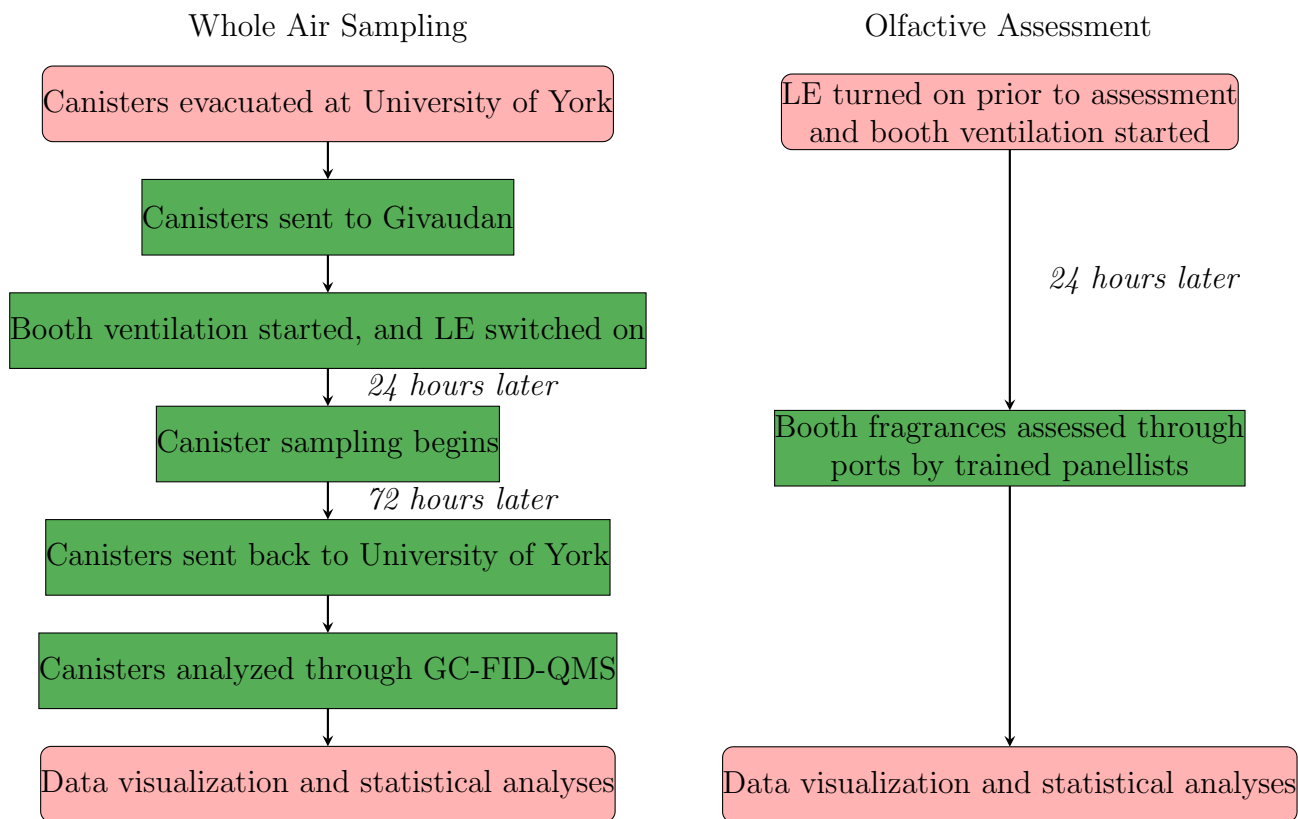
Fragrance VOCs and SVOCs can be perceived at low ambient concentrations<sup>[48,49]</sup>, and so here we assess the VOC emissions from LEs coupled with fragrance strength perception by trained sensory panellists. It is hypothesised that excessive and/or off-instruction use of LEs, such as using multiple LEs simultaneously in rooms with low ACRs, is less likely to occur than for other household VOC-containing products, since usage may be attenuated by human tolerance of the resulting odours created. This was evaluated using controlled test booths of different sizes for in-room monitoring of VOC concentrations in addition to human olfactory testing. A comparison to real world indoor air studies measuring VOC contributions from LEs was also conducted to assess the ability to apply these artificial room studies as a model for estimating normal consumer home environments. The combination of indoor air quality measurements with olfactory evaluation is undocumented in research literature to our knowledge. Assessing personal responses to VOCs is technically challenging owing to person-to-person variance in perception and odour detection threshold, different effects of fragrances to physiological responses, pre-existing expectations of product performance, and time required in establishing robust methodology to account for these possible person-to-person discrepancies.<sup>[17,50-52]</sup> Here we combine state-of-the-art fragrance industry testing

---

protocols, a trained sensory panel and indoor air quality measurements to assess strength perception of a typical fragrance releasing household product.

## 4.4 Methodology

The following sections give detailed explanations of the methodological processes followed in this study, while summary flowcharts can be found in Fig. 4.1.



Scheme 4.1: Flowcharts showing air sampling and olfactive assessment method flows. The flowchart begins at the top and works methodically through the steps downwards through to the bottom. Unless specifically stated, the time taken between the steps tended to vary based on logistics.

### 4.4.1 Canister preparation

Whole air samplers were used to collect in-room samples using 6 L vacuum-intake stainless steel canisters internally treated with silica (Entech, CA, USA) using flow-restrictive inlets (Entech, CA, USA) resulting in samples being drawn over 72 hours, found by Heeley-Hill *et al.* to be linear over the first 48 hours with a reducing flow rate over the last 24 hours.<sup>[29]</sup> Prior to

---

deployment, canisters were evacuated to 0.01 Pa, or 29.9 Hg vacuum (gauge). Canister valves were checked prior to deployment to qualitatively assess valve seal integrity by attaching a vacuum gauge atop the closed canister valve and leaving for at least 2 hours. Failed valves were replaced like-for-like, and the evacuation and valve integrity process repeated.

#### 4.4.2 Sample collection and preparation for analysis

Evacuated canisters were placed in one of two laboratory test rooms ('booths') at Givaudan Ltd, Ashford, UK, either designed to mimic a small bathroom ( $W$  1.92 m  $\times$   $D$  1.90 m  $\times$   $H$  2.6 m) or a medium-sized living room ( $W$  3.0 m  $\times$   $D$  4.45 m  $\times$   $H$  2.49 m). These were mechanically ventilated with outdoor air with an air change rate of 7.5  $\text{h}^{-1}$ . Top-down schematics of the large booth and the toilet booth are given in the Fig. 4.1 and 4.2, respectively. It is noted that an ACR of 7.5  $\text{hr}^{-1}$  is high, and most residential houses would expect an ACR range of between 0.5  $\text{hr}^{-1}$  and 2  $\text{hr}^{-1}$ . For the booths used here, a proprietary control panel was used which had no variable settings, and only allowed an ACR of 7.5  $\text{hr}^{-1}$ . Additionally, the booths used here were constructed primarily for panellist fragrance strength perception training and evaluation, which would require low ambient concentrations to ensure panellists could detect subtle differences in fragrance composition. Between 1 and 5 identical LEs of known formulation were placed together in each of the rooms. Canisters for sampling were placed at identical distances from the LEs. LEs were turned on 24 hours before the sampling period began to aid equilibration of output and for mixing of the airspace; after 24 hours the canisters would begin sampling. After 72 hours had elapsed, the valves were closed, and when sampling had finished across all booths, the canisters were returned to University of York for analysis.

LE emissions were measured through oil mass loss over the sampling period. LEs were weighed both pre- and post-sampling. Mass loss ranged between 1.80 g and 3.70 g with a standard deviation of 0.49 g. Mean oil mass loss was 2.66 g, and median oil mass loss was 2.54 g. Commercial comparable LEs draw between 2 and 4 W of power, and the LE used here drew 2.8 W (UK 230/240 V, AC current with a frequency of 50 Hz).

An equal number of samples were taken for each LE multiple (between 1 and 5). Controls were taken of empty booths over the same time-period to allow for background (fresh air ventilation) air composition to be quantified.

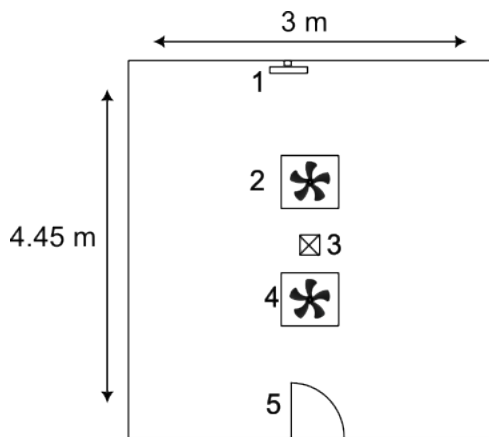


Figure 4.1: Top-down view of the large booth layout. Numbered elements are as follows: 1 - LE plug location, 2 - Air in flow vent, 3 - Canister sampling location, 4 - Air out flow vent, 5 - Access door. The height of the booth was 2.49 m, giving a final volume of  $33.24 \text{ m}^3$ .

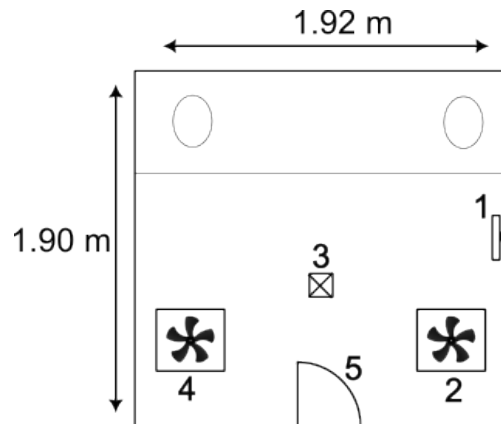


Figure 4.2: Top-down view of the toilet booth layout. Numbered elements are as follows: 1 - LE plug location, 2 - Air in flow vent, 3 - Canister sampling location, 4 - Air out flow vent, 5 - Access door. Ovals at the top of the schematic represent two toilets fitted on a plinth. The height of the booth was 2.6 m, giving a final volume of  $9.48 \text{ m}^3$ .

The entrance and exit doors of both booths were made of wood and glass, and set within a glass-panelled internal wall. The remaining three walls in each booth were constructed from plasterboard with a skim coat of plaster and finished with a white, non-gloss paint. No internal furnishings were present in either booth at any point during the sampling campaign, aside from the two permanently installed toilets in the smaller booths. Air inflow fans were sited in the ceiling for both the large and toilet booths, while the outflow fan was sited in the ceiling of the large booth, and 30cm from the floor in the toilet booth.

---

### 4.4.3 Sample analysis

Filled canisters were pressurised to 1 bar (gauge) with highly purified air free of VOCs, generated from a custom-built thermal catalytic oxidiser with compressed ambient air passed over platinum beads at 400 °C to fully oxidise any VOCs in the compressed air (hereafter referred to as ‘blank gas’). Samples were analysed following the method detailed in Warburton *et al.*<sup>[26]</sup> In brief, 500 mL of canister air was drawn through a 16-port Valco electrically-actuated multi-position valve (VICI Valco Instruments Co. Inc., TX, USA) into a custom-built thermal desorption unit (TDU), comprised of (sequentially) a water trap, a sample pre-concentration trap and finally a pre-injection focus trap. The first GC column was a 60 m long, 150  $\mu\text{m}$  internal diameter (ID) VF-WAX column with a film thickness of 0.50  $\mu\text{m}$  (Agilent Technologies, CA, USA) at a flow rate of 1.6 mL min<sup>-1</sup> (carrier gas pressure of 35 psi). The early eluting unresolved analytes (C<sub>2</sub> to C<sub>6</sub> hydrocarbons) were passed to an Na<sub>2</sub>SO<sub>4</sub>-deactivated Al<sub>2</sub>O<sub>3</sub> porous-layer open tubular (PLOT) column (50 m  $\times$  320  $\mu\text{m}$  ID, with a film thickness of 5  $\mu\text{m}$ , Agilent Technologies, CA, USA), through a Deans switch (Agilent Technologies, CA, USA) with detection via flame ionisation detection (FID). After 8.3 minutes, the Deans switch diverted the analyte flow through a section of fused silica (2 m  $\times$  150  $\mu\text{m}$  ID) to both balance column flows at the Deans switch and split analyte flow between the second FID and the quadrupole mass spectrometer (QMS) for simultaneous detection, through sections of 150  $\mu\text{m}$  ID fused silica of length 0.91 m and 2.1 m, respectively. GC elution data was acquired through MassHunter Qualitative Analysis (Agilent Technologies, CA, USA). The QMS ionisation was achieved through electron impact (EI) ionisation, with the QMS scanning for ions with an  $m/z$  between 30 and 150 units. Ion source temperature was 230 °C and an electron energy of 70 eV, with a quadrupole temperature of 150 °C.

Sample calibration was achieved by using a thirty-component mix of non-methane hydrocarbons (NMHCs) in nitrogen, with each gas at a mole fraction of approximately 4 ppb, provided by the National Physical Laboratory, Teddington, UK (cylinder number D933515, hereafter referred to as ‘NPL 30’) for VOCs contained therein, with remaining VOCs calibrated using equivalent carbon responses (ECN), using n-heptane as the proxy for ECN calculations. Blank gas was sampled three times after each canister sequence to confirm complete sample transfer and to allow for any artifacts to be corrected. After the blank gas samples, five NPL 30 calibrations were run, followed by three carrier gas/internal samples (‘no flow blanks’). The no flow blank method resembled a regular canister sample method, however no sample was drawn (sample fill volume was set to 0 mL), but the carrier gas flow rate and flow time remained unchanged, resulting in an equal volume of carrier gas flowing through the TDU, and subsequently the GC, as would occur in a regular sampling method. Combined, this

allowed for canister samples to be corrected for blank gas diluent contamination (none seen) and carrier gas, or system, contamination (consistently  $0.95 \mu\text{g m}^{-3}$  benzene only). Canisters would then be re-evacuated according to the previously described method. Canisters were randomly selected to check for contamination by filling from fully evacuated to 1 bar (gauge) with blank gas and run according to the previous method. Instrument limits of detection (LOD) and quantification (LOQ) for the six fragrance-originating VOCs in this paper are given in Table 4.1. LODs were calculated using a signal-to-noise ratio (SNR) of 3:1, and LOQ an SNR of 10:1.

Table 4.1: Instrument limits of detection (LOD) and quantification (LOQ) for the six fragrance species  $\alpha$ -pinene,  $\beta$ -pinene,  $\gamma$ -terpinene, *p*-cymene, eucalyptol, and benzaldehyde.

Species	LOD (ppt) / LOD ( $\text{ng m}^{-3}$ )	LOQ (ppt) / LOQ ( $\text{ng m}^{-3}$ )
$\alpha$ -pinene	2.93 / 16.3	9.76 / 54.4
$\beta$ -pinene	2.93 / 16.3	9.76 / 54.4
$\gamma$ -terpinene	2.93 / 16.3	9.76 / 54.4
<i>p</i> -cymene	2.93 / 16.1	9.76 / 53.6
eucalyptol	3.16 / 20.0	10.5 / 66.6
benzaldehyde	4.88 / 21.2	16.3 / 70.6

Chromatogram peak integration was completed using *GCWerks* (GC Soft Inc., CA, USA). Over 120 VOC species were identified and included in the automated analysis. Only the VOCs associated with the LE formulation are reported in this paper to simplify the presentation of results, however the entire VOC dataset is open-access from the Centre for Environmental Data Analysis (CEDA) repository at <https://www.ceda.ac.uk/>.

The fragrance formulation was known to the investigation team at University of York, however the formulation is commercially sensitive information and, beyond what is shown in this work, therefore cannot be disclosed in its entirety.

#### 4.4.4 Data visualisation and statistical analysis

All data analysis and manipulation were conducted using the R language, through RStudio software. The *tidyverse* package was used in all data processing. Data plotting used *ggplot2* for all figures except quantile–quantile plots (qq-plots) for data normality which used *ggpubr*. Boxplots show values in the order of (from bottom-to-top): lower outliers, 5th percentile, 25th percentile, median value, 75th percentile, 95th percentile, and upper outliers. Regression statistics were calculated using Spearman’s rho using *stat\_cor* from the *ggpubr* package.

---

A confidence interval of 95% ( $\alpha = 0.05$ ) was used to indicate significance. Diffuser increment plots were produced using the raster and *contour-filled* functions in *ggplot2*, with additional contour lines and contour line labels added using the *contour2* and *geom\_text\_contour* functions in the *metR* package.

For statistical analysis of VOC concentrations difference arising from different numbers of LE used in each booth, all data were first transformed by natural logarithm. Following this a Kruskal–Wallis test was completed on the transformed data with a *post-hoc* Dunn tests for species which returned a positive result for significance following the initial Kruskal–Wallis test, indicated by a *p*-value lower than the  $\alpha = 0.05$  level. Statistical analysis methodology for the olfactive results is given later.

#### 4.4.5 Olfactory methodology

Human olfactory testing was completed using a group of trained panellists from a sensory panel at Givaudan, UK. The members of the panel were selected based on their olfactory sensory acuity and then trained for a period of 4-6 months to enable them to discriminate between products and score consistently. The sensory panellist training programme at Givaudan, UK consists of several stages including: (1) discrimination through triangle tests, to enhance skills for differentiating between different odour types or odour intensities, (2) ranking, to develop skills for comparing the relative strength of sample, (3) scaling, to develop the ability to quantify differences between samples and (4) scoring against a control, to further develop the ability to use the scale. The trained panellists assessed the strength of the LEs from 10 m<sup>3</sup> toilet booths, following the same LE usage as with VOC sampling.

Samples were monadically assessed blind and sequentially. Panellists were not aware of the purpose of the investigation. The trained panellists were asked to rate the overall perceived intensity of the fragrance inside the 10 m<sup>3</sup> toilet booths using a linear 0-100 scale. Sample orders were randomised using a Latin square design to control experimental error. Replicates were included within the sample set, and panellists were not told there were replicates within the assessments. Sampled panellist data was assessed for reliability using published methods in Talsma (2018).<sup>[53]</sup> Statistical analysis was completed using analysis of variance (ANOVA) followed by a Benjamini–Hochberg *post-hoc* assessment to observe significance between levels. The ANOVA was additionally used to assess and ensure no significant interaction between products and replicates. As with sample VOC analysis, a confidence interval of 95% ( $\alpha = 0.05$ ) was used to indicate significance. Panellists sampled the LE scent through a porthole from the chamber so as to not interfere with booth airspace composition, and panellists were unaware of the number of LEs present within the booth.

---

#### 4.4.6 VOC metrics and modelling

In this paper, the metric “TVOC” is defined as the sum of all quantifiable VOCs within a sample, making it an operationally defined term specific to the analytical methods used. Additionally, we introduce the metric “fragrance TVOC,” which is operationally defined as the sum of the concentrations of six VOCs:  $\alpha$ -pinene,  $\beta$ -pinene,  $\gamma$ -terpinene, benzaldehyde, *p*-cymene, and eucalyptol. While this metric does not represent the entire fragrance formulation, it includes all fragrance-origin VOCs that were sampled and resolved using our methodology. The “fragrance TVOC” metric was adopted for brevity when describing the behaviour of VOCs originating from the LE fragrance. In specific cases, discussed later, individual fragrance VOCs were highlighted, particularly when some compounds were missing from samples or fell below detection limits.

Warburton *et al.* (2023)<sup>[26]</sup> reported a simple method for determining a steady-state increment of a species with a known emission rate, shown in equation 4.1:

$$A_H = \frac{6 \times 10^4 n G_p}{V(C_{in} - C_{ex})} \quad (4.1)$$

where  $C$  is the concentration of the species within an airspace ( $\mu\text{g m}^{-3}$ ),  $q$  is the emission rate of the species ( $\text{g h}^{-1}$ ),  $A_H$  is the air change rate ( $\text{h}^{-1}$ ) and  $V$  is the room volume ( $\text{m}^3$ ). This equation assumes a steady-state airspace in a well-mixed, one-box compartment with no chemical loss. In this study a more complete model was used which solves the ordinary differential equation (ODE) given in Carslaw (2007),<sup>[54]</sup> shown in equation 4.2, with some term symbols changed to match those used in equation 4.1. For the analysis in this study,  $\alpha$ -pinene was chosen to model concentrations, as it represented a considerable portion of the volatile fraction within the LE oil itself.

$$\frac{dC_s}{dt} = -V_d \left( \frac{A}{V_c} \right) C_s + \lambda f C_{out} - \lambda C_s + \frac{q_s}{V_c} + \sum_{j=1}^n R_{ij} \quad (4.2)$$

where  $C_s$  is the concentration of the species within the airspace ( $\text{molecule cm}^{-3}$ ),  $t$  is time (s),  $V_d$  is the deposition velocity of the species ( $\text{cm s}^{-1}$ ),  $A$  is the surface area of the room ( $\text{cm}^2$ ),  $V_c$  is the volume of the room ( $\text{cm}^3$ ),  $\lambda$  is air change rate ( $\text{h}^{-1}$ ),  $f$  is the outdoor-to-indoor penetration factor (dimensionless),  $q_s$  is the species emission rate ( $\text{molecule s}^{-1}$ ), and  $R_{ij}$  is the rate of reaction between species  $i$  and  $j$  ( $\text{molecule cm}^{-3} \text{s}^{-1}$ ). In this study, it was assumed there was no surface deposition, that the outdoor-to-indoor penetration factor was equal to 1 as in Dimitroulopoulou *et al.* (2001),<sup>[55]</sup> and chemical removal was via oxidation reactions with OH and  $\text{NO}_3$  radicals, as well as with  $\text{O}_3$ . Reaction rates were calculated for the oxidation of  $\alpha$ -

---

pinene to form APINAO<sub>2</sub>, APINBO<sub>2</sub>, APINCO<sub>2</sub>, NAPINAO<sub>2</sub>, NAPINBO<sub>2</sub>, APINOOA, and APINOOB, rate constants for which were obtained using the Master Chemical Mechanism (MCM) *via* <http://www.mcm.york.ac.uk>.<sup>[56,57]</sup> The ozone concentration was originally set to  $2.46 \times 10^{11}$  molecule cm<sup>-3</sup> (10 ppb) to give a model for  $\alpha$ -pinene increment expected in residential homes, but was set to  $8.61 \times 10^{11}$  molecule cm<sup>-3</sup> (35 ppb) to be reflective of the air make-up within the booths used in this study. OH and NO<sub>3</sub> radicals were given maximum concentrations of  $2 \times 10^6$  molecule cm<sup>-3</sup> and  $9.2 \times 10^8$  molecule cm<sup>-3</sup> respectively, in a sinusoidal circadian rhythm, with OH concentrations peaking at 12 pm and NO<sub>3</sub> concentrations peaking at 2 am. Low concentrations used for OH and NO<sub>3</sub> were  $1 \times 10^5$  molecule cm<sup>-3</sup> and  $1 \times 10^6$  molecule cm<sup>-3</sup>, respectively. NO<sub>3</sub> radicals, while important in VOC oxidation, do not typically see very high indoor concentrations and are normally not a major consideration for indoor modelling.<sup>[54]</sup> However, in this study the booths were supplied with outdoor air throughout, and additionally were allowed to equilibrate for one day before sampling began. As such the air makeup in the booths over the sampling period was treated as if it were outdoor air and subject to circadian outdoor behaviours.

The rooms are based at a large industrial facility in Ashford, UK where similar sensory science investigations take place and were compared against available data for comparable locations and times of year when samples were obtained, with ozone fractions taken from <http://www.gov.uk/government/statistical-data-sets/env02-air-quality-statistics>, OH radical concentrations were informed from Heard et al. (2004)<sup>[58]</sup> and Rivett et al. (2003),<sup>[59]</sup> and NO<sub>3</sub> radical concentrations were informed from Asaf et al. (2009),<sup>[60]</sup> Abdalmogith and Harrison (2006)<sup>[61]</sup> and Khan et al. (2015).<sup>[62]</sup> This model, which assumes a well-mixed one-box compartment, was run for each emission rate with a 5 second resolution over one day of constant emission and was then iterated over a variety of air change rates and volumes to give an array of simulations for each LE emission load. As each simulation progressed, the room concentration of  $\alpha$ -pinene reached a constant concentration, indicating the simulation had reached a steady-state. The simulated steady-state concentrations were then plotted as a  $z$ -axis colour contour against room volume and air change rate.

Using equation 4.2 to model indoor VOC concentrations provided a more comprehensive prediction than equation 4.1, as it accounted for VOC loss through various pathways, most importantly oxidation. Monoterpenes and monoterpenoids, which are highly reactive indoors, underwent oxidation particularly with ozone, as well as with nitrate and hydroxyl radicals. This oxidation served as a substantial sink for these compounds. For upper-bound estimates, equation 4.1 provided a straightforward method for approximating concentrations; however, for this more detailed analysis of one specific VOC, equation 4.2 yielded a fuller

---

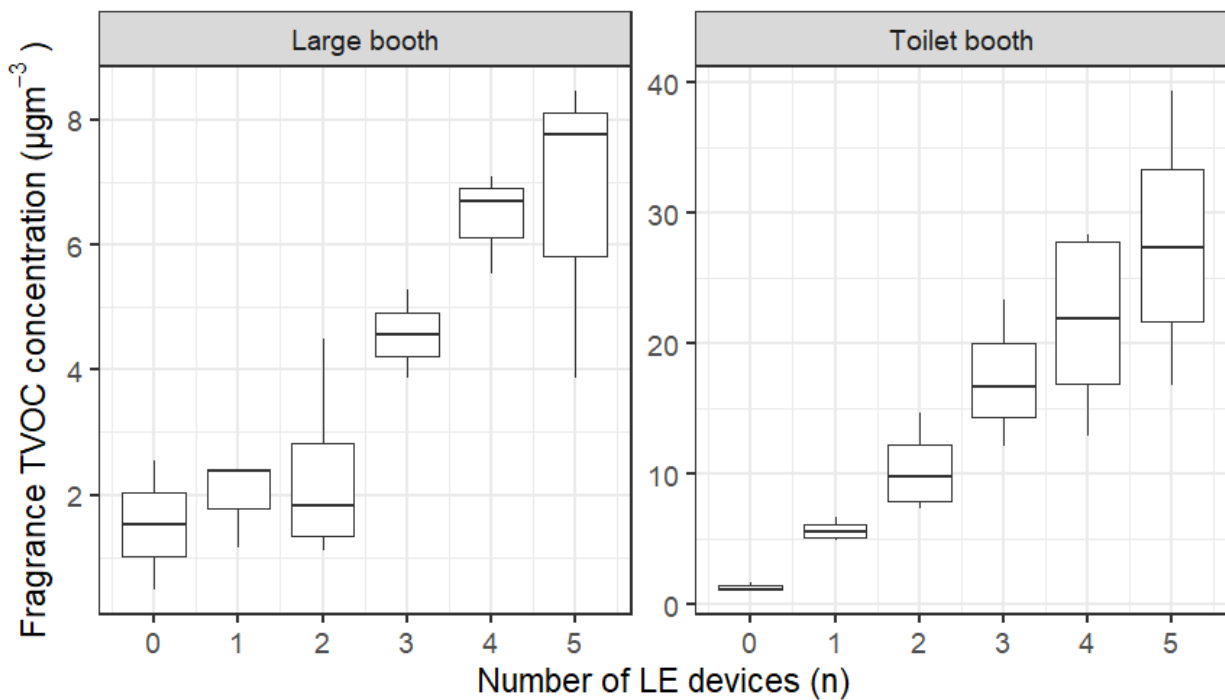
representation.

## 4.5 Results and discussion

### 4.5.1 TVOC and fragrance species concentrations

Boxplots of fragrance TVOC concentration at discrete levels of LEs (0–5) are shown in Fig. 4.3. As would be expected, the VOC concentrations in the smaller booths were higher than in the larger room, however both increased linearly as the number of LE devices increased. Fig. 4.4 shows the change in mean individual species concentrations and linear regression statistics for the large room as number of LE devices increases, with Fig. 4.5 showing the same for the small booth. Spearman’s Rho was used in the calculation of regression statistics, and  $R$  and  $p$ -values are given on each plot. Significant linearities were found for  $\alpha$ -pinene and  $p$ -cymene for the large booth, and all quantifiable species in the toilet booth. The effect of additional LEs in the large booth was more scattered and at lower concentrations than the toilet booth. Neither showed any indication of concentration plateauing at a high number of concurrent LEs. Note that significance in linearity does not reflect significance in the pairwise comparison of concentrations across LE levels, which is discussed later on. Benzaldehyde 0 LE concentrations in the large booth appeared to be a potential outlier, as this higher-than-expected concentration skewed the linearity significantly. Ignoring the 0 LE result, LE additions resulted in a linear and roughly stepwise trend. Replacing this outlier with the 0 LE benzaldehyde concentration from toilet booth data resulted in a significant linearity with  $R = 1$  and  $p = 0.0028$  (figure 4.6).

It has been previously reported that VOCs with lower vapour pressures tend to have lower human odour detection limits (ODLs).<sup>[63,64]</sup> Value-based definitions of VOCs vary, but vapour pressure-based definitions separating VOCs from lower-vapour pressure species is generally between 0.075 mmHg and 0.1 mmHg.<sup>[65,66]</sup> Tamas *et al.* (2006)<sup>[67]</sup> demonstrated a plateauing of perception of limonene (vapour pressure/ $V_p = 1.5$  mmHg) within test chambers up to 115 ppb, or approximately  $641 \mu\text{g m}^{-3}$ . The same study also reported an ODL for limonene of around 40 ppb, or approximately  $220 \mu\text{g m}^{-3}$ . Yoshio *et al.* (2003)<sup>[46]</sup> reported a limonene ODL of approximately 40 ppb also, and an  $\alpha$ -pinene ( $V_p = 4.75$  mmHg) ODL of 18 ppb, or roughly  $101 \mu\text{g m}^{-3}$ , with a  $\beta$ -pinene ( $V_p = 2.93$  mmHg) ODL of approximately 33 ppb, or roughly  $184 \mu\text{g m}^{-3}$ . Yoshio *et al.* (2003)<sup>[46]</sup> also report the ODL for the sesquiterpenoid geosmin ( $V_p = 0.003$  mmHg) at 6.5 ppt, or  $0.05 \mu\text{g m}^{-3}$ , and Schoenauer and Schieberle (2016)<sup>[68]</sup> reporting an ODL for grapefruit mercaptan ( $V_p = 0.1$  mmHg) of 0.0049 ppt, or approximately  $0.000034 \mu\text{g m}^{-3}$ . All vapour pressure values were obtained from The



Note - Fragrance TVOC is the sum of the concentrations for  $\alpha$ -pinene,  $\beta$ -pinene,  $\gamma$ -terpinene, eucalyptol, p-cymene and benzaldehyde

Figure 4.3: Boxplots of the spread of fragrance TVOC concentrations in the large booth (left panel) and toilet booth (right panel). From bottom to top, each boxplot shows 5th percentile, 25th percentile, 50th percentile/median, 75th percentile, 95th percentile. Any outliers are given as single dots above or below the 5th/95th whisker.

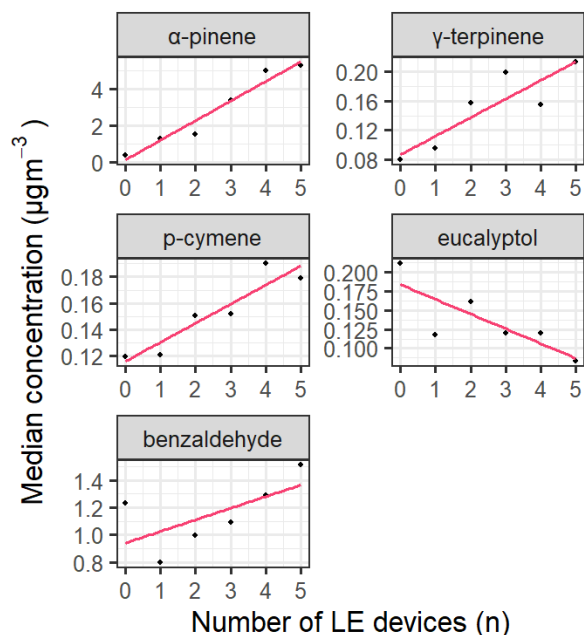


Figure 4.4: Scatter plot showing median concentration results for fragrance species at each LE level (0 to 5) for the large booth. Regression statistics for each species:  $\alpha$ -pinene  $R = 1$ ,  $p = 0.0028$ ;  $\gamma$ -terpinene  $R = 0.83$ ,  $p = 0.058$ ;  $p$ -cymene  $R = 0.94$ ,  $p = 0.017$ ; eucalyptol  $R = -0.6$ ,  $p = 0.24$ ; benzaldehyde  $R = 0.66$ ,  $p = 0.18$

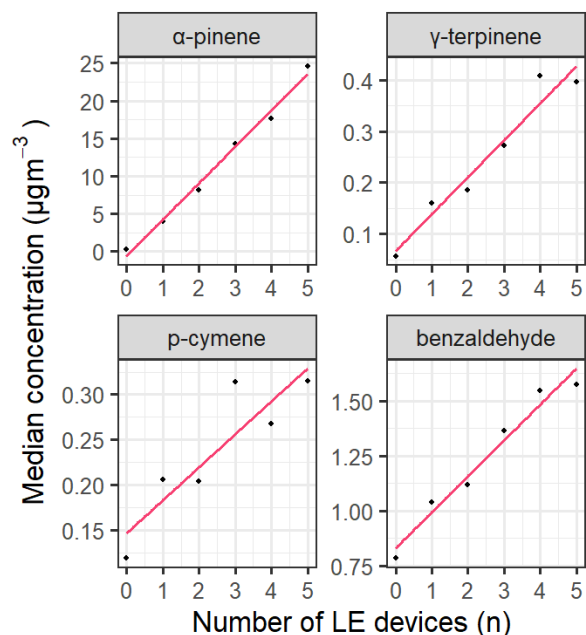


Figure 4.5: Scatter plot showing median concentration results for fragrance species at each LE level (0 to 5) for the toilet booth. Regression statistics for each species:  $\alpha$ -pinene  $R = 1$ ,  $p = 0.0028$ ;  $\gamma$ -terpinene  $R = 0.94$ ,  $p = 0.017$ ;  $p$ -cymene  $R = 0.89$ ,  $p = 0.033$ ; benzaldehyde  $R = 1$ ,  $p = 0.0028$ .

Concentrations are given in  $\mu\text{g m}^{-3}$ . Regression statistics were calculated using Spearman's Rho. Note -  $\beta$ -pinene plots are missing from both figures 4.4 and 4.5 as all values were below the LOQ for  $\beta$ -pinene. Eucalyptol is missing from figure 4.5 due to only having values above LOQ for LE levels 5 and 6, resulting in an incomplete plot.

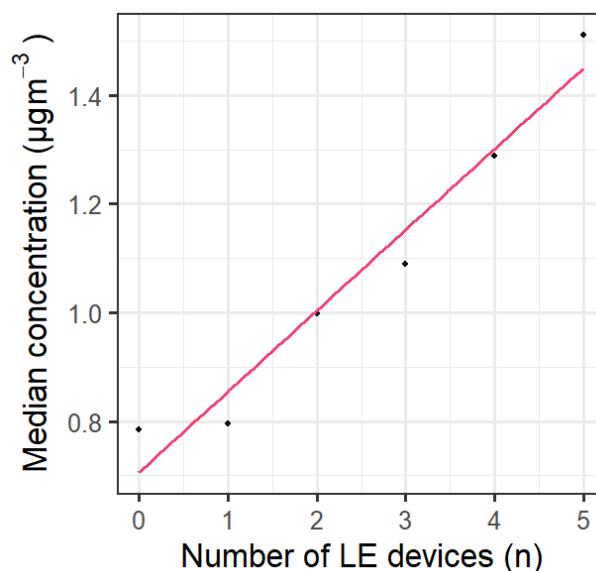


Figure 4.6: Re-plot large booth benzaldehyde linearity, using the 0 LE concentration from the toilet booth to attempt to de-skew the regression caused by the outlying 0 LE large booth benzaldehyde concentration. The resulting linearity was of significance. Regression statistics ( $R = 1$ ,  $p = 0.0028$ ) were calculated using Spearman's Rho.

Good Scents Company (<http://www.thegoodscentcompany.com/>). As described in later sections of this paper, toilet booths were perceived by sensory panellists to have detectable fragrance odour when any number of LEs (1–5) were present, however the ‘measurable’ VOC component of the fragrance (monoterpenes and other higher vapour pressure species) were at concentrations below their individually reported ODLs, suggesting that the detectable odour arose from less volatile species from the fragrance formulation such as  $\gamma$ -undecalactone and  $\beta$ -caryophyllene – likely present at ppt and sub-ppt mixing ratios and below measurable limits.

#### 4.5.2 Comparison of LE emission rates

LEs were weighed before and after sample collection to determine oil mass loss over the sampling period. Median diffuser mass loss was 2.54 g, average mass loss was 2.67 g, with a standard deviation of 0.50 g. Using mean mass loss, this resulted in an overall LE oil emission rate of 0.028 g h<sup>-1</sup>. Using the known fragrance formulation this gave an  $\alpha$ -pinene emission rate of  $1.60 \times 10^{-3}$  g h<sup>-1</sup>. The LE emission rate was compared against available literature, shown in Table 1. There was little literature available which disclosed LE emission rates directly or contained data from which an emission rate could be calculated. Values were taken from Warburton *et al.* (2023),<sup>[26]</sup> Angulo-Milhem *et al.* (2023)<sup>[24]</sup> and Angulo-Milhem

Table 4.2: Comparison of LE emission rates and booth properties between this study and several other studies available in literature.

	This study	Warburton <i>et al.</i> (2023) <sup>[26]</sup>	Angulo-Milhem <i>et al.</i> (2023) <sup>[24]</sup>	Angulo-Milhem <i>et al.</i> (2021) <sup>[23]</sup>
<b>Diffuser emission rate (g hr<sup>-1</sup>)</b>	0.028	0.024	0.053	0.044
<b>Chamber volume (m<sup>3</sup>)</b>	33.73 (large booth) 9.49 (toilet booth)	-	40	1
<b>Air change rate/ACR (hr<sup>-1</sup>)</b>	7.5	-	0.3 ±0.1	0.3 ±0.05

*et al.* (2021).<sup>[23]</sup> In Angulo-Milhem *et al.* (2021)<sup>[23]</sup> it was noted the LE was placed on a medium intensity, resulting in an emission rate of 0.044 g h<sup>-1</sup>. It is common for commercial LE devices to have both variable and fixed output settings, however the LE used in this study had a fixed output. Given the lack of available emission rate statistics of LEs in literature, it was not possible to contextualise these emission rates, however the impact of a higher oil emission rate would be seen in both elevated concentrations of emitted VOCs, as well as increased fragrance perception. Section 3.4 discusses the estimation of indoor concentrations from known emission rates and sources.

### 4.5.3 Perceived intensity of LEs

Trained sensory panellists were asked to give an overall perceived intensity rating from 0 to 100 for the toilet booths, containing between 0 and 5 LEs. Panellists were blind to the number of LEs present in the room during each assessment. Fig. 4.7 gives mean results from the difference in perceived fragrance intensity as pairwise values. A stepwise increase in LE number, *i.e.* from 1 to 2 to 3 *etc.*, resulted in increasing small perceived differences in odour intensity once the first LE was added. The most marked increase in step-wise perception of change in fragrance odour was between rooms containing 0 and 1 LE. Testers identified limited differences in their perception of the fragrance intensity between 2 and 3 or more devices. For olfactive results, pairwise analysis was completed on difference in perceived intensity using an Analysis of Variation (ANOVA) test, with a Benjamini–Hochberg *post-hoc* assessment, *p*-values for which are shown as a matrix in Fig. 4.8. These results confirmed a step-wise incremental increase in significance for the addition of LEs up to 2, after which the significance of the difference in perceived intensity drops and did not give rise to further significant increase in perceived fragrance intensity. Fragrance TVOC concentrations were assessed across LE levels using a Kruskal-Wallis test, which returned a positive stochastic result for significance. All samples were used in this assessment, and the data were transformed by

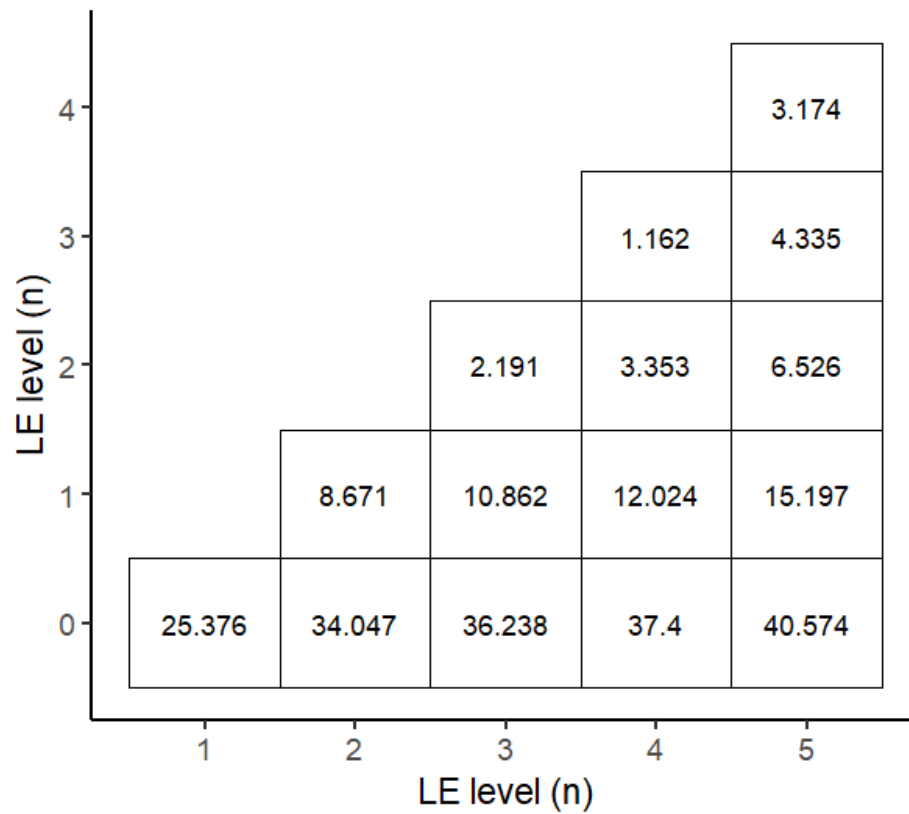


Figure 4.7: A matrix which shows the mean change in perceived fragrance intensity at each combination of LE level from a scale of 0 to 100, 0 being the lowest/no change in perceived intensity and 100 being the highest.

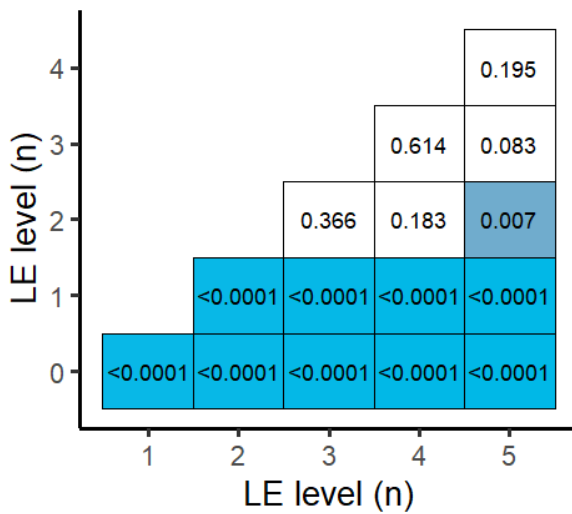


Figure 4.8: Matrix showing  $p$ -value results for each LE level pair following ANOVA and Benjamini-Hochberg *post-hoc* analysis for fragrance perception.

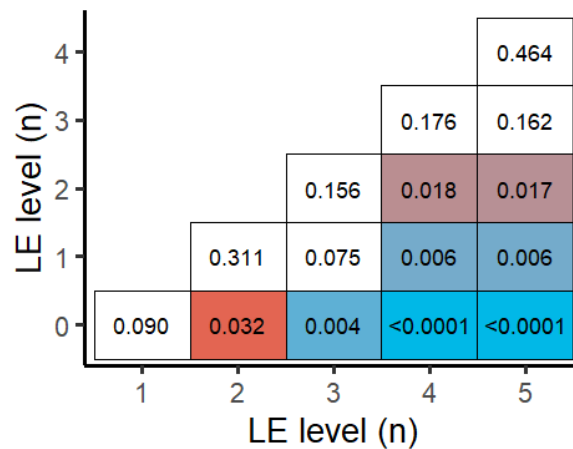


Figure 4.9: Matrix which shows  $p$ -value results for each LE level pair following Kruskal-Wallis and Dunn *post-hoc* analysis for fragrance TVOC concentrations.

Insignificant results are given in white, and results of significance graduate from red ( $p = 0.05$ ) to blue ( $p \rightarrow 0$ ).

---

natural logarithm prior to Kruskal–Wallis analysis. A *post-hoc* Dunn test was then performed, which gave the *p*-value results shown in Fig. 4.9. Pairwise analysis of fragrance TVOC concentrations yielded insignificant results when comparing a stepwise increase in LE number, with significant pairwise increases in fragrance TVOC concentration only found when multiple LEs were added into the airspace at once.

The lack of significance in perception of change in intensity may lead to a real-world consequence where the use of LEs in a single room is to a degree self-limiting because of limited perception of further benefit to the user if additional LEs are added. We however note that other factors such as user tolerance and fragrance acceptability will also contribute to end-user-based limitation of LE use, and future work would be required to identify whether LE use could be labelled as self-limiting. In the larger room and with the maximum of 5 LEs operating, a median  $\alpha$ -pinene concentration of  $5 \mu\text{g m}^{-3}$  and an upper  $\alpha$ -pinene concentration of  $7 \mu\text{g m}^{-3}$  was generated. This is a surprisingly low concentration given the number of LEs present. The concentration of  $\alpha$ -pinene in the larger room was typical of concentrations (within the 50th percentile) found in real-world homes with comparable room sizes in the work of Heeley-Hill *et al.* (2021)<sup>[29]</sup> and within the 60th percentile of homes in Warburton *et al.* (2023).<sup>[26]</sup> Monoterpene emissions are undoubtedly associated with the use of fragranced products and are often species with the higher emission fractions within product formulations such as in air fresheners, surface cleaners and shampoos.<sup>[69,70]</sup> However even in an exaggerated product perturbation experiment the concentrations of monoterpenes generated in realistically sized and ventilated rooms are low, hence their presence or absence may not be a good indicator for whether a room would have perceptible fragrance odour.

#### 4.5.4 Modelling $\alpha$ -pinene increments

Fig. 4.10 shows the resulting contour plot for the increment of  $\alpha$ -pinene from the use of one diffuser. As the increment increases, the colour of the contour graduates from blue through to red. This model shows that plausibly high concentrations are possible in very small rooms combined with low ACRs. Spaces in homes with this combination of low volume and low ACR are likely to be rooms where occupancy is incidental and episodic however, rather than over longer periods of time, such as under-the-stairs cloakrooms or porch cupboards. The short-term (30 min) exposure limit for  $\alpha$ -pinene in indoor settings in the UK is  $45000 \mu\text{g m}^{-3}$ ,<sup>[71]</sup> which may give rise to noticeable effects to the consumer's comfort. Using 1 LE with the lowest feasible model combination of room volume and ACR in the above model ( $V = 0.5 \text{ m}^3$ ,  $A_H = 0.5 \text{ h}^{-1}$ ) gave an  $\alpha$ -pinene increment of  $3700 \mu\text{g m}^{-3}$ , more than an order of magnitude lower than the short-term exposure limit, and also lower than the long-term

---

exposure limit (1 day of constant exposure) of  $4500 \mu\text{g m}^{-3}$ .<sup>[71]</sup> However, spaces in homes with this combination of room volume and ACR are likely small cupboards (kitchen cupboards, under-the-stairs storage cupboards) where VOC exposure would be incidental, and LE use is unlikely. A comparison of sampled concentrations from this study, along with exposure thresholds are given in Table 4.3.

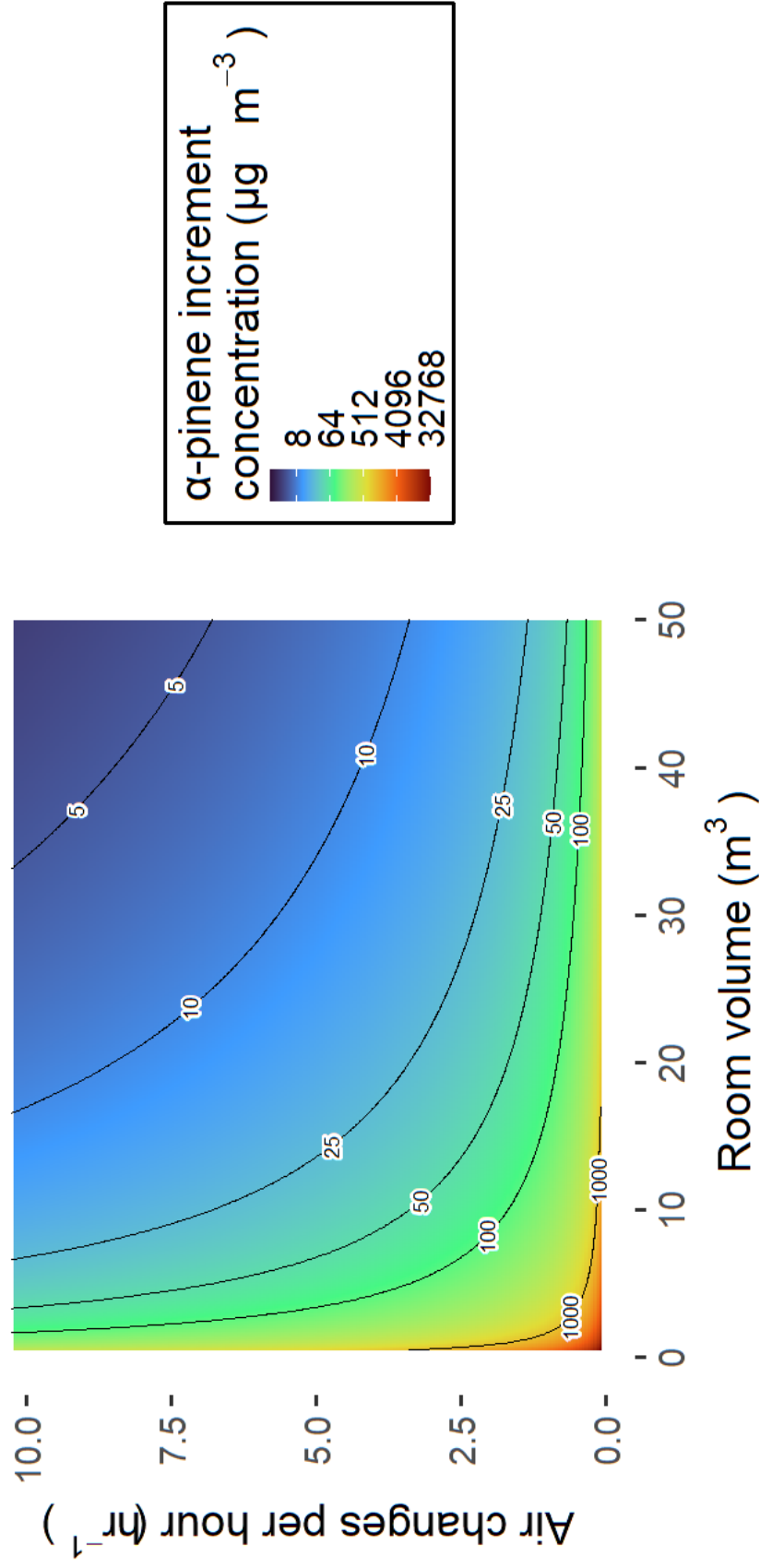


Figure 4.10: Raster plot showing expected increment concentration of  $\alpha$ -pinene in  $\mu\text{g m}^{-3}$ , against ventilation rates in units of  $\text{h}^{-1}$ , and room volumes in units of  $\text{m}^3$ . Concentrations were calculated using mean LE emission rates from this study. Increment concentrations graduate on a low-to-high colour scale from blue to red.

Table 4.3: Comparison of median sampled concentrations from this study against UK indoor exposure thresholds available from Public Health England.<sup>[74]</sup> All concentrations are shown in  $\mu\text{g m}^{-3}$ .

Species	1 LE (small booth)	1 LE (large booth)	5 LE (small booth)	5 LE (large booth)	Indoor short- term limit	Indoor long- term limit
$\alpha$ -pinene	3.980	1.264	24.580	5.289	45 000 <sup>a</sup>	4500 <sup>c</sup>
Limonene	0.162	0.038	0.947	0.117	90 000 <sup>a</sup>	9000 <sup>c</sup>
Acetaldehyde	4.800	4.881	4.799	5.710	1420 <sup>b</sup>	280 <sup>c</sup>
Benzene	0.632	0.485	0.644	0.435	0 <sup>d</sup>	0 <sup>d</sup>

<sup>a</sup> 30 min exposure

<sup>b</sup> 1 hour exposure

<sup>c</sup> 1 day exposure

<sup>d</sup> No safe exposure limit to benzene has been published, however England and Wales have a  $5 \mu\text{g m}^{-3}$  benzene concentration target according to European (EU) ambient air quality directive 2008/50/EC.

---

### 4.5.5 Comparison with real-world analogues

Chambers or booths are used extensively to measure emissions of VOCs from household products and also have applications in sensory sciences.<sup>[72-74]</sup> Chambers for VOC analysis are typically of stainless steel construction with glass panels and sampling ports, and while they can range in sizes, they are typically smaller volumes for ease of use and space in laboratories. While smaller testing chambers allow for potentially better analysis of emitted VOCs through product use for instruments with higher detection limits, they do not necessarily replicate the same conditions found in real-world analogues. In this study, two sizes of booths were used, a smaller booth of approximately 10 m<sup>3</sup> and a larger booth of approximately 30 m<sup>3</sup>, representing the size of a bathroom and living room, respectively. The booths used in this study additionally had more real-world representative surfaces within the volume, such as painted walls and wooden doors.

Fig. 4.11 shows a comparison of the concentrations of samples from this study compared with real-world concentrations of VOCs through LE use found in Warburton *et al.* (2023).<sup>[26]</sup> The same LE device and liquid formulation was used across both studies. It should be noted that the rooms used in Warburton *et al.* (2023)<sup>[26]</sup> were the main living area of the house and ranged from between 20 m<sup>3</sup> and 50 m<sup>3</sup> in volume. Whilst the data showed incremental fragrance VOC increases in the booth plot (especially so for the more confined space of the toilet booth), comparison with a cohort of real-world homes from Warburton *et al.* (2023)<sup>[26]</sup> showed little difference in both the overall VOC concentrations found, and in the concentrations of individual fragrance VOCs between the two studies. This may, of course, arise from the differences in ACR levels between homes and the test booths, although comparative data for one LE in both situations shows little difference in concentrations reported. From a consumer perspective, the concentrations generated in the large booths when multiple devices were used did not lead to elevated fragrance VOC concentrations above those seen typically in homes, remaining well below the short-term and long-term exposure limit (1 day of constant exposure) as outlined by UK indoor exposure thresholds available from Public Health England (Table 4.3).<sup>[71]</sup> Although assessing potential health impacts is beyond the scope of this study, modelling indicated that high VOC concentrations approaching exposure limit thresholds could occur only in rooms with an unrealistic combination of low ACRs and small volumes. Typically, product packaging provides user guidance on proper usage, including recommendations for adequate ventilation and suitable room size. Using the device in small, poorly ventilated spaces would therefore be considered off-label use.

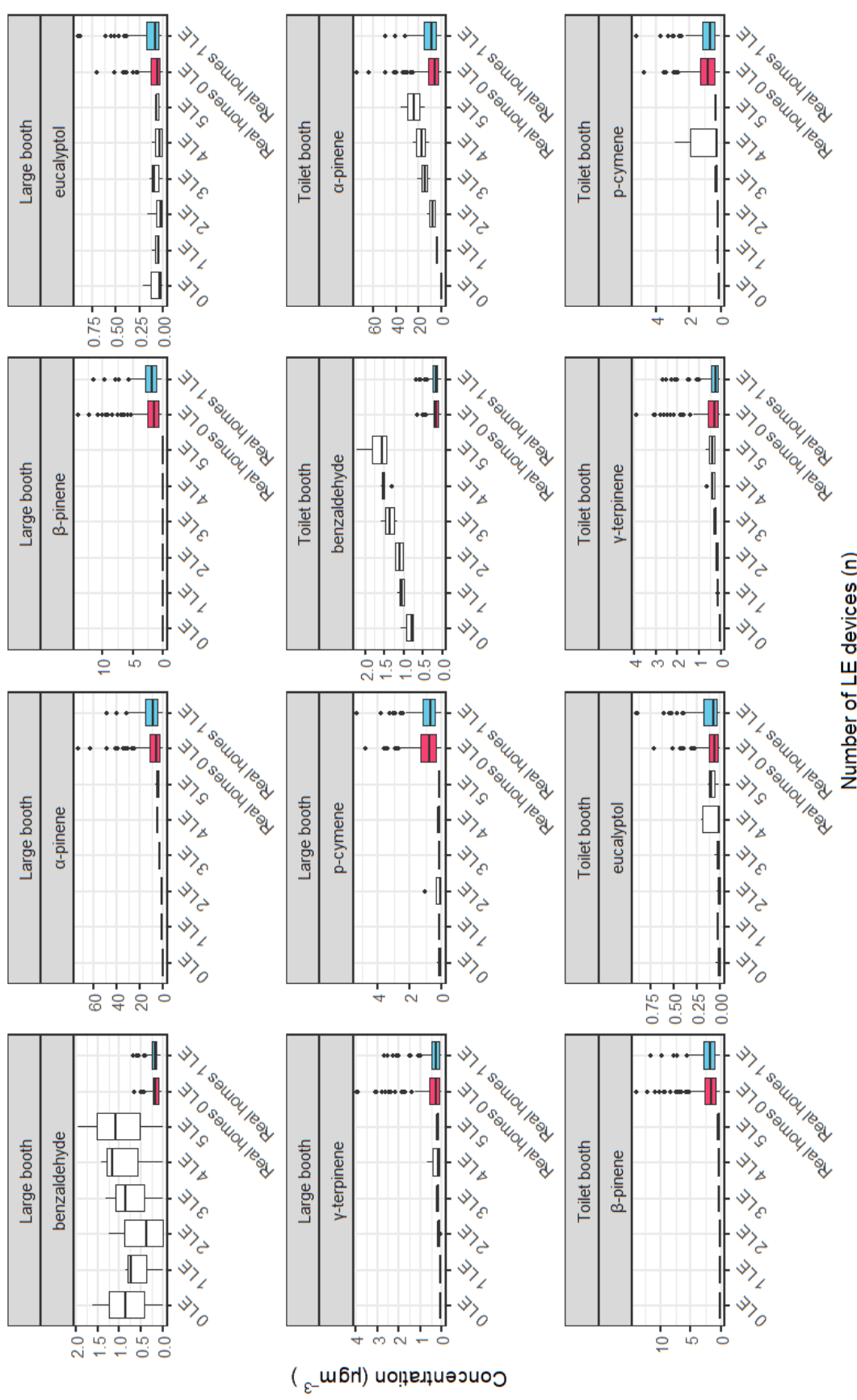


Figure 4.11: Comparison of concentrations collected in this study against the concentrations found in Warburton *et al.* (2023), [26] using the same LE device and liquid formulation. All concentrations are shown in  $\mu\text{g m}^{-3}$ . Concentrations from Warburton *et al.* (2023) [26] are displayed on the plots as 'Real homes'. From bottom to top, each boxplot shows 5th percentile, 25th percentile, 50th percentile/median, 75th percentile, 95th percentile. Any outliers are given as single dots above or below the 5th/95th whisker.

---

Comparisons between chamber-based studies and real-world studies are complex by nature. In real-world scenarios, there is more than likely no one single point emission source of VOCs throughout the sampling period, and air makeup is highly changeable between samples.<sup>[75]</sup> Additionally, in booths there are typically in-flows and out-flows to create air exchange, which may interfere with VOC release and mixing into the volume. Such molecular-level disturbances may be difficult to detect through typical means such as the use of anemometers. However, in this study, the booths were made to be as reflective of real-world conditions as possible, given the sensory science-based nature of the regular use of the booths used in this study.

## 4.6 Conclusions

In this study the olfactive perception and VOC concentrations arising from fragrance LE use in controlled but realistically sized and ventilated test rooms were assessed. As the number of LEs deployed in a room increased, concentrations of VOCs increased linearly, although individual VOC concentrations lower than  $10 \mu\text{g m}^{-3}$  were generated in the larger room. Based on intensity feedback reported by trained panelists, the perception of the intensity change arising from incrementally adding LEs into a room was not of significance above 2 LEs in the  $10 \text{ m}^3$  toilet booths. The potential exists for multiple devices to be added to a single room space. In these cases, there was limited difference in fragrance intensity when 2 or more LEs were added concurrently. The lack of human perception of increased fragranced intensity with the use of multiple LEs within an airspace may however limit the potential for such off-instruction use, since little end user benefit is likely to be detected or where the consumer felt that 1 LE was performing adequately.

When 5 LEs were used in test rooms, concentrations of volatile monoterpenes remained relatively low despite testers reporting intense fragrance.  $\alpha$ -pinene concentrations generated in the test rooms using 5 LEs were comparable to typical concentrations found ordinarily in residential homes, with upper  $\alpha$ -pinene concentrations comparing between the 50th to 60th percentile of real-home data in available literature. The in-room concentrations of  $\alpha$ -pinene were below the literature reported individual ODL.

Analysis between this study and a real-world study using an LE showed generally comparable VOC release and in-room concentrations across both studies. The use of controlled but realistic booths and chambers could be a reasonable substitute to predict VOC exposure for regular LE consumer uses.

There are broader implications however for indoor air quality. Reactive VOCs can impact

---

indoor air quality through atmospheric reactions that generate by-products such as formaldehyde, acetaldehyde and secondary organic particulate matter. Ultimately, the contribution that a fragranced-derived compound will make to increasing secondary pollutants indoors will be a combination of the amount emitted and available for oxidation in air, the available oxidants (*e.g.* O<sub>3</sub>, Cl, NO<sub>3</sub>, OH), and the bimolecular rate coefficients. It is clear that some components of the LE fragrance tested here create strong perceptible odours for humans but generate only very low concentrations in the gas phase. These were not detectable by the sampling and TD-GC-QMS methods used here, and it can be hypothesised that concentrations are likely to be in the low part per trillion range or below, rather than part per billion which was typical of more volatile species such as monoterpenes.

Much literature discussion of the possible indoor impacts of fragranced products considers the ultimate fate of the emissions following gas phase oxidation reactions. If a fragrance contains monoterpenes and the use of the product generates in-room increments in the order of tens of  $\mu\text{g m}^{-3}$  in indoor air, that in turn has the potential to create comparable  $\mu\text{g m}^{-3}$  increments of formaldehyde (having a VOC to HCHO yield in the region 5–10%).<sup>[76]</sup>

In this study whilst monoterpenes were a substantial component of the fragrance formulation and the major type of VOC generated indoors from the use of LE products, they did not appear to be a major contributor to the perception of fragrance by human testers. Often concentrations were below their reported ODL. Reduction of monoterpene content from raw materials might be a means to reduce possible indoor air pollution in low-ventilation homes without necessarily substantially changing human-perceived product performance.

#### 4.6.1 Future work

Future work aimed at identifying the olfactive intensity of fragrances in controlled settings should consider assessments under variable ACRs, as this could illuminate perception gradients by varying the concentration of LE-emitted VOCs. A challenge in such studies would be the pairing of air sampling and analytical methods to resolve both the highly volatile fractions of fragrance formulations, as achieved in this study, and the less volatile fractions, which are likely present at  $\leq$ ppt gas-phase mixing ratios. However, the use of sensitive on-line analytical techniques, such as proton transfer reaction (PTR) or selected ion flow tube (SIFT) mass spectrometry, could enable assessments of the emitted concentrations of these lower volatility species, as well as offer a time series of emissions and decays of LE-originating VOCs.

---

## 4.6.2 Limitations and considerations

In this study, the booths were supplied with a fixed ventilation rate, resulting in an ACR of  $7.5 \text{ hr}^{-1}$ . This is significantly higher than typical values for most residential settings, unless mechanical ventilation is actively running. However, this higher ACR for the toilet booths was more consistent with conditions expected in a residential bathroom with extraction ventilation in operation. To improve the relevance of findings to residential environments, future experiments should be conducted under a range of ACRs to assess potential perception gradients and evaluate how ventilation affects perceived fragrance strength.

Because this study combined VOC emission analysis with human olfactive strength assessments, it was essential that the booth atmosphere remained undisturbed aside from the controlled air exchange. Opening the main booth door would have caused a rapid influx of air, diluting the VOCs and compromising both the integrity of the olfactive assessments and the time-integrated air sampling. As a result, the experiment could not be conducted under conditions of variable occupancy during the LE emission period. Future studies incorporating either actual or simulated occupancy, without undermining experimental rigour, could provide further insight. Simulated occupancy could be achieved by introducing a controlled emission of a blend of biogenically-derived VOCs over time to mimic human presence in the space.

All booths were controlled for relative humidity and temperature in this study. For olfactive assessments, these variables must be controlled. However to ensure relevance in real residential settings, repeated assessments with varying temperatures and relative humidities would offer further insight into potential strength perception gradients.

---

## 4.7 References

- [1] Narayanaganesh Balasubramanian. “Scented Oils and Perfumes”. In: *Chemical Technology in Antiquity*. Vol. 1211. American Chemical Society, 2015, pp. 219–244. ISBN: 9780841231122. DOI: [doi : 10 . 1021 / bk - 2015 - 1211 . ch00810 . 1021 / bk - 2015 - 1211 . ch008](https://doi.org/10.1021/bk-2015-1211.ch00810.1021/bk-2015-1211.ch008). URL: <https://doi.org/10.1021/bk-2015-1211.ch008>.
- [2] Dimitra Voudouri and Christine Tesseromatis. “Perfumery from myth to antiquity”. In: *International Journal of Medicine and Pharmacy* 3 (2015), pp. 41–55.
- [3] Muhammad Thalal. “Fragrances from Heaven: The relevance of smelling in understanding the early history of Islam”. In: *Jurnal Ilmiah Islam Futura* 20.1 (2020), p. 35. DOI: [10.22373/jiif.v20i1.5831](https://dx.doi.org/10.22373/jiif.v20i1.5831). URL: <https://dx.doi.org/10.22373/jiif.v20i1.5831>.
- [4] Weiyang Chen, Ilze Vermaak, and Alvaro Viljoen. “Camphor—A Fumigant during the Black Death and a Coveted Fragrant Wood in Ancient Egypt and Babylon—A Review”. In: *Molecules* 18.5 (2013), pp. 5434–5454. DOI: [10.3390/molecules18055434](https://dx.doi.org/10.3390/molecules18055434). URL: <https://dx.doi.org/10.3390/molecules18055434>.
- [5] Neda Nematollahi, Spas D Kolev, and Anne Steinemann. “Volatile chemical emissions from 134 common consumer products”. In: *Air Quality, Atmosphere & Health* 12.11 (2019), pp. 1259–1265. DOI: [10.1007/s11869-019-00754-0](https://dx.doi.org/10.1007/s11869-019-00754-0). URL: <https://dx.doi.org/10.1007/s11869-019-00754-0>.
- [6] Peder Wolkoff and Gunnar D Nielsen. “Effects by inhalation of abundant fragrances in indoor air – An overview”. In: *Environment International* 101 (2017), pp. 96–107. DOI: <https://doi.org/10.1016/j.envint.2017.01.013>. URL: <https://www.sciencedirect.com/science/article/pii/S0160412016305955>.
- [7] Dong Sik Yang, Ki-Cheol Son, and Stanley J Kays. “Volatile Organic Compounds Emanating from Indoor Ornamental Plants”. In: *HortScience* 44.2 (2009), pp. 396–400. DOI: [10.21273/hortsci.44.2.396](https://dx.doi.org/10.21273/hortsci.44.2.396). URL: <https://dx.doi.org/10.21273/hortsci.44.2.396>.
- [8] Sylwia Król, Jacek Namieśnik, and Bożena Zabiegała. “ $\alpha$ -Pinene, 3-carene and d-limonene in indoor air of Polish apartments: The impact on air quality and human exposure”. In: *Science of The Total Environment* 468-469 (2014), pp. 985–995. DOI: [10.1016/j.scitotenv.2013.08.099](https://dx.doi.org/10.1016/j.scitotenv.2013.08.099). URL: <https://dx.doi.org/10.1016/j.scitotenv.2013.08.099>.
- [9] Felix Klein et al. “Indoor terpene emissions from cooking with herbs and pepper and their secondary organic aerosol production potential”. In: *Scientific Reports* 6.1 (2016), p. 36623. DOI: [10.1038/srep36623](https://dx.doi.org/10.1038/srep36623). URL: <https://dx.doi.org/10.1038/srep36623>.

- 
- [10] S Angulo Milhem et al. “Indoor use of essential oil-based cleaning products: Emission rate and indoor air quality impact assessment based on a realistic application methodology”. In: *Atmospheric Environment* 246 (2021), p. 118060. DOI: [10.1016/j.atmosenv.2020.118060](https://doi.org/10.1016/j.atmosenv.2020.118060). URL: <https://dx.doi.org/10.1016/j.atmosenv.2020.118060>.
- [11] Chunting Michelle Wang et al. “Unexpectedly high concentrations of monoterpenes in a study of UK homes”. In: *Environmental Science: Processes & Impacts* 19.4 (2017), pp. 528–537. DOI: [10.1039/c6em00569a](https://doi.org/10.1039/c6em00569a). URL: <https://dx.doi.org/10.1039/c6em00569a>.
- [12] N Carslaw and D Shaw. “Secondary product creation potential (SPCP): A metric for assessing the potential impact of indoor air pollution on human health”. In: *Environmental Science: Processes and Impacts* 21.8 (2019), pp. 1313–1322. DOI: [10.1039/c9em00140a](https://doi.org/10.1039/c9em00140a).
- [13] Helen L Davies et al. “A measurement and modelling investigation of the indoor air chemistry following cooking activities”. In: *Environmental Science: Processes & Impacts* 25.9 (2023), pp. 1532–1548. DOI: [10.1039/d3em00167a](https://doi.org/10.1039/d3em00167a). URL: <https://dx.doi.org/10.1039/d3em00167a>.
- [14] Shalit Moshe et al. “Volatile compounds emitted by rose cultivars: Fragrance perception by man and honeybees”. In: *Israel journal of plant sciences*. 52.3 (2004), pp. 245–255.
- [15] Elizabeth Tomasino, Mei Song, and Claudio Fuentes. “Odor Perception Interactions between Free Monoterpene Isomers and Wine Composition of Pinot Gris Wines”. In: *Journal of Agricultural and Food Chemistry* 68.10 (2020), pp. 3220–3227. DOI: [10.1021/acs.jafc.9b07505](https://doi.org/10.1021/acs.jafc.9b07505). URL: <https://dx.doi.org/10.1021/acs.jafc.9b07505>.
- [16] Kandhasamy Sowndhararajan et al. “Effect of olfactory stimulation of isomeric aroma compounds, (+)-limonene and terpinolene on human electroencephalographic activity”. In: *European Journal of Integrative Medicine* 7.6 (2015), pp. 561–566. DOI: <https://doi.org/10.1016/j.eujim.2015.08.006>. URL: <https://www.sciencedirect.com/science/article/pii/S1876382015300287>.
- [17] Kandhasamy Sowndhararajan and Songmun Kim. “Influence of Fragrances on Human Psychophysiological Activity: With Special Reference to Human Electroencephalographic Response”. In: *Scientia Pharmaceutica* 84.4 (2016), pp. 724–751. DOI: [10.3390/scipharm84040724](https://doi.org/10.3390/scipharm84040724). URL: <https://dx.doi.org/10.3390/scipharm84040724>.
- [18] Keun Hyung Park et al. “Evaluation of human electroencephalogram change for sensory effects of fragrance”. In: *Skin Research and Technology* 25.4 (2019), pp. 526–531. DOI: [10.1111/srt.12682](https://doi.org/10.1111/srt.12682). URL: <https://dx.doi.org/10.1111/srt.12682>.

- 
- [19] Lutfun Nahar et al. “Ruta Essential Oils: Composition and Bioactivities”. In: *Molecules* 26.16 (2021), p. 4766. DOI: [10.3390/molecules26164766](https://doi.org/10.3390/molecules26164766). URL: <https://dx.doi.org/10.3390/molecules26164766>.
- [20] Patrícia Sartorelli et al. “Chemical composition and antimicrobial activity of the essential oils from two species of Eucalyptus”. In: *Phytotherapy Research* 21.3 (2007), pp. 231–233. DOI: [10.1002/ptr.2051](https://doi.org/10.1002/ptr.2051). URL: <https://dx.doi.org/10.1002/ptr.2051>.
- [21] Şeyda Kivrak. “Essential oil composition and antioxidant activities of eight cultivars of Lavender and Lavandin from western Anatolia”. In: *Industrial Crops and Products* 117 (2018), pp. 88–96. DOI: <https://doi.org/10.1016/j.indcrop.2018.02.089>. URL: <https://www.sciencedirect.com/science/article/pii/S0926669018302097>.
- [22] E Uhde and N Schulz. “Impact of room fragrance products on indoor air quality”. In: *Atmospheric Environment* 106 (2015), pp. 492–502. DOI: [10.1016/j.atmosenv.2014.11.020](https://doi.org/10.1016/j.atmosenv.2014.11.020).
- [23] Shadia Angulo-Milhem et al. “Indoor use of essential oils: Emission rates, exposure time and impact on air quality”. In: *Atmospheric Environment* 244 (2021), p. 117863. DOI: <https://doi.org/10.1016/j.atmosenv.2020.117863>. URL: <https://www.sciencedirect.com/science/article/pii/S1352231020305975>.
- [24] Shadia Angulo-Milhem et al. “Full-scale determination of essential oil diffusion: Impact on indoor air quality”. In: *Atmospheric Environment* 315 (2023), p. 120141. DOI: <https://doi.org/10.1016/j.atmosenv.2023.120141>. URL: <https://www.sciencedirect.com/science/article/pii/S1352231023005678>.
- [25] Wen-Hsi Cheng, Yi-Chian Chen, and Song-You Shih. “Volatile Organic Compound Emissions from Indoor Fragrance Diffusers”. In: *Atmosphere* 14.6 (2023), p. 1012. DOI: [10.3390/atmos14061012](https://doi.org/10.3390/atmos14061012). URL: <https://dx.doi.org/10.3390/atmos14061012>.
- [26] Thomas Warburton et al. “The impact of plug-in fragrance diffusers on residential indoor VOC concentrations”. In: *Environ. Sci.: Processes Impacts* 25.4 (2023), pp. 805–817. DOI: [10.1039/D2EM00444E](https://doi.org/10.1039/D2EM00444E). URL: <http://dx.doi.org/10.1039/D2EM00444E>.
- [27] Toshio Itoh et al. “Examination of VOC Concentration of Aroma Essential Oils and Their Major VOCs Diffused in Room Air”. In: *International Journal of Environmental Research and Public Health* 19.5 (2022), p. 2904. DOI: [10.3390/ijerph19052904](https://doi.org/10.3390/ijerph19052904). URL: <https://dx.doi.org/10.3390/ijerph19052904>.
- [28] I Myers and R L Maynard. “Polluted air—outdoors and indoors”. In: *Occupational Medicine* 55.6 (2005), pp. 432–438. DOI: [10.1093/occmed/kqi137](https://doi.org/10.1093/occmed/kqi137). URL: <https://doi.org/10.1093/occmed/kqi137>.

- 
- [29] A C Heeley-Hill et al. “Frequency of use of household products containing VOCs and indoor atmospheric concentrations in homes”. In: *Environmental Science: Processes and Impacts* 23.5 (2021), pp. 699–713. DOI: [10.1039/d0em00504e](https://doi.org/10.1039/d0em00504e).
- [30] A T Hodgson et al. “Effect of outside air ventilation rate on volatile organic compound concentrations in a call center”. In: *Atmospheric Environment* 37.39-40 (2003), pp. 5517–5527. DOI: [10.1016/j.atmosenv.2003.09.028](https://doi.org/10.1016/j.atmosenv.2003.09.028). URL: <https://dx.doi.org/10.1016/j.atmosenv.2003.09.028>.
- [31] Y Jia et al. “Investigation of indoor total volatile organic compound concentrations in densely occupied university buildings under natural ventilation: Temporal variation, correlation and source contribution”. In: *Indoor and Built Environment* 30.6 (2021), pp. 838–850. DOI: [10.1177/1420326X20914000](https://doi.org/10.1177/1420326X20914000).
- [32] German Hernandez et al. “The effect of ventilation on volatile organic compounds produced by new furnishings in residential buildings”. In: *Atmospheric Environment: X* 6 (Apr. 2020), p. 100069. DOI: [10.1016/j.aeaoa.2020.100069](https://doi.org/10.1016/j.aeaoa.2020.100069).
- [33] Peder Wolkoff, Kenichi Azuma, and Paolo Carrer. “Health, work performance, and risk of infection in office-like environments: The role of indoor temperature, air humidity, and ventilation”. In: *International Journal of Hygiene and Environmental Health* 233 (Apr. 2021), p. 113709. DOI: [10.1016/j.ijheh.2021.113709](https://doi.org/10.1016/j.ijheh.2021.113709).
- [34] Tun Zan Maung et al. “Indoor Air Pollution and the Health of Vulnerable Groups: A Systematic Review Focused on Particulate Matter (PM), Volatile Organic Compounds (VOCs) and Their Effects on Children and People with Pre-Existing Lung Disease”. In: *International Journal of Environmental Research and Public Health* 19 (July 2022), p. 8752. DOI: [10.3390/ijerph19148752](https://doi.org/10.3390/ijerph19148752).
- [35] Betty Bridges. “Fragrance: emerging health and environmental concerns”. In: *Flavour and Fragrance Journal* 17.5 (2002), pp. 361–371. DOI: [10.1002/ffj.1106](https://doi.org/10.1002/ffj.1106). URL: <https://dx.doi.org/10.1002/ffj.1106>.
- [36] Anne Steinemann. “Fragranced consumer products: sources of emissions, exposures, and health effects in the UK”. In: *Air Quality, Atmosphere & Health* 11.3 (2018), pp. 253–258. DOI: [10.1007/s11869-018-0550-z](https://doi.org/10.1007/s11869-018-0550-z). URL: <https://dx.doi.org/10.1007/s11869-018-0550-z>.
- [37] Landelle Caroline et al. “Poisoning by lavandin extract in a 18-month-old boy”. In: *Clinical Toxicology* 46.4 (2008), pp. 279–281. DOI: [10.1080/15563650701281098](https://doi.org/10.1080/15563650701281098). DOI: [doi/10.1080/15563650701281098](https://doi.org/10.1080/15563650701281098).
- [38] Alan Woolf. “Essential Oil Poisoning”. In: *Journal of Toxicology: Clinical Toxicology* 37.6 (1999), pp. 721–727. DOI: [10.1081/CLT-100102450](https://doi.org/10.1081/CLT-100102450). URL: <https://doi.org/10.1081/CLT-100102450>.

- 
- [39] Mihoko Ago, Kazutoshi Ago, and Mamoru Ogata. “A fatal case of n-butane poisoning after inhaling anti-perspiration aerosol deodorant”. In: *Legal Medicine* 4.2 (2002), pp. 113–118. DOI: [https://doi.org/10.1016/S1344-6223\(01\)00063-3](https://doi.org/10.1016/S1344-6223(01)00063-3). URL: <https://www.sciencedirect.com/science/article/pii/S1344622301000633>.
- [40] Stéphane Cariou et al. “Odor concentration prediction by gas chromatography and mass spectrometry (GC-MS): importance of VOCs quantification and odor detection threshold accuracy”. In: *Chemical Engineering Transactions* 54 (2016), pp. 67–72. DOI: [10.3303/cet1654012](https://doi.org/10.3303/cet1654012). URL: <https://imt-mines-ales.hal.science/hal-02913982>.
- [41] Michael H Abraham et al. “A Model for Odour Thresholds”. In: *Chemical Senses* 27.2 (2002), pp. 95–104. DOI: [10.1093/chemse/27.2.95](https://doi.org/10.1093/chemse/27.2.95). URL: <https://doi.org/10.1093/chemse/27.2.95>.
- [42] Manuel Zarzo. “Effect of Functional Group and Carbon Chain Length on the Odor Detection Threshold of Aliphatic Compounds”. In: *Sensors* 12.4 (2012), pp. 4105–4112. DOI: [10.3390/s120404105](https://doi.org/10.3390/s120404105). URL: <https://dx.doi.org/10.3390/s120404105%2010.3390/s120404105>.
- [43] Johannes Polster and Peter Schieberle. “Structure–Odor Correlations in Homologous Series of Alkanethiols and Attempts To Predict Odor Thresholds by 3D-QSAR Studies”. In: *Journal of Agricultural and Food Chemistry* 63.5 (2015), pp. 1419–1432. DOI: [10.1021/jf506135c](https://doi.org/10.1021/jf506135c). URL: <https://dx.doi.org/10.1021/jf506135c%2010.1021/jf506135c>.
- [44] Vicente Ferreira. “Revisiting psychophysical work on the quantitative and qualitative odour properties of simple odour mixtures: a flavour chemistry view. Part 1: intensity and detectability. A review”. In: *Flavour and Fragrance Journal* 27.2 (2012), pp. 124–140. DOI: [10.1002/ffj.2090](https://doi.org/10.1002/ffj.2090). URL: <https://dx.doi.org/10.1002/ffj.2090%2010.1002/ffj.2090>.
- [45] John Greenman et al. “Assessing the relationship between concentrations of malodor compounds and odor scores from judges”. In: *The Journal of the American Dental Association* 136.6 (2005), pp. 749–757. DOI: <https://doi.org/10.14219/jada.archive.2005.0258>. URL: <https://www.sciencedirect.com/science/article/pii/S0002817714629986>.
- [46] Yoko Yoshio and Eiichiro Nagata. *Measurement of Odor Threshold by Triangular Odor Bag Method*. Tech. rep. Japan Ministry of the Environment, 2003, pp. 118–127. URL: [https://www.env.go.jp/en/air/odor/measure/02\\_3\\_2.pdf](https://www.env.go.jp/en/air/odor/measure/02_3_2.pdf).
- [47] Agnieszka Sabiniewicz, Marnie Brandenburg, and Thomas Hummel. “Odor Threshold Differs for Some But Not All Odorants Between Older and Younger Adults”. In: *The*

- 
- Journals of Gerontology: Series B* 78.6 (2023), pp. 1025–1035. DOI: [10.1093/geronb/gbad019](https://doi.org/10.1093/geronb/gbad019). URL: <https://doi.org/10.1093/geronb/gbad019>.
- [48] Friedrich Jüttner and B Watson Susan. “Biochemical and Ecological Control of Geosmin and 2-Methylisoborneol in Source Waters”. In: *Applied and Environmental Microbiology* 73.14 (2007), pp. 4395–4406. DOI: [10.1128/AEM.02250-06](https://doi.org/10.1128/AEM.02250-06). URL: <https://doi.org/10.1128/AEM.02250-06>.
- [49] F A Fazzalari and W H Stahl. *Compilation of Odor and Taste Threshold Values Data*. DS48A-EB. ASTM International, 1978. DOI: <https://doi.org/10.1520/DS48A-EB>. URL: <https://books.google.co.uk/books?id=M1BJvgEACAAJ>.
- [50] Julien W Hsieh et al. “SMELL-S and SMELL-R: Olfactory tests not influenced by odor-specific insensitivity or prior olfactory experience”. In: *Proceedings of the National Academy of Sciences* 114.43 (2017), pp. 11275–11284. DOI: [10.1073/pnas.1711415114](https://doi.org/10.1073/pnas.1711415114). URL: <https://dx.doi.org/10.1073/pnas.1711415114>.
- [51] Anne M Cleary et al. “Odor recognition without identification”. In: *Memory & Cognition* 38.4 (2010), pp. 452–460. DOI: [10.3758/mc.38.4.452](https://doi.org/10.3758/mc.38.4.452). URL: <https://dx.doi.org/10.3758/mc.38.4.452>.
- [52] Andreas Scharf and Hans-Peter Volkmer. “The impact of olfactory product expectations on the olfactory product experience”. In: *Food Quality and Preference* 11.6 (2000), pp. 497–503. DOI: [https://doi.org/10.1016/S0950-3293\(00\)00028-8](https://doi.org/10.1016/S0950-3293(00)00028-8). URL: <https://www.sciencedirect.com/science/article/pii/S0950329300000288>.
- [53] Paul Talsma. “How much sensory panel data do we need?” In: *Food Quality and Preference* 67 (2018), pp. 3–9. DOI: <https://doi.org/10.1016/j.foodqual.2016.12.005>. URL: <https://www.sciencedirect.com/science/article/pii/S0950329316302634>.
- [54] Nicola Carslaw. “A new detailed chemical model for indoor air pollution”. In: *Atmospheric Environment* 41.6 (2007), pp. 1164–1179.
- [55] C Dimitroulopoulou et al. “Modelling of indoor exposure to nitrogen dioxide in the UK”. In: *Atmospheric Environment* 35.2 (2001), pp. 269–279. DOI: [https://doi.org/10.1016/S1352-2310\(00\)00176-X](https://doi.org/10.1016/S1352-2310(00)00176-X). URL: <https://www.sciencedirect.com/science/article/pii/S135223100000176X>.
- [56] Michael E Jenkin, Sandra M Saunders, and Michael J Pilling. “The tropospheric degradation of volatile organic compounds: a protocol for mechanism development”. In: *Atmospheric Environment* 31.1 (1997), pp. 81–104. DOI: [https://doi.org/10.1016/S1352-2310\(96\)00105-7](https://doi.org/10.1016/S1352-2310(96)00105-7). URL: <https://www.sciencedirect.com/science/article/pii/S1352231096001057>.

- 
- [57] S M Saunders et al. “Protocol for the development of the Master Chemical Mechanism, MCM v3 (Part A): tropospheric degradation of non-aromatic volatile organic compounds”. In: *Atmos. Chem. Phys.* 3.1 (2003), pp. 161–180. DOI: [10.5194/acp-3-161-2003](https://doi.org/10.5194/acp-3-161-2003). URL: <https://acp.copernicus.org/articles/3/161/2003/>.
- [58] D E Heard et al. “High levels of the hydroxyl radical in the winter urban troposphere”. In: *Geophysical Research Letters* 31.18 (2004). DOI: [10.1029/2004gl020544](https://doi.org/10.1029/2004gl020544). URL: <https://dx.doi.org/10.1029/2004gl020544%2010.1029/2004gl020544>.
- [59] A C Rivett et al. “The role of volatile organic compounds in the polluted urban atmosphere of Bristol, England”. In: *Atmospheric Chemistry and Physics* 3.4 (2003), pp. 1165–1176. DOI: [10.5194/acp-3-1165-2003](https://doi.org/10.5194/acp-3-1165-2003). URL: <https://dx.doi.org/10.5194/acp-3-1165-2003%2010.5194/acp-3-1165-2003>.
- [60] David Asaf et al. “Long-Term Measurements of NO<sub>3</sub> Radical at a Semiarid Urban Site: Extreme Concentration Events and Their Oxidation Capacity”. In: *Environmental Science & Technology* 43.24 (2009), pp. 9117–9123. DOI: [10.1021/es900798b](https://doi.org/10.1021/es900798b). URL: <https://dx.doi.org/10.1021/es900798b%2010.1021/es900798b>.
- [61] Salah S Abdalmogith and Roy M Harrison. “An analysis of spatial and temporal properties of daily sulfate, nitrate and chloride concentrations at UK urban and rural sites”. In: *Journal of Environmental Monitoring* 8.7 (2006), p. 691. DOI: [10.1039/b601562j](https://doi.org/10.1039/b601562j). URL: <https://dx.doi.org/10.1039/b601562j%2010.1039/b601562j>.
- [62] M A H Khan et al. “Estimation of Daytime NO<sub>3</sub> Radical Levels in the UK Urban Atmosphere Using the Steady State Approximation Method”. In: *Advances in Meteorology* 2015 (2015), pp. 1–9. DOI: [10.1155/2015/294069](https://doi.org/10.1155/2015/294069). URL: <https://dx.doi.org/10.1155/2015/294069%2010.1155/2015/294069>.
- [63] Brett J Doleman, Erik J Severin, and Nathan S Lewis. “Trends in odor intensity for human and electronic noses: Relative roles of odorant vapor pressure vs. molecularly specific odorant binding”. In: *Proceedings of the National Academy of Sciences* 95.10 (1998), pp. 5442–5447. DOI: [10.1073/pnas.95.10.5442](https://doi.org/10.1073/pnas.95.10.5442). URL: <https://dx.doi.org/10.1073/pnas.95.10.5442>.
- [64] Jonathan Williams and Akima Ringsdorf. “Human odour thresholds are tuned to atmospheric chemical lifetimes”. In: *Philosophical Transactions of the Royal Society B: Biological Sciences* 375.1800 (2020), p. 20190274. DOI: [10.1098/rstb.2019.0274](https://doi.org/10.1098/rstb.2019.0274). URL: <https://dx.doi.org/10.1098/rstb.2019.0274>.
- [65] Erik Olsen and Frands Nielsen. “Predicting Vapour Pressures of Organic Compounds from Their Chemical Structure for Classification According to the VOC Directive and Risk Assessment in General”. In: *Molecules* 6.4 (2001), pp. 370–389. DOI: [10.3390/60400370](https://doi.org/10.3390/60400370). URL: <https://dx.doi.org/10.3390/60400370>.

- 
- [66] Uyên-Uyên T Vỡ and Michael P Morris. “Nonvolatile, semivolatile, or volatile: Redefining volatile for volatile organic compounds”. In: *Journal of the Air & Waste Management Association* 64.6 (2014), pp. 661–669. DOI: [10.1080/10962247.2013.873746](https://doi.org/10.1080/10962247.2013.873746). URL: <https://dx.doi.org/10.1080/10962247.2013.873746>.
- [67] G Tamas et al. “Influence of ozone-limonene reactions on perceived air quality”. In: *Indoor Air* 16.3 (2006), pp. 168–178. DOI: [10.1111/j.1600-0668.2005.00413.x](https://doi.org/10.1111/j.1600-0668.2005.00413.x). URL: <https://dx.doi.org/10.1111/j.1600-0668.2005.00413.x>.
- [68] Sebastian Schoenauer and Peter Schieberle. “Structure–Odor Activity Studies on Monoterpenoid Mercaptans Synthesized by Changing the Structural Motifs of the Key Food Odorant 1- $\beta$ -Menthene-8-thiol”. In: *Journal of Agricultural and Food Chemistry* 64.19 (2016), pp. 3849–3861. DOI: [10.1021/acs.jafc.6b01645](https://doi.org/10.1021/acs.jafc.6b01645). URL: <https://dx.doi.org/10.1021/acs.jafc.6b01645>.
- [69] B C Singer et al. “Cleaning products and air fresheners: emissions and resulting concentrations of glycol ethers and terpenoids”. In: *Indoor Air* 16.3 (2006), pp. 179–191. DOI: [10.1111/j.1600-0668.2005.00414.x](https://doi.org/10.1111/j.1600-0668.2005.00414.x). URL: <https://dx.doi.org/10.1111/j.1600-0668.2005.00414.x>.
- [70] Amber M Yeoman et al. “Simplified speciation and atmospheric volatile organic compound emission rates from non-aerosol personal care products”. In: *Indoor Air* 30.3 (2020), pp. 459–472. DOI: <https://doi.org/10.1111/ina.12652>. URL: <https://onlinelibrary.wiley.com/doi/abs/10.1111/ina.12652>.
- [71] C Shrubsole et al. “IAQ guidelines for selected volatile organic compounds (VOCs) in the UK”. In: *Building and Environment* 165 (2019), p. 106382. DOI: <https://doi.org/10.1016/j.buildenv.2019.106382>. URL: <https://www.sciencedirect.com/science/article/pii/S036013231930592X>.
- [72] Tunga Salthammer. “Acetaldehyde in the indoor environment”. In: *Environmental Science: Atmospheres* 3.3 (2023), pp. 474–493. DOI: [10.1039/d2ea00146b](https://doi.org/10.1039/d2ea00146b). URL: <https://dx.doi.org/10.1039/d2ea00146b>.
- [73] Claudia Silva Cortez-Pereira et al. “Sensory approach to measure fragrance intensity on the skin”. In: *Journal of Sensory Studies* 24.6 (2009), pp. 871–901. DOI: [10.1111/j.1745-459x.2009.00242.x](https://doi.org/10.1111/j.1745-459x.2009.00242.x). URL: <https://dx.doi.org/10.1111/j.1745-459x.2009.00242.x>.
- [74] Emily Upstill, Claire Rowland, and Caroline Jordan. “Delivering context for fragrance evaluation: A study using trained sensory panellists”. In: *Food Quality and Preference* 102 (2022), p. 104636. DOI: <https://doi.org/10.1016/j.foodqual.2022.104636>. URL: <https://www.sciencedirect.com/science/article/pii/S0950329322001112>.

- 
- [75] Frank J Kelly and Julia C Fussell. “Improving indoor air quality, health and performance within environments where people live, travel, learn and work”. In: *Atmospheric Environment* 200 (2019), pp. 90–109. DOI: [10.1016/j.atmosenv.2018.11.058](https://doi.org/10.1016/j.atmosenv.2018.11.058). URL: <https://dx.doi.org/10.1016/j.atmosenv.2018.11.058>.
- [76] Anita Lee et al. “Gas-phase products and secondary aerosol yields from the ozonolysis of ten different terpenes”. In: *Journal of Geophysical Research: Atmospheres* 111.D7 (2006). DOI: [10.1029/2005jd006437](https://doi.org/10.1029/2005jd006437). URL: <https://dx.doi.org/10.1029/2005jd006437>.

# Chapter 5

## Yearlong study of indoor VOC variability: Insights into spatial, temporal, and contextual dynamics of indoor VOC exposure

### 5.1 Declaration, contributions and conflicts

This chapter is based on the following publication:

Warburton T, Hamilton JF, Carslaw N, McEachan RRC, Yang TC, Hopkins JR, Andrews SJ, Lewis AC. Yearlong study of indoor VOC variability: Insights into spatial, temporal, and contextual dynamics of indoor VOC exposure. *Environ. Sci.: Processes & Impacts*, (2025), **27**, 1025-1040.<sup>†</sup>

Supplementary tables 5 and 6 have been omitted from this thesis for brevity, however remain freely available within the original publication's supplementary information.

The study was conceptualised and designed by ACL, JFH, RRCM, and NC. Methodological development was carried out by TW, ACL, JFH, RRCM, TCY, JRH, SJA, and NC. TW led the investigation, data curation, formal analysis, visualisation, and validation. TCY and RRCM supported aspects of the investigation. TW prepared the original draft of the manuscript. All authors contributed to the reviewing and editing of the manuscript. Funding for the study was secured by ACL, JFH, RRCM, and NC.

---

<sup>†</sup>[doi.org/10.1039/D4EM00756E](https://doi.org/10.1039/D4EM00756E)

---

There are no conflicts of interest to declare.

## 5.2 Abstract

Volatile organic compounds (VOCs) are released from many sources indoors, with ingress of outdoor air being an additional source of these species indoors. We report indoor VOC concentrations for 124 homes in Bradford in the UK, collected between March 2023 and April 2024. Whole air samples were collected over 72-hours in the main living area of the home. Total VOC (TVOC) concentrations in the homes were highly variable, ranging from  $100 \mu\text{g m}^{-3}$  to  $> 8000 \mu\text{g m}^{-3}$  (*median* concentration  $\approx 1000 \mu\text{g m}^{-3}$ ). Acetaldehyde and 1,3-butadiene concentrations in  $> 75\%$  of homes were found to be in exceedance of the 1 in 1,000,000 lifetime cancer risk threshold. Higher concentrations of benzene, toluene, ethylbenzene and xylene (BTEX) as well as trimethylbenzenes were found in urban homes (summed xylene *median*  $2.35 \mu\text{g m}^{-3}$ ) compared to rural homes (summed xylene *median*  $1.22 \mu\text{g m}^{-3}$ ,  $p$ -value = 0.02), driven by ingress of elevated outdoor BTEX and trimethylbenzenes (outdoor urban BTEX *median*  $1.69 \mu\text{g m}^{-3}$ , outdoor rural BTEX *median*  $0.78 \mu\text{g m}^{-3}$ ). Inferred air change rate (ACR) exhibited a degree of seasonality, with average ACR varying between median values of  $1.2 \text{ hr}^{-1}$  in the summer and  $0.70 \text{ hr}^{-1}$  in winter. Time-averaged emission rate data provided additional insight compared to measured concentrations, such as seasonal variability, with highest total VOC time-averaged emission rates occurring in summer months (*median*  $51,953 \mu\text{g hr}^{-1}$ ), potentially a product of both increased occupancy times during school holidays as well as off-gassing of VOCs from surfaces. This comprehensive analysis underscores the critical role of seasonal, spatial, and contextual factors in shaping indoor VOC exposure, as well as potential health risks associated with consistently elevated concentrations of specific VOCs.

## 5.3 Introduction

Volatile organic compounds (VOC) are a class of air pollutants that are found both indoors and outdoors.<sup>[1–3]</sup> Activities indoors such as cooking, using personal care products (PCPs), cleaning products and building and furnishing materials can all lead to VOC emissions; if these occur in poorly ventilated spaces then markedly elevated indoor VOC concentrations can result.<sup>[4–7]</sup> The same sources can also lead to the emission of semi-volatile organic compounds (SVOCs) which can undergo gas-to-particle phase partitioning, or produce new products following oxidation, as with VOCs. Both processes influence the total mass of particulate matter indoors, and hence the ability to cause harm to human health.<sup>[8,9]</sup> As up to

---

90% of time is spent indoors,<sup>[10]</sup> quantification of both VOC emissions and concentrations is an essential precursor to effective indoor air quality management.

Whilst acute VOC exposure has been associated with serious medical conditions, such as breathing difficulties and cardiac arrhythmia,<sup>[11,12]</sup> the effects of long-term exposure to lower concentrations of VOCs remains relatively understudied. Ambient indoor concentrations of VOCs in typical UK settings are generally not high enough to give rise to acute health effects. Indoor measurements rarely show concentrations that exceed guidelines for acute effects, e.g. as in Shrubsole *et al.* (2019) and adopted by Public Health England as “UK guidelines for volatile organic compounds in indoor spaces”.<sup>[3,13–15]</sup> However, as of yet, there are no long-term data sets that allow for assessments of the health effects of exposure to VOCs with confidence.

Incidental release of VOCs through activities such as cooking and cleaning gives rise to sudden and often large increases in associated VOC concentrations. Concentrations decrease once the activity has concluded, dependent on variables such as room volume, air exchange rate, gas-surface partitioning of VOCs, and oxidation, and can take several hours.<sup>[6,16–19]</sup> VOCs with the highest measured indoor concentrations in the UK are typically propane, butane and ethanol.<sup>[3,14]</sup> A common source of propane and butane is from the use of aerosol products where they are propellants, including as home care and PCPs. Propane and butane concentrations greater than  $3000\mu\text{g m}^{-3}$  have previously been reported in homes.<sup>[3,14]</sup> Ethanol is used as an ingredient in some personal care products such as hairspray, but also arises from fragrance and disinfectant use, as well as from cooking.<sup>[20–24]</sup> Increasing ventilation rates and controlling source emissions can aid in mitigating high VOC concentrations indoors.<sup>[25,26]</sup>

Air change rate (ACR) is defined as the number of air changes within a volume over a time period, usually per hour. ACR is inherently difficult to accurately determine in residential settings, and is usually calculated/inferred through tracer or decay methods and models.<sup>[27,28]</sup> Low ACRs have been shown to give rise to an increase in indoor VOC concentrations and hence exposure.<sup>[14,29,30]</sup> Residential ACRs are typically around  $0.5\text{ hr}^{-1}$  to  $2\text{ hr}^{-1}$ , however, ACRs in general can vary greatly depending on whether the space is in a residential or commercial setting, the time of year, the air permeability of the building envelope, and human behaviour, among other factors.<sup>[31–33]</sup>

Ambient temperature can impact indoor VOC exposure through increased material off-gassing of surface-bound VOCs.<sup>[34,35]</sup> This process is uneven however,<sup>[36]</sup> with newer building materials having generally higher off-gassing VOC emission rates than older materials regardless of temperature effects.

---

Indoor-outdoor (IO) ratios of VOCs can be used to highlight those VOCs which have large indoor concentrations; reactive species such as monoterpenes and other double-bond-containing hydrocarbons often have higher indoor concentrations compared to outdoors.<sup>[3,13,37,38]</sup> These compounds are noteworthy because of the potential for secondary product formation when they are oxidised, such as secondary organic aerosols (SOAs).<sup>[39–41]</sup> Chronic exposure to SOAs is potentially linked to an increase in mortality.<sup>[42,43]</sup>

Datasets on indoor VOC concentrations in UK homes remain sparse, particularly for lower-income households. Limited measurements have been conducted across the broader range of VOCs present in the UK.<sup>[3,13,14]</sup> This paper reports on VOC concentrations observed in 124 occupied homes as part of the INGENIOUS (Understanding the sourceEs, traNsformations and fates of IndOor air pollUtantS) project.<sup>[44]</sup> It quantifies the concentrations and time-averaged emission rates of indoor VOCs, and how these are influenced by seasonal effects of ACR.

## 5.4 Experimental and methodology

### 5.4.1 Study area

Bradford is a city in the West Yorkshire Combined Authority in the North of England, in the UK. With a population of 560,000,<sup>[45]</sup> Bradford encompasses a large geographic envelope, with rural and urban areas often within short distances. Bradford is located east of the Pennine hills, and the city centre sits in a bowl-like position, flanked by inclines on almost all sides. A Clean Air Zone (CAZ) was introduced to Bradford within the outer ring road and extending up to Shipley in North Bradford in late-September 2022, currently the largest of its type in England outside of Greater London, covering 9.35 square miles. The Bradford CAZ applies to all vehicles other than private cars and motorbikes in an effort to reduce vehicle-related emissions within the Bradford area, such as NO<sub>x</sub>. While it may be too soon to definitively identify the effects on outdoor air pollution of the introduction of the Bradford CAZ, preliminary results show a potential reduction in vehicle emissions since the introduction of the Bradford CAZ.<sup>[46]</sup> More established CAZs, such as the Greater London Low Emission Zone (LEZ) and the Ultra-low Emission Zone (ULEZ), have been shown to reduce vehicle-related pollution levels more so than nearby CAZ-free areas.<sup>[47,48]</sup> Given the potential for outdoor air penetration indoors, this could have a potential impact on indoor air quality in CAZ-enveloped areas.

Bradford's history is mainly industrial, being a centre of wool-based production and trade in the 1800s.<sup>[49]</sup> Following the collapse of industrialisation in the UK, Bradford saw a decline

---

in living standards, along with several other Northern English and other post-industrial cities across Europe.<sup>[50-52]</sup> In the 21st century, Bradford has higher-than-average levels of socioeconomic disadvantage, as well as disproportionately lower life expectancy and health prospects when compared to the rest of England.<sup>[53-56]</sup> Bradford is a highly diverse city with high levels of ethnic diversity.<sup>[57]</sup>

Studies have previously linked areas with higher deprivation levels with worse outdoor air quality across the entire UK and within countries and regions which make up the UK, especially so in comparable post-industrial cities.<sup>[58-61]</sup> Outdoor air pollution in Bradford has been monitored continuously since 1999, with one continuous automatically-reporting monitoring site located on Mayo Avenue, Bradford measuring NO and NO<sub>2</sub>, as well as wind direction, speed and ambient temperature, forming part of the Defra national monitoring network.<sup>[62]</sup> Despite over 20 years of continuous outdoor air pollution data collection, there are no reported datasets on indoor VOC concentrations for Bradford, or similar cities with high degrees of socioeconomic and ethnic diversity.

## 5.4.2 Participant selection and questionnaires

The methodology for participant selection and sampling regime, more broadly including the development and analysis of questionnaires, are detailed in Ikeda *et al.* (2023).<sup>[63]</sup> In brief, 310 homes were monitored for indoor air pollutants using low-cost sensors.<sup>[44]</sup> A subset of sampled homes participated in VOC analysis where a whole air canister was deployed and a time-integrated sample (up to 72 hours) was collected. The participants in this study were part of the Born in Bradford (BiB) birth cohort study.<sup>[64]</sup> Homeowners were asked to complete home, health and behaviour surveys during sampling. This captured a large quantity of information that could be linked with each air sample. From these questionnaires, daily statistics of aerosol product and fragrance product use was taken for analysis in this study and summed for a total product use over the canister sampling period. A building audit was completed by BiB research assistants, capturing information about the different microenvironments in which samples were taken, of which the room volume was of specific interest to this study for the calculation of ACR (explained in section 5.4.5). The full questionnaires are available in the supplementary information in Ikeda *et al.* (2023).<sup>[63]</sup> Of the targeted 150 homes, a total of 124 homes had usable whole air samples taken for VOC analysis. All the samples had home, health, behaviour and building survey responses available. However, response rates to individual questions within the surveys were sometimes < 100% (*min* 41%, *max* 100%, *median* 90%).

---

### 5.4.3 Sample preparation, collection and preparation for analysis

Whole air samples inside each home were collected using 6 L vacuum-intake stainless steel canisters treated internally with a proprietary silica-based ceramic (Entech, CA, USA). Flow-restrictive inlets (Entech, CA, USA) were used to time-integrate samples up to 72 hours (sampling flow rates through low surface area sapphire orifice restrictors varied between 1.4 and 1.9 mL min<sup>-1</sup>). Canisters were evacuated to 0.01 Pa (29.9 ” Hg vacuum gauge, 99.99% vacuum) prior to use. Canister valves were assessed for seal integrity using a vacuum gauge fitted to the sealed canister valve.

Canisters and flow-restrictive inlets, which remained paired throughout the study, were deployed in homes across Bradford from March 2023 to April 2024, with each sample collected over a 72-hour period. Canisters were consistently placed in the main living area, which was not always a designated ‘living room’ and often included open-plan spaces such as combined living, kitchen, and dining areas. Consequently, some canisters may have been exposed to episodic VOC emissions from activities like cooking and food preparation. Canisters were positioned within the living area, no higher than 1 m above ground level and, where feasible, away from doorways. After sampling, the canisters were returned to the University of York for analysis.

### 5.4.4 Sample analysis

Samples were analysed following the method detailed in Warburton *et al.* (2023).<sup>[56]</sup> Briefly, canister samples were initially diluted to 1 bar (gauge) with 6 L of humidified highly purified air free of VOCs (hereafter ‘blank gas’), produced by flowing compressed ambient air through a bed of platinum beads at >375 °C. 500 mL of diluted canister air was then drawn through a 16-port solenoid-actuated pneumatic valve manifold (Swagelok Company, OH, USA) at 15 mL min<sup>-1</sup> into a custom-built thermal desorption unit (TDU), sequentially comprising a water trap, pre-concentration trap and finally a pre-injection focus trap. The water trap was held at -40 °C during sample intake, while the pre-concentration and focus traps were held at the lowest achievable temperature, always below -110 °C.

Following flash heating from the focus trap, dried, pre-concentrated and focused samples were injected into a two-column gas chromatograph (GC, Agilent 7890A, Agilent Technologies, CA, USA) fitted with flame ionisation detectors (FIDs) and a quadrupole mass spectrometer (QMS, Agilent 5977A, Agilent Technologies, CA, USA). Samples were first separated on a 60 m, 150 µm internal diameter (ID) VF-WAX column with a film thickness of 0.50 µm (Agilent Technologies, CA, USA) at 1.6 mL min<sup>-1</sup> (helium carrier gas pressure of 35 psi).

---

This resulted in a long elution of unresolved  $C_2$  to  $C_6$  hydrocarbons from the VF-WAX column, which were passed through a Deans switch (Agilent Technologies, CA, USA) to a 50 m, 320  $\mu\text{m}$  ID  $\text{Na}_2\text{SO}_4$ -deactivated  $\text{Al}_2\text{O}_3$  porous-layer open tubular (PLOT) column with a wall coating thickness of 5  $\mu\text{m}$  (Agilent Technologies, CA, USA). Eluent from the PLOT column directly flowed through to an FID. Once the unresolved species had finished eluting through the VF-WAX column (at 8.3 minutes) the Deans switch diverted the analyte flow through a section of fused silica (2 m x 150  $\mu\text{m}$  ID) to both balance column flows at the Deans switch and split analyte flow between a second FID and the QMS for simultaneous detection, through sections of 150  $\mu\text{m}$  ID fused silica of length 0.91 m and 2.1 m, respectively.

A thirty-component mix of non-methane hydrocarbons (NMHCs) in nitrogen was used for sample calibration. Each VOC was at a mixing ratio of approximately 4 ppb, provided by the National Physical Laboratory, Teddington, UK (cylinder number D933515, hereafter referred to as ‘NPL 30’). Sampled VOCs contained within the NPL 30 mix were directly calibrated, with remaining VOCs calibrated using equivalent carbon responses. Table 5.1 gives the identify of the thirty directly-calibrated species. Following each canister batch, blank gas was sampled three times, followed by five NPL 30 calibrations and finally three carrier gas/internal samples (‘no flow blanks’). A no flow blank method involved the TDU operating with the sample volume set to 0 mL and the sample time set to 33.3 minutes, the time a regular 500 mL sample would take to be drawn. This process resulted in only carrier gas flowing through the TDU traps over the sampling period, resulting in canister sample correction for both blank gas diluent impurities (none found) and wider carrier gas and system impurities (consistently 0.95  $\mu\text{g m}^{-3}$  benzene only). Following analysis, canisters were re-evacuated according to the previous method. Evacuated canisters were spot checked for impurities by filling from evacuated to 1 bar (gauge) with humidified blank gas and run on a regular canister sampling method.

Following GC analysis, a subset of  $n = 90$  samples was further processed for greenhouse gas analysis, by flowing the canister samples at 600  $\text{mL min}^{-1}$  into a laser absorption spectrometer (Ultraportable Greenhouse Gas Analyser, Los Gatos Research Inc., CA, USA). This additional analysis allowed carbon dioxide mixing ratios to be quantified.

Chromatograms for each sample were initially qualitatively analysed using MassHunter (Agilent Technologies, CA, USA) to assess the quality of chromatographic separation and resolution. Chromatograms were then integrated using GCWerks (GC Soft Inc., CA, USA). FID data was mostly used for peak integration and concentration data analysis. However, QMS data was required to deconvolve benzene, monoterpenes, chlorinated species and cyclosiloxanes. Over 120 VOC species were identified and included in the analysis. Instrument limits

Table 5.1: A table of the 30 VOCs contained within the 30-component NPL30 calibration standard used in this study.

1,2,3-trimethylbenzene	ethane	<i>n</i> -heptane
1,2,4-trimethylbenzene	ethene	<i>n</i> -octane
1,3,5-trimethylbenzene	ethylbenzene	<i>n</i> -pentane
1,3-butadiene	hexane	<i>o</i> -xylene
1-butene	isobutane	propane
2-methylpentane	isooctane	propene
acetylene	isopentane	<i>p</i> -xylene
benzene	isoprene	toluene
<i>cis</i> -2-butene	<i>m</i> -xylene	<i>trans</i> -2-butene
<i>cis</i> -2-pentene	<i>n</i> -butane	<i>trans</i> -2-pentene

of detection (LOD) and limits of quantification (LOQ) were calculated using a signal-to-noise ratio of 3:1 and 10:1 respectively, and are shown in Table 5.2 for all VOCs measured by the instrument (including some otherwise not explicitly mentioned in this paper).

The entire VOC dataset is open-access and available at <https://doi.org/10.15124/24fd1762-0e98-4773-a74c-7dd87ef59aa8>.

### 5.4.5 Calculation of ACR

Several methods exist to calculate and infer ACR. A common method is to use real-time CO<sub>2</sub> mixing ratios (or another tracer gas) and monitor decay rates.<sup>[65,66]</sup> The work presented here used assumptions about the natural generation of CO<sub>2</sub> by home occupants (adjusted for time spent in the main living area assessed through available data on room occupancy statistics<sup>[67,68]</sup>), the room volume, and the difference between internal and external CO<sub>2</sub> mixing ratios. Within the wider scope of the INGENIOUS project, real-time CO<sub>2</sub> mixing ratios were measured by low-cost sensors and used to calculate ACR, and these results will form the basis of a future paper.

Here, ACR was inferred according to an adapted method identified in Warburton *et al.* (2023),<sup>[14]</sup> which itself used methods described by Batterman (2017),<sup>[69]</sup> shown in eqn 5.1:

$$ACR = \frac{[(n_A \cdot G_{p,A}) + (n_C \cdot G_{p,C})]6 \times 10^4}{V \cdot (C_{in} - C_{out})} \quad (5.1)$$

Where *ACR* is the inferred air change rate (hr<sup>-1</sup>), *n<sub>A</sub>* and *n<sub>C</sub>* is the number of adult and child occupants respectively, *G<sub>p,A</sub>* and *G<sub>p,C</sub>* are the natural generation rate of CO<sub>2</sub> (L min<sup>-1</sup> for adults and children respectively, *V* is the volume of the room the sample was taken in

Table 5.2: Limits of detection (LOD) and quantification (LOQ) for VOCs resolved by the GC analysis. LODs were calculated by a signal-to-noise (SNR) ratio of 3:1, and LOQ using an SNR of 10:1.

VOC name	LOD $\mu\text{g m}^{-3}$	LOQ $\mu\text{g m}^{-3}$	VOC name	LOD $\mu\text{g m}^{-3}$	LOQ $\mu\text{g m}^{-3}$
1,2,3-TMB	0.0217	0.0724	$\gamma$ -terpinene	0.0227	0.0755
1,2,4-TMB	0.0222	0.0741	hexane	0.0239	0.0796
1,3,5-TMB	0.0222	0.0741	isobutane	0.0242	0.0806
2-carene	0.0227	0.0755	isoprene	0.0227	0.0755
2-chloropropane	0.0436	0.145	isopropanol	0.0444	0.148
3-carene	0.0227	0.0755	levomenthol	0.0281	0.0937
4-carene	0.0227	0.0755	limonene	0.0227	0.0755
acetaldehyde	0.0733	0.244	methanol	0.0711	0.237
acetone	0.0483	0.161	methylenechloride	0.141	0.471
acetonitrile	0.0455	0.152	n-butane	0.0242	0.0806
$\alpha$ -phellandrene	0.0227	0.0755	n-pentane	0.024	0.08
$\alpha$ -pinene	0.0227	0.0755	o-cymene	0.0223	0.0744
$\alpha$ -terpinene	0.0227	0.0755	p-cymene	0.0223	0.0744
$\beta$ -myrcene	0.0227	0.0755	propan-1-ol	0.04	0.133
$\beta$ -phellandrene	0.0227	0.0755	propanal	0.0483	0.161
$\beta$ -terpinene	0.0227	0.0755	propane	0.0245	0.0815
$\beta$ -thujene	0.0227	0.0755	styrene	0.0217	0.0722
camphene	0.0227	0.0755	tert-butyl-benzene	0.0223	0.0744
camphor	0.0281	0.0938	1,1-dichloroethene	0.101	0.336
carbendisulfide	0.127	0.422	cyanogenchloride	0.128	0.426
$\delta$ -terpinene	0.0227	0.0755	carbontetrachloride	1.02	3.41
ethanol	0.0511	0.17	chloroform	0.496	1.65
ethylbenzene	0.0221	0.0736	benzene	0.0217	0.0722
toluene	0.0219	0.073	xylene	0.0221	0.0736

---

(m<sup>3</sup>), and  $C_{in}$  and  $C_{ex}$  are respectively the internal and external CO<sub>2</sub> mixing ratios (ppm). The total room volume was calculated from measured room lengths, widths and heights. Volume was then reduced by 7% to account for volume occupied by internal furnishings, as in Manuja (2019),<sup>[70]</sup> transforming the  $V$  term to be representative of available diluent volume. Here,  $C_{ex}$  was assumed to be 450 ppm.  $G_{p,A}$  and  $G_{p,C}$  used in this study were 0.312 L min<sup>-1</sup> for an adult and 0.174 L min<sup>-1</sup> for a child.<sup>[71]</sup> Calculation by this method assumes the occupants were all present over the entire sampling period, which is unrealistic for up to 72-hour time-integrated sampling. Therefore, using available data on typical times spent in main living areas in the home, which was inclusive of time spent in other rooms in the home and working/school patterns, occupancy was adjusted to 20% to account for time not spent in the main living area.<sup>[67,68]</sup> Clearly, assumptions have had to be made about external CO<sub>2</sub> mixing ratios, occupancy patterns and CO<sub>2</sub> generation rates in this approach, but the assumptions have been applied consistently across the data set based on knowledge of the number of occupants in each of our sampled houses.

## 5.4.6 VOC metrics and manipulation

For VOC analysis, a total of  $n = 124$  samples were used. For each sample a metric of total VOC ("TVOC") concentration was defined as the sum of all quantified VOC concentrations for each sample. This would often be a subset of the total number of VOCs quantified in this study, owing to variation in sample composition. Therefore, TVOC presented here is an operational air quality metric specific to this study and analytical method.

### 5.4.6.1 Modified *Z-score* calculation

Modified *Z-scores* were calculated for VOCs for the analysis contained within Section 5.5.1.2. A 'regular' *Z-score* measures a value's deviation from the mean of the group it belongs to. In this study, it reflects how a VOC concentration deviates from the mean of all measured values for that VOC. A modified *Z-score* is similar but relies on the group median instead of the mean, making it less susceptible to skewing by outliers.

Indoor VOC sources such as paints and other decorating products can emit BTEX species (benzene, toluene, ethylbenzene, and xylene) and trimethylbenzenes (TMB) in intense but episodic bursts, especially immediately following the use of paints,<sup>[72]</sup> potentially producing extreme outliers that distort data and statistical analyses. However, given the inherently variable nature of indoor air, a data treatment approach was needed that could accommodate natural variations while mitigating the impact of extreme values. Modified *Z-scores* were

---

therefore calculated for indoor BTEX and TMB according to eqn 5.2:

$$mz_i = \frac{0.6745 \cdot (x_i - i_{med})}{MAD} \quad (5.2)$$

where  $mz_i$  is the modified  $Z$ -score,  $x_i$  is the value the modified  $Z$ -score is being calculated for (the VOC concentration for BTEX and TMB),  $i_{med}$  is the median of the group  $i$  to which  $x_i$  belongs (the median of all concentrations for the given BTEX or TMB VOC), and  $MAD$  is the median absolute deviation. Here, 0.6745 ( $1/\sqrt{1.4826}$ ) acts to scale the modified  $Z$ -score to compare against ‘regular’  $Z$ -scores.  $MAD$  itself is the median value of the absolute deviation of each data point in group  $i$  from the median of group  $i$ , and can be calculated according to eqn 5.3:

$$MAD = median(|x_i - i_{med}|) \quad (5.3)$$

In this context,  $mz_i$  may be used analogously to a standard  $Z$ -score for evaluating deviations from the central tendency. However, because  $mz_i$  is based on group median and MAD, it is more resistant to the effects of outliers. Typically, if a value has an absolute  $mz_i$  greater than 3.5, it is said to be an outlier, and this threshold was used here.<sup>[73]</sup>

To address skewing by the largest outliers and reduce the number of false positives when identifying outliers through the  $mz_i$  calculation, the data were first logarithmically transformed. Outliers were then identified by calculating according to eqn 5.2, with datapoints grouped by VOC having an  $mz_i$  higher than 3.5 being filtered out. The typical lower threshold of -3.5 was not necessary in this case as the lowest modified  $Z$ -score for this analysis was -3.46. Finally, the data were transformed back to the original concentration values by applying an exponential to the filtered dataset.

#### 5.4.6.2 Time-averaged emission rate calculation

Time-averaged emission rates of VOCs from each sample were estimated by using measured indoor and outdoor concentrations, the room volume the sample was taken in, and the inferred ACR for each sample. Time-averaged emission rates were calculated using a simple model adapted from Warburton *et al.* (2023),<sup>[14]</sup> shown in eqn 5.4:

$$q = \frac{(C_{in} - C_{out})}{10^6} \cdot ACR \cdot V \quad (5.4)$$

Where  $q$  is the VOC time-averaged emission rate (g hr<sup>-1</sup>), and  $C_{in}$  and  $C_{out}$  are the measured indoor and outdoor concentrations of the VOC respectively ( $\mu\text{g m}^{-3}$ ). In using eqn 5.4, it is assumed that the concentrations of the VOC are reflective of a steady-state value, and

that VOC removal is a function solely of ventilation. The volume term ( $V$ ) here reflected the 7% reduction of total room volume set out in Section 5.4.5. Equation 5.4 does not give an instantaneous emission rate, rather a time-averaged emission rate of a VOC over the sampling period. While high VOC emission events will be captured by this methodology, they are smoothed given the low sampling flow rates. The method for emission rate calculation here is mathematically equivalent to the methods of Sarwar *et al.* (2002).<sup>[74]</sup>

### 5.4.6.3 Sensitivity analysis

To assess the impact of compounding errors on the emission rate (eqn 5.4), the propagation of errors formula can be used:

$$\sigma_q^2 = \left( \frac{\partial q}{\partial C_{in}} \cdot \sigma_{C_{in}} \right)^2 + \left( \frac{\partial q}{\partial C_{out}} \cdot \sigma_{C_{out}} \right)^2 + \left( \frac{\partial q}{\partial V} \cdot \sigma_V \right)^2 + \left( \frac{\partial q}{\partial ACR} \cdot \sigma_{ACR} \right)^2 \quad (5.5)$$

Where  $\frac{\partial q}{\partial x}$  is the partial derivative of the emission rate  $q$  with respect to variable  $x$ , and  $\sigma_x$  is the absolute error of variable  $x$ . The partial derivatives can be calculated using the product rule as such:

$$\frac{\partial q}{\partial C_{in}} = V \cdot ACR \quad (5.6)$$

$$\frac{\partial q}{\partial C_{out}} = -V \cdot ACR \quad (5.7)$$

$$\frac{\partial q}{\partial V} = (C_{in} - C_{out}) \cdot ACR \quad (5.8)$$

$$\frac{\partial q}{\partial ACR} = (C_{in} - C_{out}) \cdot V \quad (5.9)$$

Substituting eqns 5.6 to 5.9 into eqn 5.5 gives the following:

$$\sigma_q = \sqrt{(V \cdot ACR \cdot \sigma_{C_{in}})^2 + (-V \cdot ACR \cdot \sigma_{C_{out}})^2 + [(C_{in} - C_{out}) \cdot ACR \cdot \sigma_V]^2 + [(C_{in} - C_{out}) \cdot V \cdot \sigma_{ACR}]^2} \quad (5.10)$$

The errors of  $C_{in}$  and  $C_{out}$  are 0.1%, which itself was determined through constructing calibration curves of a target gas of increasing concentration. As conservative estimates, errors in  $V$  and  $ACR$  were assigned as 10% and 20%, respectively. This resulted in an average 22% uncertainty in the calculated emission rate. However, this likely represents a ‘worst case’ scenario as the volume and air change rate uncertainties are likely upper-bound estimates of the actual uncertainties. Assigning errors in  $V$  and  $ACR$  of 10% for both gives an average 14% uncertainty in the calculated emission rate.

---

### 5.4.7 IRIS benchmark calculations

In this study, benzene exhibited a significantly lower median indoor concentration ( $0.70 \mu\text{g m}^{-3}$ ) compared to substances such as ethanol (median  $320 \mu\text{g m}^{-3}$ ). Despite this, the health risks associated with chronic benzene overexposure are well-documented, with safe exposure thresholds set at notably low levels. Consequently, evaluating indoor concentrations against established exposure benchmarks offers additional insight into the potential long-term impacts of VOC exposure. Inhalation unit risks (IURs), defined as ‘the upper-bound excess lifetime cancer risk estimated to result from continuous exposure to an agent at a concentration of  $1 \mu\text{g m}^{-3}$  in air for a lifetime’,<sup>[75]</sup> for lifetime cancer risk (LCR) assessments and reference concentrations for hazard quotient (HQ) calculations were sourced from the Integrated Risk Information System (IRIS) database.<sup>[76]</sup>

Calculation of both LCR and HQ for homeowners follow methods established by both the United States Environmental Protection Agency (US EPA)<sup>[75,76]</sup> and the Agency for Toxic Substances and Disease Registry (ATSDR),<sup>[77]</sup> also using freely available data on UK working patterns obtained from the Office for National Statistics (ONS)<sup>[78]</sup> to better inform assumptions made.

#### 5.4.7.1 Lifetime cancer risk calculation

Lifetime cancer risk (LCR) can be calculated according to the following:

$$LCR = C_{A,C} \cdot IUR \quad (5.11)$$

Where  $C_{A,C}$  is the exposure factor-adjusted indoor concentration ( $\mu\text{g m}^{-3}$ ),  $T_Y$  is the residential time per lifetime (years), and  $T_L$  is the life expectancy (years), and  $IUR$  is the inhalation unit risk [ $\mu\text{g m}^{-3-1}$ ]. Cancer IURs were identified for 6 VOCs in this study, and were obtained from the IRIS database, shown in Table 5.3, hosted by the US EPA.<sup>[76]</sup> The exposure factor-adjusted indoor concentration was calculated using eqn 5.12:

$$C_{A,C} = C_I \cdot E_{f,C} \quad (5.12)$$

Where  $C_I$  is the measured indoor concentration obtained from whole air samples ( $\mu\text{g m}^{-3}$ ), and  $E_{f,C}$  is the atmospheric exposure factor for the LCR calculation (dimensionless). The atmospheric exposure factor serves to adjust the measured indoor concentrations into an ‘effective’ concentration to account for time not spent within the setting  $C_I$  was measured in.

Table 5.3: Measured VOCs used for LCR analysis using inhalation unit risk data available from IRIS.

Species name	Inhalation unit risk (per $\mu\text{g m}^{-3}$ )
1,3-butadiene	0.0003
Chloroform	0.000 023
Carbon tetrachloride	0.000 006
Acetaldehyde	0.000 002 2
Benzene	0.000 002 2
Methylene chloride	0.000 000 08

$E_{f,C}$  was calculated according to the following:

$$E_{f,C} = \frac{T_R \cdot 7 \frac{\text{days}}{\text{week}} \cdot 52.14 \frac{\text{weeks}}{\text{year}} \cdot T_Y}{24 \frac{\text{hours}}{\text{day}} \cdot 7 \frac{\text{days}}{\text{week}} \cdot 52.14 \frac{\text{weeks}}{\text{year}} \cdot T_L} \quad (5.13)$$

Where  $T_R$  is the residential time per day (hours),  $T_Y$  is the residential time per lifetime (years), and  $T_L$  is the life expectancy (years). Average UK work hours (obtained from the Office for National Statistics<sup>[78]</sup>) were subtracted from 24 to give  $T_R=16.72$ . Values of  $T_Y=33$  and  $T_L=78$  were obtained from available guidance provided by the Agency for Toxic Substances and Disease Registry (ATSDR).<sup>[77]</sup> This gave a calculated  $E_{f,C}$  of 0.30, reflecting that for this calculation it is assumed that 30% of an individual's lifetime is spent in the residential environment studied here.

#### 5.4.7.2 Hazard quotient calculation

The calculation of a hazard quotient (HQ) for a VOC concentration starts similarly to the estimation of LCR in the calculation of an exposure factor, shown in eqn 5.14:

$$E_{f,NC} = \frac{T_R \cdot 7 \frac{\text{days}}{\text{week}} \cdot 52.14 \frac{\text{weeks}}{\text{year}}}{24 \frac{\text{hours}}{\text{day}} \cdot 7 \frac{\text{days}}{\text{week}} \cdot 52.14 \frac{\text{weeks}}{\text{year}}} \quad (5.14)$$

Where  $E_{f,NC}$  is the atmospheric exposure factor for non-cancer hazard quotient calculation (dimensionless).  $E_{f,NC}$  in this study was calculated to be 0.70. The exposure factor-adjusted concentration of VOCs for non-cancer hazard quotient calculation,  $C_{A,NC}$  was calculated as in eqn 5.12. Finally, hazard quotients were calculated as in eqn 5.15:

$$HQ = \frac{C_{A,NC}}{R_f C} \quad (5.15)$$

Where  $HQ$  is the hazard quotient for non-cancer related risk (dimensionless), and  $R_fC$  is the reference concentration for each VOC ( $\mu\text{g m}^{-3}$ ).  $R_fC$  values were gathered from the IRIS database, and are shown in Table 5.4.<sup>[76]</sup> The preceding equations follow guidance from the EPA and the ATSDR. Cancer IURs were calculated using specific exposure pathways, as inhalation risks increase through defined routes. In contrast,  $R_fC$  values consider total indoor time, reflecting broader exposure patterns in the calculation of exposure factors.

Table 5.4: Measured VOCs used for HQ analysis using reference concentration data available from IRIS.

Species name	Reference concentration ( $\mu\text{g m}^{-3}$ )
1,3-butadiene	2
Propanal	8
Acetaldehyde	9
Benzene	30
1,2,3-trimethylbenzene	60
1,2,4-trimethylbenzene	60
1,3,5-trimethylbenzene	60
Acetonitrile	60
m-xylene	100
o-xylene	100
p-xylene	100
Methylenechloride	600
Carbondisulfide	700
Hexane	700
1,3-dichlorobenzene	800
Ethylbenzene	1000
Styrene	1000
t-butyl-benzene	5000
Toluene	5000
Methanol	20 000
Carbon tetrachloride	100
Cyclohexane	6000
Naphthalene	3
t-butyl-alcohol	5000

#### 5.4.8 Data visualisation and statistical analysis

All data analysis and manipulation were conducted through *RStudio* software. The *tidyverse* package was used in all data processing. Data plotting used *ggplot2* for all figures. Box-plots show values in the order of (from bottom-to-top): lower outliers, 5th percentile, 25th

---

percentile, median value, 75th percentile, 95th percentile, and upper outliers. Error bars on plots represent 95% confidence intervals, calculated using 1,000 bootstrap resamples of the data.

Multiple statistical testing methods were employed in this study. Data normality was first assessed using QQ plots, which indicated that all VOCs followed non-normal distributions. To evaluate stochastic dominance within data subsets, Brunner-Munzel tests (also known as the "generalized Wilcoxon test") were conducted, grouping samples based on a binary variable. The Brunner-Munzel test was chosen over the more commonly used Mann-Whitney U test (Wilcoxon rank-sum test) because it does not assume equal variances or a location shift between groups, unlike the Mann-Whitney U test. Given the variability of indoor air due to personal behaviours, these assumptions could not be reliably made, necessitating a more robust testing method. For datasets with multiple levels within groupings (e.g., seasons), an initial Kruskal-Wallis test was performed to assess overall differences across the primary binary grouping variable. *Post-hoc* Dunn tests were then used to identify pairwise differences and determine specific levels exhibiting stochastic dominance.

All  $p$ -values were adjusted using Holm's correction for multiple comparisons. A significance level of  $\alpha = 0.05$  (95% confidence interval) was applied throughout the analysis, with  $p$ -values below this threshold indicating statistical significance.

## 5.5 Results and discussion

### 5.5.1 Indoor VOC concentrations

#### 5.5.1.1 Indoor concentrations of select VOCs

Fig. 5.1 displays a logarithmic plot of TVOC and a selected group of VOCs found in indoor air samples in this study. The VOCs displayed in Fig. 5.1 were picked either due to their mass contribution to TVOC (methanol, ethanol, isopropanol, butane and propane), their inclusion as common ingredients in fragranced products ( $\alpha$ -pinene and limonene), or being of note due to potential health concerns (benzene, ethylbenzene). On average across the 124 homes, ethanol, n-butane, methanol, propane and i-butane represented 11-93 wt% of the most abundant VOCs, with a median value of 68 wt%.

Indoor sources of butane and propane were dominated by emissions from compressed aerosol products such as deodorants, cleaning aerosols, hairsprays and other aerosolised personal care products (PCPs), where they act as propellants.<sup>[5]</sup> Methanol is a commonly found emission from cooking, but also originates as an endogenous human breath emission, as well as in small

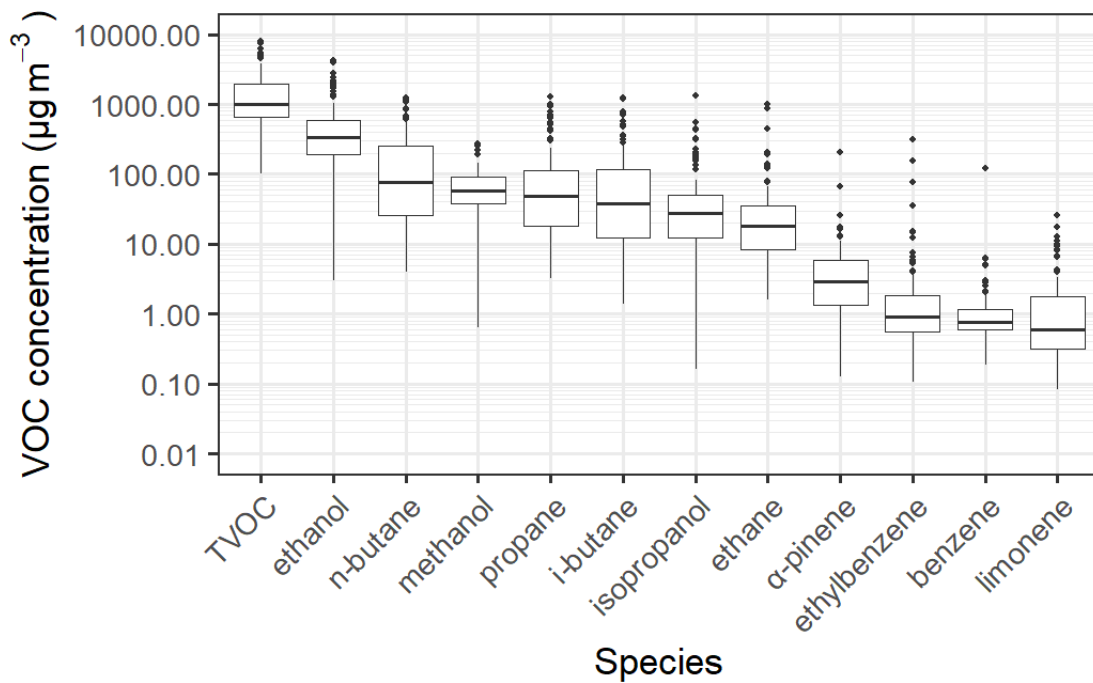


Figure 5.1: Measured indoor concentrations of a select group of VOCs measured in the INGENIOUS homes. Boxplots show values in the order of (from bottom-to-top): lower outliers, 5th percentile, 25th percentile, median value, 75th percentile, 95th percentile, and upper outliers. The y-axis has been logarithmically transformed to aid presentation.

---

amounts in some household products and, more rarely, PCPs.<sup>[16,79,80]</sup> Ethanol is commonly found indoors, arising from multiple sources such as household products and PCPs, alcohol consumption and cooking.<sup>[3,16,79]</sup>

### 5.5.1.2 Effect of geography on indoor VOC concentrations

Boxplots for indoor aromatic concentrations (once treated to account for extreme outliers) across rural and urban homes are shown in Fig. 5.2. The increase in indoor xylene concentrations between rural and urban homes was of significance ( $p$ -value = 0.02). There were modest but insignificant increases in median concentrations for 1,2,4- and 1,2,3-trimethylbenzene and toluene between rural and urban samples. There were minor increases in median benzene and ethylbenzene concentrations between rural and urban houses. Notably, urban homes exhibited a greater frequency of extreme concentration values compared to rural homes, further highlighting the trend that urban environments generally had higher concentrations of these species relative to rural settings. A similar analysis was applied to indoor-outdoor (IO) ratios for these species (Fig. 5.3), which were generally lower in urban compared to rural households, indicating that outdoor sources of these species were generally more prevalent in urban areas than in rural areas. An increase in indoor aromatic VOC concentrations in houses in urban areas, appeared to be driven by higher outdoor concentrations of aromatics.

### 5.5.1.3 Lifetime cancer risk estimates

Boxplots showing the spread of calculated LCRs for samples in this study are given in Fig. 5.4. A dashed horizontal line is shown at  $y = 1 \times 10^{-6}$ , which indicates a lifetime cancer risk of 1 in 1,000,000. Median values for acetaldehyde, carbon tetrachloride, chloroform and 1,3-butadiene were above the 1 in 1,000,000 threshold. Indeed, >60% of homes had concentrations of these four species above this threshold, with values sometimes exceeding 1 in 100,000, comparable to LCRs derived from chronic exposure to second- and third-hand smoke.<sup>[81,82]</sup> However, LCRs in this study were highly variable and in general appeared to be somewhat lower than LCRs for chronic exposure to indoor airborne particulates and outdoor airborne nitrosamines.<sup>[82-85]</sup> Carbon tetrachloride has been phased out of publicly available products since the Montreal Protocol came into effect, as well as being a potent hepatotoxic suspected human carcinogen. Given the variability in calculated LCRs and indoor concentrations, it is clear that there was at least one indoor source of emission of carbon tetrachloride in this study, likely arising as a secondary by-product of atmospheric reactions rather than as a primary emission from the product formulation itself. Carbon

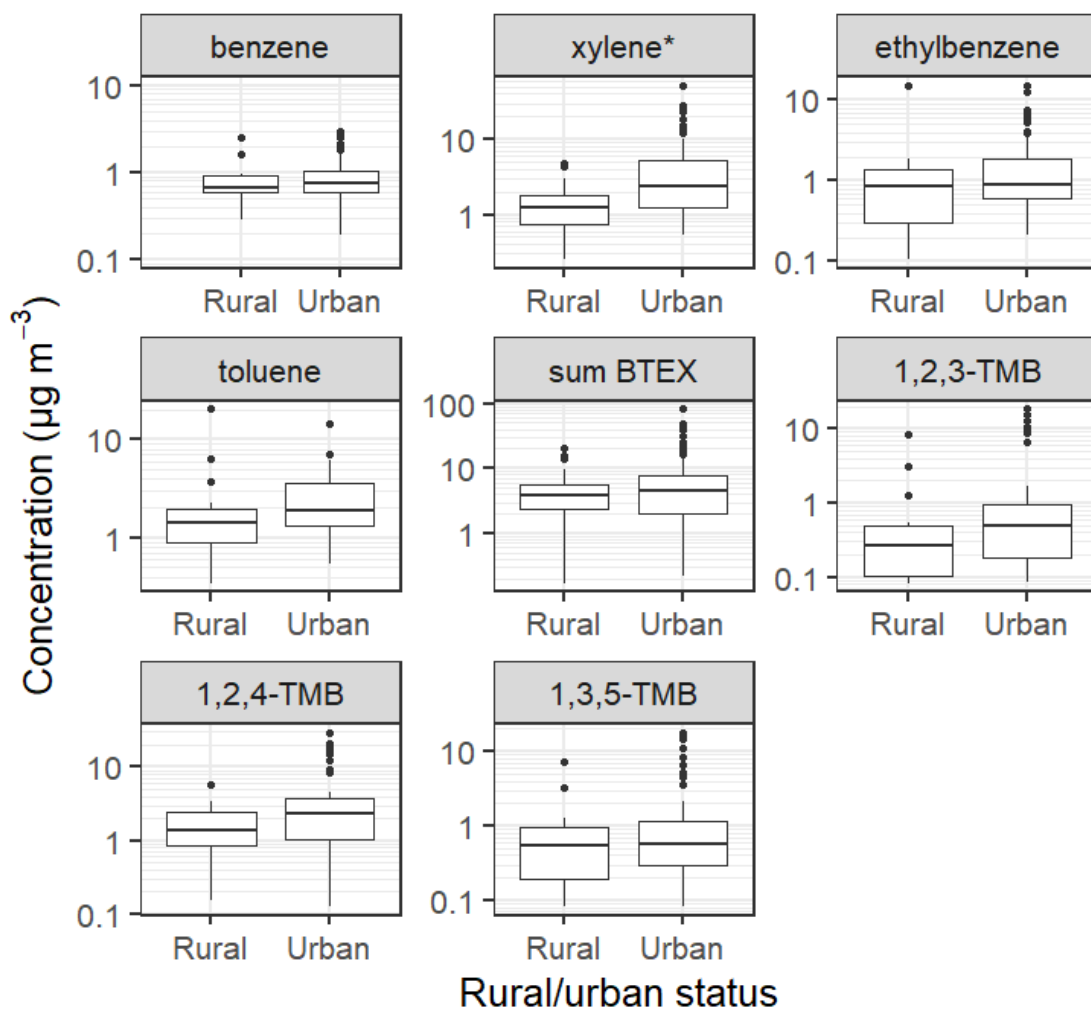


Figure 5.2: Indoor concentrations of aromatic VOCs, treated through modified  $Z$ -score analysis, and separated by rural or urban status. Boxplots show values in the order of (from bottom-to-top): lower outliers, 5th percentile, 25th percentile, median value, 75th percentile, 95th percentile, and upper outliers. The y-axis has been logarithmically transformed to aid presentation. TMB = trimethylbenzene, BTEX = benzene, toluene, ethylbenzene and xylene. \* denotes a change of significance ( $p$ -value $\leq 0.05$ ).

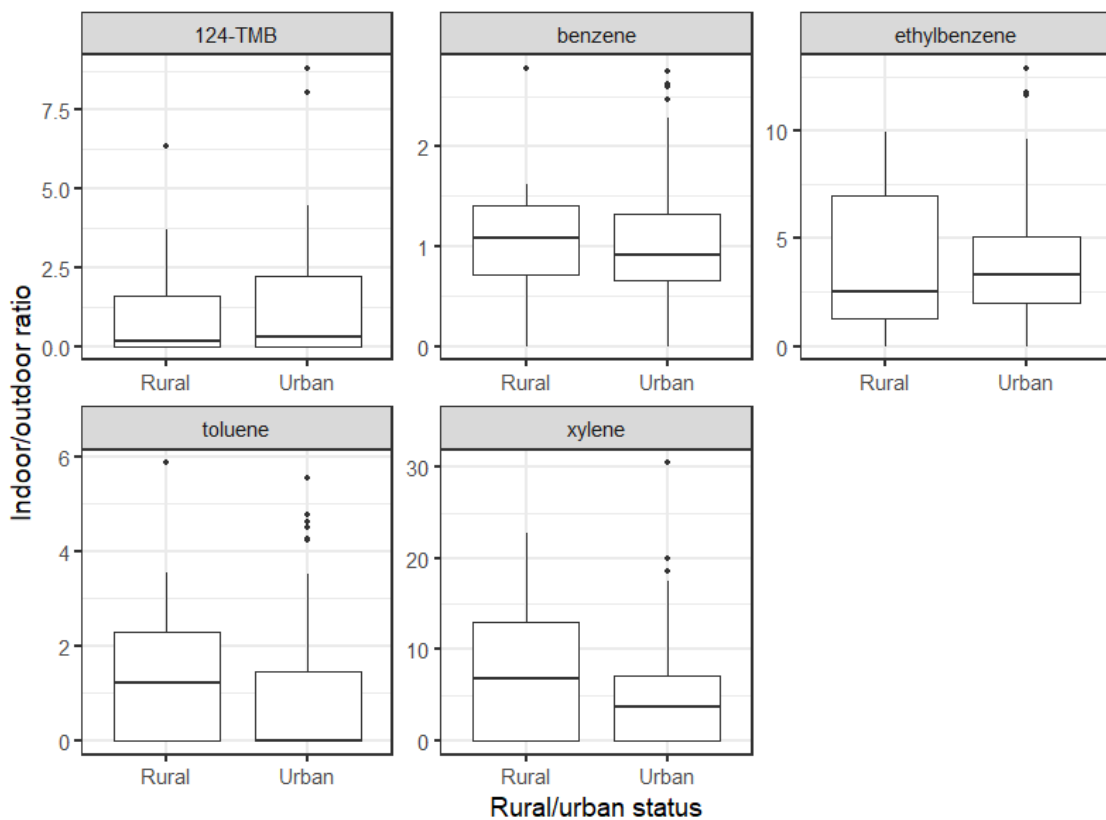


Figure 5.3: Boxplots indoor-outdoor ratios of aromatic VOCs, separated by rural or urban status. Indoor-outdoor ratios were split into Boxplots show values in the order of (from bottom-to-top): lower outliers, 5th percentile, 25th percentile, median value, 75th percentile, 95th percentile, and upper outliers. TMB = trimethylbenzene. Here, individual xylene isomers have been grouped for consistency with the main text.

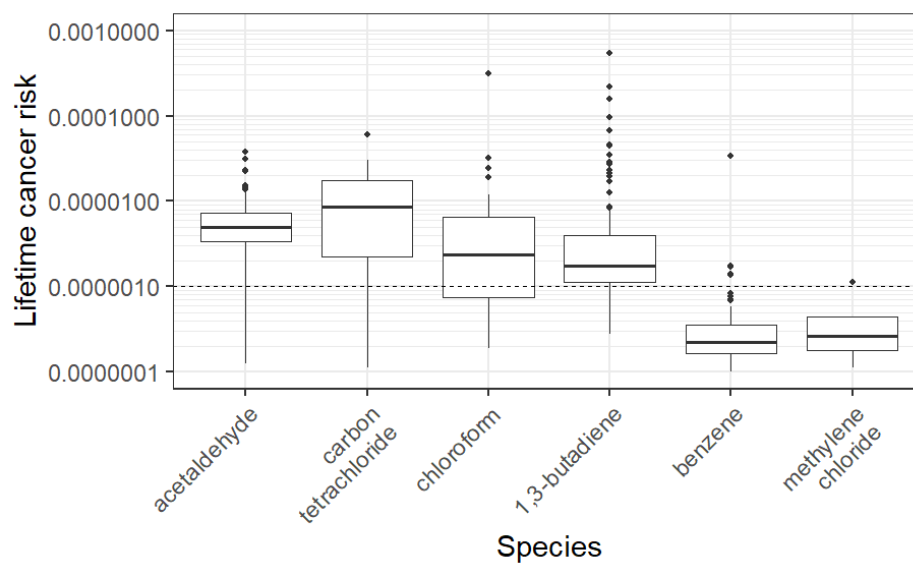


Figure 5.4: Calculated lifetime cancer risks (LCRs) for six VOCs. A horizontal dotted line is placed at the 0.000001 mark, representing the 1 in 1,000,000 chance threshold of developing cancer through a lifetime exposure to the exposure factor-adjusted concentration of the displayed VOC. Boxplots show values in the order of (from bottom-to-top): lower outliers, 5th percentile, 25th percentile, median value, 75th percentile, 95th percentile, and upper outliers. The y-axis has been logarithmically transformed to aid presentation.

tetrachloride, as well as other halogenated hydrocarbons have been shown to be emitted from the use of chlorinated bleach indoors.<sup>[86,87]</sup> The use of chlorinated products indoors may have been a potential source of indoor carbon tetrachloride secondary emissions here.

#### 5.5.1.4 Hazard quotients

Hazard quotients for all available VOCs are shown in Fig. 5.5. A dashed line was added at  $HQ = 1$ , as any value above this threshold is identified as exceeding the non-cancer health guidelines established by IRIS, defined as the threshold concentration above which a lifetime exposure risk not associated with cancer but other health outcomes is significantly possible.<sup>[76]</sup> Fig. 5.5 shows that concentrations for nine of the twenty-one analysed VOCs did not rise above the  $HQ = 1$  threshold in any home. The highest number of total instances above  $LCR = 1 \times 10^{-6}$  and  $HQ = 1$  thresholds were for acetaldehyde and 1,3-butadiene. Most notable is the number of outlier observations in which 1,3-butadiene was markedly raised above  $LCR = 1 \times 10^{-6}$  ( $n = 98$  out of 124 total observations). Both acetaldehyde and 1,3-butadiene originate from, among other sources, wood products, combustion and use of cigarettes and e-cigarettes.<sup>[88-90]</sup> Mean concentrations of acetaldehyde and 1,3-butadiene in this study were  $22.2 \mu\text{g m}^{-3}$  and  $3.6 \mu\text{g m}^{-3}$ , respectively, placing mean indoor concentrations

---

in Bradford homes for both species markedly higher than those found in literature.<sup>[3,14,88,91]</sup>

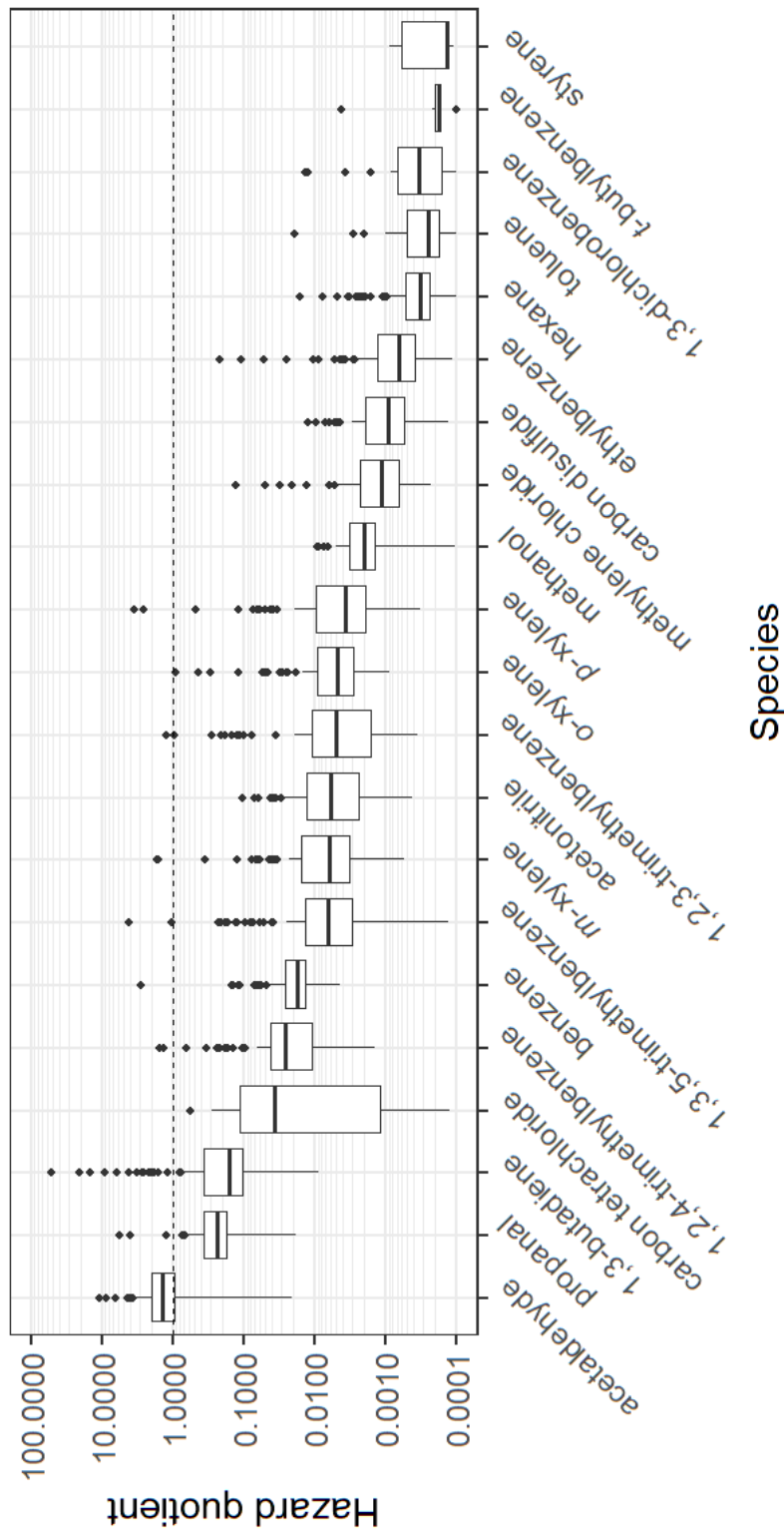


Figure 5.5: Calculated hazard quotients (HQs) for the VOCs measured in this study with available reference concentration data from the integrated risk information system (IRIS). A horizontal dotted line is placed at  $HQ = 1$ , above which a home occupant could develop symptoms based on a lifetime exposure to the exposure factor-adjusted concentration for the displayed VOC. Boxplots show values in the order of (from bottom-to-top): lower outliers, 5th percentile, 25th percentile, median value, 75th percentile, 95th percentile, and upper outliers. The y-axis has been logarithmically transformed to aid presentation.

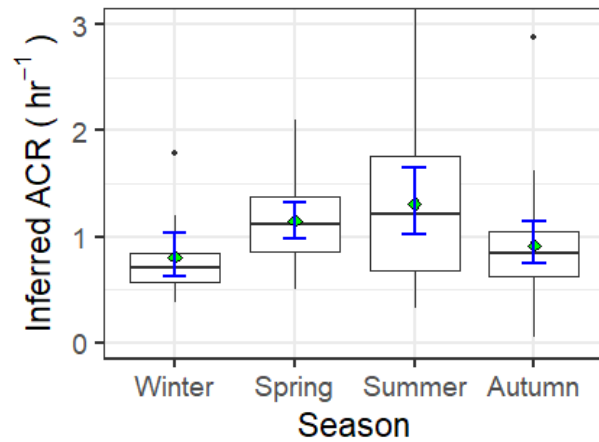


Figure 5.6: The inferred air change rates ( $\text{hr}^{-1}$ ) by season. Boxplots show values in the order of (from bottom-to-top): lower outliers, 5th percentile, 25th percentile, median value, 75th percentile, 95th percentile, and upper outliers. The green diamonds indicate seasonal mean ACR. Error bars are calculated as 95% confidence intervals for the mean value using 1000 bootstrap resamples of the data.

### 5.5.2 Air change rates

Fig. 5.6 illustrates inferred ACR across the four seasons: winter (December, January, February), spring (March, April, May), summer (June, July, August), and autumn (September, October, November). The data reveal two distinct phases: an increase in ACR during spring and summer, followed by a decline in autumn and winter. Meteorological data gathered from UK Met Office (Fig. 5.7 and Fig. 5.8) shows that autumn had higher *mean* maximum ( $14.6\text{ }^{\circ}\text{C}$ ) and minimum ( $8.4\text{ }^{\circ}\text{C}$ ) temperatures in Bradford compared to spring (*max mean*  $13.1\text{ }^{\circ}\text{C}$ , *min mean*  $5.2\text{ }^{\circ}\text{C}$ ). The gradual warming in spring, following the extended winter cold, likely heightened sensitivity to rising temperatures, prompting increased ventilation via open windows. Additionally, spring had more sunshine hours (*mean*  $139.6\text{ hrs month}^{-1}$ ) than autumn (*mean*  $91.1\text{ hrs month}^{-1}$ ), potentially leading to higher solar heating of buildings and warmer indoor temperatures, which may have contributed to the higher ACR in spring through windows and doors potentially being opened for longer. Meteorological data for June 2023 indicated Bradford's highest mean temperature of the year ( $21.6\text{ }^{\circ}\text{C}$ ), while summer saw the most sunshine (*mean*  $177\text{ hrs months}^{-1}$ ). These meteorological patterns likely explain the elevated ACR observed in spring, which remained high throughout the summer as outdoor temperatures rose. The wider error bars for the mean summer ACR in Fig. 5.6 reflect greater variability in ACR during the summer months.

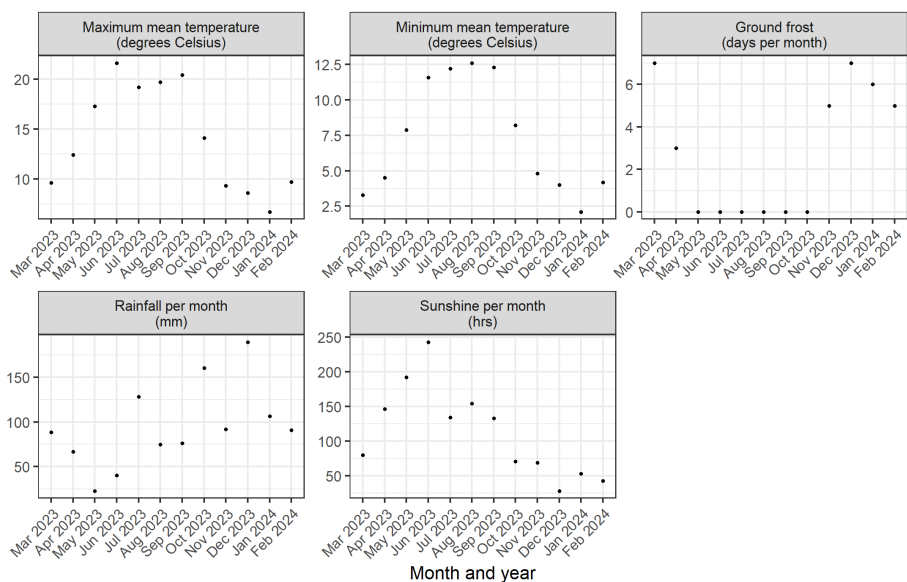


Figure 5.7: Meteorological data gathered from UK Met Office for Bradford over 2023 and 2024, taken from a weather station at 53°48'46.8"N 1°46'19.2"W. Values were taken for each month. Data was collected for maximum and minimum mean temperature (°C), ground frost days per month, total rainfall (mm) and total sunshine hours per month.

### 5.5.3 Seasonality in VOC emissions

Indoor VOC concentrations are primarily influenced by VOC emission rates, diluent room volume, and ACR. However, the observed seasonality in ACR suggested that raw indoor concentrations may not have fully captured the dynamics of indoor VOC exposure. Since VOC exposure is unique to the occupants of each sampled house, normalising concentrations by room volume and inferred ACR to calculate VOC time-averaged emission rates enables more robust comparisons across the cohort.

Figs. 5.9 and 5.10 shows a comparison between the seasonal TVOC concentrations and seasonal total VOC time-averaged emission rates, respectively. There were no patterns in indoor TVOC concentration over the seasons (Fig. 5.9), but clear seasonality in total indoor VOC emissions (Fig. 5.10). Seasonality for individual VOC emissions is shown in Fig. 5.11. In general, time-averaged emission rates were at a minimum in winter and a maximum in summer, as seen in total time-averaged emission rates in Fig. 5.10.

Total monoterpene time-averaged emission rates displayed the opposite seasonality however (Fig. 5.11), with a low in summer and autumn months (*median* 492  $\mu\text{g hr}^{-1}$  and 380  $\mu\text{g hr}^{-1}$  respectively), and a high in winter and spring months (*median* 731  $\mu\text{g hr}^{-1}$  and 966  $\mu\text{g hr}^{-1}$  respectively). This was most likely driven by heightened emission rates of limonene in winter months, which was the single biggest contributor to the total monoterpene time-

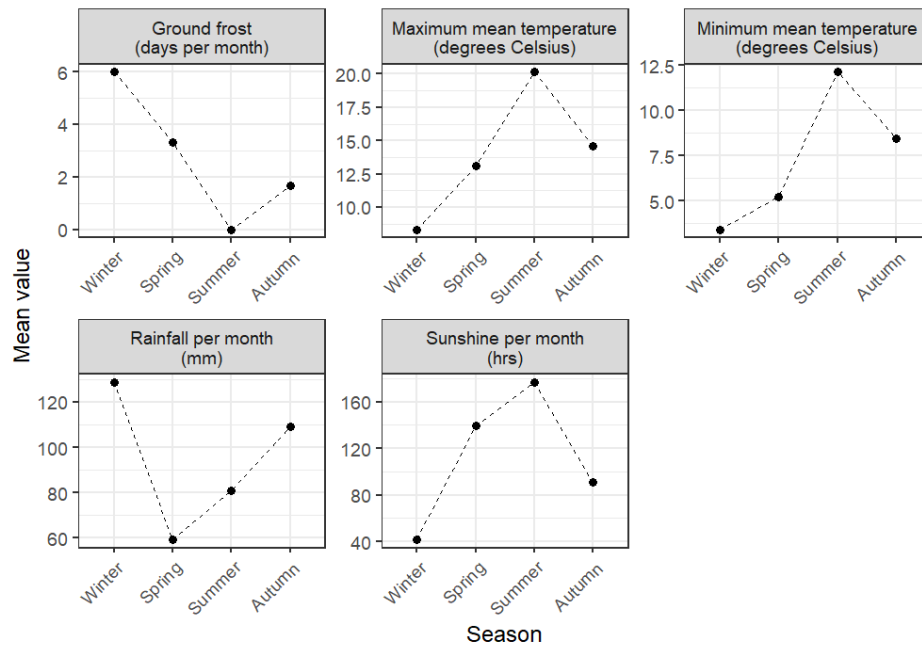


Figure 5.8: Meteorological data gathered from UK Met Office for Bradford over 2023 and 2024, taken from a weather station at 53°48'46.8" N 1°46'19.2" W. Values were taken for each month. Data was collected for maximum and minimum mean temperature (°C), ground frost days per month, total rainfall (mm) and total sunshine hours per month. Values were taken for each month, with each month then being grouped into four seasons: winter (December, January, February), spring (March, April, May), summer (June, July, August), and autumn (September, October, November), and mean values for each meteorological measurement taken for each season.

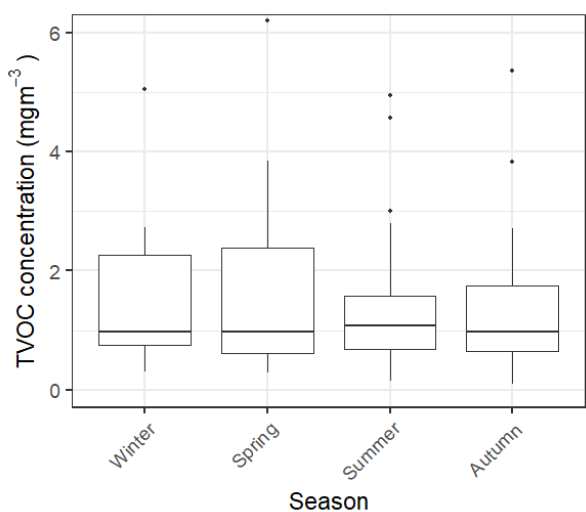


Figure 5.9: Indoor TVOC concentrations by season.

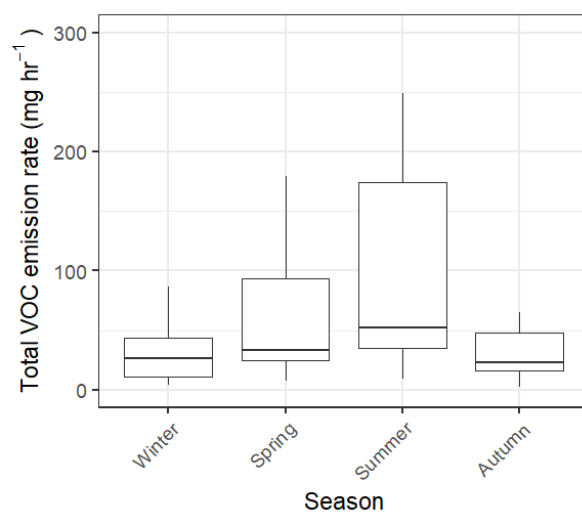


Figure 5.10: Total indoor VOC emission rates by season.

Boxplots show values in the order of (from bottom-to-top): lower outliers, 5th percentile, 25th percentile, median value, 75th percentile, 95th percentile, and upper outliers.

averaged emission rate metric. The reported elevated median use of fragrance products in winter months (Fig. 5.12) is a likely source of elevated limonene emission rates in winter. A similar winter-high, summer-low pattern was seen in isopropanol, indicating the potential for common emission sources. However, emission sources are complex with variable dynamics, such as building materials which have variable rates of VOC off-gassing.<sup>[36,92]</sup> As with indoor concentrations, indoor time-averaged emission rates were dominated by ethanol, butane and propane (Fig. 5.11). However, the seasonality in time-averaged emission rates for these species does not match with the product use patterns (Fig. 5.12). It is noted that in a small subset of homes ( $n = 13$ ), portable space heaters were used including those using bottled gas, which could be a non-typical source of indoor butane and propane. The use of bottled gas for cooking stoves is not common in the UK and was not found in this study. We further note that product use behaviours were consolidated in the questionnaires. For example, daily usage statistics of room fragrance products, such as air fresheners, electric diffusers and candles were grouped together. As a result, the grouping of product use behaviours provided a broader overview of behaviour, rather than allowing a highly specific breakdown of each product type.

Time-averaged emission rates of ethanol were markedly higher in summer months compared to others, with the summer median time-averaged emission rate ( $30,510 \mu\text{g hr}^{-1}$ ) being more

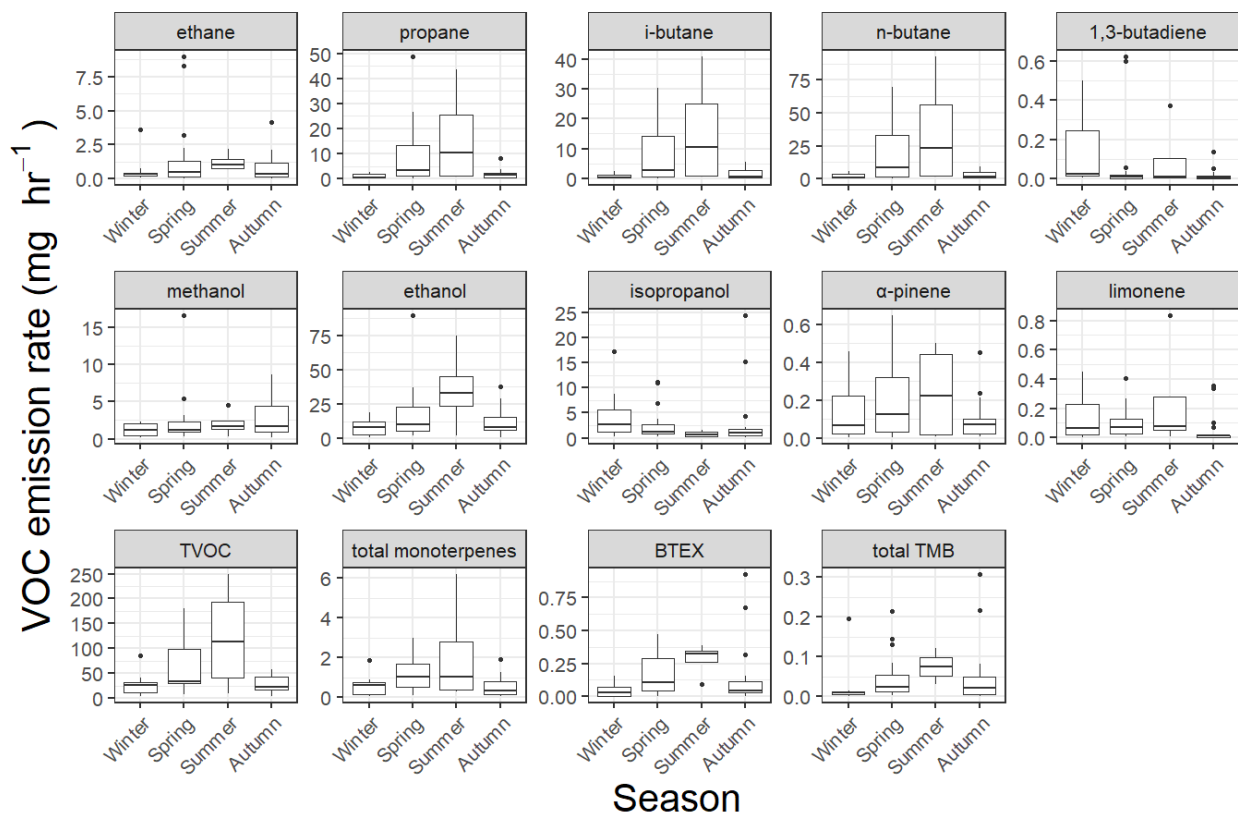


Figure 5.11: Calculated individual VOC emission rates over the seasons. Outliers above 10 mg hr<sup>-1</sup> were removed from ethane and sum BTEX plots, and outliers above 1 mg hr<sup>-1</sup> were removed from 1,3-butadiene and sum TMB plots to aid presentation, but did not affect the calculation of quartiles for boxplots. Boxplots show values in the order of (from bottom-to-top): lower outliers, 5th percentile, 25th percentile, median value, 75th percentile, 95th percentile, and upper outliers. The y-axis has been logarithmically transformed to aid presentation. TMB = trimethylbenzene, BTEX = benzene, toluene, ethylbenzene and xylene.

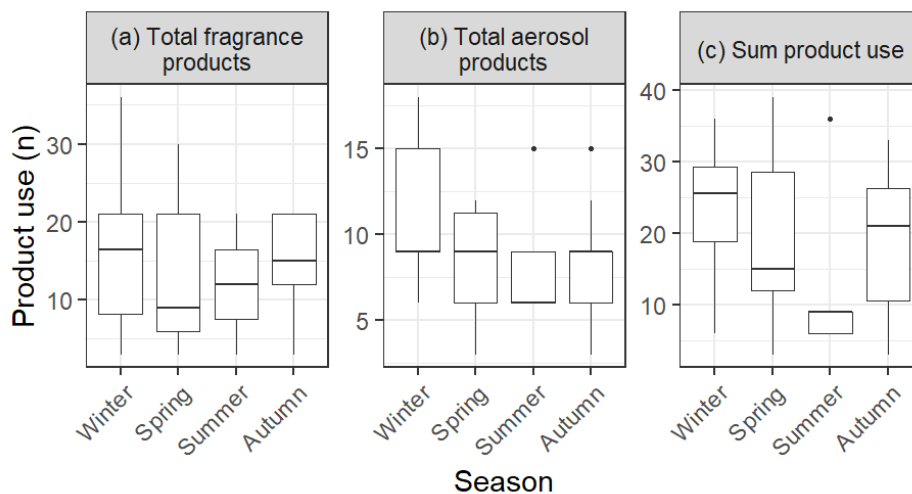


Figure 5.12: (a) Total fragrance product use, (b) total aerosol product use and (c) the sum of fragrance and aerosol product use. Statistics were gathered daily and then added together over the 72-hour sampling period. Boxplots show values in the order of (from bottom-to-top): lower outliers, 5th percentile, 25th percentile, median value, 75th percentile, 95th percentile, and upper outliers.

than three times the next highest median time-averaged emission rate in spring ( $9698 \mu\text{g hr}^{-1}$ ). While inferred ACRs were higher in summer, there does not appear to be a significant seasonality in ethanol concentrations outdoors, and so higher outdoor air exchange in summer is unlikely to be the source of this trend.<sup>[93]</sup>

To account for single dominant time-averaged emission rates such as ethanol, propane and butane, VOC time-averaged emission rates were normalised on a scale of 0 to 1 using equation 5.16, where  $X'_a$  is the normalised time-averaged emission rate value of VOC  $a$ ,  $X_a$  is the original time-averaged emission rate of VOC  $a$  ( $\text{g hr}^{-1}$ ), and  $X_{a,max}$  and  $X_{a,min}$  are the maximum and minimum time-averaged emission rates of VOC  $a$  ( $\text{g hr}^{-1}$ ), respectively. Normalised values were then summed together, as shown in Fig. 5.13, along with summed normalised monoterpene time-averaged emission rates in Fig. 5.14 .

$$X'_a = \frac{X_a - X_{a,min}}{X_{a,max} - X_{a,min}} \quad (5.16)$$

Total normalised VOC time-averaged emission rates were at their highest in summer and lowest in autumn. While Kruskal-Wallis testing on the non-normalised time-averaged emission rate data set indicated no significant change in total VOC time-averaged emission rates across the seasons, significance in total normalised VOC time-averaged emission rate and to-

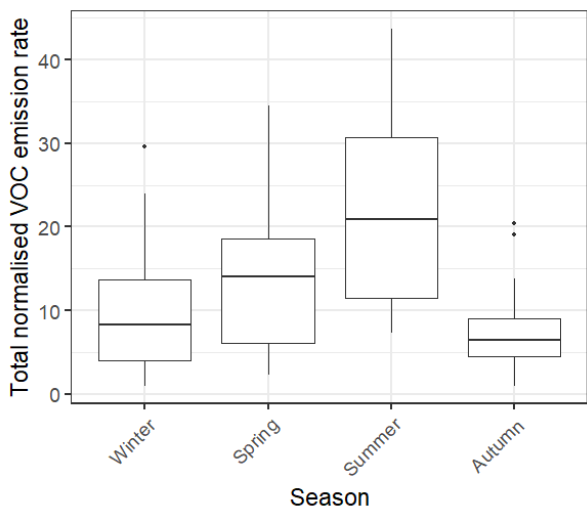


Figure 5.13: Seasonality in the summed normalised total VOC emissions.

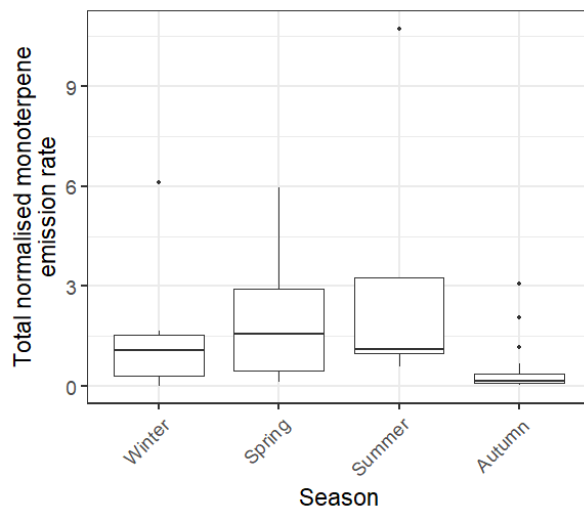


Figure 5.14: Seasonality in the summed normalised monoterpene emissions.

Boxplots show values in the order of (from bottom-to-top): lower outliers, 5th percentile, 25th percentile, median value, 75th percentile, 95th percentile, and upper outliers.

tal normalised monoterpene time-averaged emission rate seasonality was observed. *Post-hoc* Dunn tests revealed significant differences between autumn - summer and autumn - spring for both total normalised time-averaged emission rates and normalised monoterpene time-averaged emission rates. *p*-values for the *post-hoc* Dunn tests are displayed as a matrix in Fig. 5.15. Normalised data analysis highlighted that dominance from specific VOC emissions could potentially skew results when comparing raw time-averaged emission rates. Among the possible sources of increased time-averaged emission rates in this study, two emerged as likely causes. Firstly, during the summer months, especially in late-July and August, children are at home more due to school holidays and as such, parents are likely to be at home more too. This could result in an increase in VOC emission rates. Secondly, it has been noted in other studies that emission rates of surface-partitioned VOCs increase with an increase in temperature.<sup>[17,94]</sup> Over colder months, it has been suggested that there may be a cumulative increase in surface-bound VOC concentrations, which resulted in increased off-gassing as temperatures increase in warmer seasons.

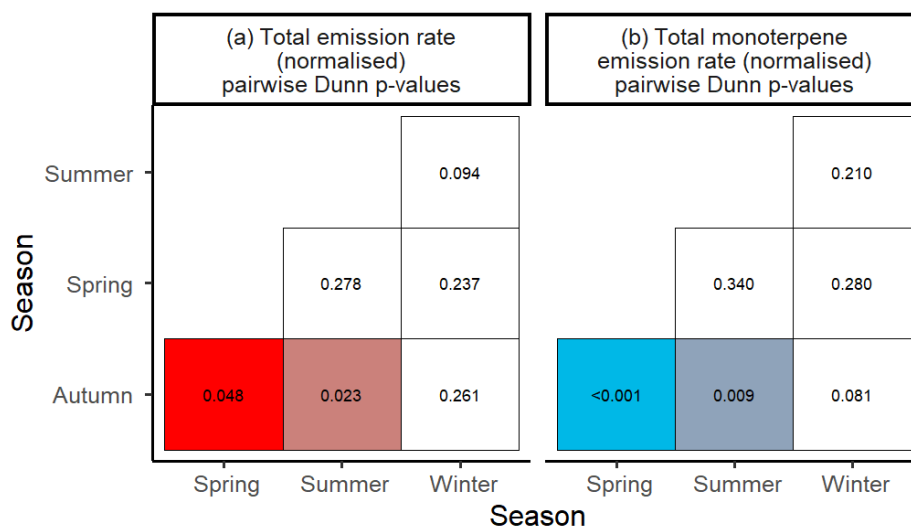


Figure 5.15: Matrices of  $p$ -values following *post-hoc* Dunn tests for seasonality in (a) summed normalised VOC emission rates and (b) summed normalised monoterpene emission rates. A white coloured matrix cell indicates the  $p$ -value for the pairwise comparison was not of significance. Significant values ( $p$ -value  $\leq 0.05$ ) graduate from red ( $p$ -value = 0.05) to blue ( $p$ -value  $\rightarrow 0$ ).

## 5.6 Conclusions

The time-integrated concentrations of  $>120$  VOCs were measured in the main living area of 124 homes in Bradford, UK. It was found, as in other studies,<sup>[3,14,95]</sup> that indoor concentrations rarely showed any associations with factors such as product use. However, evaluation and estimation of personal VOC exposure using simple indoor concentrations against LCR benchmarks showed exceedances for all measured species against the US EPA 1 in 1,000,000 threshold, with exceedances in  $>75\%$  of homes for acetaldehyde, carbon tetrachloride and 1,3-butadiene. HQ assessment showed an exceedance above an HQ of 1 in 75% of homes for acetaldehyde, and there were measured exceedances in HQ for propanal, 1,3-butadiene, trimethylbenzenes, benzene and xylenes. While not the aim of this paper to make direct claims regarding the health prospects of the participants of this study, there was a clear pattern of elevated concentrations of VOCs that have been shown to be harmful to health.

Of particular interest is carbon tetrachloride. As an ozone-depleting substance, as well as a hepatotoxic suspected human carcinogen, the inclusion of this VOC in any product has been phased out in many countries including the UK through the Montreal Protocol. However, the variation seen in this study ( $min\ 4.83\ \mu\text{g m}^{-3}$ ,  $max\ 81\ \mu\text{g m}^{-3}$ ,  $median\ 15.5\ \mu\text{g m}^{-3}$ ) suggests that carbon tetrachloride has at least one secondary emission source indoors, likely as an atmospheric by-product of bleach or other chlorinated-product use. Previous studies have

---

shown that carbon tetrachloride is a measurable emission from the use of bleach or other chlorinated-product use indoors.<sup>[86,87]</sup> Further investigation into indoor production of carbon tetrachloride, other halogenated hydrocarbons and other VOCs from the use of household products would therefore be warranted.<sup>[44]</sup>

Once the effects of short-term emissions of BTEX species from painting and decorating had been accounted for, indoor BTEX species had higher median concentrations in urban homes than in rural homes, with xylene concentrations being significantly higher in urban homes (rural *median* concentration  $1.22 \mu\text{g m}^{-3}$ , urban *median* concentration  $2.35 \mu\text{g m}^{-3}$ ). Additionally, there was a generally lower I/O ratio in urban houses for BTEX species compared with rural houses, indicating generally higher concentrations of BTEX species in urban outdoor areas. Indoor concentrations appeared to be impacted by outdoor concentrations with higher indoor concentrations for BTEX seen in urban homes compared to rural.

ACR was inferred using an adjusted method from Warburton *et al.* (2023)<sup>[14]</sup> through CO<sub>2</sub> exchange and room diluent volume. ACR was at a high in summer with a median ACR of  $1.2 \text{ hr}^{-1}$  and at a low in winter with a median ACR of  $0.7 \text{ hr}^{-1}$ . ACR itself was most variable in summer, and presented a study-wide range of between  $0.41 \text{ hr}^{-1}$  and  $3.05 \text{ hr}^{-1}$ .

Once seasonal changes in inferred ACR and individual room sizes were accounted for through the calculation of time-averaged emission rates, then highest VOC time-averaged emission rates were found for the summer months. Summer had the highest median total VOC time-averaged emission rate ( $51,950 \mu\text{g hr}^{-1}$ ), while autumn had the lowest median total VOC time-averaged emission rate ( $22,760 \mu\text{g hr}^{-1}$ ), closely followed by winter ( $26,161 \mu\text{g hr}^{-1}$ ). Additionally, the variability in total VOC time-averaged emission rates rose to a maximum in summer (*min*  $9472 \mu\text{g hr}^{-1}$ , *max*  $249,300 \mu\text{g hr}^{-1}$ ). This trend could not be attributed solely to any seasonality in product use in this study. This was likely a product of increased surface-adsorbed VOCs off-gassing as ambient temperature increased, as well as increased occupancy times over the summer months with parents and children spending more time in the homes.

## 5.6.1 Limitations and strengths

### 5.6.1.1 Limitations

In this study, CO<sub>2</sub> mixing ratios were used to infer an ACR. This clearly can have limitations since there may be unaccounted for sources of CO<sub>2</sub> within indoor environments. While the samples from this study were time integrated thus smoothing short-term effects, this may have impacted the calculated value. In calculating time-averaged emission rates, only indoor

---

and outdoor VOC concentrations, ACR and total room volume was considered. VOC loss through oxidation or surface losses may also have occurred, however accounting for these factors is not possible in a model given the state of knowledge of these processes at this time, and difficulties in estimating individual surface area-to-volume ratios and indoor oxidant concentrations for the large number of houses sampled here. Additionally, there remains little information available on surface deposition rates for many of the VOCs assessed here. Sensitivity analysis of the implications of assumptions based on ACR and room volume were completed and are included within the supplementary information.

In calculating LCRs and HQs for indoor VOCs, assumptions must be made regarding expected lifetimes, residential times as well as a greater assumption that the sampled concentration of VOC is indicative of the concentration an occupant will always be exposed to. By nature, these calculations must make these assumptions, and the resulting values are only meant to be regarded as indicative values and not absolute.

Within the scope of the larger INGENIOUS study, participants answered several large questionnaires gathering information on many aspects of the occupants and their home. As such, aspects of the questionnaires had to be consolidated, such as product use. The resulting groupings were therefore relatively coarse.

#### **5.6.1.2 Strengths**

A long-term analysis of indoor air quality has provided new insights into the multiple factors influencing indoor VOC exposure. By examining compounding seasonal effects and time-averaged emission rates, this study identifies key patterns in VOC variability. Previous research has shown that raw time-integrated VOC concentration data often fail to reveal meaningful relationships. However, through the application of transformative analytical methods, this study uncovers structured patterns in indoor VOC exposure. To our knowledge, this is one of the longest indoor VOC datasets collected to date.

This study offers a comprehensive dataset of indoor VOC concentrations and time-averaged emission rates across a large sample of homes ( $n = 124$ ), serving as a valuable resource for the air pollution research community. The wide range of VOC species measured provides a detailed understanding of the factors shaping indoor air quality. By incorporating seasonal and spatial analyses, this work identifies key drivers of indoor VOC exposure, such as outdoor air ingress and emission variability throughout the year.

A key strength of this study is its contribution to understanding indoor VOC dynamics. For instance, the observed increase in ACR during warmer months suggests greater ventilation-

---

driven transport of VOCs from indoors to the immediate outdoor environment. When scaled across millions of homes, this process may represent a significant and largely unaccounted-for source of outdoor VOC pollution. Currently, most outdoor air pollution models do not adequately consider indoor VOC emissions, yet this study demonstrates that indoor spaces could play a major role in shaping outdoor VOC concentrations.

### 5.6.2 Future work

Further in-home studies should attempt to specify product use as much as possible. The realities of widely variable product formulation and composition will naturally result in assumptions having to be made when considering source apportionment of VOCs to specific groups of products, however. Future indoor air analyses should consider the effects of ACR and diluent room volume on indoor VOC concentrations. While indoor concentrations can be used to compare against benchmarks, the effects of intra-study ACR and volume variability on measured concentrations may result in difficulty in drawing conclusions from concentration data across and within studies. Compounding this with sampling and analytical differences between studies, transformation of indoor concentrations into emission rates may allow for better VOC exposure comparison between studies. Additional consideration of the potential for increased VOC-surface partitioning in colder months and increased off-gassing of surface-bound VOCs in warmer months would provide additional insight into population exposure to VOCs.

Future studies should also consider the impact indoor air pollution may have on outdoor air pollution. As is evident from this study, indoor VOC concentrations can be orders of magnitude higher than outdoor concentrations, and activities such as cooking and cleaning are known to give rise to substantial VOC emissions. Indoor reactions appear capable of producing halocarbons of significance to stratospheric ozone depletion such as carbon tetrachloride, species that are not used as raw ingredients in product formulation, but may still be emitted due to unaccounted for indoor chemistry. Mitigating indoor VOC exposure by increased ventilation will directly lead to elevated outdoor VOC concentrations in the immediate surroundings of the indoor area, and the magnitude of this effect should be further studied and quantified.

---

## 5.7 References

- [1] Andrea Bergomi et al. “Outdoor trends and indoor investigations of volatile organic compounds in two high schools of southern Italy”. In: *Air Quality, Atmosphere & Health* (2024). ISSN: 1873-9318. DOI: [10.1007/s11869-024-01509-2](https://doi.org/10.1007/s11869-024-01509-2). URL: <https://dx.doi.org/10.1007/s11869-024-01509-2>.
- [2] Busoon Son, Patrick Breyse, and Wonho Yang. “Volatile organic compounds concentrations in residential indoor and outdoor and its personal exposure in Korea”. In: *Environment International* 29.1 (2003), pp. 79–85. ISSN: 0160-4120. DOI: [https://doi.org/10.1016/S0160-4120\(02\)00148-4](https://doi.org/10.1016/S0160-4120(02)00148-4). URL: <https://www.sciencedirect.com/science/article/pii/S0160412002001484>.
- [3] A C Heeley-Hill et al. “Frequency of use of household products containing VOCs and indoor atmospheric concentrations in homes”. In: *Environmental Science: Processes and Impacts* 23.5 (2021), pp. 699–713. DOI: [10.1039/d0em00504e](https://doi.org/10.1039/d0em00504e).
- [4] Toby J Carter et al. “Indoor cooking and cleaning as a source of outdoor air pollution in urban environments”. In: *Environmental Science: Processes & Impacts* 26.6 (2024), pp. 975–990. ISSN: 2050-7887. DOI: [10.1039/d3em00512g](https://doi.org/10.1039/d3em00512g). URL: <https://dx.doi.org/10.1039/d3em00512g>.
- [5] Amber M Yeoman, Marvin Shaw, and Alastair C Lewis. “Estimating person-to-person variability in VOC emissions from personal care products used during showering”. In: *Indoor Air* 31.4 (2021), pp. 1281–1291. ISSN: 0905-6947. DOI: [10.1111/ina.12811](https://doi.org/10.1111/ina.12811). URL: <https://dx.doi.org/10.1111/ina.12811>.
- [6] Ellen Harding-Smith et al. “Does green mean clean? Volatile organic emissions from regular versus green cleaning products”. In: *Environmental Science: Processes & Impacts* 26.2 (2024), pp. 436–450. ISSN: 2050-7887. DOI: [10.1039/d3em00439b](https://doi.org/10.1039/d3em00439b). URL: <https://dx.doi.org/10.1039/d3em00439b>.
- [7] Amber M Yeoman and Alastair C Lewis. “Global emissions of VOCs from compressed aerosol products”. In: *Elementa: Science of the Anthropocene* 9.1 (2021), p. 177. DOI: [10.1525/elementa.2020.20.00177](https://doi.org/10.1525/elementa.2020.20.00177). URL: <https://doi.org/10.1525/elementa.2020.20.00177>.
- [8] Kasper Kristensen et al. “Gas–Particle Partitioning of Semivolatile Organic Compounds in a Residence: Influence of Particles from Candles, Cooking, and Outdoors”. In: *Environmental Science & Technology* 57.8 (2023), pp. 3260–3269. ISSN: 0013-936X. DOI: [10.1021/acs.est.2c07172](https://doi.org/10.1021/acs.est.2c07172). URL: <https://dx.doi.org/10.1021/acs.est.2c07172>.

- 
- [9] Joe L Mauderly and Judith C Chow. “Health Effects of Organic Aerosols”. In: *Inhalation Toxicology* 20.3 (2008), pp. 257–288. ISSN: 0895-8378. DOI: [10.1080/08958370701866008](https://doi.org/10.1080/08958370701866008). URL: <https://doi.org/10.1080/08958370701866008>.
- [10] Christopher M Long et al. “Using Time- and Size-Resolved Particulate Data To Quantify Indoor Penetration and Deposition Behavior”. In: *Environmental Science & Technology* 35.10 (2001), pp. 2089–2099. ISSN: 0013-936X. DOI: [10.1021/es001477d](https://dx.doi.org/10.1021/es001477d). URL: <https://dx.doi.org/10.1021/es001477d>.
- [11] Utku Pamuk et al. “A rare cause of fatal cardiac arrhythmia: Inhalation of butane gas”. In: *The Turkish Journal of Pediatrics* 60.6 (2018), pp. 755–756. ISSN: 2791-6421. DOI: [10.24953/turkjped.2018.06.021](https://dx.doi.org/10.24953/turkjped.2018.06.021). URL: <https://dx.doi.org/10.24953/turkjped.2018.06.021>.
- [12] Klaus Abraham et al. “Elevated internal exposure of children in simulated acute inhalation of volatile organic compounds: effects of concentration and duration”. In: *Archives of Toxicology* 79.2 (2005), pp. 63–73. ISSN: 0340-5761. DOI: [10.1007/s00204-004-0599-3](https://dx.doi.org/10.1007/s00204-004-0599-3). URL: <https://dx.doi.org/10.1007/s00204-004-0599-3>.
- [13] Chunting Michelle Wang et al. “Unexpectedly high concentrations of monoterpenes in a study of UK homes”. In: *Environmental Science: Processes & Impacts* 19.4 (2017), pp. 528–537. DOI: [10.1039/c6em00569a](https://dx.doi.org/10.1039/c6em00569a). URL: <https://dx.doi.org/10.1039/c6em00569a>.
- [14] Thomas Warburton et al. “The impact of plug-in fragrance diffusers on residential indoor VOC concentrations”. In: *Environ. Sci.: Processes Impacts* 25.4 (2023), pp. 805–817. DOI: [10.1039/D2EM00444E](https://dx.doi.org/10.1039/D2EM00444E). URL: <http://dx.doi.org/10.1039/D2EM00444E>.
- [15] C Shrubsole et al. “IAQ guidelines for selected volatile organic compounds (VOCs) in the UK”. In: *Building and Environment* 165 (2019), p. 106382. DOI: <https://doi.org/10.1016/j.buildenv.2019.106382>. URL: <https://www.sciencedirect.com/science/article/pii/S036013231930592X>.
- [16] Jenna C Ditto et al. “Indoor and outdoor air quality impacts of cooking and cleaning emissions from a commercial kitchen”. In: *Environmental Science: Processes & Impacts* 25.5 (2023), pp. 964–979. ISSN: 2050-7887. DOI: [10.1039/d2em00484d](https://dx.doi.org/10.1039/d2em00484d). URL: <https://dx.doi.org/10.1039/d2em00484d>.
- [17] Han N Huynh et al. “VOC emission rates from an indoor surface using a flux chamber and PTR-MS”. In: *Atmospheric Environment* 338 (2024), p. 120817. ISSN: 1352-2310. DOI: <https://doi.org/10.1016/j.atmosenv.2024.120817>. URL: <https://www.sciencedirect.com/science/article/pii/S1352231024004928>.
- [18] Jie Yu, Frank Wania, and Jonathan P D Abbatt. “A New Approach to Characterizing the Partitioning of Volatile Organic Compounds to Cotton Fabric”. In: *Environmental*

- 
- Science & Technology* 56.6 (2022), pp. 3365–3374. ISSN: 0013-936X. DOI: [10.1021/acs.est.1c08239](https://doi.org/10.1021/acs.est.1c08239). URL: <https://dx.doi.org/10.1021/acs.est.1c08239>.
- [19] Helen L Davies et al. “A measurement and modelling investigation of the indoor air chemistry following cooking activities”. In: *Environmental Science: Processes & Impacts* 25.9 (2023), pp. 1532–1548. DOI: [10.1039/d3em00167a](https://doi.org/10.1039/d3em00167a). URL: <https://dx.doi.org/10.1039/d3em00167a>.
- [20] Wei Liu et al. “Tracking indoor volatile organic compounds with online mass spectrometry”. In: *TrAC Trends in Analytical Chemistry* 171 (2024), p. 117514. ISSN: 0165-9936. DOI: <https://doi.org/10.1016/j.trac.2023.117514>. URL: <https://www.sciencedirect.com/science/article/pii/S0165993623006015>.
- [21] Wen-Hsi Cheng, Yi-Chian Chen, and Song-You Shih. “Volatile Organic Compound Emissions from Indoor Fragrance Diffusers”. In: *Atmosphere* 14.6 (2023), p. 1012. DOI: [10.3390/atmos14061012](https://dx.doi.org/10.3390/atmos14061012). URL: <https://dx.doi.org/10.3390/atmos14061012>.
- [22] William Bruchard, Aakriti Bajracharya, and Nancy A C Johnston. “Volatile Organic Compound Emissions from Disinfectant Usage in the Home and Office”. In: *Environmental Health Perspectives* 131.4 (2023), p. 47701. DOI: [doi:10.1289/EHP11916](https://doi.org/10.1289/EHP11916). URL: <https://ehp.niehs.nih.gov/doi/abs/10.1289/EHP11916>.
- [23] Felix Klein et al. “Characterization of Gas-Phase Organics Using Proton Transfer Reaction Time-of-Flight Mass Spectrometry: Cooking Emissions”. In: *Environmental Science & Technology* 50.3 (2016), pp. 1243–1250. ISSN: 0013-936X. DOI: [10.1021/acs.est.5b04618](https://doi.org/10.1021/acs.est.5b04618). URL: <https://dx.doi.org/10.1021/acs.est.5b04618>.
- [24] Hanyu Zhang et al. “Chemical characterization of volatile organic compounds (VOCs) emitted from multiple cooking cuisines and purification efficiency assessments”. In: *Journal of Environmental Sciences* 130 (2023), pp. 163–173. ISSN: 1001-0742.
- [25] Sangin Park et al. “VOC concentrations in houses in Japan: correlations with housing characteristics and types of ventilation”. In: *Journal of Asian Architecture and Building Engineering* (2024), pp. 1–17. ISSN: 1346-7581. DOI: [10.1080/13467581.2024.2325463](https://doi.org/10.1080/13467581.2024.2325463). URL: <https://dx.doi.org/10.1080/13467581.2024.2325463>.
- [26] A T Hodgson et al. “Effect of outside air ventilation rate on volatile organic compound concentrations in a call center”. In: *Atmospheric Environment* 37.39-40 (2003), pp. 5517–5527. DOI: [10.1016/j.atmosenv.2003.09.028](https://doi.org/10.1016/j.atmosenv.2003.09.028). URL: <https://dx.doi.org/10.1016/j.atmosenv.2003.09.028>.
- [27] William J Fisk and David Faulkner. “Air exchange effectiveness in office buildings: measurement techniques and results”. In: *International Symposium on Room Air Convection and Ventilation Effectiveness*. Tokyo, July 1992, pp. 1–15.

- 
- [28] Michael S Breen et al. “A review of air exchange rate models for air pollution exposure assessments”. In: *Journal of Exposure Science & Environmental Epidemiology* 24.6 (2014), pp. 555–563. DOI: [10.1038/jes.2013.30](https://doi.org/10.1038/jes.2013.30). URL: <https://dx.doi.org/10.1038/jes.2013.30>.
- [29] A Rackes and M S Waring. “Do time-averaged, whole-building, effective volatile organic compound (VOC) emissions depend on the air exchange rate? A statistical analysis of trends for 46 VOCs in U.S.offices”. In: *Indoor Air* 26.4 (2016), pp. 642–659. DOI: [10.1111/ina.12224](https://doi.org/10.1111/ina.12224). URL: <https://dx.doi.org/10.1111/ina.12224>.
- [30] L Du et al. “Air exchange rates and migration of VOCs in basements and residences”. In: *Indoor Air* 25.6 (2015), pp. 598–609. DOI: [10.1111/ina.12178](https://doi.org/10.1111/ina.12178). URL: <https://dx.doi.org/10.1111/ina.12178>.
- [31] David Thickett, Frances David, and Naomi Luxford. “Air exchange rate - the dominant parameter for preventive conservation?” In: *The Conservator* 29.1 (2005), pp. 19–34. DOI: [10.1080/01410096.2005.9995210](https://doi.org/10.1080/01410096.2005.9995210). URL: <https://dx.doi.org/10.1080/01410096.2005.9995210>.
- [32] Nicola Carslaw. “A new detailed chemical model for indoor air pollution”. In: *Atmospheric Environment* 41.6 (2007), pp. 1164–1179.
- [33] M T R Hill et al. “Measurement and Modelling of Short-Term Variations in Particle Concentrations in UK Homes”. In: *Indoor and Built Environment* 10.3-4 (2002), pp. 132–137. ISSN: 1420-326X. DOI: [10.1159/000049227](https://doi.org/10.1159/000049227). URL: <https://doi.org/10.1159/000049227>.
- [34] Chen Zhou et al. “Combined effects of temperature and humidity on indoor VOCs pollution: Intercity comparison”. In: *Building and Environment* 121 (2017), pp. 26–34. DOI: <https://doi.org/10.1016/j.buildenv.2017.04.013>. URL: <https://www.sciencedirect.com/science/article/pii/S0360132317301737>.
- [35] Yingrui Zhu, Shan Guo, and Weihui Liang. “A literature review investigating the impact of temperature and humidity on volatile organic compound emissions from building materials”. In: *Building and Environment* 262 (2024), p. 111845. ISSN: 0360-1323. DOI: <https://doi.org/10.1016/j.buildenv.2024.111845>. URL: <https://www.sciencedirect.com/science/article/pii/S0360132324006875>.
- [36] Sverre B Holøs et al. “VOC emission rates in newly built and renovated buildings, and the influence of ventilation – a review and meta-analysis”. In: *International Journal of Ventilation* 18.3 (2019), pp. 153–166. ISSN: 1473-3315. DOI: [10.1080/14733315.2018.1435026](https://doi.org/10.1080/14733315.2018.1435026). URL: <https://doi.org/10.1080/14733315.2018.1435026>.
- [37] Jing Xu et al. “Estimation of indoor and outdoor ratios of selected volatile organic compounds in Canada”. In: *Atmospheric Environment* 141 (2016), pp. 523–531. DOI:

- 
- <https://doi.org/10.1016/j.atmosenv.2016.07.031>. URL: <https://www.sciencedirect.com/science/article/pii/S1352231016305519>.
- [38] Rufus D Edwards et al. “VOC concentrations measured in personal samples and residential indoor, outdoor and workplace microenvironments in EXPOLIS-Helsinki, Finland”. In: *Atmospheric Environment* 35.27 (2001), pp. 4531–4543. DOI: [https://doi.org/10.1016/S1352-2310\(01\)00230-8](https://doi.org/10.1016/S1352-2310(01)00230-8). URL: <https://www.sciencedirect.com/science/article/pii/S1352231001002308>.
- [39] N Carslaw and D Shaw. “Secondary product creation potential (SPCP): A metric for assessing the potential impact of indoor air pollution on human health”. In: *Environmental Science: Processes and Impacts* 21.8 (2019), pp. 1313–1322. DOI: [10.1039/c9em00140a](https://doi.org/10.1039/c9em00140a).
- [40] Anita Lee et al. “Gas-phase products and secondary aerosol yields from the ozonolysis of ten different terpenes”. In: *Journal of Geophysical Research: Atmospheres* 111.D7 (2006). DOI: [10.1029/2005jd006437](https://doi.org/10.1029/2005jd006437). URL: <https://dx.doi.org/10.1029/2005jd006437>.
- [41] Anita Lee et al. “Gas-phase products and secondary aerosol yields from the photooxidation of 16 different terpenes”. In: *Journal of Geophysical Research: Atmospheres* 111.D17 (2006). DOI: [10.1029/2006jd007050](https://doi.org/10.1029/2006jd007050). URL: <https://dx.doi.org/10.1029/2006jd007050>.
- [42] Pratiti Home Chowdhury et al. “Exposure of Lung Epithelial Cells to Photochemically Aged Secondary Organic Aerosol Shows Increased Toxic Effects”. In: *Environmental Science & Technology Letters* 5.7 (2018), pp. 424–430. DOI: [10.1021/acs.estlett.8b00256](https://doi.org/10.1021/acs.estlett.8b00256). URL: <https://dx.doi.org/10.1021/acs.estlett.8b00256>.
- [43] Urs Baltensperger et al. “Combined Determination of the Chemical Composition and of Health Effects of Secondary Organic Aerosols: The POLYSOA Project”. In: *Journal of Aerosol Medicine and Pulmonary Drug Delivery* 21.1 (2008), pp. 145–154. DOI: [10.1089/jamp.2007.0655](https://doi.org/10.1089/jamp.2007.0655). URL: <https://doi.org/10.1089/jamp.2007.0655>.
- [44] Nicola Carslaw et al. “The INGENIOUS project: towards understanding air pollution in homes”. In: *Environmental Science: Processes & Impacts* 27.2 (2025), pp. 355–372. ISSN: 2050-7887. DOI: [10.1039/D4EM00634H](https://doi.org/10.1039/D4EM00634H). URL: [http://dx.doi.org/10.1039/D4EM00634H](https://dx.doi.org/10.1039/D4EM00634H).
- [45] City of Bradford Metropolitan District Council. *Population — Understanding Bradford District*. 2024. URL: <https://ubd.bradford.gov.uk/about-us/population/>.
- [46] Teumzghi F Mebrahtu et al. “Impact of an urban city-wide Bradford clean air plan on health service use and nitrogen dioxide 24 months after implementation: An interrupted time series analysis”. In: *Environmental Research* 270 (2025), p. 120988.

- 
- ISSN: 0013-9351. DOI: <https://doi.org/10.1016/j.envres.2025.120988>. URL: <https://www.sciencedirect.com/science/article/pii/S0013935125002397>.
- [47] Richard B Ellison, Stephen Greaves, and David A Hensher. “Medium term effects of London’s low emission zone”. In: *Transportation Research Board Annual Meeting, Washington DC*. 2013.
- [48] Hajar Hajmohammadi and Benjamin Heydecker. “Evaluation of air quality effects of the London ultra-low emission zone by state-space modelling”. In: *Atmospheric Pollution Research* 13.8 (2022), p. 101514. DOI: <https://doi.org/10.1016/j.apr.2022.101514>. URL: <https://www.sciencedirect.com/science/article/pii/S1309104222001969>.
- [49] Liu Jinghua. “Regional Specialization and Urban Development in England during the Industrial Revolution”. In: *Social Sciences in China* 39.1 (2018), pp. 199–216. DOI: [10.1080/02529203.2018.1414420](https://dx.doi.org/10.1080/02529203.2018.1414420). URL: <https://dx.doi.org/10.1080/02529203.2018.1414420>.
- [50] Robert Rowthorn. “Combined and Uneven Development: Reflections on the North–South Divide”. In: *Spatial Economic Analysis* 5.4 (2010), pp. 363–388. DOI: [10.1080/17421772.2010.516445](https://doi.org/10.1080/17421772.2010.516445). URL: <https://doi.org/10.1080/17421772.2010.516445>.
- [51] David Walsh, Martin Taulbut, and Phil Hanlon. “The aftershock of deindustrialization—trends in mortality in Scotland and other parts of post-industrial Europe”. In: *European Journal of Public Health* 20.1 (2009), pp. 58–64. ISSN: 1101-1262. DOI: [10.1093/eurpub/ckp063](https://doi.org/10.1093/eurpub/ckp063). URL: <https://doi.org/10.1093/eurpub/ckp063>.
- [52] Luke Telford. “‘There is nothing there’: Deindustrialization and loss in a coastal town”. In: *Competition & Change* 26.2 (2022), pp. 197–214. DOI: [10.1177/10245294211011300](https://doi.org/10.1177/10245294211011300). URL: <https://journals.sagepub.com/doi/abs/10.1177/10245294211011300>.
- [53] Hawraman Ramadan et al. “Incidence of first stroke and ethnic differences in stroke pattern in Bradford, UK: Bradford Stroke Study”. In: *International Journal of Stroke* 13.4 (2018), pp. 374–378. DOI: [10.1177/1747493017743052](https://doi.org/10.1177/1747493017743052). URL: <https://dx.doi.org/10.1177/1747493017743052>.
- [54] Ahmed Elhakeem et al. “OP125 Socioeconomic differences in pregnancy metabolic profiles: evidence from the multi-ethnic Born in Bradford cohort study”. In: *Journal of Epidemiology and Community Health* 77.Suppl 1 (2023), A122–A123. DOI: [10.1136/jech-2023-SSMabstracts.255](https://doi.org/10.1136/jech-2023-SSMabstracts.255). URL: [https://jech.bmj.com/content/jech/77/Suppl\\_1/A122.2.full.pdf](https://jech.bmj.com/content/jech/77/Suppl_1/A122.2.full.pdf).
- [55] David Buck and David Maguire. *Inequalities in life expectancy*. Tech. rep. London: The King’s Fund, Aug. 2015.

- 
- [56] Matthew Warburton et al. “Risk of not being in employment, education or training (NEET) in late adolescence is signalled by school readiness measures at 4–5 years”. In: *BMC Public Health* 24.1 (2024). DOI: [10.1186/s12889-024-18851-w](https://doi.org/10.1186/s12889-024-18851-w). URL: <https://dx.doi.org/10.1186/s12889-024-18851-w>.
- [57] City of Bradford Metropolitan District Council. *Ethnicity and religion — Understanding Bradford District*. 2024. URL: <https://ubd.bradford.gov.uk/about-us/ethnicity-and-religion/>.
- [58] Nathan R Gray, Alastair C Lewis, and Sarah J Moller. “Deprivation based inequality in NOx emissions in England”. In: *Environmental Science: Advances* 2.9 (2023), pp. 1261–1272.
- [59] H Brunt et al. “Air pollution, deprivation and health: understanding relationships to add value to local air quality management policy and practice in Wales, UK”. In: *Journal of Public Health* 39.3 (2016), pp. 485–497. ISSN: 1741-3842. DOI: [10.1093/pubmed/fdw084](https://doi.org/10.1093/pubmed/fdw084). URL: <https://doi.org/10.1093/pubmed/fdw084>.
- [60] S Morrison, F M Fordyce, and E Marian Scott. “An initial assessment of spatial relationships between respiratory cases, soil metal content, air quality and deprivation indicators in Glasgow, Scotland, UK: relevance to the environmental justice agenda”. In: *Environmental Geochemistry and Health* 36.2 (2014), pp. 319–332. ISSN: 0269-4042. DOI: [10.1007/s10653-013-9565-4](https://dx.doi.org/10.1007/s10653-013-9565-4). URL: <https://dx.doi.org/10.1007/s10653-013-9565-4>.
- [61] Anil Namdeo and Claire Stringer. “Investigating the relationship between air pollution, health and social deprivation in Leeds, UK”. In: *Environment International* 34.5 (2008), pp. 585–591. ISSN: 0160-4120. DOI: <https://doi.org/10.1016/j.envint.2007.12.015>. URL: <https://www.sciencedirect.com/science/article/pii/S0160412007002309>.
- [62] United Kingdom Department for Environment and Food Rural Affairs. *Automatic Urban and Rural Network (AURN) - Defra, UK*. 2024. URL: <https://uk-air.defra.gov.uk/networks/network-info?view=aurn>.
- [63] Erika Ikeda et al. “Understanding the patterns and health impact of indoor air pollutant exposures in Bradford, UK: a study protocol”. In: *BMJ Open* 13.12 (2023), e081099–e081099. DOI: [10.1136/bmjopen-2023-081099](https://doi.org/10.1136/bmjopen-2023-081099). URL: <https://dx.doi.org/10.1136/bmjopen-2023-081099>.
- [64] Rosemary R C McEachan et al. “Cohort Profile Update: Born in Bradford”. In: *International Journal of Epidemiology* 53.2 (2024). ISSN: 1464-3685. DOI: [10.1093/ije/dyae037](https://doi.org/10.1093/ije/dyae037). URL: <https://doi.org/10.1093/ije/dyae037>.

- 
- [65] Shuqing Cui et al. “CO<sub>2</sub> tracer gas concentration decay method for measuring air change rate”. In: *Building and Environment* 84 (2015), pp. 162–169. ISSN: 0360-1323. DOI: [10.1016/j.buildenv.2014.11.007](https://doi.org/10.1016/j.buildenv.2014.11.007). URL: <https://dx.doi.org/10.1016/j.buildenv.2014.11.007>.
- [66] Roulet Claude-Alain and Flavio Foradini. “Simple and Cheap Air Change Rate Measurement Using CO<sub>2</sub> Concentration Decays”. In: *International Journal of Ventilation* 1.1 (2002), pp. 39–44. ISSN: 1473-3315. DOI: [10.1080/14733315.2002.11683620](https://doi.org/10.1080/14733315.2002.11683620). URL: <https://dx.doi.org/10.1080/14733315.2002.11683620>.
- [67] Iman Khajehzadeh and Brenda Vale. “How do people use large houses?” In: *International Conference of the Architectural Science Association*. Melbourne, Dec. 2015.
- [68] Iman Khajehzadeh, Brenda Vale, and Nigel Isaacs. “Time-use in different rooms of selected New Zealand houses and the influence of plan layout”. In: *Indoor and Built Environment* 27.1 (2018), pp. 19–33. DOI: [10.1177/1420326x16665161](https://doi.org/10.1177/1420326x16665161). URL: <https://journals.sagepub.com/doi/abs/10.1177/1420326X16665161>.
- [69] S Batterman. “Review and extension of CO<sub>2</sub>-based methods to determine ventilation rates with application to school classrooms”. In: *International Journal of Environmental Research and Public Health* 14.2 (2017). DOI: [10.3390/ijerph14020145](https://doi.org/10.3390/ijerph14020145).
- [70] Archit Manuja et al. “Total surface area in indoor environments”. In: *Environmental Science: Processes & Impacts* 21.8 (2019), pp. 1384–1392. ISSN: 2050-7887. DOI: [10.1039/C9EM00157C](https://doi.org/10.1039/C9EM00157C). URL: <http://dx.doi.org/10.1039/C9EM00157C>.
- [71] A Persily and L De Jonge. “Carbon dioxide generation rates for building occupants”. In: *Indoor Air* 27.5 (2017), pp. 868–879. DOI: [10.1111/ina.12383](https://doi.org/10.1111/ina.12383). URL: <https://dx.doi.org/10.1111/ina.12383>.
- [72] Seong Kwang Lim et al. “Risk Assessment of Volatile Organic Compounds Benzene, Toluene, Ethylbenzene, and Xylene (BTEX) in Consumer Products”. In: *Journal of Toxicology and Environmental Health, Part A* 77.22-24 (2014), pp. 1502–1521. ISSN: 1528-7394. DOI: [10.1080/15287394.2014.955905](https://doi.org/10.1080/15287394.2014.955905). URL: <https://doi.org/10.1080/15287394.2014.955905>.
- [73] Boris Iglewicz and David Caster Hoaglin. *How to Detect and Handle Outliers (The ASQC Basic Reference in Quality Control)*. 1993.
- [74] Golam Sarwar et al. “Hydroxyl radicals in indoor environments”. In: *Atmospheric Environment* 36.24 (2002), pp. 3973–3988. DOI: [https://doi.org/10.1016/S1352-2310\(02\)00278-9](https://doi.org/10.1016/S1352-2310(02)00278-9). URL: <https://www.sciencedirect.com/science/article/pii/S1352231002002789>.

- 
- [75] United States Environmental Protection Agency. *Basic Information about the Integrated Risk Information System*. 2023. URL: <https://www.epa.gov/iris/basic-information-about-integrated-risk-information-system>.
- [76] United States Environmental Protection Agency. *IRIS Assessments*. 2024. URL: [https://iris.epa.gov/AtoZ/?list\\_type=alpha](https://iris.epa.gov/AtoZ/?list_type=alpha).
- [77] Agency for Toxic Substances and Disease Registry. *Guidance for Inhalation Exposures*. 2021. URL: <https://www.atsdr.cdc.gov/pha-guidance/resources/ATSDR-EDG-Inhalation-508.pdf>.
- [78] Office for National Statistics. *Average hours worked and economic growth, UK: 1998 to 2022*. 2024. URL: <https://www.ons.gov.uk/economy/grossdomesticproductgdp/articles/averagehoursworkedandeconomicgrowth/2024-01-22>.
- [79] Xiaochen Tang et al. “Volatile Organic Compound Emissions from Humans Indoors”. In: *Environmental Science & Technology* 50.23 (2016), pp. 12686–12694. ISSN: 0013-936X. DOI: [10.1021/acs.est.6b04415](https://doi.org/10.1021/acs.est.6b04415). URL: <https://dx.doi.org/10.1021/acs.est.6b04415>.
- [80] Amber M Yeoman et al. “Inhalation of VOCs from facial moisturizers and the influence of dose proximity”. In: *Indoor Air* 32.1 (2022). ISSN: 0905-6947. DOI: [10.1111/ina.12948](https://doi.org/10.1111/ina.12948). URL: <https://dx.doi.org/10.1111/ina.12948>.
- [81] Ruiling Liu et al. “Assessment of risk for asthma initiation and cancer and heart disease deaths among patrons and servers due to secondhand smoke exposure in restaurants and bars”. In: *Tobacco Control* 23.4 (2014), pp. 332–338. ISSN: 0964-4563. DOI: [10.1136/tobaccocontrol-2012-050831](https://doi.org/10.1136/tobaccocontrol-2012-050831). URL: <https://dx.doi.org/10.1136/tobaccocontrol-2012-050831>.
- [82] Noelia Ramírez et al. “Exposure to nitrosamines in thirdhand tobacco smoke increases cancer risk in non-smokers”. In: *Environment International* 71 (2014), pp. 139–147. ISSN: 0160-4120. DOI: [10.1016/j.envint.2014.06.012](https://doi.org/10.1016/j.envint.2014.06.012). URL: <https://dx.doi.org/10.1016/j.envint.2014.06.012>.
- [83] Sonja N Sax et al. “A Cancer Risk Assessment of Inner-City Teenagers Living in New York City and Los Angeles”. In: *Environmental Health Perspectives* 114.10 (2006), pp. 1558–1566. DOI: [doi:10.1289/ehp.8507](https://doi.org/10.1289/ehp.8507). URL: <https://ehp.niehs.nih.gov/doi/abs/10.1289/ehp.8507>.
- [84] H Guo et al. “Risk assessment of exposure to volatile organic compounds in different indoor environments”. In: *Environmental Research* 94.1 (2004), pp. 57–66. ISSN: 0013-9351. DOI: [https://doi.org/10.1016/S0013-9351\(03\)00035-5](https://doi.org/10.1016/S0013-9351(03)00035-5). URL: <https://www.sciencedirect.com/science/article/pii/S0013935103000355>.

- 
- [85] Naomi J Farren et al. “Estimated Exposure Risks from Carcinogenic Nitrosamines in Urban Airborne Particulate Matter”. In: *Environmental Science & Technology* 49.16 (2015), pp. 9648–9656. ISSN: 0013-936X. DOI: [10.1021/acs.est.5b01620](https://doi.org/10.1021/acs.est.5b01620). URL: <https://doi.org/10.1021/acs.est.5b01620>.
- [86] Mustafa Odabasi. “Halogenated Volatile Organic Compounds from the Use of Chlorine-Bleach-Containing Household Products”. In: *Environmental Science & Technology* 42.5 (2008), pp. 1445–1451. ISSN: 0013-936X. DOI: [10.1021/es702355u](https://dx.doi.org/10.1021/es702355u). URL: <https://dx.doi.org/10.1021/es702355u>.
- [87] Mustafa Odabasi et al. “Halogenated volatile organic compounds in chlorine-bleach-containing household products and implications for their use”. In: *Atmospheric Environment* 92 (2014), pp. 376–383. ISSN: 1352-2310. DOI: [10.1016/j.atmosenv.2014.04.049](https://dx.doi.org/10.1016/j.atmosenv.2014.04.049). URL: <https://dx.doi.org/10.1016/j.atmosenv.2014.04.049>.
- [88] Tunga Salthammer. “Acetaldehyde in the indoor environment”. In: *Environmental Science: Atmospheres* 3.3 (2023), pp. 474–493. DOI: [10.1039/d2ea00146b](https://dx.doi.org/10.1039/d2ea00146b). URL: <https://dx.doi.org/10.1039/d2ea00146b>.
- [89] W Liu et al. “Estimating contributions of indoor and outdoor sources to indoor carbonyl concentrations in three urban areas of the United States”. In: *Atmospheric Environment* 40.12 (2006), pp. 2202–2214. DOI: <https://doi.org/10.1016/j.atmosenv.2005.12.005>. URL: <https://www.sciencedirect.com/science/article/pii/S1352231005011672>.
- [90] Pernilla Gustafson et al. “The impact of domestic wood burning on personal, indoor and outdoor levels of 1,3-butadiene, benzene, formaldehyde and acetaldehyde”. In: *J. Environ. Monit.* 9.1 (2007), pp. 23–32. DOI: [10.1039/b614142k](https://dx.doi.org/10.1039/b614142k). URL: <https://dx.doi.org/10.1039/b614142k>.
- [91] Lai Nguyen Huy, Shun Cheng Lee, and Zhuozhi Zhang. “Human cancer risk estimation for 1,3-butadiene: An assessment of personal exposure and different microenvironments”. In: *Science of The Total Environment* 616-617 (2018), pp. 1599–1611. DOI: [10.1016/j.scitotenv.2017.10.152](https://dx.doi.org/10.1016/j.scitotenv.2017.10.152). URL: <https://dx.doi.org/10.1016/j.scitotenv.2017.10.152>.
- [92] A T Hodgson et al. “Volatile organic compound concentrations and emission rates in new manufactured and site-built houses.” In: *Indoor Air* 10 (2000), p. 178.
- [93] Rachel E Dunmore et al. “Atmospheric ethanol in London and the potential impacts of future fuel formulations”. In: *Faraday Discussions* 189 (2016), pp. 105–120. ISSN: 1359-6640. DOI: [10.1039/c5fd00190k](https://dx.doi.org/10.1039/c5fd00190k). URL: <https://dx.doi.org/10.1039/c5fd00190k>.
- [94] Tamara Braish et al. “Evaluation of the seasonal variation of VOC surface emissions and indoor air concentrations in a public building with bio-based insulation”. In:

---

*Building and Environment* 238 (2023), p. 110312. ISSN: 0360-1323. DOI: [10.1016/j.buildenv.2023.110312](https://doi.org/10.1016/j.buildenv.2023.110312). URL: <https://dx.doi.org/10.1016/j.buildenv.2023.110312>.

- [95] Robin E Dodson et al. “Evaluating methods for predicting indoor residential volatile organic compound concentration distributions”. In: *Journal of Exposure Science & Environmental Epidemiology* 19.7 (2009), pp. 682–693. ISSN: 1559-0631. DOI: [10.1038/jes.2009.1](https://doi.org/10.1038/jes.2009.1). URL: <https://dx.doi.org/10.1038/jes.2009.1>.



## Chapter 6

# Speciation and contaminant analysis of personal and home care aerosol products

While the primary aim of this thesis was to evaluate population exposure to indoor VOCs, an emerging area of indoor air analysis is the contribution of product use to IAQ. Product emission assessments can present considerable difficulties for sampling by sensitive methods for analysis of potential trace contaminants. Generated concentrations of VOCs from product use emissions can exceed several ppm. An area of current confusion due to lack of standard procedures is the sampling of these products.

The work presented in this chapter forms part of the methodology for another study, the manuscript of which is currently under consideration in Scientific Reports Household Air Pollution special issue.<sup>†</sup> JRH and SJA devised the original GC-based instrument setup and methods. TW, JRH, and SJA developed the updated GC-based methods applied here. TW and NKS conducted the experimental benzene analysis and visualised the resulting data, while TW performed the general speciation experiments described subsequently. TW also designed the experimental sampling methodology detailed in this chapter and carried out further method development. In the scope of the entire study, including details not presented here, AMY, TW, and ACL designed the original experiments. AMY, TW, and NS performed the laboratory experiments. SJA, MS, and JRH provided technical support, with MS and JRH also contributing substantive revisions. AMY and TW analysed the data, and AMY

---

<sup>†</sup>Yeoman AM, Warburton T, Sidhu NK, Andrews SJ, Shaw M, Hopkins JR, Lewis AC. Updated speciation of VOCs emitted from European-market aerosol dispenser consumer products. Unpublished.

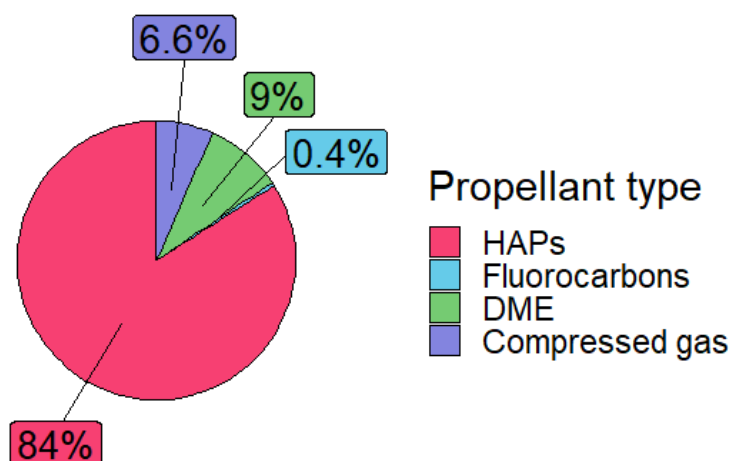


Figure 6.1: Pie chart showing the contribution of individual propellant types to the total 2012 propellant budget. HAP = hydrocarbon aerosol propellant; DME = dimethyl ether. Reproduced from Yeoman and Lewis (2021).<sup>[1]</sup>

and ACL interpreted the results. All authors contributed to the writing of the manuscript and the development of its conclusions.

## 6.1 Background

Most products used in everyday life have an aerosolised option, such as deodorants, hair care products, sunscreen, boot polish, air fragrance products and furniture polish. Each of these products have a more manual ('un-aerosolised') alternative, such as wax sticks for deodorant, wax for furniture polish, and topical cream for sun care. However, aerosolised products (APs) can provide a faster and less manual application of the same products, and as such are often the more pervasive delivery method for products.

APs have varied formulations, however all APs require propellants and solvents (and active ingredients). The role of the propellant is to dispense the product from the canister, while the solvent simply acts to dissolve the active ingredient(s) within the formulation. Hydrocarbon aerosol propellants (HAPs), a blend of propane, *n*- and *i*-butane and sometimes *n*- and *i*-pentane, are the most common propellants used in APs, accounting for over 80% of the total propellant budget.<sup>[1]</sup> Combined with roughly 9% of the propellant budget originating from dimethyl ether, roughly 93% of the propellant budget originates from VOCs, shown in figure 6.1.<sup>[1]</sup> The active ingredient(s) is/are the components within the formulation intended for application.

---

There are several methods by which contaminants could be introduced into product formulations. For example, HAPs such as propane originate from the refinement of natural gas and crude oil.<sup>[2]</sup> Crude oil is typically refined through fractional distillation within a crude oil distillation unit (CDU). Simplified, a CDU can be thought of as a large tank into which the crude oil is introduced at the bottom and is heated to around 398 °C. C<sub>1</sub> to C<sub>4</sub> hydrocarbons (with some C<sub>5</sub> hydrocarbons) separate as a gaseous fraction, with heavier hydrocarbons separating as either liquid or solid fractions. While distillation itself is a purification process, the potential for azeotropic distillation exists, and has been demonstrated.<sup>[3-5]</sup> Manufacturers of APs rely on the purity of their feedstocks to give an assurance of purity in the final product.

At the time of writing, there has been no standardised method written for broad VOC speciation in compressed APs. There have been several studies which have aimed to speciate VOC emissions from personal or home care products, including compressed aerosols, typically using headspace GC-MS or dispensing a dose of the product into a small chamber and then using on-line methodologies such as selective ion flow tube (SIFT) MS or proton transfer reaction (PTR) MS.<sup>[6-8]</sup>

On-line methodologies such as SIFT-MS and PTR-MS allow for a VOC evolution profile to be constructed, from which mixing rates, emission rates and emission factors can then be calculated. Rather than reporting on specific separated species, results are given separated by  $m/z$  channel. This can give difficulties on the reporting on species whose molecular formula is used to define their grouping, for example monoterpenes, which are defined as any chemical with the molecular formula C<sub>10</sub>H<sub>16</sub>. In this specific case, monoterpenes evaluated through SIFT-MS or PTR-MS are often reported in totality as 'total monoterpenes', or sometimes reported as the main monoterpene ingredient in the product formulation. Without carefully monitoring results, this could result in erroneous or misleading reporting. It would be a rare occurrence for only one resulting analyte ion to be reported on an  $m/z$  channel. GC-MS can provide the separative resolution which on-line methodologies may not be able to, but inherently only provide a 'snapshot' of composition at the time the sample was drawn. GC-MS method lengths give additional time resolution implications. A combination of the two types of methodology may therefore be beneficial for the analysis of trace components, both through reporting in depth speciation as well as species emission and decay patterns.

### 6.1.1 Contextualising previous work

In 2021, American independent laboratory Valisure LLC reported benzene detection in many sunscreen and after-sun products, and filed a citizen petition calling for the recall of the identified products reportedly found to contain benzene.<sup>[7]</sup> Reported ratios of benzene found

---

were up to 2 ppm. This was clearly an alarming find, and as such led to several voluntary recalls of indicated products. Valisure LLC additionally found the suspected carcinogen *N*-Nitrosodimethylamine (NDMA) in ranitidine (trade name Zantac) tablets which resulted in recalls and an eventual settlement of over \$2 billion,<sup>[9–11]</sup> as well as finding benzene in benzoyl peroxide-containing products.<sup>[12,13]</sup>

The presence of any contaminant in personal and home care products is of concern. While potentially not defined as a cosmetic according to the UK Cosmetic Products Enforcement Regulations (regulation 2009/1223), which defines a cosmetic as a product which makes purposeful contact with external parts of the human body, many of these products will make unavoidable, incidental contact with external parts of human bodies. For instance, using an aerosolised air freshener will inevitably result in the dispersion of fine aerosols, which will make incidental contact with skin. The presence of potentially harmful contaminants is therefore a crucial concern of such products, and so a robust sampling methodology must be developed to analyse potential trace contaminants.

## 6.2 Methodology

The methodology set out hereafter was developed in two phases to allow for the analysis of trace VOC contaminants in commercially available aerosol sprays: quantification of potential benzene, and then a broad VOC speciation. This requirement for a method to be developed was as a result of reported presence of benzene in APs, including sunscreen and dry shampoo.<sup>[7]</sup> While some untargeted analysis has been completed on APs, generally analysis of APs is targeted to specific species, or literature reviews of listed ingredients.<sup>[14–17]</sup> Naturally, targeted analysis is better when quantifying specific VOCs, however it may miss other potential contaminants. Additionally, reviews of listed ingredients will give insight into the frequency of use of specific ingredients, but will also miss potential contaminants. A requirement of this methodology was to give a broad speciation of the VOC content of a panel of APs, insodoing giving insight into the emissions an end-user may be exposed to. It was therefore decided to dispense an amount of the spray (dose measured through canister mass differential) into an emission chamber which was connected to the gas chromatograph (GC) through a sample line.

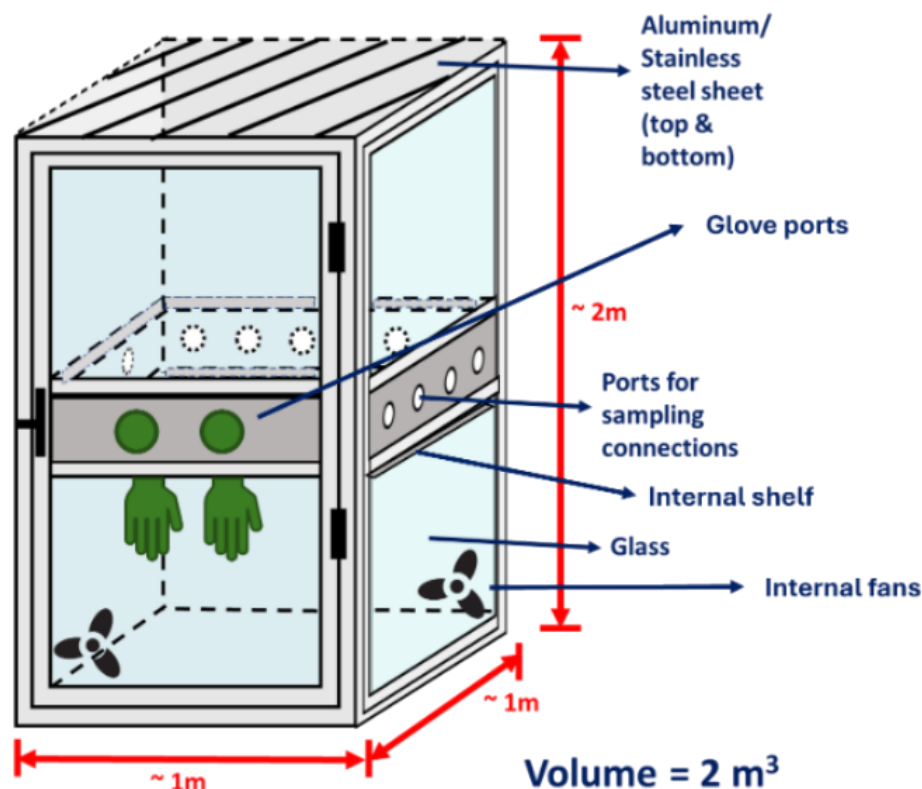


Figure 6.2: Diagram of the chamber used in the aerosol speciation study (not to scale). Reproduced from Yeoman *et al.* (Unpublished).

## 6.2.1 Aerosol dispensing and sampling

### 6.2.1.1 Emission chamber

This work was completed at the Wolfson Atmospheric Chemistry Laboratories, at the University of York. In the laboratory, the emission chamber used in this work was a 2 m<sup>3</sup> chamber constructed with aluminium extrusion profiling with tempered glass panels, shown in figure 6.2. The chamber was roughly 5 m displaced from the GC instrument, so a sample line was therefore required. Whole air sampling canisters were initially used for trial sampling, however this was not deemed suitable. Primarily, a substantial number of canisters would be needed for the analysis and the canister evacuation and preparation methods would cause large time constraints on the analysis, given this work was completed in the context of a busy laboratory with several other projects running simultaneously. Additionally, it was known the mixing ratios of VOCs emitted from the aerosols would be in the order of potentially several hundred parts per million in totality, and there were concerns that such high mixing ratios could cause canister contamination. Samples would therefore need to be pumped to the GC.

---

### 6.2.1.2 Sample line

A sample line was constructed to facilitate analysis through GC. The sample line construction is given in figure 6.3. Following the conclusion the metal bellows pump would not contribute to quantifiable contaminations in samples (discussed in section 6.2.1.3, the pump was placed upstream of the GC, resulting in a pressurised flow of chamber gas passing the GC. Typically, pumps would be placed downstream of the GC, resulting in a negative-pressure flow of gas passing the GC and the GC then sub-sampling this flow. However in this case, the GC sucking pump was not sufficient to draw against the negative pressure caused by the sample line pump suction, and so a positive pressure was required. An additional requirement was not to artificially increase the air exchange rate of the chamber by simply venting the pumped gas to the atmosphere - to counter this, the sample line was routed to flow back into the sampling chamber. As such, there had to be confidence that there would be no contamination introduced into the chamber through the bellows of the pump itself.

### 6.2.1.3 Metal bellows pump

A metal bellows pump was used throughout the sampling campaign. The operating principle for such a pump is that gas movement occurs through the expansion and contraction of stainless steel bellows, controlled through a drive shaft attached to an eccentric shaft, with gas inlets and outlets fitted with check (directional) valves. Through the movement of the drive shaft and the expansion and contraction of gases, the bellows heat up to temperatures reaching 70 °C. Such a temperature would not be hot enough to thermally decompose any of the VOCs quantified in this study, and additionally would keep any of the more 'sticky' VOCs, such as benzene, toluene, xylene and trimethylbenzene, to stay in the gas-phase and not deposit onto the bellows. To preserve the integrity of the bellows, a 7 µm filter was added inline to the pump inlet.

The pump was assessed as a potential source of VOC contamination by filling a fully evacuated 45 L canister with blank gas to 1.5 bar (gauge), and attaching the pump inlet and outlet to either side of the canister through short lengths of PFA tubing. Before attaching the tubing to the pump and canister, each end of the tubing was fitted with a lever ball valve, the valves opened and blank gas flowed through the tubing for 10 seconds. The valves were then closed to encapsulate the blank gas within the tubing, and was then directly attached to the canister and pump, thus clearing as much ambient air from the system as possible. Before circulating the canister blank gas through the pump, the canister was directly attached to the GC (bypassing the pump, so as to not draw the sample through the pump bellows) and a 500 mL sample was drawn and analysed in the same methods as in previous chapters. Once

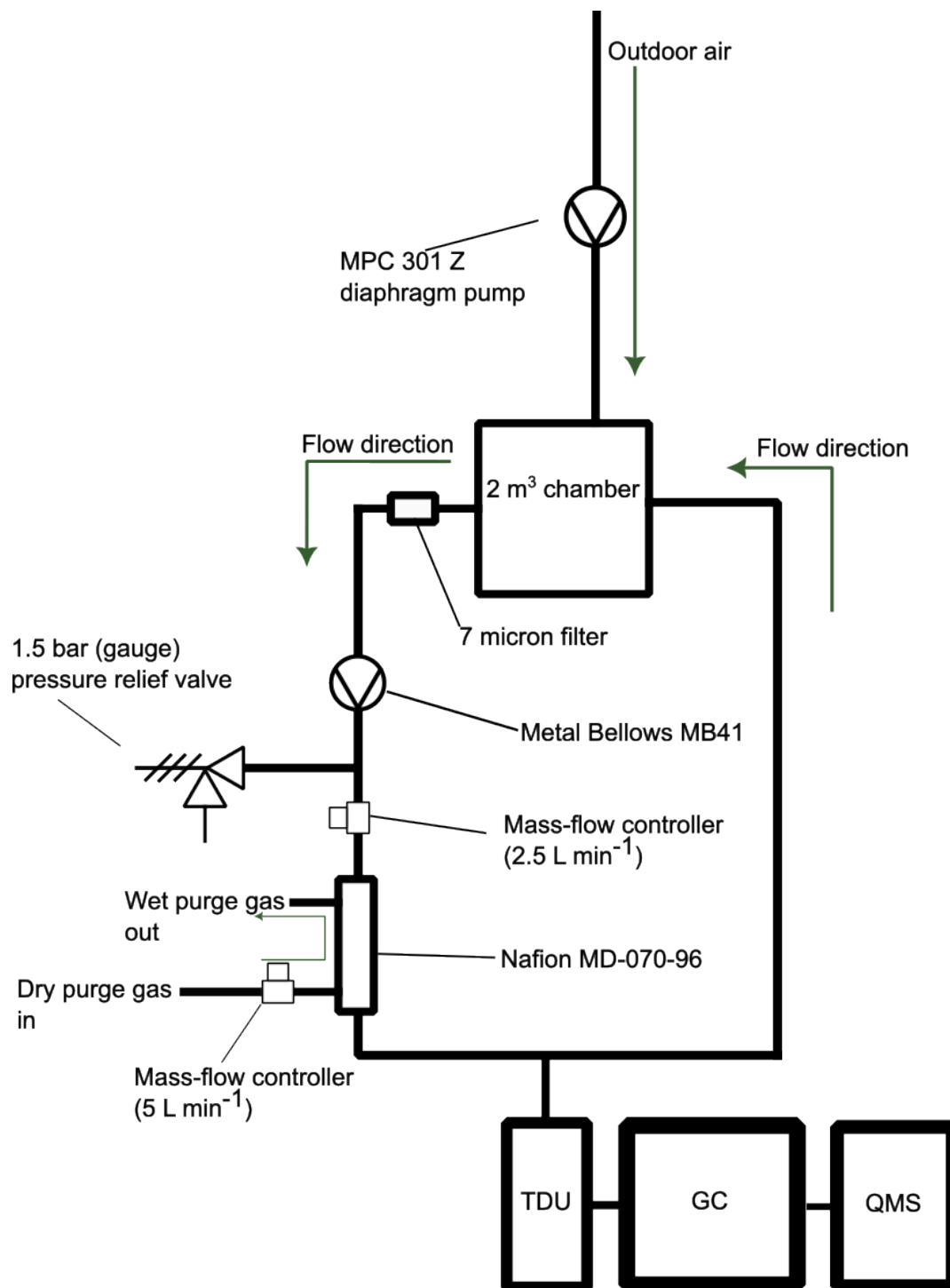


Figure 6.3: Schematic diagram of the AP sample line used for benzene analysis. During the main sampling campaign, the main line mass-flow controller, Nafion MD-070-96 and associated parts were removed, with all other components remaining. Symbols used within the diagram are as prescribed by the Piping and Instrument Diagrams (P&ID) standards.

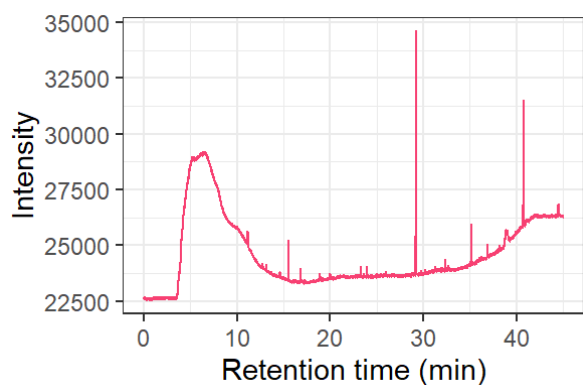


Figure 6.4: PLOT chromatogram for 500 mL sample of blank gas drawn through the sampling manifold used to process the canister and pump blank samples.

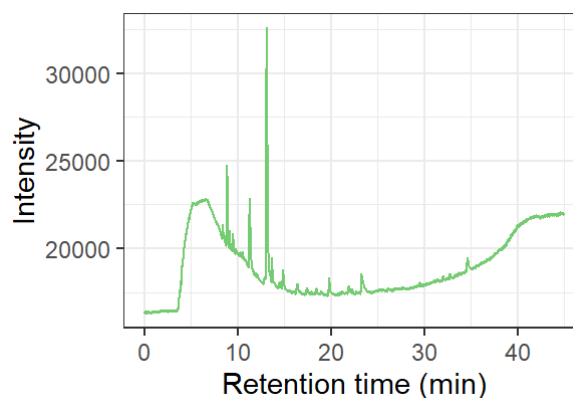


Figure 6.5: WAX chromatogram for 500 mL sample of blank gas drawn through the sampling manifold used to process the canister and pump blank samples.

the sample had been drawn, the canister was then disconnected from the GC, topped up with blank gas back to a pressure of 1.5 bar (gauge) to replace the volume sampled. The blank gas-containing tubing was then attached between the canister and the pump inlets and outlets. The canister valves and pump valves were opened and the pump switched on. The pump was allowed to run for a full day. Once this time had elapsed, the canister valves were closed and the pump taken out of line. The canister was then directly attached to the GC for another sample. The purpose of this was not to quantitatively account for any potential contributions from the pump, but to assess whether there was any potential contamination from the use of the pump, and the impact this might have on aerosol sample reporting. A blank gas sample was also analysed through the same sampling manifold as for the canister and pump samples, to assess any potential impurities through the sampling manifold.

During analysis, it became clear the sampling manifold itself had considerable sources of contamination, as shown in figures 6.4 and 6.5. As the bulk aerosol sampling campaign did not involve this sampling manifold, this was not of concern for the integrity of the aerosol samples. However here, canister and pump blank samples would need to be corrected for this contamination. Incidentally, this contamination was found to be mostly breakdown products of siloxanes, large concentrations of which had been sampled through this sampling manifold previous to this analysis. Following replacement of pneumatic valves on the manifold, the contaminations were cleared. No samples of indoor air used throughout this thesis, indeed in any published work, were included in any analyses during this period of siloxane contamination.

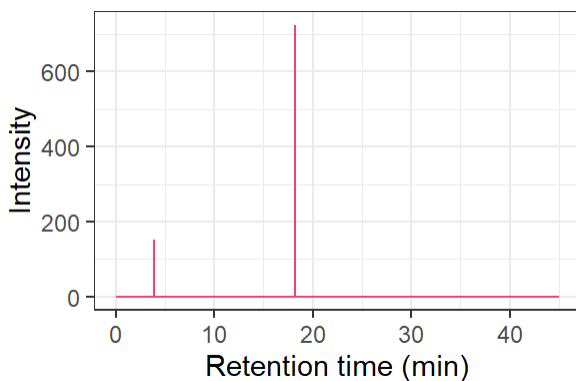


Figure 6.6: Plot showing PLOT channel intensities following canister blank intensities being subtracted from the pump blank.

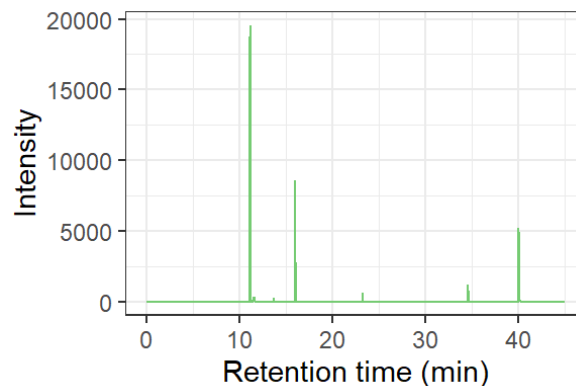


Figure 6.7: Plot showing WAX channel intensities following canister blank intensities being subtracted from the pump blank.

Chromatographic intensities from canister and pump blank samples were analysed, with canister blank intensities being subtracted from those of pump blanks to isolate the relevant differences, with the resulting intensities shown in figures 6.6 and 6.7. Naturally some negative numbers were introduced during the variable regions of noise, ranging from -300 to -1, and so any negative intensities were set to 0. This did not impact the identification of any identifiable contamination through the use of the pump.

There were no pump contaminations found from the PLOT elutions (figure 6.6). There were two spikes in intensity at  $\approx 4$  min and  $\approx 17.5$  min, however these were due to electrical noise within the system and were not due to chemical elution from the PLOT column. There were four larger elutions from the WAX column, the largest being at  $\approx 11$  min. The three other notable elutions were at  $\approx 15$  min,  $\approx 35$  min and  $\approx 40$  min, along with a very small elution at  $\approx 23$  min. In order from the first elution to last, the species were identified as acetone, a cyclosiloxane (likely D4/octamethylcyclotetrasiloxane), styrene, benzaldehyde and naphthalene. Through the subtraction process, the acetone peak split into two separate peaks, however this was likely due to the peak tailing in the canister blank not subtracting totally due to the slightly different retention times of acetone across the two samples (shown in figures 6.8 and 6.9). These differences in retention time likely account for the presence of acetone in the subtraction process itself and therefore an artifact of the canister. There is no realistic mechanism by which acetone would be preferentially created in the pumping process in the total absence of common precursor species, and as such was not of concern for aerosol sampling.

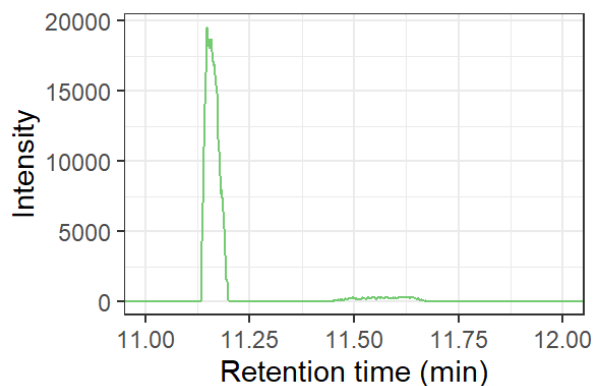


Figure 6.8: Plot showing the difference between canister and pump blank samples, zoomed in to the acetone peak, here showing splitting of the peak due to differences between acetone retention time between the canister and pump blank sample runs.

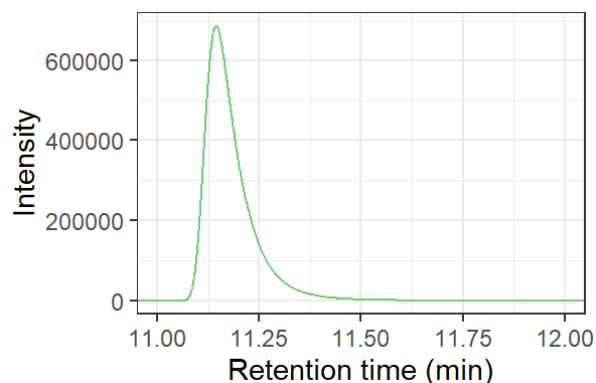


Figure 6.9: Original pump blank sample showing the acetone peak, with significant peak tailing, indicating there was band broadening due to high quantities of acetone in the volume sampled.

The cyclosiloxane was not properly identified as the mass spectrometer (MS) scan range used in this analysis ran between 30 and 150 units  $m/z$  units. The mass spectrum for the elution showed substantial peaks at (highest to lowest) 133, 73 and 125  $m/z$  units in a ratio of 1:0.6:0.3. It was suspected that this cyclosiloxane was D4/octamethylcyclotetrasiloxane, the 'real' base peak of which fell out the MS  $m/z$  scan range at 281  $m/z$  units. To confirm this, a 1  $\mu\text{L}$  injection of D4 liquid was injected into a 3 L Tedlar bag through a septum, and then diluted to 3 L with blank gas. The resulting suspected D4 elution is shown in figure 6.10, alongside the mass spectrum for the suspected D4 elution (figure 6.11). The suspected D4 elution at  $\approx 16$  min in figure 6.7 is shown in figure 6.12, the mass spectrum of which is shown in figure 6.13.

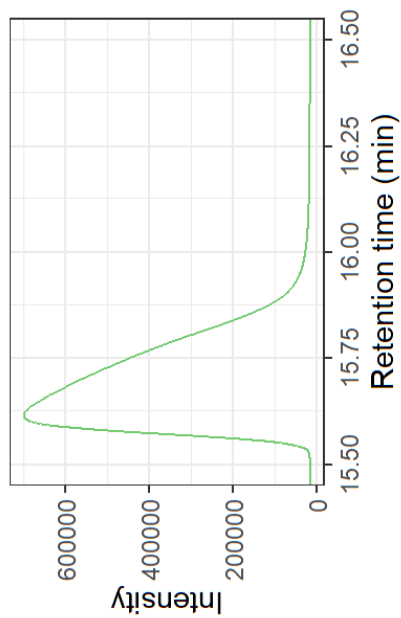


Figure 6.10: WAX elution for suspected D4 following liquid injection of 1  $\mu\text{L}$  into 3 L of blank gas into a Tedlar bag. The peak shows significant non-Gaussian characteristics, indicating an overloading of the column. While not ideal, it was evidence this was the elution of D4.

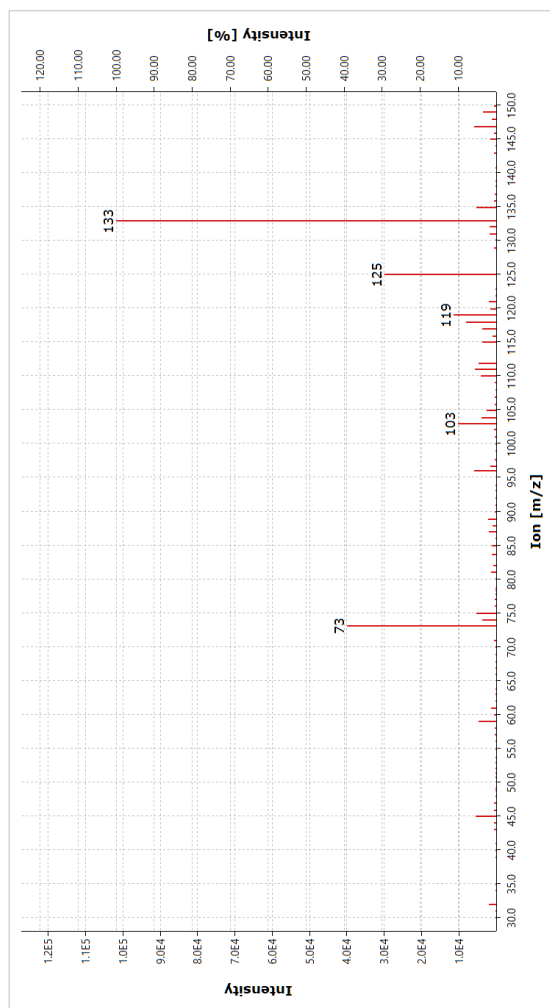


Figure 6.11: Mass spectrum for the peak shown in figure 6.10.

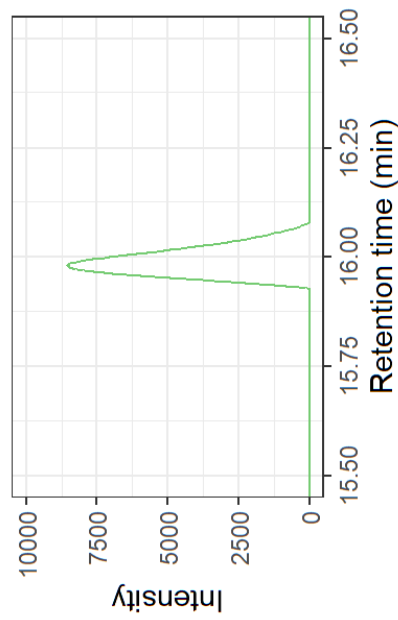


Figure 6.12: WAX elution for suspected D4 - originating from the same plot as figure 6.7, just scaled to retention times of 15.5 min and 16.5 min.

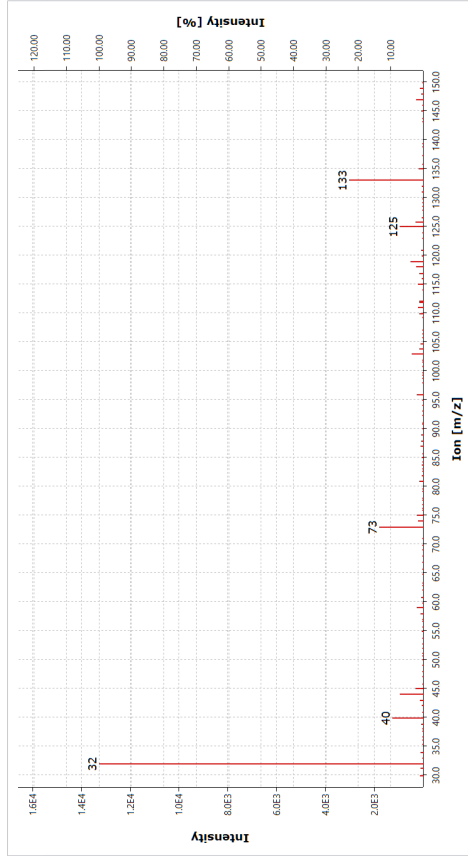


Figure 6.13: Mass spectrum for the peak shown in figure 6.12. Significant peaks at 32, 40 and 45  $m/z$  units originate from the background, identified as oxygen, argon, and small amounts of  $CO_2$ , likely to originate from air due to a small leak.

---

Given the significant overlap between mass spectra for the suspected cyclosiloxane and the D4 injection, it was determined that the cyclosiloxane present at  $\approx 16$  min in figure 6.7 was D4/octamethylcyclotetrasiloxane.

After 24 hours of continuous use, the pump appeared to contribute small levels of octamethylcyclotetrasiloxane, styrene, benzaldehyde and naphthalene. Of these species, only benzaldehyde was included in speciation. The mixing ratio of benzaldehyde present in the pumped blank sample was 79 ppt,  $\approx 0.34 \mu\text{g m}^{-3}$ . However during the sampling campaign, the pumped chamber sample flowed directly back into the chamber itself, meaning any contamination produced was diluted into 2000 L of air, and the chamber itself was vented regularly between samples. As such, the contaminants produced likely had no quantifiable effect on the quantified aerosol samples.

### 6.2.2 Benzene analysis

A particular feature of the instrument used throughout this thesis was the co-elution of ethanol and benzene, shown in figure 6.14. Under normal conditions, reporting of benzene by using flame ionisation detection (FID) data would only be possible in the total absence of ethanol. As for indoor air ethanol is a considerable mass contributor to the summed total of analysed VOCs in any given study, and given the usual presence of substantial quantities of ethanol in APs, benzene would have to be quantified using quadrupole mass spectrometry (QMS) data to deconvolve the coeluted peak. While this would usually be acceptable for general characterisation of indoor air samples, this would not be sufficient for the specific analysis of benzene as a possible trace contaminant in a product formulation.

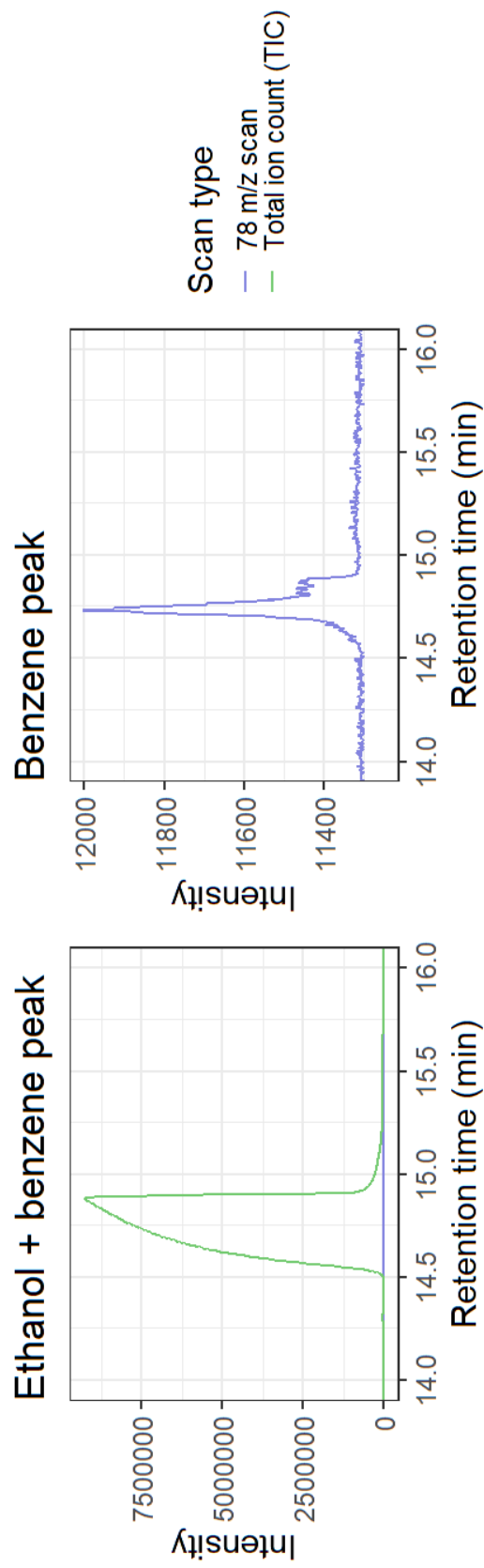


Figure 6.14: QMS data from both total ion count (TIC) in green, and the 78  $m/z$  scan showing the benzene detection during the wide ethanol detection. The ethanol detection showed significant band broadening in the column due to the quantity of ethanol within the sample.

---

### 6.2.2.1 Sample drying

Ethanol would therefore have to be removed from the AP sample in order to properly quantify benzene using FID data. To achieve this, ethanol was chemically separated from the raw sample gas flow using Nafion, which was originally discussed in section 2.1.2.2. In summary, Nafion, being a trademarked name for a fluoropolymer-copolymer, acts as a chemical membrane through which susceptible species are chemically transformed and pass through the membrane into a purge gas flow, shown previously in figure 2.5. At this point, up to 90% of the ethanol contained within the sample gas was removed. However, as shown in figure 6.14, this could leave detectable quantities of ethanol remaining within the gas flow given the large quantities of ethanol in the original aerosol sample.

### 6.2.2.2 GC heartcutting

On a standard sample run (shown as a flowchart in figure 3.1), the dried, preconcentrated and focused sample would flow from the focus trap straight through the VF-WAX column, and (after 8.3 min) through a Deans switch and then through a split to both an FID and the QMS detector. However for benzene analysis here, immediately prior to the ethanol and benzene co-elution at 14.3min, the Deans switch was actuated to divert the elution flow to the PLOT column. At 15.5 min once the co-elution had finished eluting, the Deans switch was once again switched off to proceed through the standard flow pathway. This is a process known as heartcutting. Ethanol was destroyed by the PLOT column used here through the dehydration of ethanol into ethylene and water. This was not a viable long-term solution as the produced water could bind to the alumina and degrade the sodium sulphate coating as well as cause an interference with ethylene analysis, however as a short-term assessment, it proved beneficial in removing the remaining traces of ethanol. In heartcutting the ethanol onto the PLOT column, this provided a final route by which ethanol was totally destroyed, leaving only benzene as a PLOT column elution quantifiable by flame ionisation detectors.

Standard GC elutions of the 30 component standard mix are shown in figures 6.15 and 6.16 for both PLOT and WAX column elutions, respectively. Here, the absence and presence (respectively) of benzene peaks in the chromatograms has been identified. Figures 6.17 and 6.18 show the PLOT and WAX elutions respectively of the same 30 component standard, however with benzene heartcut from the WAX column to the PLOT column. Comparing relative intensities between benzene peaks for WAX and heartcut-PLOT elutions (figures 6.16 and 6.17 respectively), it appeared there was an increase in benzene response between FID detectors. This was to be expected however, as in a normal sample run as in figure 6.16, WAX elution flow was split after 8.3 minutes between a flame ionisation detector and a mass

---

spectrometer, resulting in reduced flow to the WAX FID.

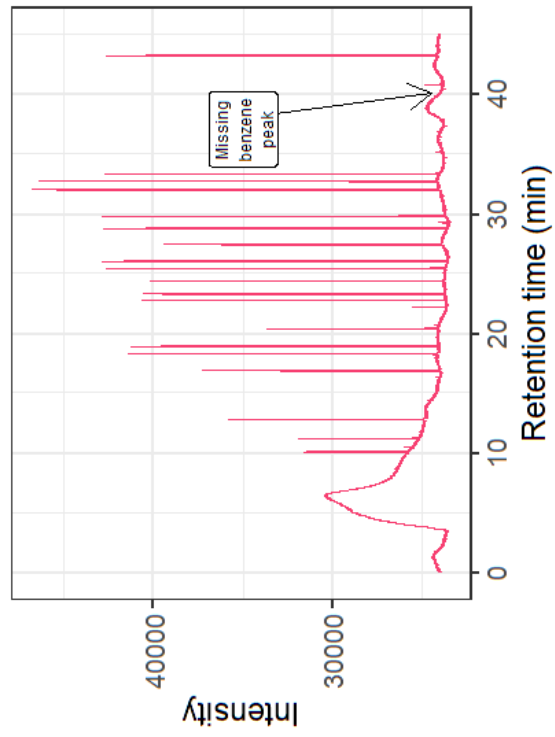


Figure 6.15: PLOT chromatogram for a 20 mL sample of the 30 component gas standard, with the absence of a benzene peak identified.

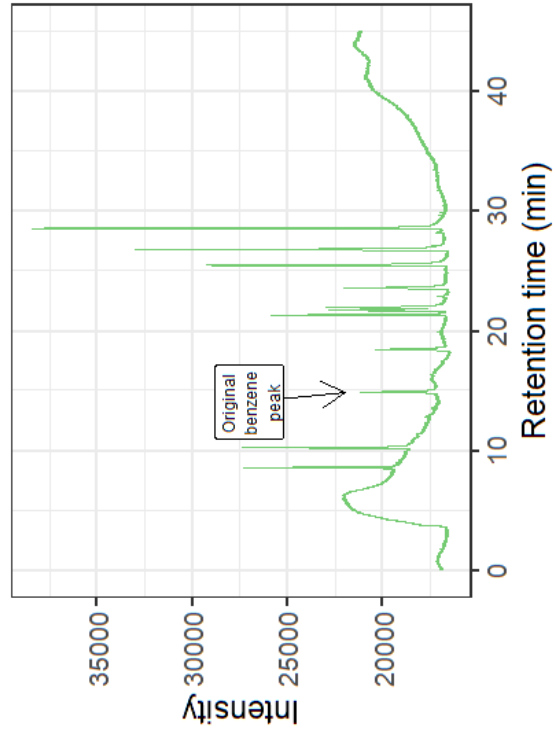


Figure 6.16: WAX chromatogram for a 20 mL sample of the 30 component gas standard, with the benzene peak identified.

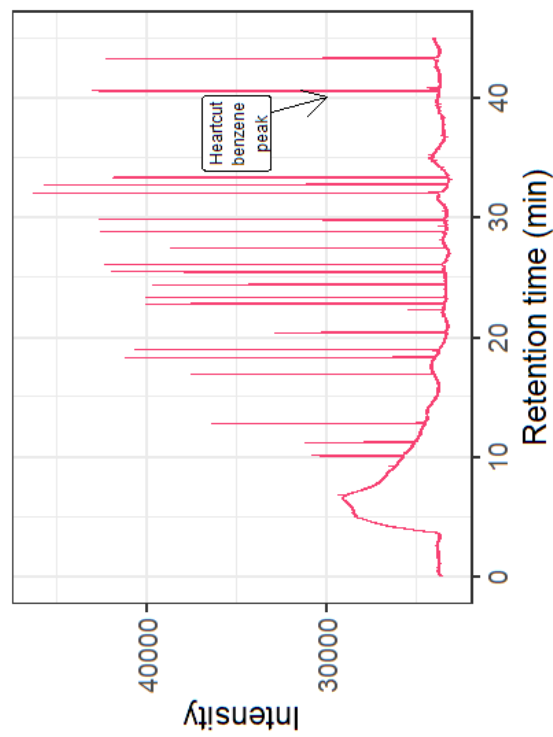


Figure 6.17: PLOT chromatogram for a 20 mL sample of the 30 component gas standard using the heartcutting method, with the benzene peak identified.

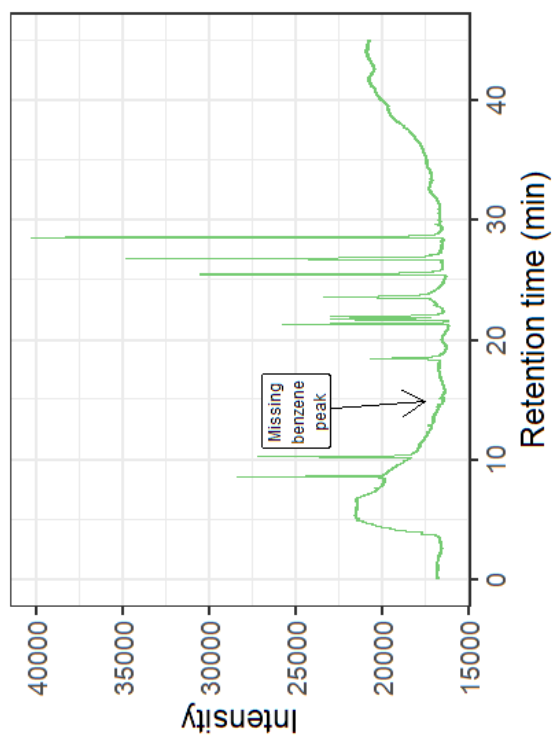


Figure 6.18: WAX chromatogram for a 20 mL sample of the 30 component gas standard using the heartcutting method, with the absence of the benzene peak identified. There was a small reduction in baseline noise during the Deans switch actuation, owing to a slight reduction in pressure as the WAX eluent flow passed through the PLOT column.

---

## 6.3 Conclusions

This chapter presented the development and validation of a sampling system for the characterisation of VOC emissions from personal and home care APs. A custom emission chamber setup incorporating a metal bellows pump, Nafion dryer for benzene analysis, and inert sampling lines enabled controlled, repeatable sampling of AP emissions and subsequent analysis via GCMS.

Key methodological elements, including rigorous blank testing, and sample drying and GC heartcutting for benzene analysis, were found to be critical in achieving sufficient analytical clarity for complex product matrices. Differences between pump and canister blanks demonstrated that careful choice of pumps allows for the positive pressurising of AP air samples without quantifiable contaminant introduction. The GC heartcutting method was successful in resolving co-elution issues, particularly for benzene FID quantification amidst high ethanol background.

Overall, this work underscores the importance of methodological transparency and reproducibility in VOC product testing. The modular nature of the sampling system and the detailed documentation of its operation provide a robust foundation for future testing campaigns. In a field often limited by too-selective and often inappropriate protocols and irreproducible conditions, the ability to generate and verify reliable emission data is a necessary step toward standardised indoor air exposure assessments.

---

## 6.4 References

- [1] Amber M Yeoman and Alastair C Lewis. “Global emissions of VOCs from compressed aerosol products”. In: *Elementa: Science of the Anthropocene* 9.1 (2021), p. 177. DOI: [10.1525/elementa.2020.20.00177](https://doi.org/10.1525/elementa.2020.20.00177). URL: <https://doi.org/10.1525/elementa.2020.20.00177>.
- [2] S R Clough. “Propane”. In: *Encyclopedia of Toxicology (Third Edition)*. Ed. by Philip Wexler. Oxford: Academic Press, 2014, pp. 1086–1088. ISBN: 978-0-12-386455-0. DOI: <https://doi.org/10.1016/B978-0-12-386454-3.00423-1>. URL: <https://www.sciencedirect.com/science/article/pii/B9780123864543004231>.
- [3] Robert F Marschner and Wendell P Cropper. “Hydrocarbon azeotropes of benzene”. In: *Industrial & Engineering Chemistry* 38.3 (1946), pp. 262–268.
- [4] Yoshimori Miyano and Walter Hayduk. “Solubilities of butane, vapor pressures, and densities for benzene+ cyclohexane, benzene+ methanol, and methanol+ cyclohexane solutions at 298 K”. In: *Journal of Chemical and Engineering Data* 38.2 (1993), pp. 277–281.
- [5] Zhilong Zhen et al. “Determination of water content of crude oil by azeotropic distillation Karl Fischer coulometric titration”. In: *Analytical and Bioanalytical Chemistry* 412.19 (2020), pp. 4639–4645. DOI: [10.1007/s00216-020-02714-5](https://doi.org/10.1007/s00216-020-02714-5). URL: <https://doi.org/10.1007/s00216-020-02714-5>.
- [6] Amber M Yeoman et al. “Simplified speciation and atmospheric volatile organic compound emission rates from non-aerosol personal care products”. In: *Indoor Air* 30.3 (2020), pp. 459–472. DOI: <https://doi.org/10.1111/ina.12652>. URL: <https://onlinelibrary.wiley.com/doi/abs/10.1111/ina.12652>.
- [7] Amber Hudspeth et al. “Independent sun care product screening for benzene contamination”. In: *Environmental Health Perspectives* 130.3 (2022), p. 37701.
- [8] Elanda Fikri and Yura Witsqa Firmansyah. “A Case Report: Benzene Contamination in Shampoo”. In: *Jurnal Serambi Engineering* 8.2 (2023).
- [9] Owen Dyer. “GSK settles most US lawsuits over Zantac for \$2.2bn”. In: *BMJ* 387 (2024), q2249–q2249. DOI: [10.1136/bmj.q2249](https://doi.org/10.1136/bmj.q2249). URL: <http://www.bmj.com/content/387/bmj.q2249.abstract>.
- [10] Vasudha Sharma and Navyug Raj Singh. “Ranitidine: recent regulatory issues”. In: *International Journal of Basic & Clinical Pharmacology* 9.8 (2020), pp. 1314–1317.
- [11] Andrew Walker. “Developments in Practice”. In: *Journal of Medicines Optimisation* 6.3 (2020), p. 77.

- 
- [12] Kucera Kaury et al. “Benzoyl Peroxide Drug Products Form Benzene”. In: *Environmental Health Perspectives* 132.3 (2024), p. 37702. DOI: [10.1289/EHP13984](https://doi.org/10.1289/EHP13984). URL: <https://doi.org/10.1289/EHP13984>.
- [13] Kaitlyn Bader. “Benzene Found in Benzoyl Peroxide-Containing Acne Products: What Comes Next?” In: *Dermatology Times* 45.4 (Apr. 2024), pp. 1–4.
- [14] Hazim M. Ali et al. “Sensitive analysis of some detrimental volatile organic compounds in fabric, carpet and air freshener using solid phase extraction and gas chromatography–mass spectrometry”. In: *Bulletin of the Chemical Society of Ethiopia* 38.6 (2024), pp. 1543–1556. DOI: [10.4314/bcse.v38i6.4](https://dx.doi.org/10.4314/bcse.v38i6.4). URL: <https://dx.doi.org/10.4314/bcse.v38i6.4>/[2010.4314/bcse.v38i6.4](https://dx.doi.org/10.4314/bcse.v38i6.4).
- [15] Suresh Chandra Rastogi et al. “Fragrances and other materials in deodorants: search for potentially sensitizing molecules using combined GC-MS and structure activity relationship (SAR) analysis”. In: *Contact Dermatitis* 39.6 (1998), pp. 293–303.
- [16] Adnan S Al-Mussallam et al. “Optimization of a gas chromatography–mass spectrometry (GCMS) method for detecting 28 allergens in various personal care products”. In: *Cosmetics* 10.3 (2023), p. 91.
- [17] Mitchell Tiessen, Naomi L Stock, and Theresa Stotesbury. “Untargeted SPME–GC–MS Characterization of VOCs Released from Spray Paint”. In: *Journal of Chromatographic Science* 59.2 (2021), pp. 103–111. DOI: [10.1093/chromsci/bmaa082](https://doi.org/10.1093/chromsci/bmaa082). URL: <https://doi.org/10.1093/chromsci/bmaa082>.



# Chapter 7

## Conclusions

Indoor environments are now widely recognised as the primary exposure setting for most people, particularly in residential spaces where time spent indoors continues to increase. Volatile organic compounds (VOCs), emitted from a diverse array of sources such as consumer products, building materials, and occupant activities, can accumulate to concentrations far exceeding those typically found outdoors. The extent of this accumulation is governed by multiple factors including emission strength, product usage behaviours, and the ventilation characteristics of the space. While ventilation can provide an effective means of mitigation, the trend toward increasingly airtight, energy-efficient homes complicates this dynamic. Within this context, a detailed understanding of real-world VOC sources and usage patterns - particularly from personal and home care products such as deodorants and fragrance diffusers - is critical to advancing indoor air quality science.

The work presented in this thesis addresses these challenges through a series of interlinked studies combining detailed fieldwork, analytical rigour, and novel methodological approaches. Drawing from over 180 homes, controlled test booths, and consumer aerosol product testing, it offers a contemporary perspective on the key drivers of indoor VOC exposure in residential environments, with a particular emphasis on ventilation behaviours, product emissions, and seasonal variation.

### 7.1 Synthesis of Key Findings

Across the three core studies, a number of consistent themes emerged. Chief among them was the central influence of air change rate (ACR) on VOC concentrations indoors. In poorly ventilated environments, even moderate emissions from everyday products like liquid electrical

---

(LE) fragrance diffusers could lead to disproportionately higher exposure levels. Conversely, increased ventilation was repeatedly shown to dilute VOC concentrations, underscoring the importance of effective air movement in mitigating indoor air quality risks.

The work demonstrated that fragranced products, particularly those containing monoterpenes, could contribute meaningfully to indoor VOC burdens. However, perceived fragrance intensity plateaued when multiple LEs were used concurrently, suggesting a potential self-limiting behaviour that might reduce the likelihood of excessive exposure. Nevertheless, real-world observations from product use statistics from the studies in Chapters 3 and 5 indicated that fragranced products were often used in high quantities, raising important questions about consumer awareness and behavioural norms. These findings emphasise not only the chemical potential of fragranced products but also the importance of understanding consumer behaviour in shaping VOC exposure outcomes. Interestingly, the compounds most responsible for VOC load from LE emissions (*e.g.* monoterpenes) were not always those driving fragrance perception, suggesting opportunities for reformulation to reduce emissions and potential secondary product creation without affecting consumer experience.

The longitudinal study conducted in Bradford provided a broader context for indoor VOC exposure, revealing clear spatial and seasonal patterns in emissions. Urban homes exhibited elevated background levels of traffic-related pollutants such as BTEX compounds, while warmer seasons were associated with increased VOC emission rates. By applying a transformational method to convert concentration data into generalised emission rates, effectively normalising for the changeable ACRs and room volumes found within the study, further patterns emerged in temporal and seasonal VOC emissions. The potential for VOCs to persist indoors - through sorption to surfaces or recirculation via limited ventilation - further underscores the complexity of managing indoor air quality over time.

## 7.2 Methodological Contributions

In addition to advancing substantive knowledge, this thesis developed and deployed several methodological innovations. High-sensitivity gas chromatography–mass spectrometry (GC-MS) with thermal desorption allowed for VOC quantification at sub-ppb levels in real-world settings. The use of sampling canisters, coupled with robust data correction techniques, strengthened the reliability of results. The work also introduced a reliable protocol for assessing VOC emissions from aerosol products, offering a scalable approach for future product testing and regulatory assessment.

These methodological contributions are relevant not only to future academic studies, but also

---

to the development of standardised VOC testing procedures for consumer products.

Throughout the real-home studies presented in Chapters 3 and 5, it became clear that raw concentration data rarely yielded meaningful results. While comparisons against benchmarks were informative, variations in ACR and room volume, as well as the presence of skewing outliers, often obscured clear conclusions. Stratifying households into ACR quantiles and normalising for ACR and room volume enabled deeper insights to be drawn from the data. The method developed for calculating generalised emission rates in Chapter 5 facilitates reliable inter- and intra-study comparisons, and supports more robust conclusions regarding indoor VOC exposure.

### **7.3 Implications for Indoor Air Quality and Policy**

Findings from this thesis have several implications for indoor air quality research and regulation. First, they support the inclusion of real-world behavioural data and housing characteristics in exposure models. Current modelling frameworks often assume idealised or averaged conditions, which might significantly underestimate exposure in low-ventilation homes.

Secondly, the work underscores the need for clear communication regarding the importance of ventilation and air exchange in relation to product use. Both experimental findings and modelled analyses showed the potential for significantly increased VOC exposure in poorly ventilated rooms through unintentional overuse of VOC-containing products. Transparency on the correct use of such products would aid in mitigating such circumstances.

Finally, this research suggests that any future public health guidance on indoor environments must grapple with the tension between consumer preferences, housing stock constraints, and the need for clean air indoors; a challenge likely to grow in importance as homes become more airtight in pursuit of energy efficiency.

### **7.4 Limitations**

While this work provides a robust and multi-faceted picture of indoor VOC exposure, certain limitations should be acknowledged. The temporal resolution of the flow-restrictive sampling approach limited its ability to resolve short-lived episodic events (*e.g.*, cooking, cleaning). A bias toward the front-end of sampling was observed, and some discrepancies in sampling duration arose from inherent variability in the sampler's restrictive orifice. While these issues were not necessarily large in magnitude, they may have introduced some uncertainty in intra-study concentration comparisons. Nonetheless, the overall integrity of the dataset remains

---

strong, and these limitations primarily reflect areas for refinement in future work.

Additionally, although the home surveys spanned diverse building types, the samples for work completed in Chapters 3 and 5 were geographically restricted to single UK cities. Broader regional studies would strengthen generalisability.

In the study presented in Chapter 4, the test booths operated at a fixed air change rate of  $7.5 \text{ hr}^{-1}$ , which is relatively high and not fully representative of larger residential spaces such as living rooms. However, it is broadly consistent with the typical ACR of residential bathrooms with mechanical extraction, as required in new UK housing. The use of variable ACRs would have enabled a more nuanced understanding of the emission dynamics of LE devices.

## 7.5 Future Research Directions

There are several clear avenues for future research. First, time-resolved instrumentation such as proton transfer reaction mass spectrometry (PTR-MS) or selected ion flow tube mass spectrometry (SIFT-MS) would allow for dynamic tracking of VOC fluctuations, capturing rapid emission events missed by time-integrated sampling.

Second, intervention-based studies—for example, altering ventilation behaviours or reducing product use—would provide valuable insights into the effectiveness of practical mitigation strategies. A longer-term goal could be to establish a population-scale VOC exposure dataset, linking household behaviours, building characteristics, and health outcomes.

Finally, as consumer product formulations evolve and new indoor technologies emerge, ongoing surveillance and method development will be essential to ensure indoor air remains a priority in environmental health research.

## 7.6 Final Remarks

Indoor VOC exposure is shaped by many interrelated aspects of daily life. Personal behaviours, such as the frequency and intensity of product use, and the degree of indoor-outdoor air exchange, have been shown throughout this thesis to play a critical role in controlling, and indeed mitigating, exposure levels. Decisions as seemingly minor as opening a window, selecting a fragranced product, or increasing the number of active diffusers can cumulatively have significant impacts on the chemical composition of the indoor environment.

This thesis offers a contemporary, evidence-based perspective on the complex drivers of indoor

---

VOC exposure, grounded in both rigorous experimental work and the development of novel methodological approaches. Through a combination of detailed field campaigns, controlled laboratory experiments, and product-specific emission assessments, it brings to light the often-underappreciated role that consumer products, ventilation practices, and behavioural norms play in shaping the air we breathe at home.

As the indoor environment increasingly becomes the primary exposure setting for most populations—particularly in the context of energy-efficient, airtight buildings—understanding the chemical consequences of everyday choices grows ever more important. The findings presented here provide not only a scientific foundation for future indoor air quality research but also a practical roadmap for interventions aimed at safeguarding health. Continued research, public engagement, and policy innovation will be essential to ensure that as our built environments evolve, the quality of the air within them does not become an unintended casualty.